A PROCEDURE FOR THE DESIGN OF STORAGE FACILITIES FOR INSTREAM EROSION CONTROL IN URBAN STREAMS

by

Craig R. MacRae

A thesis
submitted under the supervision of
Dr. Paul E. Wisner

in partial fulfillment of the
requirements for the degree of
Doctor of Philosophy
in
Civil Engineering

Department of Civil Engineering
University of Ottawa
Ottawa, Canada
K1N 9B4

ISBN 0-315-75097-9

UNIVERSITÉ D'OTTAWA
UNIVERSITY OF OTTAWA

This thesis is dedicated to my wife, Trudy. If it were in my power I would confer upon her the higher degree of sacrifice, loyalty and perseverance. I am indebted to her beyond my ability to pay.

ACKNOWLEDGEMENTS

Special appreciation is given to my advisor, Dr. Paul Wisner, who from his wealth of experience provided insights, encouragement and critical advise. Thanks also to Mr. Brian Morse, Dr. Alan Fok, and particularly Dr. Charles Rowney who contributed much through discussions and critical evaluations. Special thanks goes to Mr. Jean-Francois Sabourin for his help on code improvements and for the development of PLOTSEC2.

This work was sponsored in part by the Rideau Valley Conservation Authority, and the Canada Housing and Mortgage Corporation, (CMHC). Without the ongoing support of CMHC this research would not have been completed.

The author would also like to acknowledge the Metropolitan Toronto and Region Conservation Authority, and Fred Schaeffer and Associates for the opportunity they provided to test the model in practical applications.

ABSTRACT

Case studies have previously demonstrated the potentially adverse effects of uncontrolled storm water runoff from urban development on stream channel form. Such effects have prompted the development of design methods for the minimization of instream erosion potential, typically using runoff storage controls. Existing techniques generally assume that the 1:2 year recurrence interval flood event is the dominant channel forming flow event, and employ a design storm approach with focus on bed degradation, using hydraulic and sediment parameters averaged over a cross-section. These techniques have met with only limited success, and in some instances have resulted in the aggravation of instream erosion.

It is demonstrated that the greatest increase in erosion potential is associated with moderate flow events (recurrence interval less then 1:1.5 years). The importance of the bank toe stratigraphic unit is also explored using field observations of bank structure. The implication on design methodology is the need to address scour potential on a point by point basis about a channel perimeter to account for variations in material characteristics and bank structure relative to the change in flow geometry.

Channel response scenarios showing initial, intermediate and

long term channel form in response to an alteration in flow and sediment regimes are developed; wherein channel form is initially determined by the relative difference between the erodibility of the bed and least resistance bank toe stratigraphic units, and ultimately by the relative difference between sediment load characteristics and stream competence. Consequently, the degree of storage control must balance erosive and sedimentation processes to ensure long term stability.

These two process are incorporated into a proposed index of scour potential. The index compares sediment mass balance at a point on the channel periphery before and after development. Scour potential is addressed by creating a sub-index which is equated with excess shear potential. Integration of the sub-index with respect to time provides an index which is a measure of the temporal variation in erosion potential. It is argued that changes in erosion potential are minimized if the index is maintained constant with pre-development values. It follows that the channel should remain stable if the transverse distribution of the index is also maintained constant with the pre-development distribution.

The ability of the index to represent scour potential is demonstrated through a one to one correspondence between the rank of index values with a ranking of depths of degradation as predicted using a one-dimensional mobile bed model. Several bed load sediment transport relations based on excess shear stress concepts are evaluated as a basis for the estimation of mass balance. It is acknowledged that the relation used will vary with site specific conditions and user preference.

The proposed index method is used to explain variations in the success of existing design techniques. A procedure is then proposed for the development of flow criteria which would limit changes in flow geometry associated with urbanization by accounting for variations in boundary material resistance to scour about the channel perimeter. The method was applied to a case study involving a stream channel formed in cohesive sediments. In this case, it is predicted that erosion potential due to scour could be minimized by emphasising storage control for flow events of less than 1:1.5 year frequency while decreasing the relative degree of control for less frequent events. The amount of storage control required was found to vary with the resistance to scour of the least resistant bed or bank stratigraphic unit.

The proposed technique represents a more comprehensive approach to the design of storage facilities for the control of instream erosion potential. The demonstrated significance of critical peripheral parts, the need for multi-event evaluation, and the index represent contributions to the area of channel erosion protection.

I hereby declare that I am the sole author of this thesis. I further authorize the University of Ottawa to reproduce this thesis by photocopying or by other means, in total or in part, at the request of other institutions or individuals for the purpose of scholarly research.

Craig R. MacRae

TABLE OF CONTENTS

LIST OF TABLES

LIST OF FIGURES

GLOSSARY

A	area, m^2
a	constant
a	a characteristic length describing the size of the system, m
a	the y-intercept in a regression equation
a_1, a_2, a_3	are polynomial coefficients,
B	channel bottom width, m
BI	semi-perimeter cross-sectional width, m
b	a typical length of the flow pattern or scour geometry, m
b	exponent
b	slope of a regression line
b_1, b_2, b_3	are calibration coefficients,
C_{av}	average sediment concentration across the section, kg/m^3
C_c	coefficient of coagulation
C_o	coefficient of cohesion
D	depth, m
E_s	scour potential, kg/m
EVI	index based on DuBoy bed load relation, Pa
EXTAU	excess boundary shear stress indicator, Pa
F	width-depth ratio, m/m
$f(B)$	a mathematical representation of bed geometry
g	acceleration due to gravity, m/s^2
g(S)	denotes the upstream sediment supply rate, kg/m/s
h_ξ	scaling factor for ξ coordinate in the (x,ξ,η) coordinate system
h_η	scaling factor for orthogonal coordinate in the (x,ξ,η) coordinate system
k	coefficient characterizing the primary flow velocity distribution, equivalent to the Von Karman constant
L_x	length of the wetted perimeter, m
L	bed load transport, kg/s
LL	Liquid Limit, %
M	mass, kg
MP	point of maximum primary flow velocity
MPM	index based on Meyer-Peter Muller transport relation
m	a calibration coefficient,
N	number of depth increments,
NEVENT	number of flow events,
n	number of obserbations
n	exponent
n	nth depth increment
n	number of bed-bank stations
n	Manning's roughness coefficient
P	wetted perimeter, m

P_λ	sinuosity, m/m
PI	Plastic Index, %
PL	Plastic Limit, %
PS	stagnation pressure, Pa
PTOT	total precipitation, mm
PWR	index of shear power, Pa.m/s
p	volume of sediment per unit area of bed layer, m
Q	discharge, m^3/s
Q_o	the discharge rate at a the elevation of the boundary station, m^3/s
Q_p	peak discharge rate for a flow event, m^3/s
Q_s	the aggregate sediment transport potential for a flow event per unit stream width, kg/m
Q_{sv}	volumetric sediment transport rate, m^3/s
q_s	sediment discharge per unit stream width, kg/m/s
q_ℓ	lateral inflow rate, m^3/s
$q_{s\ell}$	lateral sediment input rate, kg/s
R	hydraulic radius, m
r	regression coefficient
r	vector in the (ξ,η) co-ordinate system,
S	slope, m/m
S_E	energy slope, m/m
S_f	friction slope, m/m
S_o	bed slope, m/m
SCORE	an index of resistance to scour
SD	standard deviation
T	time interval for an event beginning at time zero, hr
t	time, hr
u	primary flow velocity, m/s
V_ξ	ξ-component of the secondary flow velocity, m/s
v	primary flow velocity, m/s
v*	shear velocity, m/s
W	channel top width, m
W_R	ratio of post- to pre-development channel bankfull width
W_y	cumulative aggregate sediment transport potential, kg/m
w	channel width, m
wn	natural water content of the soil, %
X1	stickiness
X2	plasticity
X3	firmness
XLENGH	total longitudinal channel length, m
x	longitudinal distance, m
Y	dimensionless depth
YBED	height of the bed-bank station, m
YELV	the elveation of the bed, m
$YELV_o$	initial elevation of the bed, m
y	depth, m
Z	dimensionless transverse distance
ZBED	horizontal distance from y-axis through MP, m
ZDIST	distance between successive bed-bank stations, m
z	transverse distance from the y-axis, m

z_o starting bed elevation

α correction factor
α_f the angle of friction
β exponent characterizing the primary flow velocity distribution
φ the angle of inclination of the channel
γ specific weight of water and sediment,
γ_s specific weight of sediment,
γ_w specific weight of water,
σ the standard deviation of the particle size distribution
σ_x normal stress in the x-direction, N/m^2
θ the angle of the side slope,
ϵ coefficient describing the primary flow velocity distribution
η orthogonal trajectory to the isovels
ρ density of water, kg/m^3
ρ_s density of sediment, kg/m^3
υ kinematic viscosity, m^2/s
ξ curvilinear coordinate of the primary flow isovel
ξ_{MAX} maximum velocity ξ-curve value
ξ_o zero velocity ξ-curve value
τ boundary shear stress, Pa
τ_e excess boundary shear stress, Pa
τ_o instantaneous boundary shear stress, Pa
τXY xy-component of boundary shear stress, Pa
Ω total stream power, m.N/s
δI velocity coefficient in the z-direction
δY velocity coefficient in the y-direction
λ meander wavelength, m
ϕ particle diameter, mm

Subscripts

AGG aggregate
ALU alluvium
BED bed
BFL bankfull
BNK bank
CMP composite
CRT critical
EVL elevation
I in
INCR increment
MIN minimum
MAX maximum
O out
pop population data set
POST post-development
PRE pre-development

samp	sample data set
2YR	1:2 year recurrence interval

Abbreviations

ABS	absolute value
BML	bed material load
Cl	clay
CMP	composite
Est.	estimate
FUT	future
IDAY	current day
IMO	current month
IYR	current year
MID	mid bank stratigraphic unit
DRC	distributed runoff control
POST	post-development
PRE	pre-development
PRECIP	precipitation
RI	recurrence interval
Sa	Sand
Si	Silt
SSL	suspended sediment load
SWM	storm water management
TOE	bank toe stratigraphic unit
w/o	without

CHAPTER 1

PROBLEM DEFINITION AND RESEARCH OBJECTIVES

1.1 General

The effect of land use alteration on the flow regime may be generalized as a change in the natural storage of a catchment (McCuen, 1979). This alteration may result in an increase in both runoff volume and peak flow rate (Figure 1.1(a)). The associated increase in flood frequency has been shown to be non-uniform with the increase diminishing with return period (Hollis, 1975).

Case studies have demonstrated the potentially adverse effects of uncontrolled urban storm water runoff on stream channel form. The concepts of detention and retention were introduced in the form of Storm Water Management (SWM) measures to mitigate these impacts. This is achieved through the reduction of flow rates by storage routing effects (Figure 1.1(b) to (d)). Consequently, storage controls are central to most SWM policies.

In Canada, millions of dollars (primarily in Ontario, British Columbia and Alberta) have been spent and thousands of storm water management ponds have been built, to control instream erosion. While the incorporation of instream erosion control measures into SWM policy, objectives and criteria

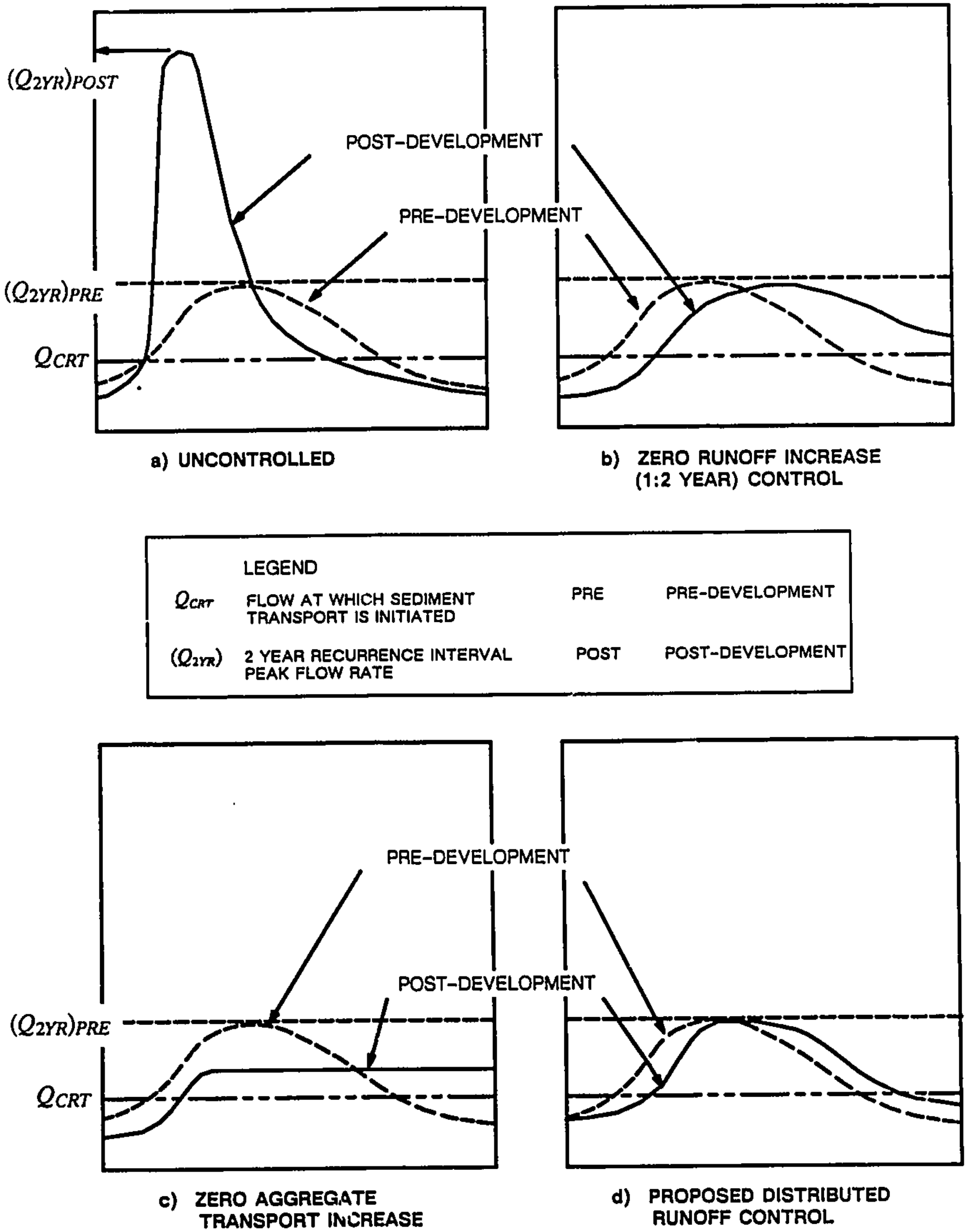

FIGURE 1.1 Comparison of Pre- and Post-Development 1:2 Year Hydrographs for Selected Control Methods

represents a significant step forward, these measures have met with limited success and in some cases, have resulted in the aggravation of instream erosion.

One of the principal concerns with these design methods is the exclusion of boundary material characteristics or the adoption of a one-dimensional approach to the estimation of scour potential. Observations of natural channels show that boundary material composition varies in both the transverse and longitudinal directions. Field observations have also shown that basal scour is the dominant mechanism controlling bank stability and channel form. This transverse variation in scour potential and the relative importance of bank erosion processes requires a three-dimensional modelling of the flow field. Consequently, a one-dimensional approximation of the channel system may not adequately describe scour potential.

A second concern is that current design methods use a design storm approach typically based on the channel forming significance of the 1:2 year flow, or a reproduction of the pre-development flood frequency curve for flows up to the 1:2 year event. However, instream erosion is a discontinuous but ongoing process which may not be sufficiently characterized by a single event approach. Further, the non-uniform increase in flood frequency may result in an increase in the channel forming importance of moderate or sub-bankfull flows.

Consequently, design methods which gradually increase storage control to a maximum at the 1:2 year level may under-control moderate flow events and hence, under-control scour potential.

The fact that SWM ponds do provide some positive benefit in terms of reducing instream erosion potential has been noted in two case studies, Upper Holmes Run in Fairfax County, Virginia (UHREMAC, 1987), and for streams in the District of Surrey, British Colombia (Lee and Ham, 1988). However, Upper Holmes Run was originally urbanized more than thirty years ago and the current development represents an "infilling". Consequently, stream morphology is that of an urban stream which has probably already undergone a significant transformation (enlargement and armouring) from its pre-development state.

The Surrey findings, one of the few Canadian studies, also reported significantly lower erosion rates for some urban streams with 1:5 year storage control in comparison to those developed without storage controls. They noted however, that channel widening, although reduced, still occurred in comparison to the control streams; and in some cases, there was no difference between basins with pond control and urbanized basins without storage control. No explanation was offered for this variation in performance. Further, a number of the streams were measured within five years of development and may not have come to an equilibrium condition. Misgivings regarding the effectiveness of SWM ponds on the control of instream erosion have also been noted elsewhere, (McCuen, 1979; Lorant, 1983 and 1988; Bishop and Mather, 1990).

It is apparent from these criticisms of current SWM criteria relating to the control of instream erosion potential that certain deficiencies exist and that analysis techniques based on these criteria may not adequately meet the intent of SWM. The major criticisms in the literature are focused primarily on event duration. The proposed solution is to increase storage control uniformly for all events up to the 1:2 year flow. However, without accounting for the transverse distribution of material resistance, this may result in excessive control and channel instability through aggradation. A systematic procedure is required for the development of control criteria which addresses the vagaries of boundary material composition and structure in terms of the alteration of flow geometry associated with urban development.

1.2 Research Objectives

Selected government agencies, municipalities, universities and consulting firms across Canada and the United States were surveyed by telephone and in person as part of this research.

It was apparent from this survey that while the need for better data collection, analytical tools, and design methods is widely recognized, very little baseline data collection or research is currently in progress.

The objective of this research is to develop a procedure for the derivation of flow criteria which would limit changes in flow geometry and the erosion potential associated with urbanization. This would require establishing;

a) the effect of urbanization on channel forming flows,

b) the significance of the transverse variation of boundary material characteristics and bank structure,

c) the development of a cumulative transversely variable index which incorporates temporal and spatial variations in the flow field and material characteristics as a means for the assessment of instream erosion potential; and,

d) the incorporation of this index into a procedure for the determination of design criteria.

The affect of urbanization on channel forming flows was investigated by dividing the channel into a number of sequential depth increments. Secondly, the flow series was segregated into individual events and the sediment transport potential was calculated for each event. The sediment transport potential for each event was then assigned to the maximum depth increment attained by the event. This was repeated for all events in the flow series until it had been translated into a sediment transport potential by increment of depth. By comparing the change in this distribution it is possible to evaluate the affect of the non-uniform increase in flood frequency on the flow field in terms of potential for scour. This analysis was carried out using a case study for which geodetic, geotechnical and hydrologic data were available.

The significance of the transverse variation in boundary materials was investigated through a field survey of seven streams in Surrey, British Columbia. The resistance to scour was evaluated for each stratigraphic unit and correlated with the increase in post-development channel width to determine the significance of material properties and bank structure. The analysis was carried out to establish the need to evaluate erosion potential on a point by point basis.

An index of erosion potential at a point along the channel boundary was derived by applying established shear stress and threshold concepts to a pre- versus post-development sediment mass balance approach through a control reach. The index was then compared to a mobile bed sediment transport model for validation.

Channel response scenarios were developed as a basis for the need to integrate the index through time and space to arrive at a sub-index which is a cumulative, transversely variable measure of scour potential. It is argued that if the magnitude of the index is maintained, then the change in scour potential is minimized. It follows that if the distribution of the sub-index is maintained then channel instability introduced as a consequence of urbanization will also be minimized.

The index method was used to develop a procedure for the determination of design criteria for storage ponds. The procedure was applied to evaluate existing design techniques and a proposed control procedure.

There are many existing theories on the hydraulic transport of sediment but none of these are well integrated into design practice. The primary area of research contribution in this work is the development of an index representing scour potential and the incorporation of this index into a design methodology for practical application to current Stormwater Management problems. This work also integrates a number of disciplines and provides insight into the prediction of channel response to an alteration in the factors determining channel form.

CHAPTER 2

LITERATURE REVIEW

2.1 Introduction

This chapter provides a review of literature dealing with,

a) an interpretation of case studies documenting the impact of urbanization on channel morphology in terms of current qualitative predictive models (Section 2.2);

b) a discussion of stream bank erosion processes (Section 2.3);

c) a review of current approaches to the mathematical modelling of bank erosion (Section 2.4);

d) a review of current methods for the design of storage ponds for the control of instream erosion hazard (Section 2.6), and the fundamental river engineering concepts upon which they are based (Section 2.5); and,

e) the rational and applicability of environmental indices for use in design procedures for instream erosion control (Section 2.7).

Section 2.8 provides a summary of the principle findings from this review.

2.2 Urbanization And Channel Morphology

The hypothesis that natural channels enlarge as a result of increased flows following urbanization was tested by Hollis and Luckett (1976) for 32 rural and 27 urban basins in West

Sussex and Canon's Brook, Harlow, Essex, England. Various measures of central tendency indicated that an increase in channel size could not be confirmed by a difference in means test suited to paired observations, even after an 18 percent paving of the basin. In some cases they observed a decrease in channel cross-sectional area similar to that reported by Leopold (1973) for Watts Branch.

Despite these studies to the contrary, most case studies of watersheds in which drainage controls were not applied, have shown channel enlargement to follow urbanization (Savini and Krammerer, 1961; Mansue and Anderson, 1974; Gregory and Walling, 1973; Keller, 1962; Guy and Ferguson, 1962; Hammer, 1972; Graf, 1975; Lazar, 1978; Allen and Narramore, 1985; Lee and Ham, 1988; Urbonas, 1980 and 1988). Wolman (1967) in a major treatise on the subject concluded that the,

> "process of urbanization constitutes a major disruption of prevailing conditions on a watershed".

Using geomorphic evidence to support his theory Wolman offered the following scenario,

a) construction results in aggradation leading to a choking of the stream channel, and

b) following development flows increase in rate and volume while sediment loads actually decrease as the surface becomes more impervious and the remaining denuded areas are stabilized with vegetation.

In Wolman's first stage of urbanization, aggradation may destabilize the active channel leading to the development of a new ultimate channel form characterized by "sedimentation patterns", (Brotherton, 1979). In the second stage, Morisawa and LaFlure (1979) hypothesized the increase in direct runoff from the urbanizing upland area, results in an increase in stream discharge and in turn instream flow velocities. Stream competence increases proportionately resulting in channel enlargement through widening, deepening or both as governed by local bed-bank characteristics (Brotherton, 1979).

The apparent discrepancy between the Hollis and Luckett (1976) and Leopold (1973) studies and those studies that support the hypothesis that urban development results in morphologic change may be explained in terms of the degree of change in sediment supply and competence in the receiver. Figure 2.1 was constructed as part of this thesis to summarize the principal factors listed in the above studies and how these factors relate to channel change.

Land use alteration in the upland zone modifies the sediment and hydrologic regimes. The degree of impact will increase;

a) as the areal extent of urban development increases in portion to the total basin area;

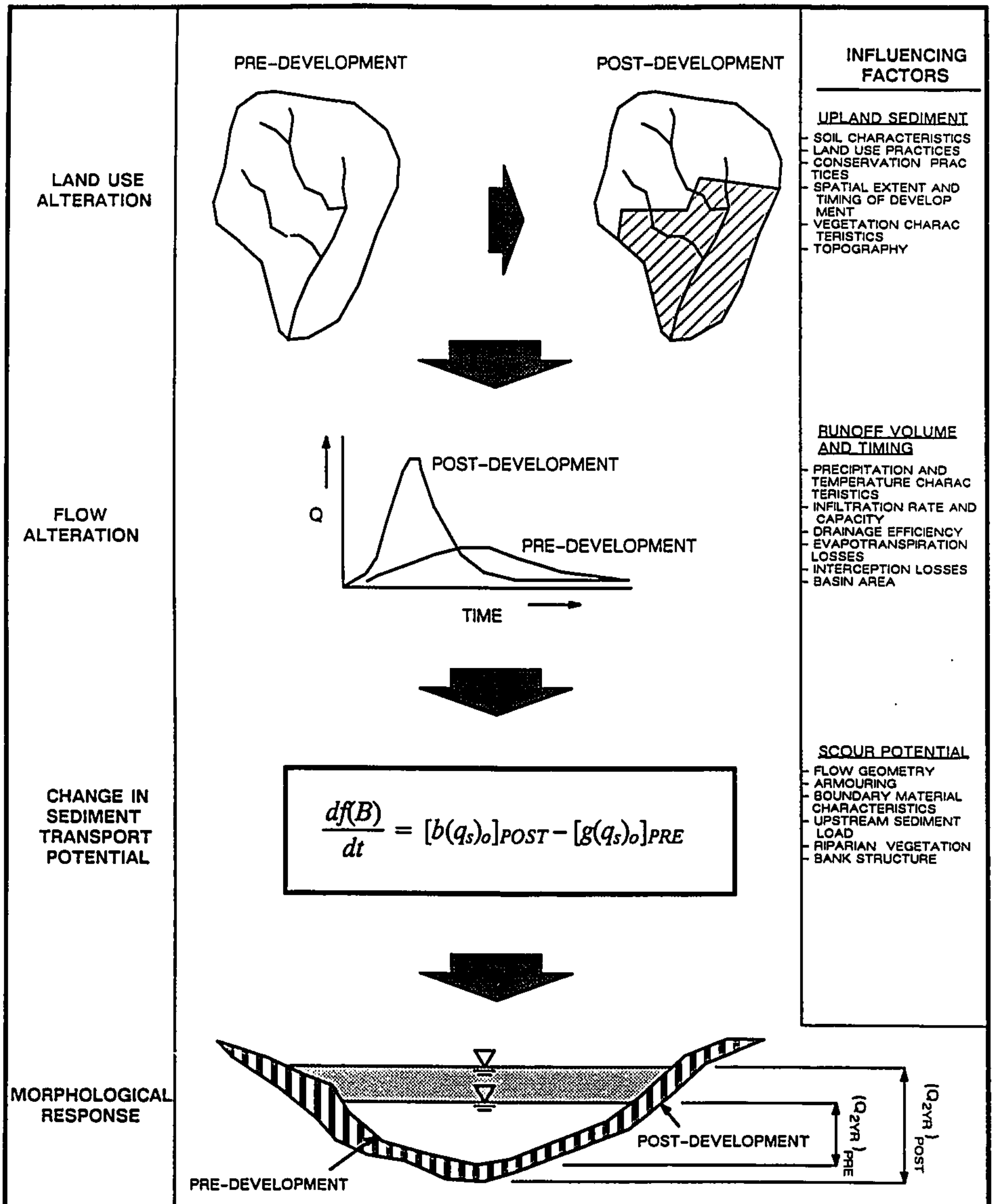

FIGURE 2.1 Schematic Overview of Channel Response to Urban Development

b) with the greatest change in surface storage characteristics, i.e. the transformation of agricultural land to low density estate residential land use on clay soils has less impact on flows then high density residential/commercial developments on sandy soils;

c) with the orientation of the spatial distribution of urban development such that stream flow rates are increased (analogous to wave interference in physics);

d) as the resistance of the channel boundary materials to scour decreases;

e) as the ability of the stream channel to adjust its plane form decreases;

f) with the physical characteristics of the upland sediment load; and,

g) as a function of the type and density of riparian vegetation.

Given these factors it may be possible that development could occur in a manner which,

a) has no net change in stream competence or sediment load and consequently no net impact on channel morphology, i.e. the erosive potential of increased flow volume is offset by a reduction in peak flows associate with a change in flow timing due to the spatial distribution of urban development (Figure 2.2 (a));

b) shows a net reduction in channel cross-section area due to a decrease in stream competence (Figure 2.2 (b)), i.e. the conversion of cropland on clay soils to low density estate residential land use; and,

c) shows a net increase in channel cross-section area resulting from a net increase in stream competence or aggradation, (Figure 2.2 (c)), i.e. a significant decrease in surface storage resulting in an increase in runoff volume and flow rate or a net increase in sediment supply over stream competence.

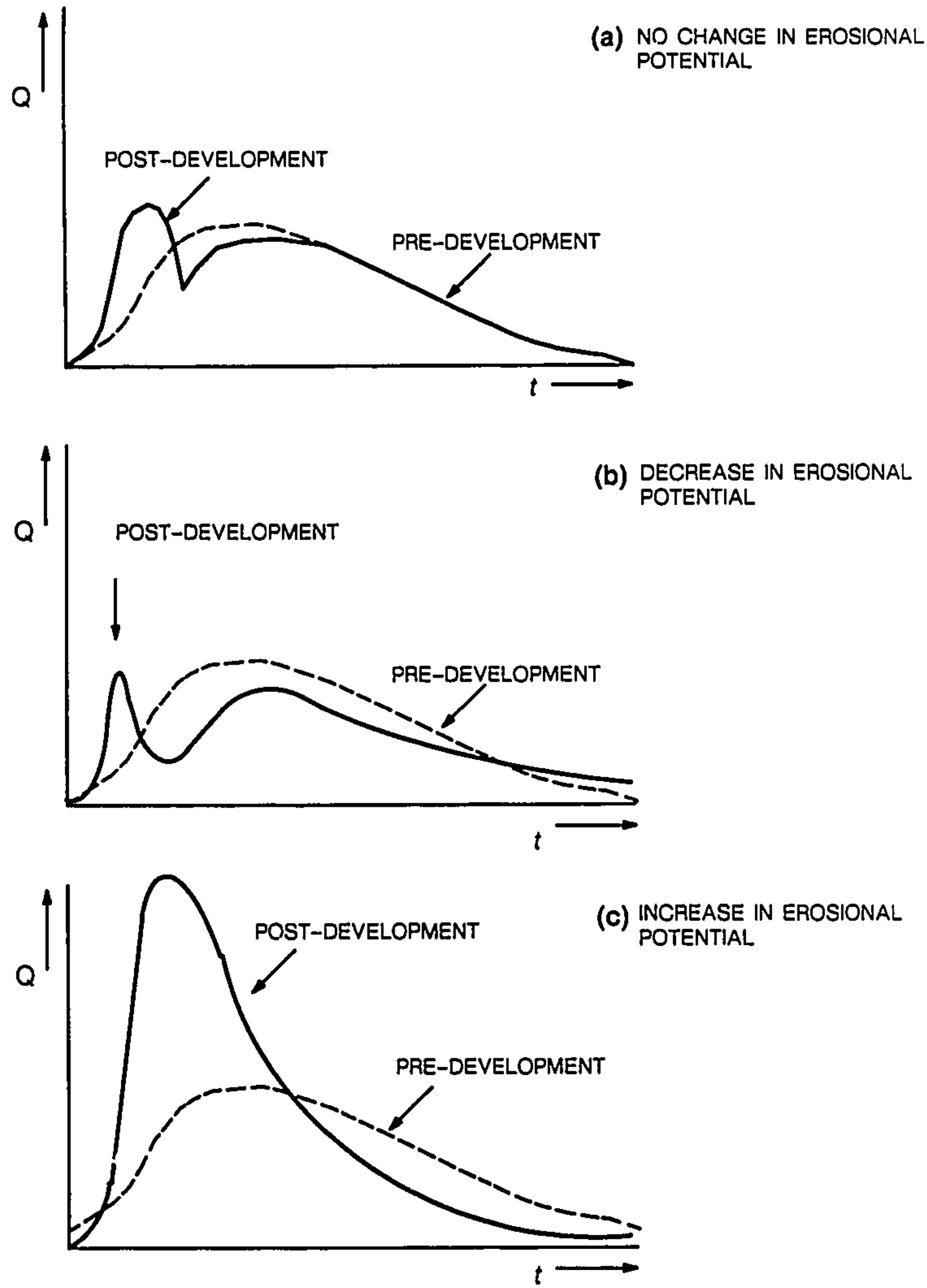

FIGURE 2.2 Possible Hydrograph Responses to Different Development and Physical Conditions.

Initially only flow depth and roughness may respond to a change in the sediment and flow regimes (Andrews, 1979). These variables tend to respond rapidly and throughout the adjustment period. Perceptible alterations in channel hydraulic geometry may not occur until after approximately a twenty percent paving of the basin (Morisawa and LaFlure, 1979; Figure 2.3). The adjustment of channel width also tends to occur over a number of years (Andrews, 1979). It is generally felt that 7 to 10 years is required for channel width to approach a new quasi-equilibrium (Lee pers. comm., 1990; Mather pers. comm., 1990). Longitudinal channel slope may adjust over 10^2 to 10^3 years assuming relative constancy in the independent variables (Andrews, 1979).

The above case studies, although somewhat contradictory, are consistent with the Morisawa and LaFlure hypothesis concerning stream competence. They are also consistent with current empirically derived relations for stable channels concerning channel response to changes in discharge and sediment load.

Simons and Li (1982) and Chorley et al., (1984) provide a synthesis of a number of empirical studies which resulted in the development of two simple relations illustrating the relationship between discharge (Q), bed load transport (L),

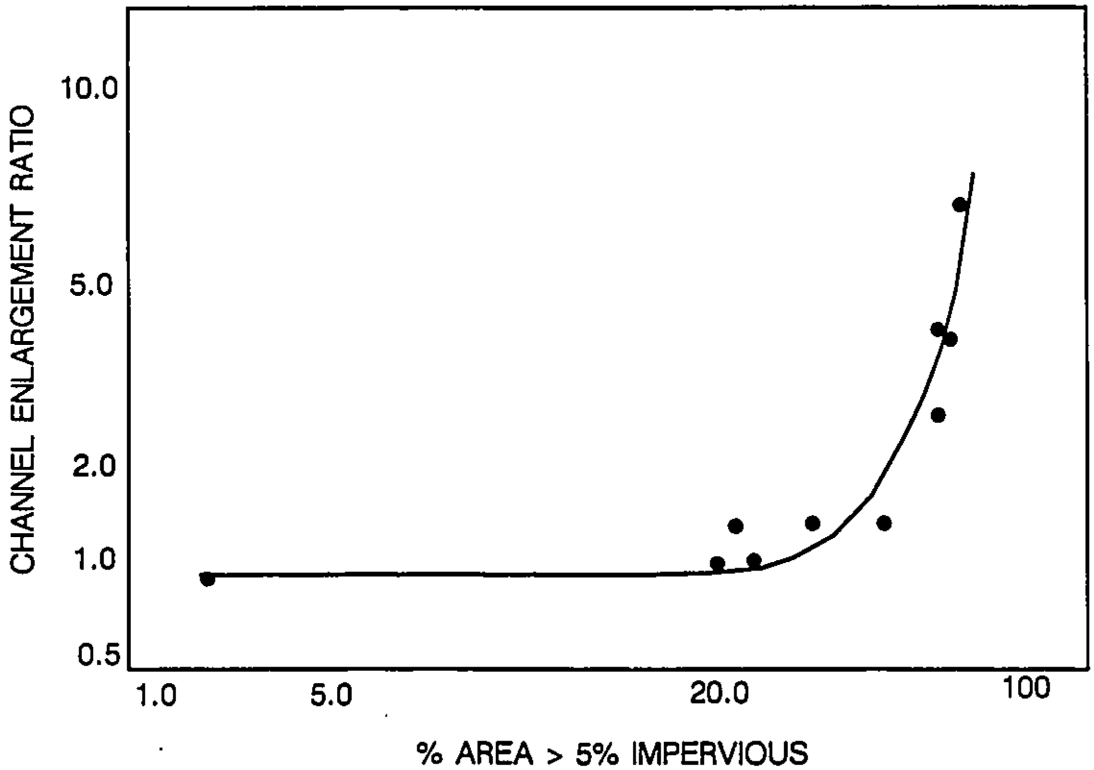

FIGURE 2.3 Channel Enlargement Ratio as a Function of Percentage of Area Greater Than 5% Impervious,
(M. Morisawa and E. LaFlure, 1979)

$$Q = \frac{(w, y, \lambda)}{S} \qquad [2.1]$$

and related measures of stream plane and cross-sectional form,

$$L \doteq \frac{(w, \lambda, S, F)}{(y, P_\lambda)} \qquad [2.2]$$

in which, w = channel width,
y = channel depth,
λ = meander wavelength,
S = slope,
P_λ = sinuosity, and
F = width-depth ratio.

These relations may be used to describe the effect of an alteration in either discharge or sediment load by using a "plus" or "minus" to indicate how the various parameters respond to an alteration in Q or L. For the relatively straightforward cases of a change in either discharge or bed material alone,

$$L+ = w+,\ y-,\ \lambda+,\ S+,\ P_\lambda-,\ F+ \qquad [2.3]$$

$$L- = w-,\ y+,\ \lambda-,\ S-,\ P_\lambda+,\ F- \qquad [2.4]$$

$$Q- = w-,\ y-,\ \lambda-,\ S+ \qquad [2.5]$$

$$Q+ = w+,\ y+,\ \lambda+,\ S- \qquad [2.6]$$

An increase in L alone, as shown in Eqn. 2.3, may correspond to the initial stages of development wherein large tracts of land are denuded and disrupted by construction activity resulting in high upland sediment yields. After revegetation of the urbanized surface sediment yield may decrease to near or slightly below pre-development levels (Wolman, 1967; Eqn. 2.4). Simultaneously, urban development may result in a net decrease (Eqn. 2.5), no net change, or a net increase in discharge (Eqn. 2.6) as described in Section 2.2. A net decrease in Q (L held constant) would result in a decrease in channel width and depth as observed by Hollis and Luckett (1976) and Leopold, (1973). A net increase in Q (L held constant) would result in the net increase in channel width and depth as noted in the remaining case studies reported above.

It is probable that an alteration in both Q and L would occur simultaneously. Using the same "plus" and "minus" system to describe the change in a variable, four combinations of changing discharge and sediment load can be considered,

$$Q+,\ L+ = w+,\ y+/-,\ \lambda+,\ S+/-,\ P_{\lambda}-,\ F+ \qquad [2.7]$$

$$Q-,\ L- = w-,\ y+/-,\ \lambda-,\ S+/-,\ P_{\lambda}+,\ F- \qquad [2.8]$$

$$Q+,\ L- = w+/-,\ y+,\ \lambda+/-,\ S-,\ P_{\lambda}+,\ F- \qquad [2.9]$$

$$Q-,\ L+ = w+/-,\ y-,\ \lambda+/-,\ S+,\ P_{\lambda}-,\ F+ \qquad [2.10]$$

Equation 2.7 may represent a situation of progressive or staged development wherein portions of the basin are developed while other regions are under construction. Equations 2.8 and 2.9 may represent a situation resulting from the imposition of Storm Water Management (SWM) controls. Equation 2.9 may also reflect a final development scenario wherein the pre-development land use produced relatively high sediment loadings from the upland area, i.e. intensive mechanical cultivation of silty soils on high gradients with poor conservation practices in comparison with a stabilized post-development land use. Equation 2.10 is perhaps the least likely of the possible scenarios although it may represent a transition period wherein the developed portion of the basin is under SWM controls while other regions are in the construction phase.

While these relations are useful as an aid to the interpretation of channel response, they are qualitative and do not explicitly account for the processes controlling bed and bank erosion. Consequently, they are limited in their use for impact assessment. They do, however, illustrate the complex feedback mechanisms operative in a process-response system as defined by an alluvial stream channel.

2.3 Bank Erosion Processes

Bank erosion is a highly spatially and temporally variable phenomenon. Leopold et al, (1964), Thorne (1978; 1982; 1988), and Simons and Li (1982) provide descriptions and classification of river bank processes which include a combination of mechanical, biological and chemical mechanisms. Mechanical processes can be differentiated into non-fluvial and fluvial processes which may be distinguished in the field on the basis of meso scale channel forms (Lewin, 1978; Appendix A). The later processes consist essentially of the scouring action created by the shear stress exerted by the flow and sediment mixture on the bed and banks.

Non-fluvial processes such as frost action (Pitty, 1971) and other complicating factors such as sapping and piping (Haggerty et al., 1986), pore water pressure (Twidale, 1964), and vegetal effects (Simons and Li, 1982) are significant factors in determining bank stability. However, process-form interpretations (Wolman, 1959; Leopold et al., 1964; Simons and Li, 1982; Hooke, 1979; Harvey and Watson, 1986) have shown that dislodgement of boundary material by the shearing action of the sediment and water mixture to be the dominant bed erosion process producing bank failure by mass movement due to basal scour (Thorne and Lewin, 1982; Yu and Wolman, 1986;

Richards and Lorriman, 1987).

The actual bank failure mechanisms (i.e. sloughing, solifluction, and/or block, cantilever, or rotational failure), depend upon bank structure, groundwater behaviour and the geotechnical properties of the bank materials (Partheniades and Paaswell, 1970; Vanoni, 1975; Thorne, 1978; Thorne and Lewin, 1982; Simons and Li, 1982; Richards and Lorriman, 1987). Yu and Wolman (1986) describe a typical stream bank erosion scenario as the occurrence of slides and slumps primarily along the concave meander bend. These mass failures are due to a combination of over steepening of the channel bank through basal scour, which undercuts the bank laterally, and by downcutting, which is referred to as valley formation.

Undercut banks typically experience shear, beam or tensile failure of cantilever overhangs (Figure 2.4). In such cases, the rate of bank failure (recession of the top of bank through time) is related to the rate of basal scour, which is in excess of rates attributed to either weathering or changes in pore water pressure (Richards and Lorriman, 1987).

Slumps of active stream channel banks are typically associated with the exceedence of threshold slopes due to downcutting (Figure 2.4). In this case, the active control of

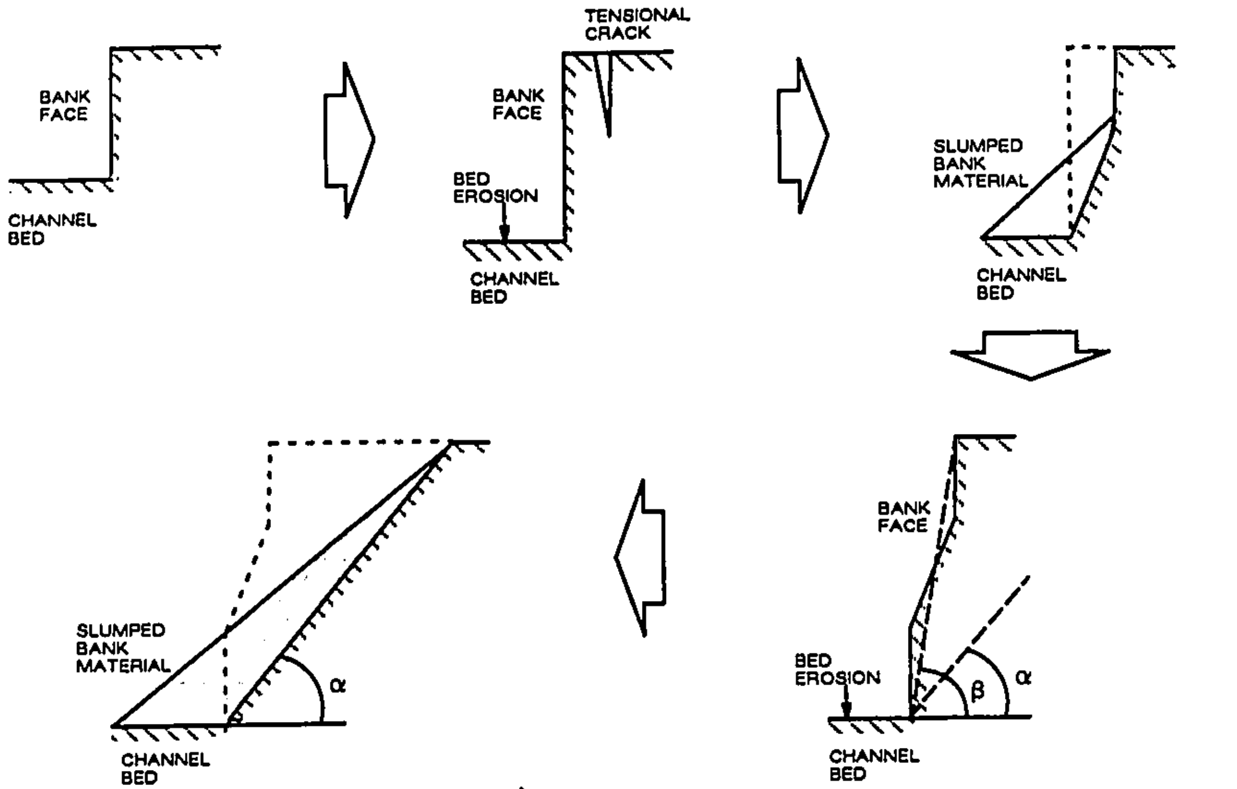

a) Hypothetical sequence of loess slope failure caused by downcutting

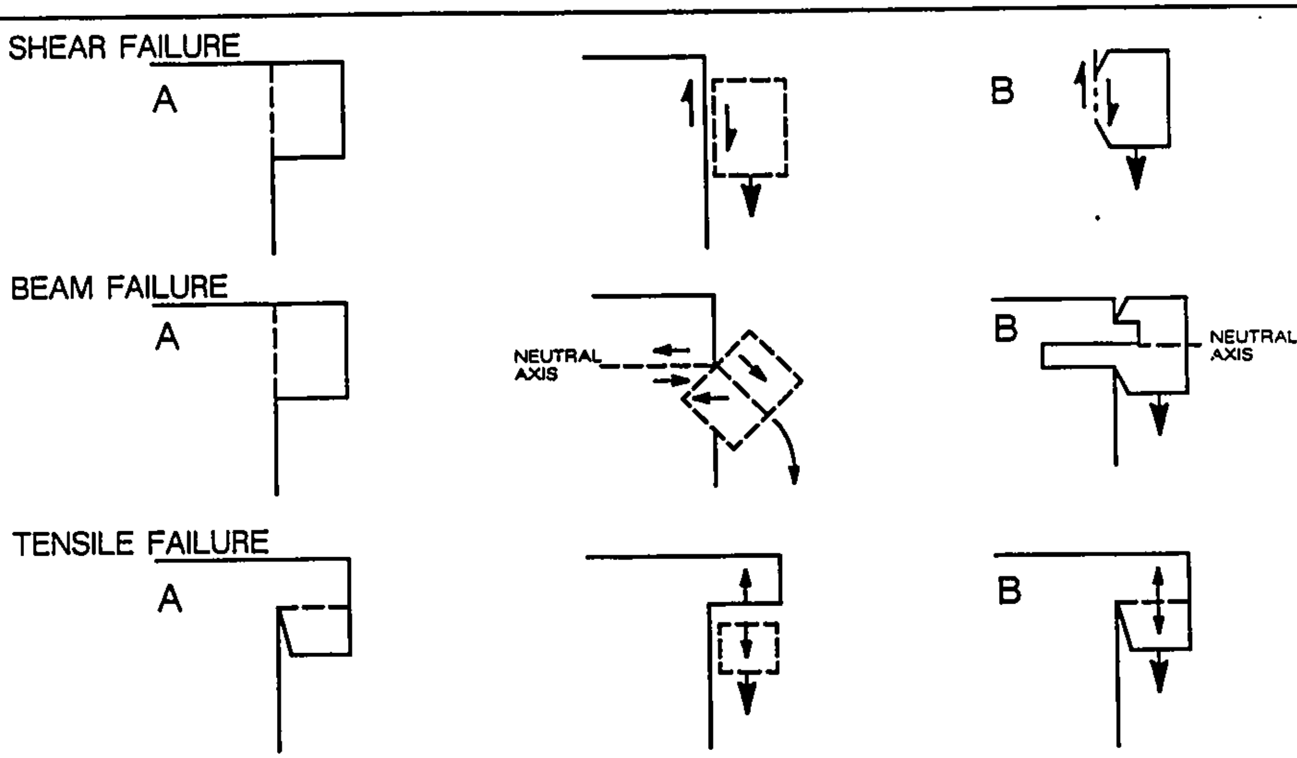

b) Definition diagrams for shear, beam and tensile failures of cantilever overhangs formed by basal undercutting

FIGURE 2.4 Schematic of Principal Slope Failure Mechanisms (Richards and Lorriman, 1987)

bank stability is the rate of weathering and changes in pore water pressure. The bank slope angle reflects the mechanical properties of the bank material and the degree of consolidation. In both undercutting and downcutting failures, the stratigraphy and lithology of the eroding slope are important considerations in determining the cyclic failure-stabilization process and relationships between short and long term slope behaviour (Richards and Lorriman, 1987). Differences in bank structure may be the cause for the disposition of a stream to actively undercut one bank while depositing floodplain sediment and colluvium on the other (Brotherton, 1979; Richards and Lorriman, 1987). The result is an asymmetric channel cross-sectional form with contrasting bank slopes (Strahler, 1950).

Yu and Wolman (1986) and PLUARG (1977) note that rivers have two major sediment sources, from erosion of the land surface (upland area), and erosion of river channel banks. They also noted that bank erosion constitutes in the order of one half of the total annual sediment load with the other half attributed to upland sources. This means that sediment supply from bed erosion is of secondary order in magnitude in comparison to bank erosion. This concurs with findings by Hooke (1979), Thorne and Lewin (1982), Simons and Li (1982), Yu and Wolman (1986), Haggerty et al., (1986), Harvey and Watson (1986), and Richards and Lorriman (1987), reporting slides due to bank undercutting as the dominant bank failure mechanism. Bank material resistance to scour consequently, is a major factor influencing channel form.

Boundary materials are typically divided into non-cohesive or cohesive sediments. The erosive characteristics of cohesive soils are controlled by electrochemical forces while non-cohesive or granular soils are controlled by gravity forces (Flaxman, 1963; Parthenides and Paaswell, 1970; Craig, 1987; Vanoni, 1975; LeFebvre, 1986). Koechlin (1924), Lane (1955) and Scheidegger (1961) have derived a stable sand channel of transverse form consistent with flume studies for non-cohesive sands under steady flow conditions, by equating gravitational and shear forces associated with fluid flow to the resistance of the boundary materials. There are, of course, few channels composed entirely of uniform, non-cohesive materials which convey a constant discharge. However, the similarity between idealized and laboratory channel forms points to the merit of using a spatially variable distribution of boundary shear stress and material properties as a means to explain changes in channel form (Davies, 1987). As noted by Leopold et al., (1964).

> "Because the flow exerts a shear stress upon the bed and banks, one "adjusted" or stable form which the channel can assume is one in which the shear stress at every point on the perimeter of the channel is just balanced by the resisting stress of the bed or bank at each point".

White (1940) derived a method for the estimation of the initiation of movement for non-cohesive particles. This technique balanced the drag force and grain weight moments acting on a spherical particle on a horizontal surface, about a fulcrum at its contact point with a downstream grain. White's balance of forces has been extended to the case of an inclined bed and expressed in terms of the critical shear stress,

$$\tau_{CRT} = (1-\gamma_s)Mg(\cos\varphi\tan\alpha-\sin\varphi) \qquad [2.11]$$

in which, τ_{CRT} = critical shear stress,
γ_s = specific weight of the boundary material,
M = the mass of an individual particle,
g = acceleration due to gravity
φ = the angle of inclination of the channel, and
α = the angle of friction.

In addition to the shear stress, a particle on the bank is subject to a component of gravitational force. In still water (Figure 2.5 (a)), the equilibrium of the particle is maintained by a balance between its submerged weight and inter-particulate friction,

$$(1-\gamma_s)Mg\sin\theta = (1-\gamma_s)Mg\cos\theta\tan\alpha \qquad [2.12]$$

where, $\tan\alpha$ = the coefficient of friction equal to the tangent of the angle of repose, and
θ = the angle of the side slope.

When water is moving along the bank, then stability of the particle requires a balance between a component of its

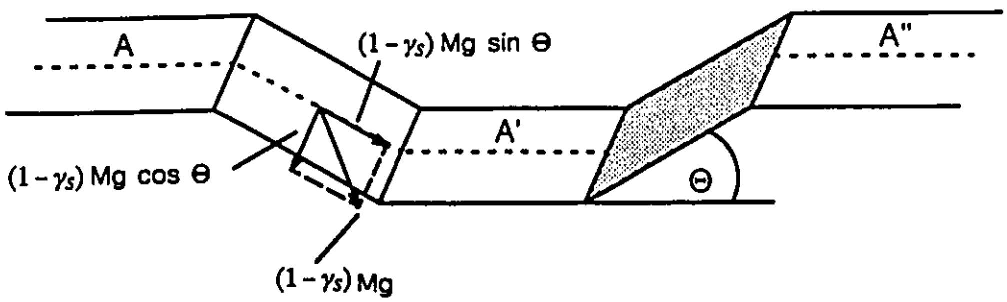

A) Force diagram in plane AA'A" perpendicular to cross section

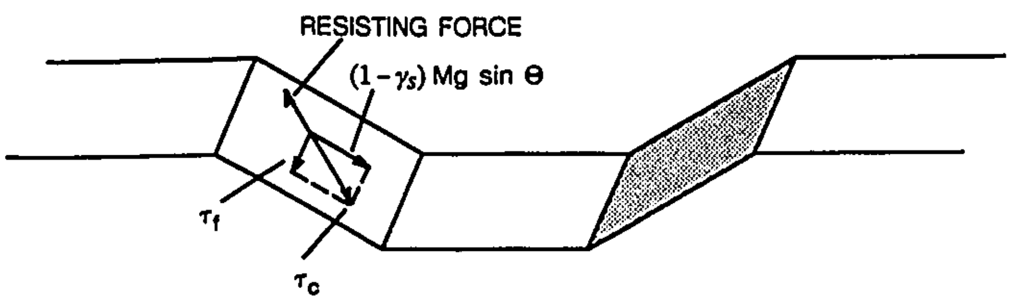

B) Force diagram in plane of sloping side of channel

FIGURE 2.5 Resolution of Forces on Submerged Particle on Sloping Channel Bank: A – No Flow. B – Flow (Leopold et al., 1964)

immersed weight and the fluid shear and gravitational forces acting on the particle (Figure 2.5 (b)). A channel which simultaneously satisfies flow and stability is referred to as a "threshold" channel (Henderson, 1961).

Vanoni (1975), using dimensional analyses and work on scour by jets by Laursen (1952) and Tarapore (1956), confirmed that scour at any point is caused by local shear stress generated by the flow velocity near that point in relation to τ_{crt}. Further, bed shear stress is a function of flow geometry and will vary with flow pattern through time and space. This means that a three-dimensional understanding of the flow field is required to properly evaluate boundary scour. Finally, Graf (1971) and Vanoni (1975) noted that for loose, non-cohesive sediments the function,

$$\tau_{crt} = f(\phi) \qquad [2.13]$$

in which ϕ, the particle diameter, was sufficient to describe the sediment.

The above analyses do not however, account for the cohesive properties of boundary sediments, heterogeneities in structure, or other influencing factors such as vegetal binding and groundwater movement. All of these factors introduce additional complexities into the relationship between the erosive forces inherent in the flow and the resistive properties of the soil particles. The property of cohesion was incorporated into the determination of threshold shear stress for cohesive sediments by Graf (1971) through a coefficient of cohesion,

$$\tau_{crt} = f(C_o, \phi) \qquad [2.14]$$

in which C_o is the coefficient of cohesion.

Gibbs (1962) suggested a trend in the erosion characteristics of fine grained cohesive material based on the Plastic Index (Figure 2.6),

$$PI = PL - LL \qquad [2.15]$$

where, PI = Plastic Index,
PL = Plastic Limit, and
LL = Liquid Limit.

as defined by Atterberg limits. Referring to Figure 2.6, Holtz and Kovacs (1981) note that for soils of equal Liquid Limit: toughness and dry strength increase with Plastic Index. Flaxman (1963), however, observed that some natural channels with sediments of low or negligible Plastic Index were stable and therefore resistant to scour. This indicates that Plastic Index alone may not be sufficient to indicate resistance to scour (Vanoni, 1975). Flaxman (1963), noted that a correlation

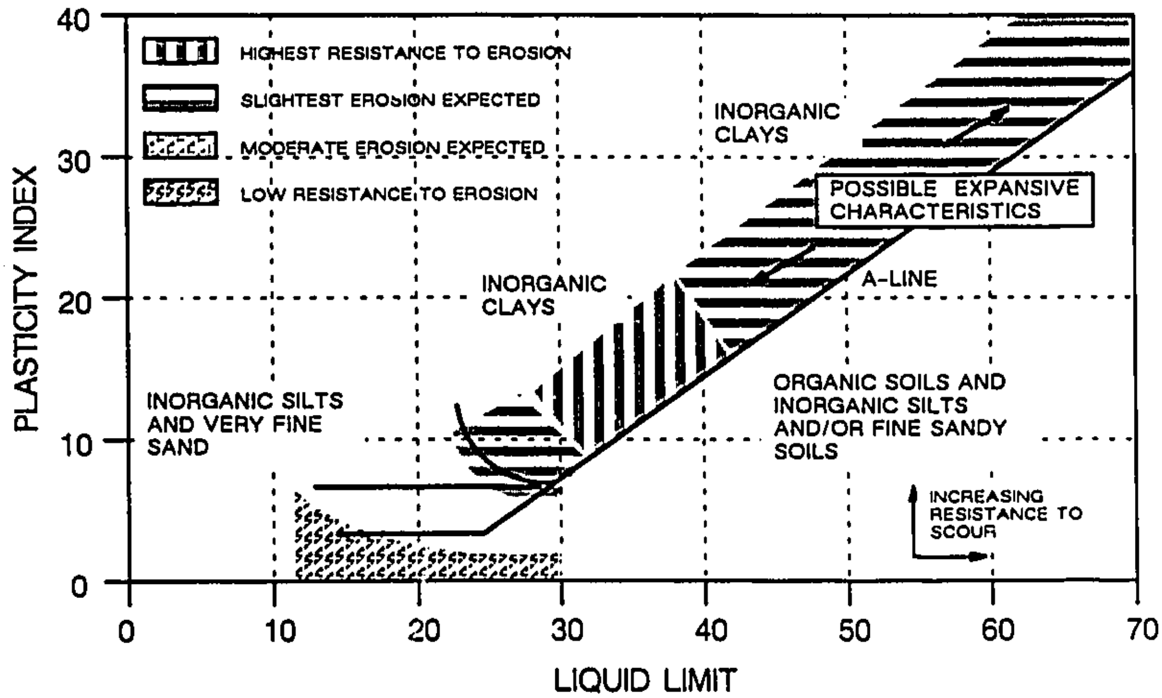

FIGURE 2.6 Suggested Trend of Erosion Characteristics for Fine-Grained Cohesive Soils with Respect to Plasticity (Gibbs, 1962)

existed between material resistance to scour an unconfined compressive strength.

Mirtskulava (1966) and Paaswell (1973), observed that aged and consolidated clay materials tend to erode as aggregates rather than at the particle level. Einsele et al., (1974), observed in laboratory studies, that only homogeneous clay materials erode at a particle level. Heterogeneous clay materials with discontinuities or planes of weakness tend to erode in chunks. This was supported by laboratory studies of intact natural unweathered clays from Eastern Canada by Rohan et al., (1980). These and additional studies lead Lefebvre and Rohan (1986), to conclude that another factor (referred to as the "structuration" of intact clay materials over time), significantly increased their resistance to scour.

Flaxman (1963), reported values of 11.5 Pa $\leq \tau_{CRT} \leq$ 72 Pa for intact cohesive sediments from natural channels. Lefebvre et al, (1985) reported values of 3.0 Pa $\leq \tau_{CRT} \leq$ 12 Pa for soft clays, 12.0 Pa $\leq \tau_{CRT} \leq$ 22 Pa for stiff clays, and 22.0 Pa $\leq \tau_{CRT} \leq$ 140 Pa for very stiff clay. In some instances $\tau_{CRT} \geq$ 140 Pa. For reworked samples, Dunn (1959) reported values of 5.7 Pa $\leq \tau_{CRT} \leq$ 23.5 Pa for materials ranging from sands to silty clay. Smerdon and Beasley (1961) reported values of 0.4 Pa $\leq \tau_{CRT} \leq$ 4.3 Pa for reworked cohesive sediments in clear water flume experiments. Suspended sediment concentrations, however, can significantly increase threshold conditions. Vanoni (1975) noted a three fold increase in permissible tractive force in flows having a high sediment concentration as opposed to clear water observations.

The importance of structure, mineralogy and consolidation on scour potential have been recognized as noted above. The variation in these factors, although noted by Thorne and Lewin (1982), Simons and Li (1982), Hagerty et al., (1986), and Richards and Lorriman (1987) have not been incorporated into current methods for the design of erosion control facilities.

2.4 Modelling Approaches To Bank Erosion

Sediment transport theory attempts to account for degradation of the bed through scouring and aggradation of the bed from sediment settling. Harvey and Watson, (1986) state that bed degradation usually precedes and predisposes channel widening, as the incised channel triggers increased mass wasting. This is not necessarily the case. Changes in hydraulic geometry are accomplished by both bed and bank erosion in response to,

a) a reduction in sediment supply in comparison to stream competence (bank erosion and/or degradation), or

b) an increase in sediment supply in comparison to stream competence (aggradation and bank erosion).

(Brotherton, 1979). In both cases however, channel widening occurs in response to a net change in bed elevation which is determined from a mass sediment balance.

It is generally accepted that no alluvial bed would be stable over the entire range of discharges experienced but that the fluctuating changes in bed elevation may be considered stable by relating bed stability to channel stability (Blench, 1951). These short term fluctuations in bed elevation are principally due to the build up and destruction of meso scale bedforms and not necessarily degradation of the underlying, intact bed. They typify the quasi-equilibrium defined by regime theory (Leopold et al., 1964). Long term changes in bed profile however, will correspond to progressive alteration of stream channel form (Bogardi, 1974; ASCE, 1982).

Mathematical models have been developed as a means to analyze transients or long term river flows and the corresponding changes in channel form if its hydrograph or sediment supply were altered through land use modification or other means. A listing of selected models is provided in Table 2.1.

In general mathematical simulation models are used to route water and sediment through an alluvial channel. The model must predict in space and time the transport rate for sediment, and the change in channel geometry resulting from aggradation or degradation of the bed and erosion of the banks. In some cases, these mobile-boundary models include the simulation of unsteady flow phenomena and the additional considerations that channel bed form and elevation, channel width, and river planform geometry are also dependent parameters that vary with time. Evaluations of these models and the relations upon which they are based is provided by Dawdy and Vanoni (1986), Kirishnappan, (1985) and Morse and Townsend (1988).

Table 2.1
Mobile Bed Sediment Transport Models

Model	Reference
MOBED	Krishnappan, (1981)
HEC-6	Hydraulic Engineering Center, (1977)
HEC-2SR	National Research Council, (1983)
KUWASER	Simons et al., (1979)
UUWSR	National Research Council, (1983)
FLUVIAL-3	Chang, (1982)
FLUVIAL-11	Chang, (1984)
IALLUVIAL	Karim and Kennedy, (1982)
USGS-1	Mengis, (1981)
USGS-2	Katzer and Bennett, (1983)
SED-4H	National Research Council, (1983)

Despite recent advances made in numerical methods, a study by the National Research Council, (1983) listed a number of deficiencies in current model approaches:

a) unreliable sediment transport functions;

b) inadequate understanding and formulation of bed armouring and its implications on sediment transport and the friction factor;

c) inadequate formulation of the friction factor for erodible channels; and,

d) inadequate understanding and formulation of bank erosion mechanics.

The inability to indicate the exact ways in which channel geometry may evolve (the relationship between bed and bank scour), has resulted in the separation of bank and bed processes with most models dealing exclusively with bed scour. These are typically one-dimensional models, some of which may distribute the amount of scour or deposition over the cross-section (bed) using a uniform distribution or a distribution based on the transverse distribution of stream capacity calculated from flow depth.

The approach upon which these models are based is essentially a sediment continuity approach proposed by Laursen (1952), in which the rate of scour may be expressed as the difference between the capacity for transport out of the scour area and the influx or rate of supply of sediment to the area. This principle may be expressed as,

$$\frac{df(B)}{dt} = g(q_s)_O - g(q_s)_I \qquad [2.16]$$

where, $f(B)$ = the mathematical description of the bed,
$g(q_s)_O$ = the sediment discharge or transport rate out

of the scour zone, and

$g(q_s)_l$ = the rate of sediment supply to the scour zone.

In simplistic terms, if the local rate of transport exceeds the rate of supply, then

$$\frac{df(B)}{dt} > 0 \qquad [2.17]$$

and scour will occur. Conversely, when

$$\frac{df(B)}{dt} < 0 \qquad [2.18]$$

deposition will occur. Finally, when

$$\frac{df(B)}{dt} = 0 \qquad [2.19]$$

there is no net change in the bed.

Solution of Eqn. 2.16 requires the development of mathematical relations describing:

a) the motion of water;

b) the continuity of water and sediment;

c) channel resistance (friction factor related to bed geometry);

d) sediment transport;

e) the relationships describing hydraulic and plane form geometry; and,

f) sediment supply.

Of the models listed in Table 2.1 only the FLUVIAL models attempt to predict bank scour. This is achieved using the concept of minimum stream power (Chang, 1982; 1984). For any given time step, stream width is adjusted for all cross-sections such that the total stream power (rate of energy expenditure) is minimized. These adjustments in width are bound by certain physical constraints such as the total amount of deposition or scour and rigid banks. The total stream power of a channel reach is given as,

$$\Omega = \int_{L_x} \gamma Q S_E \, dx \qquad [2.20]$$

in which, Ω = total stream power of the reach,
L_x = length of the reach,
γ = specific weight of water and sediment mixture,
Q = flow discharge,
S_E = energy gradient.

For streams with non-rigid banks this approach does not appear to differentiate between the erodibility of intact versus recently deposited sediments and bank structure is not incorporated into the analysis. A further limitation is the absence of bed armouring and consequently, the models are limited to sand bed streams (Dawdy and Vanoni, 1986). Dawdy and Vanoni (1986) also question the validity of using the local energy slope in the computation of sediment transport because of the instability (oscillations) which can be introduced by the numerical approach.

As noted above, bank erosion is a dynamic and spatially variable process which requires a three-dimensional model of the flow field, due to the significance of secondary currents. Leopold (1982) explains meander development and bar formation in terms of secondary currents. Chang (1983) demonstrated the apparent relationship between transverse variations in lateral mixing coefficients and secondary currents along a meander reach. Brotherton (1979) gives a qualitative explanation of channel formation in terms of helical secondary currents.

The importance of secondary currents appears to be in their affect on the distribution of shear forces throughout the flow field and particularly along the channel boundary. Chiu et al., (1978) developed mathematical relations describing three-dimensional flow in open channels including the effects of secondary currents (Appendix B). Existing sediment transport models, however, do not account for the role of secondary currents.

2.5 Some Fundamental Concepts In River Engineering

There are two major concepts in river engineering which form the basis for channel stability design methods employed in Canada, namely regime theory and the significance of bankfull stage. These concepts are briefly discussed in the following subsections.

2.5.1 Regime Concept

The premise of many engineering approaches to river form assessment is that a river is in a state of quasi-equilibrium referred to as "in-regime". That is, river form may vary with changes in flow and sediment yield, and the alignment of the channel may be in a constant state of flux, but the average dimensions (as measured by hydraulic geometry parameters such as width, depth, meander length, sinuosity, etc.) do not change significantly over small time periods (Blench, 1957). These channels are referred to as "in-regime" or "equilibrium" systems.

Catastrophic flood flow events in these channel systems are responsible for only minor geomorphic effects (Carlston, 1965; Collins and Schalk, 1937; Wolman and Eiler, 1958; Dury, 1973;

Costa, 1974; Gardner, 1977). These systems are typical of humid regions in which riparian vegetation is believed to play a significant role in stabilizing bank materials (Leopold et al., 1964). In contrast, Burkham (1981), citing studies in arid and semi-arid regions by Bryan (1927), Smith (1940), Schumm and Lichty (1963), Hack and Goodlett (1960), Stewart and LaMarche (1967), Scott (1973) and his own work (Burkham, 1972) noted catastrophic changes in channel form with each successive flood and channel infilling during smaller intervening flows. In these cases, the in-regime concept may not be valid.

2.5.2 Geomorphic Significance Of Bankfull Stage

It is accepted that the cross-sectional shape of a channel is formed by flows which apply sufficient force on boundary materials to cause deformation. Figure 2.7 demonstrates that channel form is the consequence of a range of such flows lying between the lower limit of competence and flows which exceed the capacity of the active channel (overbank flows). For in-regime systems, floodplain inundation acts to limit maximum boundary shear stresses (Barishnikov, 1967). Further, Burkham (1981) noted that correlations between the average annual flood and hydraulic geometry parameters, such as channel width and depth at bankfull stage, was usually good for in-regime

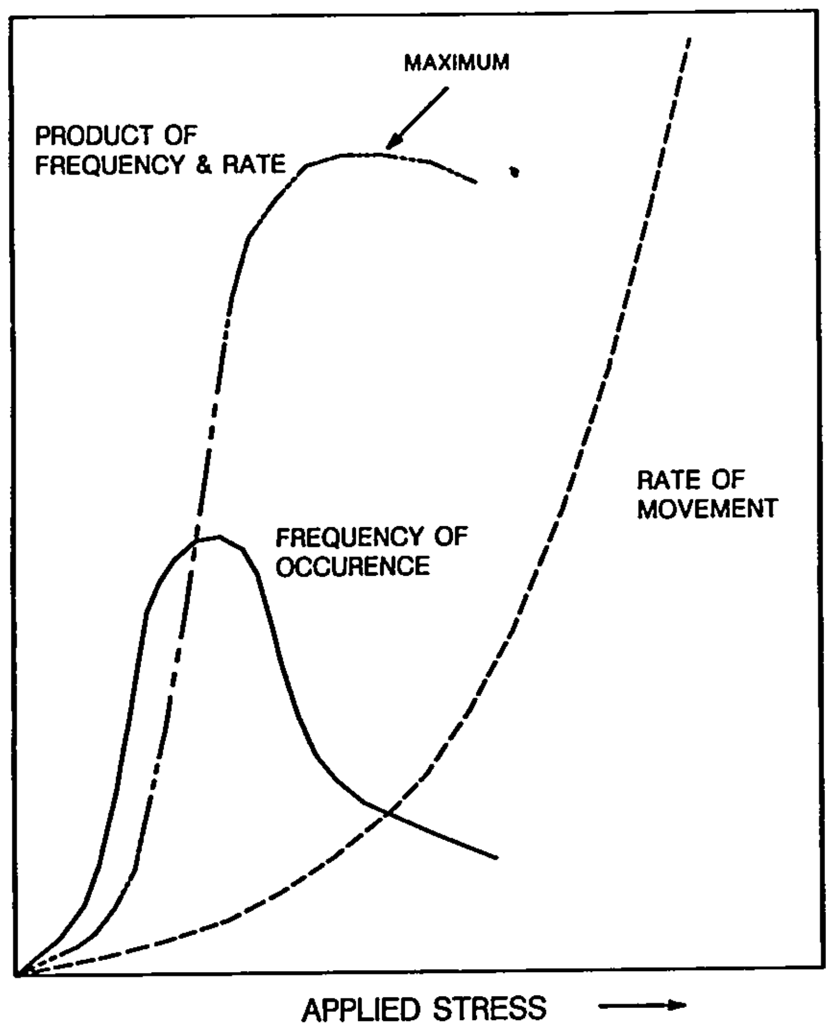

FIGURE 2.7 Generalized Relation of Effective Work Done by Events of Different Magnitudes (Leopold et al., 1964)

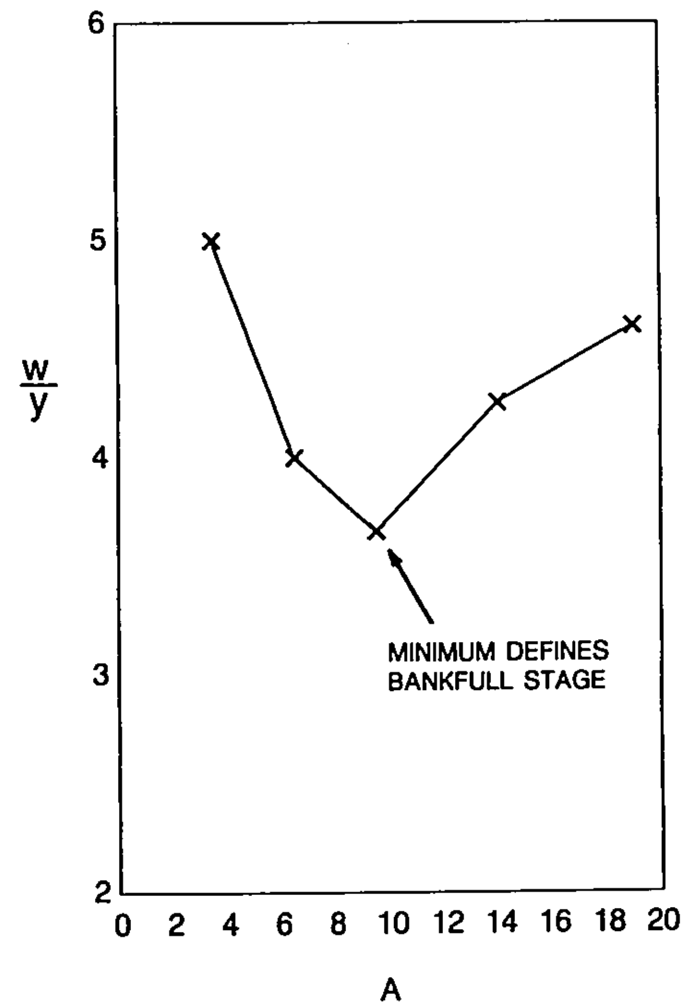

FIGURE 2.8 Definition of Bankfull stage

streams because they reflect the temporal dominance of the flows contained within the active stream channel.

From the viewpoint of work done in erosion and transport, Leopold et al., (1964) deduced, from observations of dissolved and suspended sediment loads, that

> "in many drainage basins a large proportion of the work is performed by relatively frequent events of moderate magnitude".

To the extent that excess shear,

$$\tau_e = (\tau_o - \tau_{CRT}) \qquad [2.21]$$

in which, τ_e = excess boundary shear stress,
τ_o = instantaneous boundary shear stress, and
τ_{CRT} = critical boundary shear stress,

represents the rate of sediment transport, and assuming a log-normal frequency distribution of such stresses, they then observed that the product of the weight of material moved times the frequency will achieve a maximum value, (Figure 2.7). Accordingly, they define the channel forming flow as that flow recurrence interval during which the maximum amount of erosional work is performed. Based on observations from particular streams, Leopold et al., (1964) suggested that the work of perennial streams in scour and fill and debris transport reflects the geomorphic dominance of flows near or above bankfull stage (recurrence interval of approximately 1:1.5 to 1:2 years). This correlation emphasizes the channel forming dominance of bankfull discharge (Wolman and Miller, 1960; Blench, 1966; Hammer, 1972). Bankfull stage is typically defined as the minimum point described by a width/depth versus channel cross-sectional area curve (Figure 2.8).

These observations, however, were for non-urban streams and may not necessarily apply to urbanized watersheds because of the non-uniform increase in flow frequency following urbanization (Hollis, 1975; Figure 2.9).

The more frequent sub-bankfull flows (those flows of RI<1:1.5 years) also contribute to sediment transport (Benson and Thomas, 1966) and may reduce the significance of bankfull flows (Carlston, 1965; Harvey, 1975), particularly in humid regions (Neff, 1967). Harvey et al., (1979) postulated that the cumulative effects brought about by changes in the relative frequency of sub-bankfull flows may influence the stability of the river system. For example, a change in channel stability may result from changes in vegetation colonization of river banks associated with the alteration in the frequency of sub-bankfull flows. Hitchcock, (1977) observed at Langden, that channel instability induced by major flow events (bankfull stage) may be enhanced where moderate flow events influence sediment availability, or cause changes

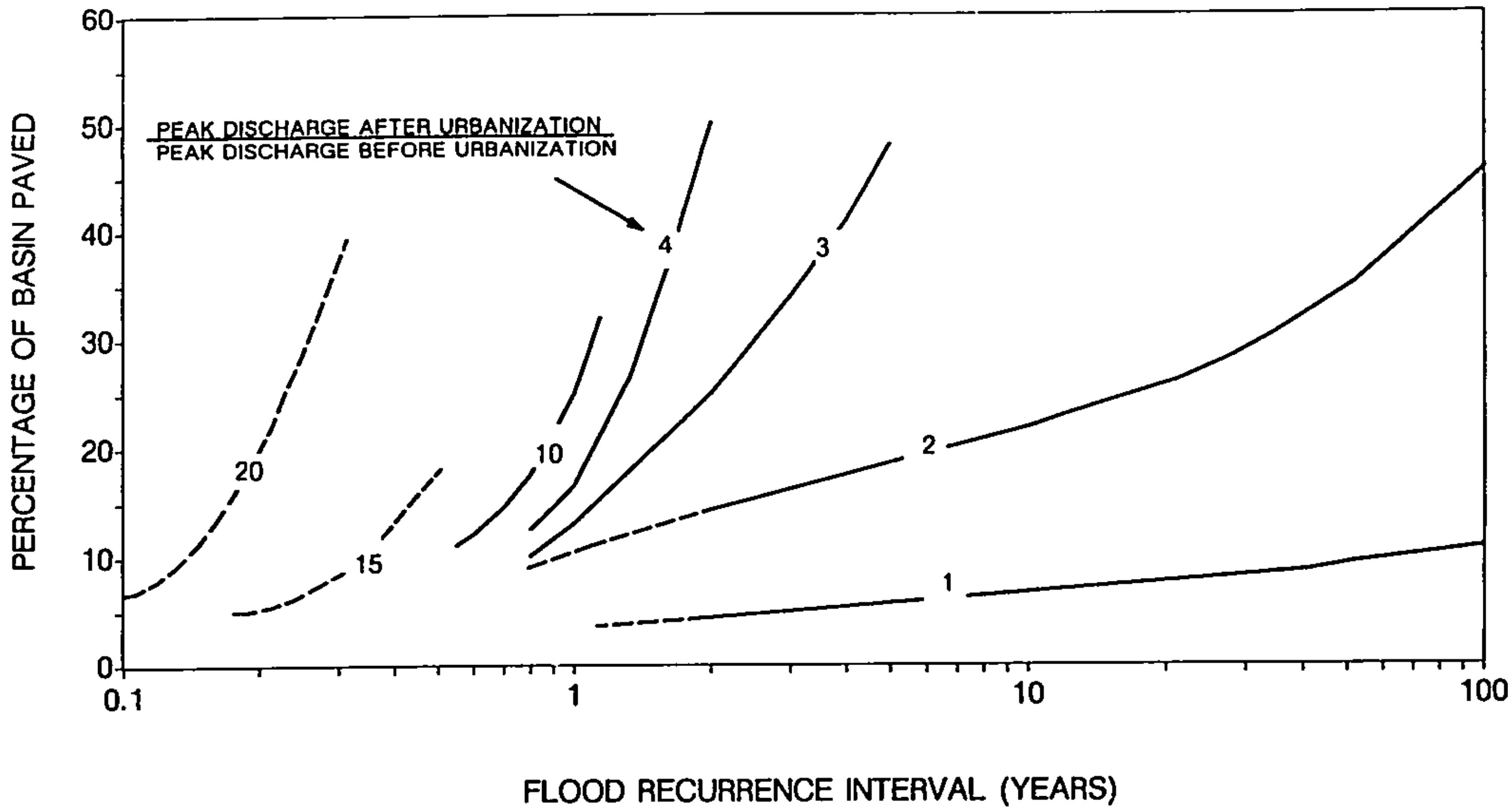

FIGURE 2.9 **Effects of Urbanization on Flood Peaks after Hollis, (1975).**

in local flow directions triggering localized instability. Such observations prompted Harvey et al. (1979) to conclude that major flow events (occurring from 4 times per year to once every 2 years) are the controlling events, but that moderate events (occurring 14 to 30 times per year) influence the adjustments within the overall morphology created by the major events. Finally, the controlling events do not equate with bankfull conditions, raising the question in their study of the utility of the bankfull stage concept. This suggests that a design procedure for the control of instream erosion potential which focuses on one point on the flood frequency curve (i.e. the 1:2 year flood) may not adequately account for the increased significance of sub-bankfull events and consequently may not adequately address the increase in erosion potential.

2.6 Current Instream Erosion Control Design Methods

2.6.1 Introduction

The concept of storage control, and its objective should be understood as a basis for evaluation of the storage approach to instream erosion control. In this research, the objective of storage control is considered to be the minimization of disruption of the morphology of the existing "natural" system by flow alteration associated with land use change. This precludes the use of channel "improvement" techniques which involve wide scale realignment, regrading, lining and reforming of the active channel plane and cross-sectional form. In practice, channel "rehabilitation" (restoration), localized channel improvements (i.e. river bends), and storage controls can and are often used in conjunction with each other. The following is a discussion of the development of storage control concepts, existing storage control methods, and whether they meet the intent of SWM policy.

2.6.2 Storage Concepts For Instream Erosion Control

The intent of detention storage in SWM is to offset changes in natural basin storage and timing characteristics. As such, the effectiveness of the storage concept in SWM control may be measured by how closely watershed storage characteristics under post-development conditions match those under pre-development conditions, (McCuen, 1979). However, while criteria for flood hazard (and somewhat less so for water quality impairment) are relatively well defined, criteria for instream erosion potential are less well established. Three criteria have been proposed:

a) the "zero runoff increase" concept (as used in Canada and parts of the United States), which is based on regime theory;

b) over control (adopted by the Ontario Ministries of Natural Resources and Environment); and,

c) "zero aggregate sediment transport increase" (McCuen and Moglen, 1988), which is based on sediment transport potential.

These three criteria are described in the following subsections.

2.6.2.1 "Zero Runoff Increase" Criteria

Perhaps one of the most influential studies on regulatory policy and criteria regarding instream erosion control was by Leopold (1968) who argued that the increase in the magnitude and frequency of the flow of bankfull recurrence interval (1:1.5 to 1:2 years) was sufficient to cause the active channel to enlarge. To offset this increase in flow, storage controls were proposed to reduce post-development peak flows, of return period equivalent to bankfull stage, back to pre-development levels (Figure 1.1 (b)).

The "Zero runoff increase" criteria, based on the 1:2 year flow, is the most commonly used approach of this type in Canada (Lorant, 1988; Lee and Ham, 1988; Bishop and Mather, 1990). Many jurisdictions in the U.S.A. and Canada, starting with Maryland in 1969 have made this policy and criteria mandatory and today millions of dollars have been spent on thousands of detention facilities designed according to these principles.

Such a criteria means that the post- and pre-development flood frequency curves intersect at only one point, the 1:2 year (bankfull) recurrence interval, (Kamedulski and McCuen, 1979). For all other frequencies the effect of storage on peak flow reduction diminishes as the recurrence interval becomes increasingly greater or less then the 1:2 year level. This has lead researchers to propose the use of more complex outflow control structures which are capable of reproducing the entire pre-development flood frequency curve up to and including the 100-year event, (Mason et al., 1982; Rossmiller, 1982).

Such facilities, while effective within the limited criterion of on-site control of peak discharges, do little if anything under current design practice to limit increases in direct runoff volume or the frequency and duration at which these high flows occur (Lorant, 1988). The impact of these aspects on instream erosion potential are generally not considered. McCuen (1979), demonstrated with the use of simulation techniques that while post-development outflow rates were controlled to pre-development levels the duration of high flows increased several fold. Using a one-dimensional application of excess velocity concepts he demonstrated that this increase in duration of high flows translates into a higher sediment transport capacity and that increase channel scour would likely result. It was concluded that the zero runoff increase concept was deficient in that it did not account for variations in boundary material resistance to erosion, nor did it account for the increased frequency or duration of bankfull or near bankfull flows (Chapter 4). Similar findings were reported by Lorant (1983, 1988) and Bishop and Mather (1990).

2.6.2.2 "Over Control" Criteria

An alternative approach has been jointly proposed by the Ontario Ministries of the Environment and Natural Resources. This approach requires that storage facilities for erosion control be sized to retain the surface runoff generated from a 25 mm precipitation event, and that this volume should be released over a minimum period of 24 hours (for areas over 20 ha). The degree of control applies uniformly to all watersheds regardless of the variation in factors affecting runoff generation or the resistance of boundary materials to scour. It differs from the 1:2 year approach in that storage volumes and the time of retention are up to two times greater. This extra degree of control is referred to as "over control".

As illustrated in Figure 1.1(c), this technique reduces the post-development peak flow rate and duration of flow exceeding Q_{CRT} below that described for the pre-development condition.

The reduction in erosion potential below pre-development levels may contribute to channel instability and bank failure through aggradation of the channel (Brotherton, 1979).

2.6.2.3 "Zero Aggregate Transport Increase" Criteria

Whipple et al., (1981) noted that it is not possible to modify post-development flows to reproduce the pre-development hydrologic regime in all aspects. They concluded that provision must be made so that the aggregate erosional effect of a series of storms will not be greater than that prescribed to a known stable state. They rationalized that this may be achieved through provision of additional detention storage over and above that required for flood hazard control. This concept is referred to as "zero aggregate transport increase" and was demonstrated using a one-dimensional discrete event analysis of sediment transport capacity by McCuen and Moglen (1988).

McCuen and Moglen (1988) reduced the peak outflow rate from a control pond until the post-development sediment transport rate, as measured by unit width bed transport potential computed from average hydraulic parameters, approached the pre-development level. For their particular case study, this represented an 85 percent reduction of post-development flows below the pre-development 1:2 year peak flow rate.

Balancing pre- and post-development erosion potential based on average hydraulic parameters may not however, be adequate by itself. Channel materials tend to vary in their resistance to erosion in both longitudinal and transverse directions, as noted earlier (Koechlin, 1924; Lane, 1955; Schedeidegger, 1961; Bathurst, 1982; Davies, 1987). In a transverse sense, a net increase in erosion potential of zero (using average hydraulic parameters) may still result in aggradation on the bed which is balanced by degradation of the banks. It is important therefore, to know how both the potential for erosion and resistance to disruption are distributed across the channel boundary.

2.6.3 Methods For The Assessment Of Channel Stability

There are two basic methods for the evaluation of stream channel response to urbanization, i) hydrologic methods based on regime theory, and ii) numerical models simulating the physical processes governing sediment transport in mobile beds (degradation models). The zero runoff increase approach is considered to be a hydrologic method while models like MOBED (Kirshnappan, 1981) is characteristic of degradation models. The zero aggregate transport increase technique, as proposed by McCuen and Moglen (1988), represents a simplified degradation approach. These methods are discussed in the following sections by way of introduction to a third procedure based on a two-dimensional index of scour potential as proposed in this research (Section 3.0).

2.6.3.1 Hydrologic Approach

Although the zero runoff increase method does implicitly link stream flow characteristics with channel form and hence the resistance of the boundary materials, it relies on hydrologic methods alone for the estimation of instream erosion potential. That is hydrologic criterion, the pre-development 1:2 year peak flow rate, establishes the stable condition and the basis for control, while the difference between pre- and post-development 1:2 year peak flow rates determines the degree of impact (the increase in-stream erosion potential).

Flow estimation is typically based on discrete event methods although multi-event methods may be used. Without the incorporation of boundary material resistance however, multi-event methods may significantly over estimate the increase in erosion potential. James and Robinson, (1981) using a continuous hydrologic simulation approach noted an increase of more than a thousand fold for very frequent events; flows not exceeding one quarter bankfull depth. He argued that this increase in flow frequency was sufficient to demonstrate the highly destructive influence of urban development of channel form. However, Leopold et al., (1964), Hooke (1979) and Harvey et al., (1979) from field observations, established that the geomorphically significant flows occur between 2 and 30 times per year. These flow events roughly correspond with flow depths exceeding one third bankfull stage. This apparent discrepancy between a hydrologic approach and field observations indicates that additional factors should be considered in the evaluation of the impact of urbanization on channel form.

2.6.3.2 Sediment Continuity Approach

The limitations of sediment transport models is presented in Section 2.4. Nevertheless, they are commonly applied for the evaluation of urban development on instream erosion potential. An implicit, finite-difference model "The unsteady, non-uniform, mobile boundary flow model - MOBED", (Krishnappan, 1981 and 1983) was selected for comparative analysis with techniques developed in this research.

The basic one-dimensional equations governing the flow over a deformable river bed are presented as:

a) The sediment continuity equation,

$$\frac{\delta Q_{sv}}{\delta x} + P\left(\frac{\delta z}{\delta t}\right)p + WC_{av}\left(\frac{\delta y}{\delta t}\right) + A\left(\frac{\delta C_{av}}{\delta t}\right) = q_{sl} \qquad [2.22]$$

b) The continuity equation,

$$\frac{\delta Q}{\delta x} + W\left(\frac{\delta y}{\delta t}\right) + P\left(\frac{\delta z}{\delta t}\right) = q_l \qquad [2.23]$$

c) The momentum equation,

$$\frac{\delta Q}{\delta t} + 2\frac{Q}{A}\left(\frac{\delta Q}{\delta t}\right) - b\frac{Q^2}{A^2}\left(\frac{\delta y}{\delta x}\right) + gA\left(\frac{\delta y}{\delta x}\right)$$

$$= gA(S_o - S_g) + q_l\left(Uq\frac{Q}{A}\right) + \frac{Q^2}{A^2}A_{(y,x)} \qquad [2.24]$$

d) The Ackers White sediment transport relations, (Ackers and White, 1973), and

e) The Kishi and Ashida, (1974) friction relations.

where, x = stream length measured along the longitudinal axis,
t = time axis,
Q_{sv} = volumetric sediment transport rate (total load),
Q = flow rate,
y = flow depth,
z = bed elevation,
P = wetted perimeter,
p = volume of sediment per unit volume of bed layer,
W = top width,

C_{av} = average sediment concentration across the section,
A = area of cross-section,
$A_{(y,x)}$ = the rate of change of A with respect to x when y is held constant,
$q_{s\ell}$ = lateral sediment input rate,
q_{ℓ} = lateral inflow rate,
g = acceleration due to gravity,
S_o = slope of the bed, and
S_E = slope of the energy grade line.

The sediment transport and friction relations are used to evaluate the variables C_{av}, Q_S, and S_f. However, the remaining variables Q, y and z must be obtained through simultaneous solution of the governing equations. Kirshnappan, following an approach described by Chen (1973), uncoupling the three governing equations of sediment and flow continuity and momentum by assuming that $(\delta z/\delta t) << (\delta y/\delta t)$. This allows for the solution of the flow continuity and momentum equations for a time step knowing the initial boundary conditions. The resulting flow conditions may then be used to solve the sediment continuity equation to evaluate the bed level variation. Flow depth is then adjusted and the next time step begins. Simultaneous solution of the flow continuity and momentum equations is obtained by using an implicit, finite-difference scheme developed by Preissmann (1961).

Comparisons of MOBED with other accepted and widely used degradation models, such as HEC-6 (HEC, 1977), have shown MOBED to compare favorably, (Krishnappan, 1985). The model has also received wide acceptance in Canada in the water resources consulting industry. For more detail on the mathematical development of the model, the reader is referred to the above manuals and reports published by Krishnappan.

2.6.3.3 Discrete Versus Multi-Event (Continuous) Simulation Approach

Observations of sediment loadings in Canadian rivers by Environment Canada have shown that 70 to 80 percent of annual loads typically occur in the spring and fall during prolonged periods of high flow (Day, 1989). This concurs with findings reported by Hooke (1979), Thorne and Lewin (1982), Yu and Wolman (1986), who found bank erosion patterns strongly correlated with multiple high flow events associated with high soil moisture levels observed in the spring of the year. Harvey (1969), Knowles, (1971), Williams (1978) and Harvey et al., (1979) suggest that alluvial channels tend to maintain a dynamic equilibrium form with events of a range of magnitudes and frequencies and they question the bankfull frequency approach. These temporal patterns for sediment transport suggest that a multi-event or continuous simulation approach may be a more appropriate analytical technique then the standard discrete event analysis currently employed. The multi-event approach for evaluation of erosion potential is also suggested by Whipple et al., (1981).

2.7 Environmental Indices

Although an exhaustive treatment of indices is not required in this work, as a matter of clarification, the following definition is offered (Ott, 1978);

> "an index or indicator is a means devised to reduce a large quantity of data down to its simplest form, retaining essential meaning for the questions that are being asked of the data".

According to Train (1973),

> "A limited number of environmental indices, obtained by aggregating and summarizing available data, could be used to illustrate major trends and highlight the existence of significant environmental conditions. These indices could provide measures of the success of federal, state, local and private programs in coping with environmental problems that must be solved."

While indices are not the sole basis for environmental decisions, they are recognized as having an important role. However, as noted in the above definition, it must be recognized that in the process of simplification, some information is lost. Indices therefore require careful and proper design, such that the loss of information will not unduly distort the answer to the question(s) being asked. It is also imperative that an index be used solely for the purpose and within the constraints for which it was designed.

2.8 Summary

The principal conclusions drawn from this review are:

a) Case studies concerning the response of channel hydraulic geometry to urbanization provide examples which vary from a net reduction to a net increase in cross-sectional channel area.

b) The apparent discrepancies between these case studies may be explained in terms of stream competence theory and qualitative relations showing the response of hydraulic and plane form geometry variables to changes in discharge and sediment loadings.

c) Scour has been shown to be the dominant erosion process controlling channel form.

d) Scour potential may be defined in terms of boundary shear stress and the resistance of the boundary materials. Boundary shear stress is a function of the flow field and boundary material resistance may be described as a function of particle size for non-cohesive sediments and a function of particle size and cohesive properties for cohesive sediments.

e) The flow field is a function of the hydraulic geometry which varies in a transverse and longitudinal sense requiring a three-dimensional approximation of the velocity field. An expression for the approximation of a three-dimensional velocity field has been developed but not incorporated into a computer simulation model for erosion hazard assessment.

f) The heterogeneous nature of the boundary materials requires consideration of bank structure and a three dimensional description of material properties.

g) The response of hydraulic geometry (bed-bank relationships) to long term changes in the flow and sediment regime are not well understood.

h) Current bank erosion modelling approaches do not include bank structure in the determination of bank erosion or the heterogenieties in the transverse distribution of boundary sediments.

i) Current erosion control design procedures do not account for the transverse variation in boundary material resistance, bank structure and stream competence. They also do not account for the non-uniform increase in flood frequency associated with urbanization.

CHAPTER 3

INSTREAM EROSION INDEX

3.1 Introduction

The index for instream erosion potential as developed in this research is designed to comply with the enforcement of Standards as described by Ott, 1978. This use entails the application of indices to specific locations, such as, channel cross-sections, to determine the extent to which legislative objectives and criteria for the control of instream erosion hazard are being met or exceeded.

3.2 Development of Instream Erosion Index

Boundary material scour at any point on the channel periphery depends on the flow pattern and the properties of the boundary materials at that point. The flow pattern may be described as a function of the hydraulic geometry and fluid properties. The properties of the boundary materials may be measured in terms of the physical and cohesive characteristics of the composite boundary sediments.

Laursen (1952) computed scour as,

$$\frac{df(B)}{dt} = g(q_s)_o - g(q_s)_I \qquad [3.1]$$

where, $f(B)$ = the mathematical description of the bed,
$g(q_s)_o$ = the sediment transport rate out of the scour zone, and
$g(q_s)_I$ = the rate of sediment supply to the scour zone.

Vanoni (1975) cites techniques of dimensional analysis, which produced the following relation for the integral form of Eqn. 3.1,

$$f(B) = \varphi\left(\frac{v}{\sqrt{\frac{\tau_{CRT}}{\rho}}}, \sigma, \frac{vt}{a}, \frac{va}{\upsilon}, \frac{v^2}{ga}, \frac{b}{a}, g(S)\right) \qquad [3.2]$$

in which, $f(B)$ = a dimensionless function of the bed configuration,
v = a velocity characterizing the kinematic properties of the flow pattern,
a = a characteristic length describing the size of the system,
t = time,
ρ = fluid density,
υ = the kinematic viscosity of the fluid,
g = acceleration due to gravity,
$g(S)$ = denotes the upstream sediment supply rate,
τ_{CRT} = critical tractive force,
σ = the standard deviation of the particle size distribution, and
b = a typical length of the flow pattern or scour geometry.

Fluid properties are incorporated into a characteristic Reynold's number, (va/υ) and a characteristic Froude number (v^2/ga). The sediment characteristics for non-cohesive sediments are described by τ_{CRT}, which is typically expressed as a function of a characteristic particle diameter. For cohesive sediments a coefficient of cohesion was introduced by Graf (1971). The upstream sediment supply rate, g(S), is a dimensionless parameter dependent upon the rate at which sediment enters the scour area. This term and those terms describing the flow pattern are also functions of time.

Particular analytical solutions to Eqn. 3.2 have been obtained in some cases, and experimental results have proven useful in other circumstances. In experiments of scour by a horizontal jet, a simpler form of Eqn. 3.2 was used (Vanoni, 1975), where

i) the supply rate of sediment $g(q_s)_I = 0$;

ii) the flow pattern is characterized by the jet velocity and size;

iii) τ_{CRT} serves to describe the sediment; and,

iv) assuming high velocities and submergence of the jet, the flow pattern was considered to be relatively independent of the Reynolds and Froude numbers.

Equation 3.2 was then simplified to,

$$f(B) = \varphi\left(\frac{V}{\sqrt{\frac{\tau_{CRT}}{\rho}}}, \frac{Vt}{a}\right) \qquad [3.3]$$

Using a form of the above relation, investigations of scour by jets has shown that the limiting extent of scour appears to be related to the ratio of the dynamic characteristics of the flow pattern as measured by a characteristic velocity (v), and the resistive properties of the boundary sediments as represented by τ_{CRT}. It was subsequently shown that the scour at any point along the channel boundary was caused by the local boundary shear stress which is a function of flow geometry and the duration of the erosion process in relation to the critical shear stress of the boundary sediments.

Extending these findings to small urban streams;

i) $g(q_s)_I > 0$, the introduction of sediment into the control reach impacts scour in terms of its effect on flow geometry through variations in bedforms and bedform roughness. Where this variation in bed roughness is significant a flow resistance term must be introduced into equation 3.3.

ii) The flow pattern is characterized by the primary flow velocity distribution as modified by secondary (transverse) currents. Consequently, primary flow velocities are not sufficient in themselves to describe the flow field.

iii) $\tau_{CRT} = f(\phi)$ serves to describe non-cohesive sediments and $\tau_{CRT} = f(C_o,\phi)$ for cohesive sediments, (Graf, 1971).

iv) $Fr \leq 1$, and consequently, downstream disturbances in the water profile will propagate upstream and affect flow geometry in the control reach. The upstream migration of knickpoints and variations in bedform geometry must be considered. In the case of knickpoint migration, the rate of migration (10^3 years) is an order magnitude lower than the rate of change in hydraulic geometry (Blench, 1957; Burkham, 1981). Consequently, characterization of the flow field is relatively independent of knickpoint migration. In cases where the variation in bedform roughness is significant a flow resistance term must be incorporated into Eqn. 3.3 as noted above.

It was concluded that the general findings of the experiments on scour by horizontal jets are applicable to channel scour in small urban streams provided that an appropriate function relating flow geometry, duration of the erosion process and material resistance can be found.

In this regard it has been established that sediment transport potential serves as a measure of scour potential (Laursen ,1952; Bogardi, 1974; Morisawa and LaFlure, 1979; Vanoni, 1975; Simons and Li, 1982), and that threshold conditions in fluvial systems is a valid concept (Henderson, 1966; Chang, 1985). To define the scour potential at any point P about a channel perimeter Laursen's relation (Eqn. 3.1) was reformulated as part of this research to form an index of scour potential at a point about the channel perimeter:

$$(E_S)_P = \int_0^T [f(q_S)_O - f(q_S)_I]_P \, dt \qquad [3.4]$$

where, $(E_S)_P$ = scour potential at point "P" about the channel perimeter,
T = the time interval for an event beginning at time zero.

In scour problems involving channel constrictions, DuBoy's bed load sediment transport function was adopted for the explicit form of Eqn. 3.4 (Vanoni, 1975),

in which, τ_o = the instantaneous boundary shear stress

$$(q_S)_P = \int_0^T b(\tau_e)_P \, dt \qquad [3.5]$$

at any boundary station 'P',

b = a calibration coefficient,

τ_e = $\max(0,(\tau_o - \tau_{CRT}))$, and

τ_{CRT} = the critical shear at boundary station 'P'.

DuBoy's relation, under different improved forms, is the basis for many commonly used bed load transport functions. These included,

$$(q_S)_P = \int_0^T b[(\tau_e)\tau_o]_P \, dt \qquad [3.6]$$

$$(q_S)_P = \int_0^T m(\tau_e)_P^n \, dt \qquad [3.7]$$

where, m = a calibration coefficient,
n = an exponent.

Relations 3.6 and 3.7 differ from Eqn. 3.5 in that they assign more weight to higher values of τ, that is they place greater emphasis on individual flow events with higher peak flow rates.

An alternative procedure is the concept of stream power. Colby (1964), demonstrated that in its simplest form the transport of sand load may be estimated in terms of the cube of velocity, which has been shown to be proportional to stream power, (Chorley et al., 1984). Stream power provides a measure of the work expended or energy loss of the stream,

$$\Omega = \gamma_w QS_E = \gamma_w wy\bar{v}S_E \qquad [3.8]$$

where, Ω = stream power,
γ_w = the specific weight of water
y = depth of flow,
v = average flow velocity,
w = width of the channel,
Q = flow rate, and
S_E = energy slope.

Expressing stream power per unit width of channel,

$$\Omega = \frac{\gamma_w wy\bar{v}S_E}{w} = \gamma_w yS_E\bar{v} \qquad [3.9]$$

and substituting into DuBoy's relation, where y ≈ R for a wide stream yields,

$$\Omega = \bar{\tau}\ \bar{v} \qquad [3.10]$$

Expressing τ in Eqn. 3.8 in terms of excess shear at some point 'P' about the channel perimeter and integrating with respect to time yields,

$$(q_S)_P \propto (\dot{\Omega})_P = \int_0^T b(\tau_e)_P\ \bar{v}\ dt \qquad [3.11]$$

in which, Ω = a measure of the stream energy expended above a threshold value at point P.

Relations 3.5 to 3.7 and 3.11 provide a synthesis of the net effect of discharge quantity, flow variability (peakedness), bankfull frequency and duration, stream slope, and hydraulic roughness in relation to the erodability and transportability of the channel materials at any point 'P' on the channel boundary.

Using a comparative pre- versus post-development analysis, where pre-development conditions represent a stable state, then the difference in the pre- and post-development magnitude of the index would represent the change in potential for channel deformation associated with land use alteration at a point. Thus,

$$(\Delta E_S)_P = [(E_S)_{POST} - (E_S)_{PRE}]_P \qquad [3.12]$$

in which, PRE = a subscript denoting pre-development conditions, and
POST = a subscript denoting post-development conditions,

represents the general form of an index of the change in scour potential associated with a change in flow geometry. From Eqn. 3.4 the functional form may be expanded to,

$$(\Delta E_S)_P=\left(\left[\int_0^T f(q_S)_O dt-\int_0^T f(q_S)_I dt\right]_{POST} - \left[\int_0^T f(q_S)_O dt-\int_0^T f(q_S)_I dt\right]_{PRE}\right)$$

[3.13]

The explicit form of the index will depend upon the exact form of the sediment transport relation. This relation should be selected such that boundary material composition in the stream to be modelled falls within the range of conditions for development of that model. Otherwise model performance is more strongly correlated with user familiarity with the adopted function and the appropriate selection of parameter values than differences in the sediment transport relations themselves.

If the index is measured about the channel perimeter, it would define a two-dimensional measure of the potential for channel deformation. An aggregate measure of the change in scour potential was also put forward as part of this research:

$$(\Delta E_S)_{AGG} = \int_0^{L_x} |(\Delta E_S)_P| \, dz \qquad [3.14]$$

where, $(\Delta E_S)_{AGG}$ = the aggregate change in scour potential about a channel cross-section,
L_x = the length of the wetted perimeter, and
z = the transverse cross-sectional axis.

When $(\Delta E_S)_{AGG} > 0$, erosion of the channel boundary will occur either along the bed (degradation), the bank (basal scour) or both. If $(\Delta E_S)_{AGG} < 0$, aggradation of the bed will occur with erosion of the bank. Finally, $(\Delta E_S)_{AGG} = 0$, as in the case of $df(B)/dt = 0$ in Laursen's model, defines a stable (no scour) scenario. The absolute value of $(\Delta E_s)_P$ is used to encompass the special case of aggradation of the bed and scour of the bank. Consequently, the transverse distribution and magnitude of ΔE_S provides a description of the potential for alteration of stream channel form and may provide a quantitative two-dimensional measure for the assessment of storage regulation of instream erosion potential.

CHAPTER 4

THE ROLE OF MODERATE FLOW EVENTS

4.1 Introduction

The channel is formed by a series of flow events, the number of occurrences of which form a positively skewed distribution. Sediment transport potential however, increases exponentially with flow rate thereby increasing the relative significance of individual rare flood events. Leopold et al., (1964) defined effective work as the product of frequency of occurrence and transport rate. They found that channel hydraulic geometry at bankfull stage accords with the flow recurrence interval coincident with maximum effective work. This recurrence interval (RI) was found to range form 1:1.5 to 1:2 years. By equating effective work with the ability of the stream to form its channel they concluded that flows corresponding to 1:1.5 $\leq$ RI $\leq$ 1:2.0 years were the flows principally responsible for the form of the active channel. The most commonly used instream erosion control method is predicated on the control of flows at RI = 1:2 year (Section 2.5.2).

Urbanization results in a non-uniform increase in flood frequency, such that the curve defining maximum effective work may increase and shift toward a lower recurrence interval (Figure 4.1). This means channel hydraulic geometry will

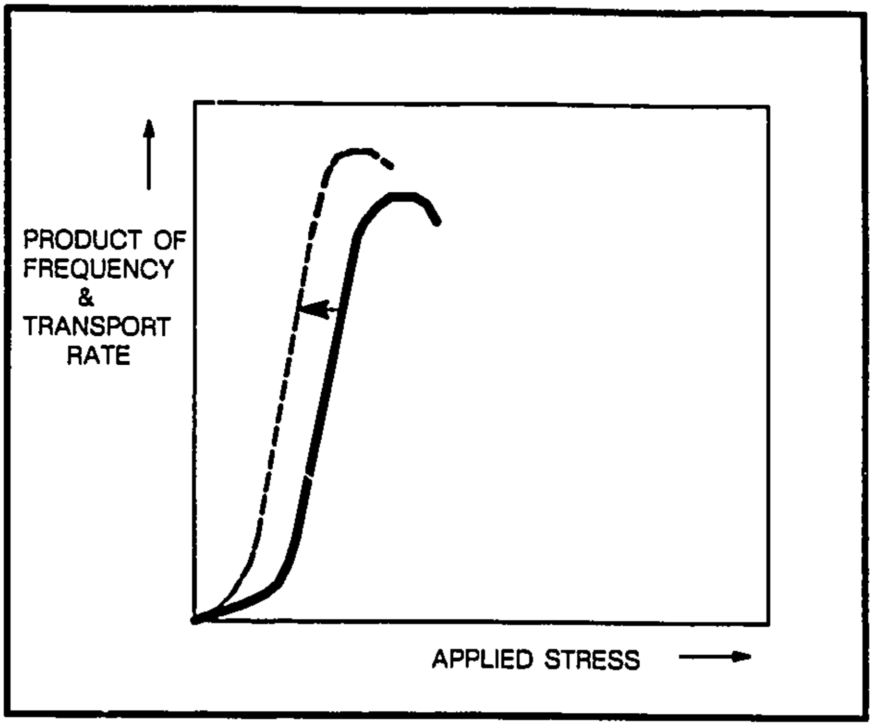

FIGURE 4.1 **Probable Alteration of Leopold et al.'s (1964) Effective Work Curve.**

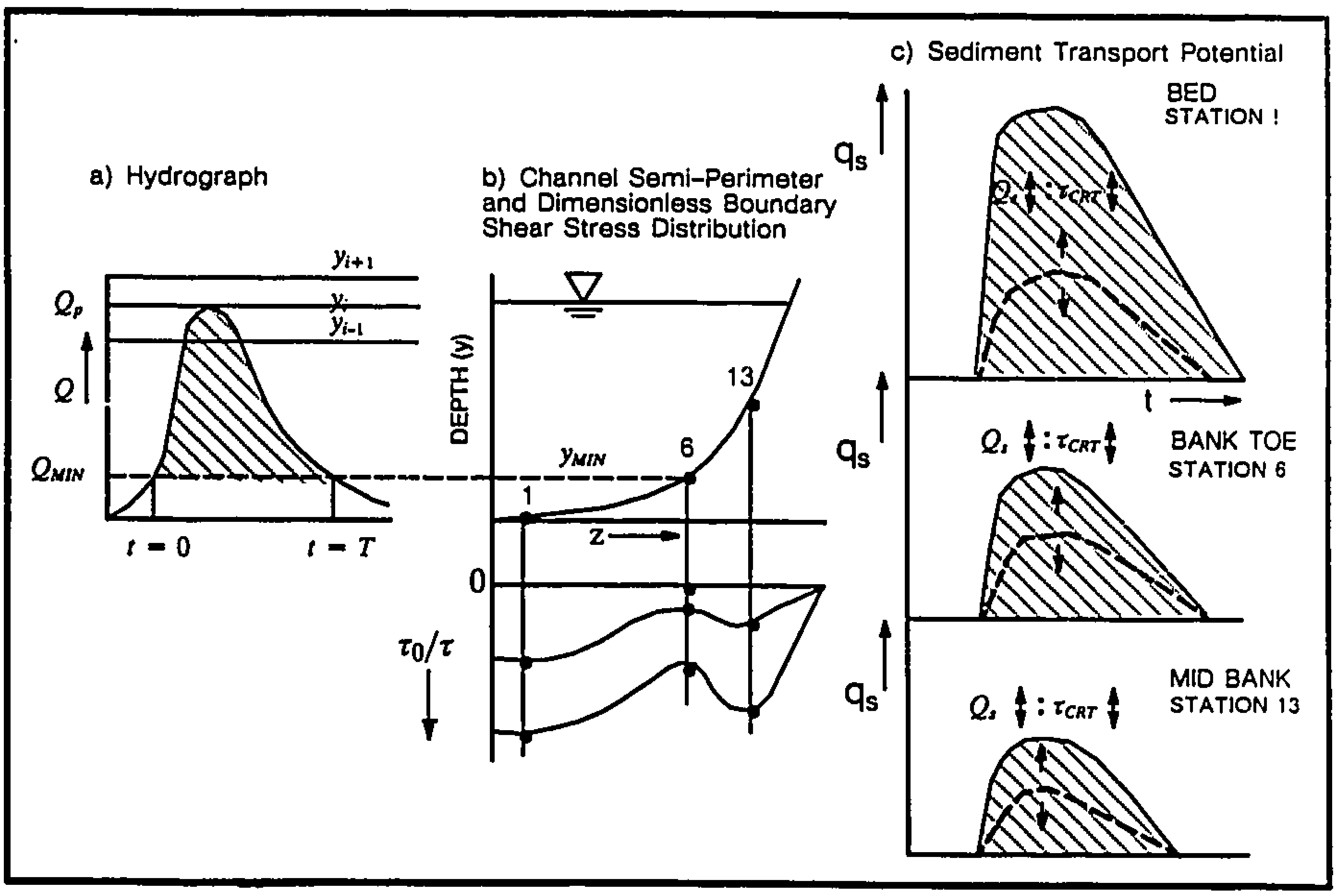

FIGURE 4.2 **Definition Sketch for Determination of Aggregate Sediment Transport Potential, (Q_S).**

evolve to conform with the scour potential described by sub-bankfull flows or moderate flow events. Consequently, control philosophies which maximize the degree of control for the 1:2 year flood may undercontrol moderate flow events and not effectively control instream erosion potential.

4.2 Sediment Transport Potential Of Moderate Flow Events

The cumulative sediment transport rate (q_s), at any point 'P' about a channel perimeter through the course of a flow event (Figure 4.2) is defined using the general form of Meyer-Peter Muller relation (Shen, 1971; Eqn. 3.7) as,

$$(q_S)_P = \int_0^T m(\tau_o - \tau_{CRT})^b \, dt \qquad [4.1]$$

where, τ_o = the instantaneous boundary shear stress at point "P",
τ_{CRT} = the critical shear stress at point "P",
b = an empirically derived exponent,
m = an expirically derived coefficient, and
T = event duration for which $q_s > 0$.

Summing Eqn. 4.1 for all points across the perimeter of the cross-section yields,

$$Q_S = \int_0^{L_x} (q_s)_P \, dz \qquad [4.2]$$

in which, Q_s = the aggregate sediment transport potential for a flow event,
z = the transverse cross-sectional axis, and
L_x = the length of the wetted perimeter.

Written in finite difference form, Eqn. 4.2 becomes,

$$Q_S = \sum_{i=0}^{N} (q_S)_{P_i} \, \Delta z \qquad [4.3]$$

in which, i = the ith boundary element, and
N = the total number of boundary elements.

To determine the significance of the sediment transport potential associated with the number of flow events that reach a particular depth of flow, the channel was divided into a number of depth increments such that,

$$\Delta y = \left(\frac{y_{BFL}}{N}\right) \qquad [4.4]$$

where, y_{BFL} = bankfull channel depth, and
N = the number of depth increments.

The depth increments were numbered consecutively from 1 to N such that,

$$(j-1)\Delta y < (y_{INCR})_j \le j(\Delta y) \qquad [4.5]$$

in which, j = 1 to N.

A flow event at peak flow rate would achieve a maximum flow depth of y_{MAX} according to a stage-discharge function. The sediment transport potential for any flow event may then be mapped to a corresponding depth increment by satisfying the condition,

$$(y_{INCR})_{i-1} < y_{MAX} \leq (y_{INCR})_i \qquad [4.6]$$

where, i = 1 to N.

Summing Q_s for all events whose maximum flow depth (y_{MAX}) falls within a specified depth increment yields,

$$(W_y)_j = \sum_{i=1}^{N} [(Q_s)_i]_j \qquad [4.7]$$

where, $(Q_s)_i$ = Q_s for an $EVENT_i$ occurring with a maximum depth (y_{MAX}) falling between $(y_{INCR})_{j-1}$ and $(y_{INCR})_j$, (j=1,10),
$(W_y)_j$ = cumulative aggregate sediment transport potential for all runoff events which reach a specified depth ($y \pm \Delta y$), and
i = the ith flow EVENT.

To examine the affect of the non-uniform increase in flood frequency on channel forming events, relations 4.1 to 4.3 and 4.7 were applied to a test channel section based on a survey of a stream in the Ottawa vicinity. Flow, geodetic and geotechnical information were available for this site (Figure

4.3; CCL, 1986). The channel configuration was representative of stable conditions as determined from an interpretation of fluvial forms and apparent activity rates (Appendix A).

The boundary materials were sampled at three locations about the perimeter of the channel as illustrated in Figure 4.3. The banks were found to be composed of a veneer of loose weathered silty clay of 3.6 to 7 cm thickness. The underlying material was composed of a firm, intact silty clay. The bed was almost entirely covered with loose alluvium composed of silty clay materials with a trace of sand. Near the center of the channel a cut was made through this material to the intact bed. The depth of alluvium at this point was approximately 0.36 m. The underlying bed material was a very firm, intact clay characterized as relatively homogeneous, fine grained and cohesive (CCL, 1986).

The channel was surveyed before and after the occurrence of a rare flood flow event (Figure 4.3). This flow, which exceeded bankfull stage, estimated recurrence interval of $1{:}50 \leq RI \leq 1{:}100$ years, removed the loose alluvial sediments lying over the intact clay bed. Comparison of pre- and post-event surveys showed only minor scouring of intact bed material (Figure 4.3).

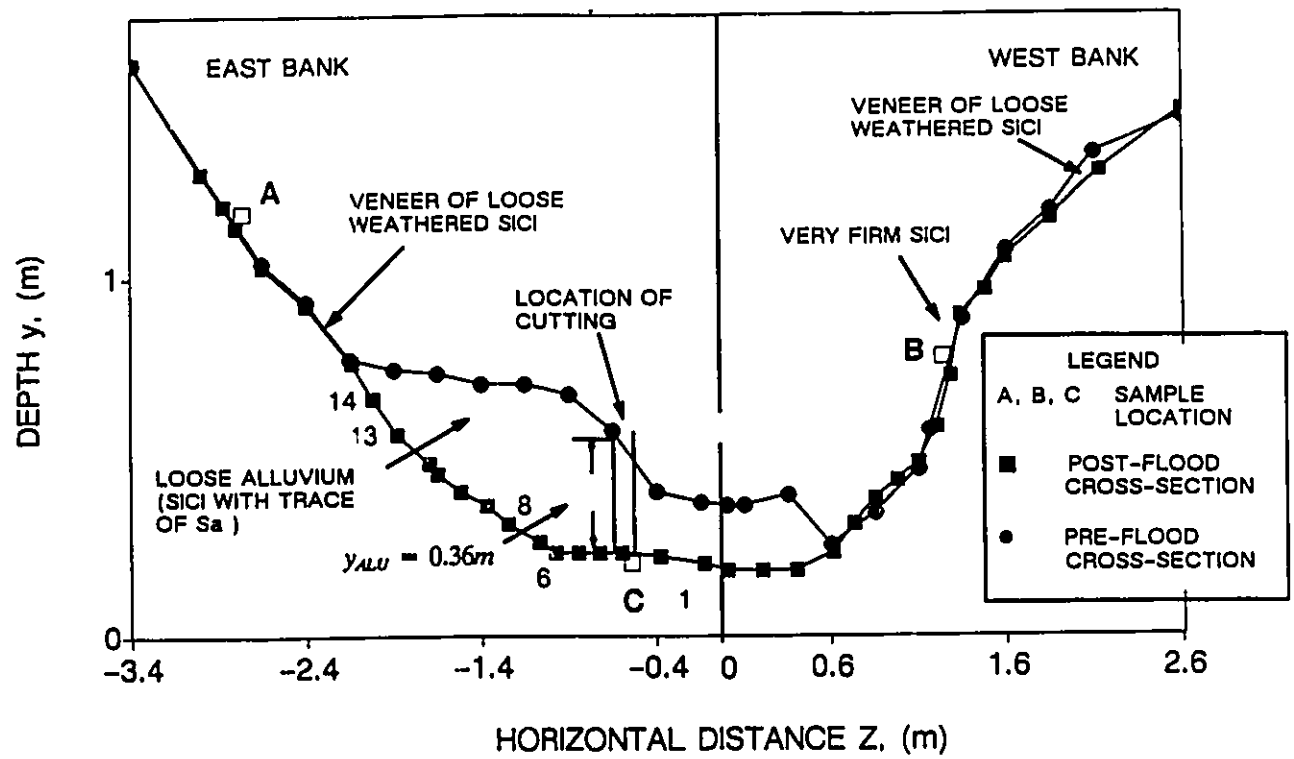

FIGURE 4.3 Bilberry Creek at Des Epinettes Ave. After Rare Flood.

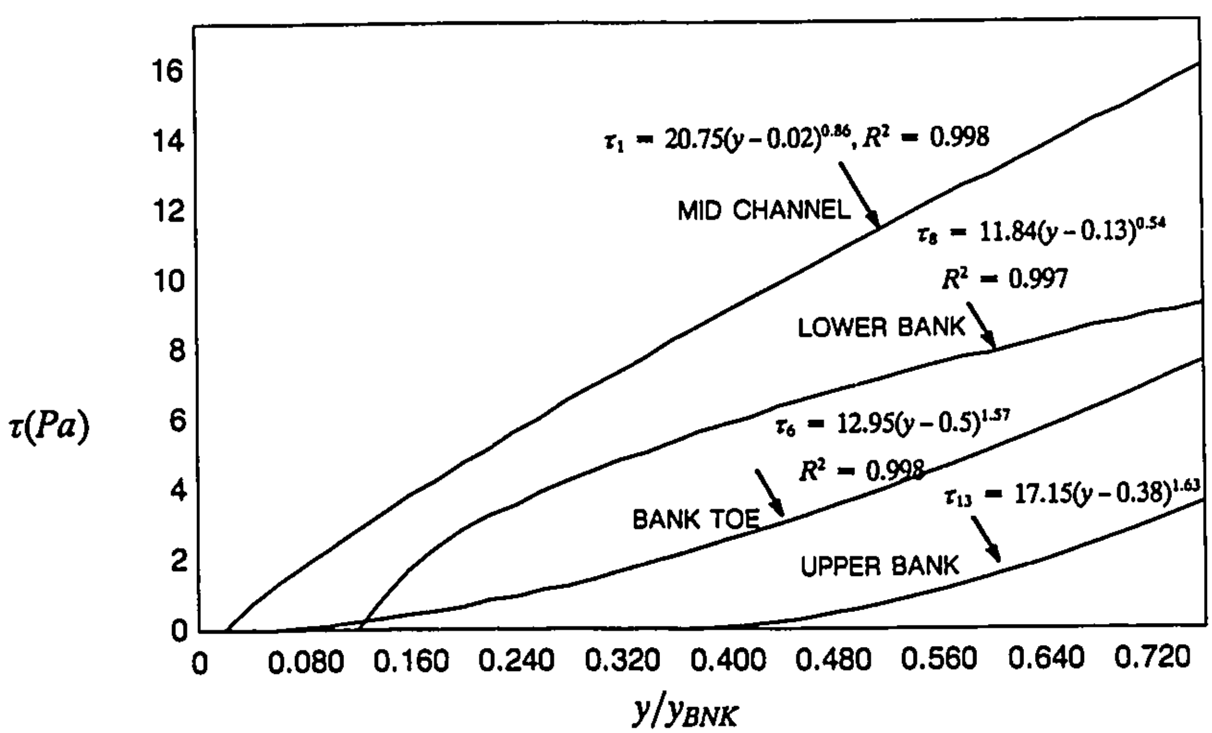

FIGURE 4.4 Boundary Shear Stress Relations for Selected Bed-Bank Stations.

A continuous hydrologic simulation model (Rowney and MacRae, 1991(a); Section 7.3) was calibrated to the watershed and used to generate flow series for a thirteen year period starting in January 01, 1971 and ending on December 31, 1983. The model was used to simulate pre- and post-development land use scenarios based on existing and future land use maps. Model parameters for the post-development state were derived from calibration studies on three urban watersheds in the Ottawa area (Rowney and MacRae, 1991(b)). These flows were used to derive a stage-discharge relation of the form,

$$Q = 2.95(y^2), \quad r^2 = .99 \tag{4.8}$$

where, Q = discharge rate, and
y = depth of flow above the thalweg.

Three boundary stations were selected for analysis; the mid bank (Station 13), the bank toe (Station 8), and the mid channel bed (Station 1).

Boundary shear stress at these stations was determined for selected depths using a calibrated boundary shear stress model (EROS1, Section 7.2; Appendix B). Correlation with flows was then performed to develop power functions of the general form,

$$\tau_o = a(Q-Q_o)^b \tag{4.9}$$

where, b = an empirically derived exponent,
a = an empirically derived coefficient, and
Q_o = the flow rate at the depth of the boundary station.

The specific relations for the three boundary stations are illustrated in Figure 4.4.

Using Eqn. 4.9, the QUALHYMO flow series were transformed into boundary shear stress time series for each Station. Cumulative aggregate sediment transport potential (W_y), was then determined at the three boundary stations. Coefficient values for the Meyer-Peter Muller sediment transport function (m=2.5 and b=1.5) were selected from studies reported in the literature (Bogardi, 1974; Shen, 1971). The computational time step was t = 0.25 hours over the 13 year period of simulation.

In this case, an event was defined as any set of contiguous time increments wherein excess boundary shear stress is greater than zero. The total number of such events (NEVENT) increased from 824 to approximately 2000 (at Station 1) following two-thirds development of the basin under predominantly residential land use. The distributions of NEVENT by depth are illustrated in Figure 4.5 (a) to (c) for Stations 1, 8, and 13 respectively.

In the thirteen year period the increase in the number of

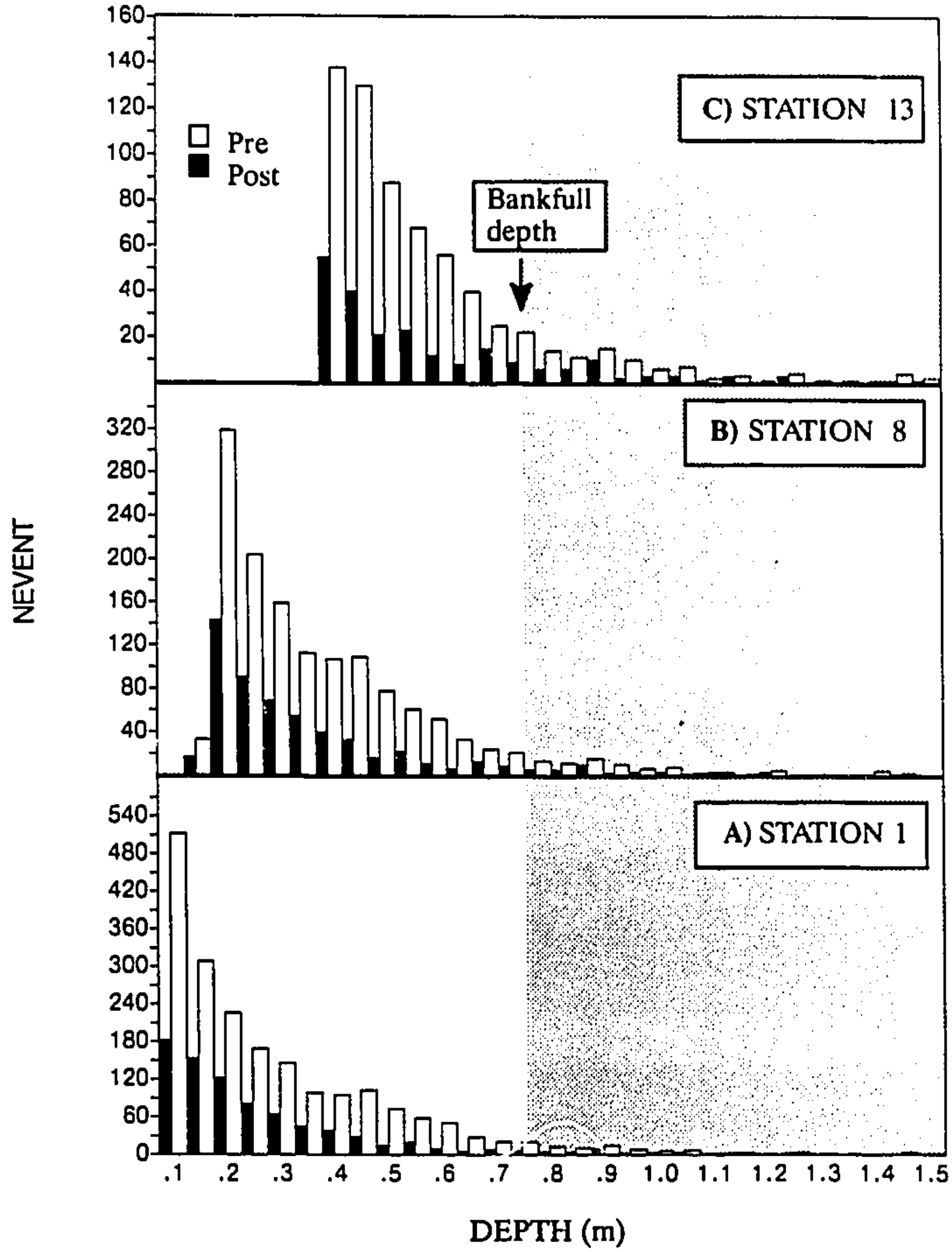

FIGURE 4.5 Number of Flow Events by Increment of Depth Under Pre– and Uncontrolled Post– Development Land Use Scenarios

events ($NEVENT_{POST}$ - $NEVENT_{PRE}$) diminishes with stage (Figure 4.6 (a) to (c)). As shown in Table 4.1 the majority of the increase in the number of events is recorded for depths of $y \leq \frac{1}{3} y_{BFL}$ at Stations 1 and 8. Over 80 percent of the increase in number of events occurs by $y \leq \frac{3}{4} y_{BFL}$ for the same two stations. The lower value for Station 13 reflects the lower boundary shear forces acting on this station.

Table 4.1

Percent Increase In NEVENT For Selected Depths

Depth y (m)	Station 1 (%)	Station 8 (%)	Station 13 (%)
$\frac{1}{3} y_{BFL}$	74	62	19
$\frac{2}{3} y_{BFL}$	85	70	56
$\frac{3}{4} y_{BFL}$	86	84	67
y_{BFL}	96	95	90

Figure 4.7 (a) to (c) compares the distribution of W_y for pre- and post-development conditions. The distribution of $(W_y)_{PRE}$ tends to support the channel forming dominance of bankfull flows at Station 13, however, scour potential is approximately an order of magnitude lower at this station relative to Stations 1 and 8. The later stations illustrate the significance of the entire range of flows in determining channel form.

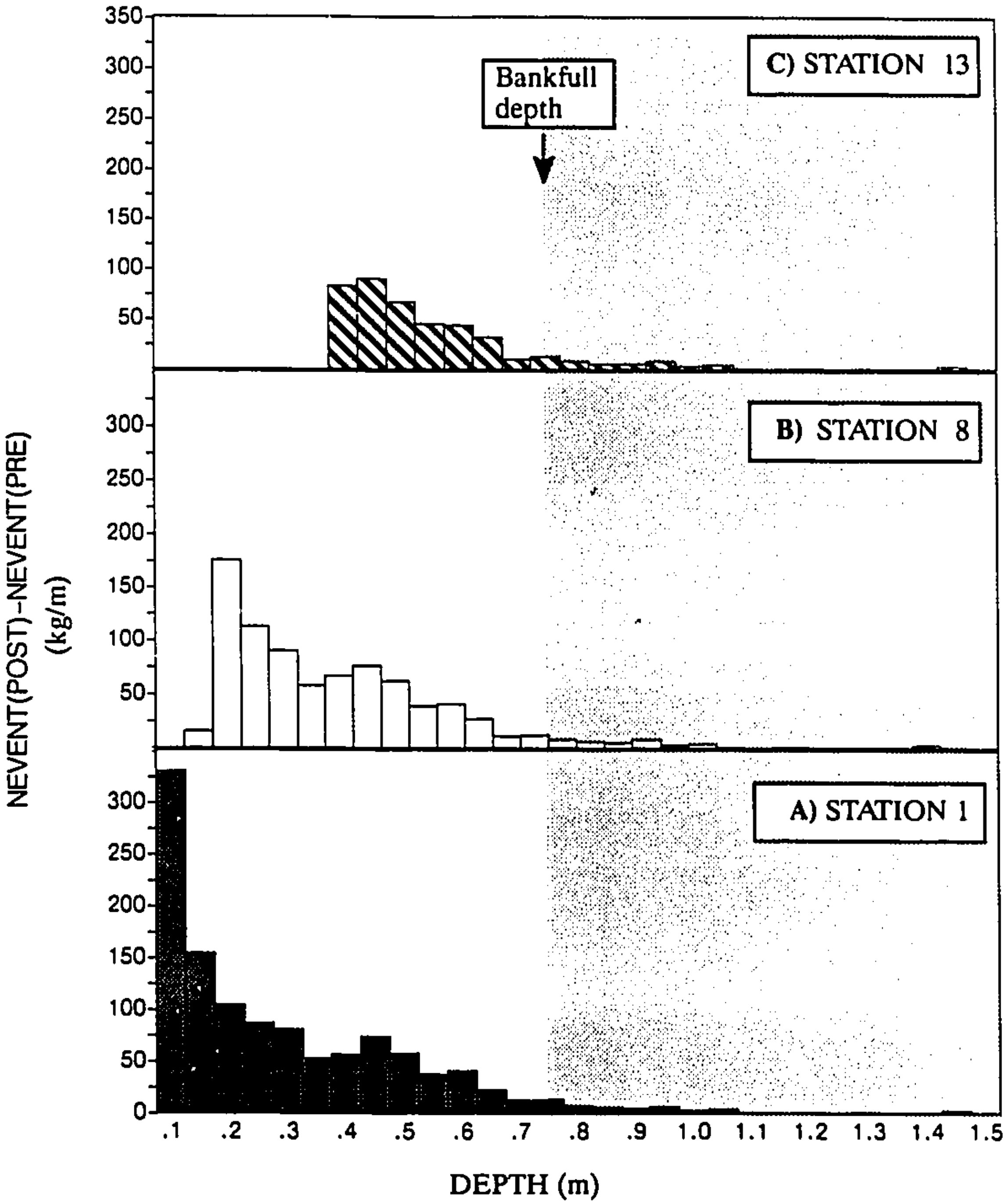

FIGURE 4.6 Increase In The Number of Flow Events by Increment of Depth Following Urbanization

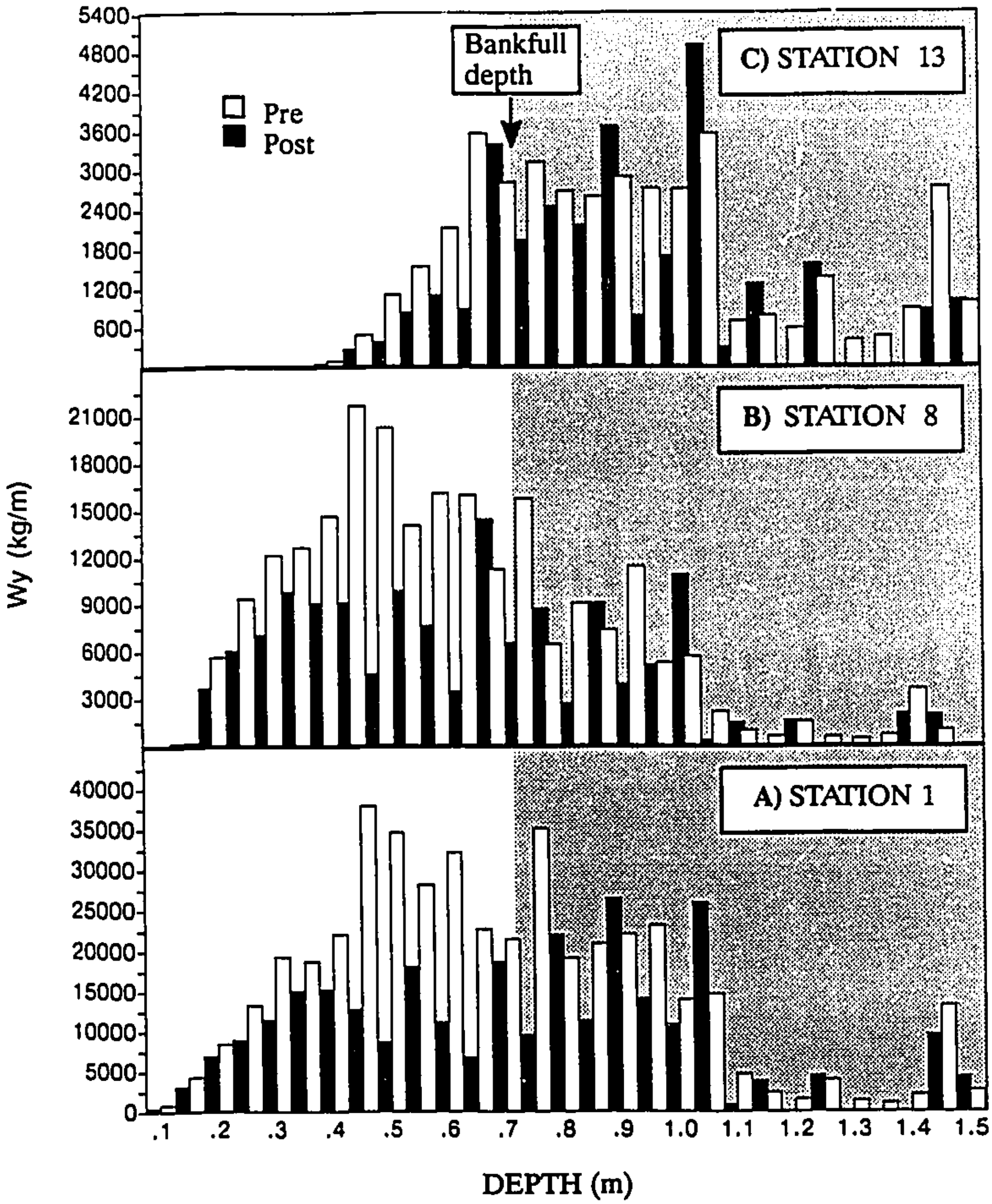

FIGURE 4.7 Cumulative Aggregate Sediment Transport Potential By Increment Of Depth

The post-development distribution of $(W_y)_n$ demonstrates the increased significance of flow events in the moderate flow range. The maximum increase occurred between $0.5y_{BFL} \leq y \leq 0.73y_{BFL}$ for Stations 1 and 8, and $0.66y_{BFL} \leq y \leq 0.8y_{BFL}$ for Station 13 (Figure 4.8 (a) to (c)). This represents an increase in scour potential in the order of 2 times for flows in the moderate event range.

The distribution of the difference in cumulative aggregate sediment transport potential is illustrated in Figure 4.9 (a) to (c). The greatest difference in (W_y) occurs at depths of $0.5y_{BFL} \leq y \leq 0.66y_{BFL}$ for Stations 1 and 8, and at approximately $y=0.85y_{BFL}$ at Station 13 This figure also shows that the majority of the total increase in cumulative aggregate sediment transport occurs for moderate flow depths. This is more clearly illustrated in Figure 4.10 (a) to (c) which shows the cumulative value of $(W_y)_{POST}$ minus $(W_y)_{PRE}$. For this case, over 67, 60 and 31 percent of the increase in scour potential occurred by $y=.75y_{BFL}$ at Stations 1, 8 and 13 respectively (Table 4.2).

The above analyses tend to support the view that stream channel form is determined by a series of flow events ranging from moderate to bankfull flows. However, scour potential associated with moderate flow events increases in the order of two times pre-development levels. The resulting distribution

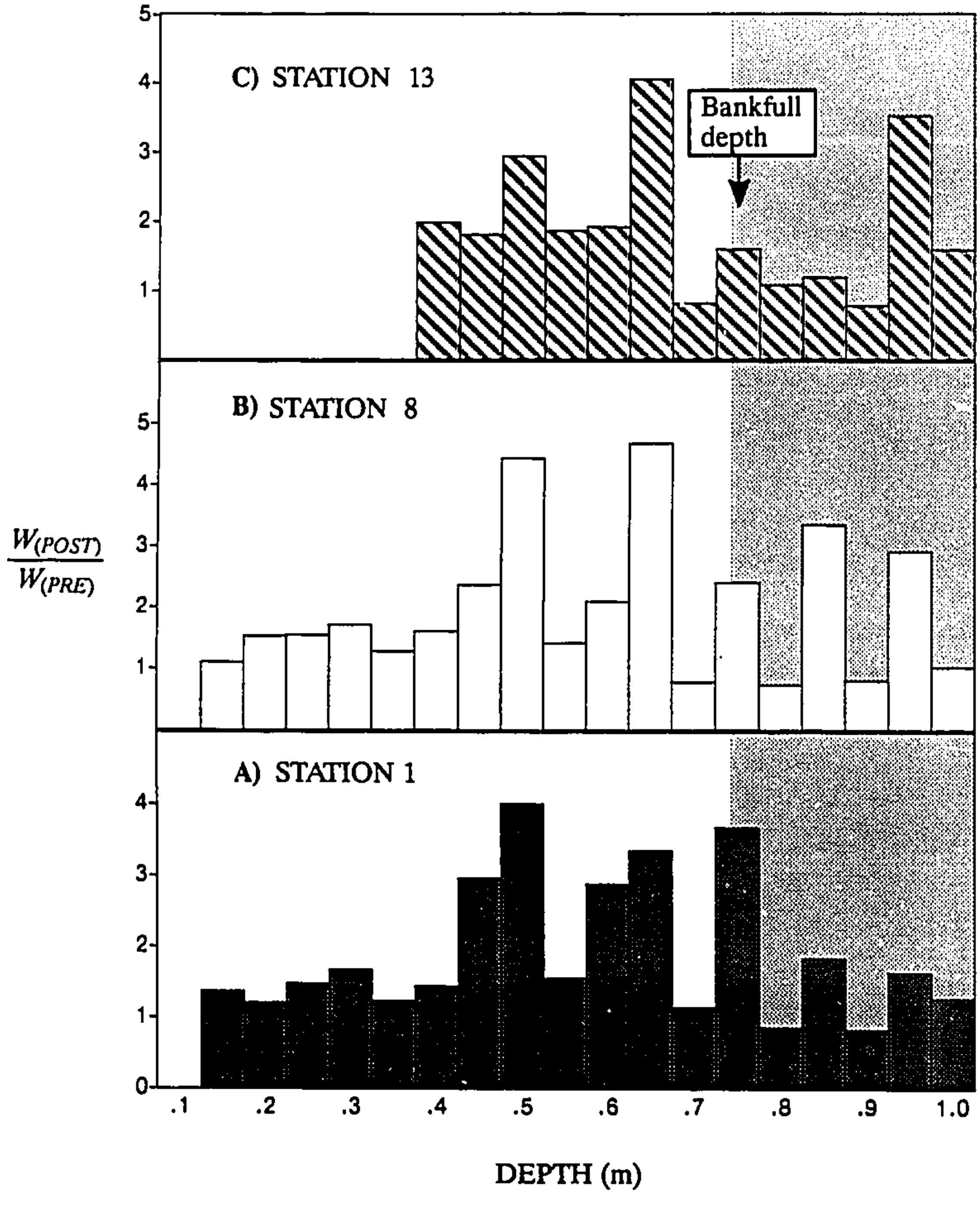

FIGURE 4.8 Post–Development Cumulative Aggregate Sediment Transport Potential As A Factor Of Pre–Development Levels By Increment Of Depth

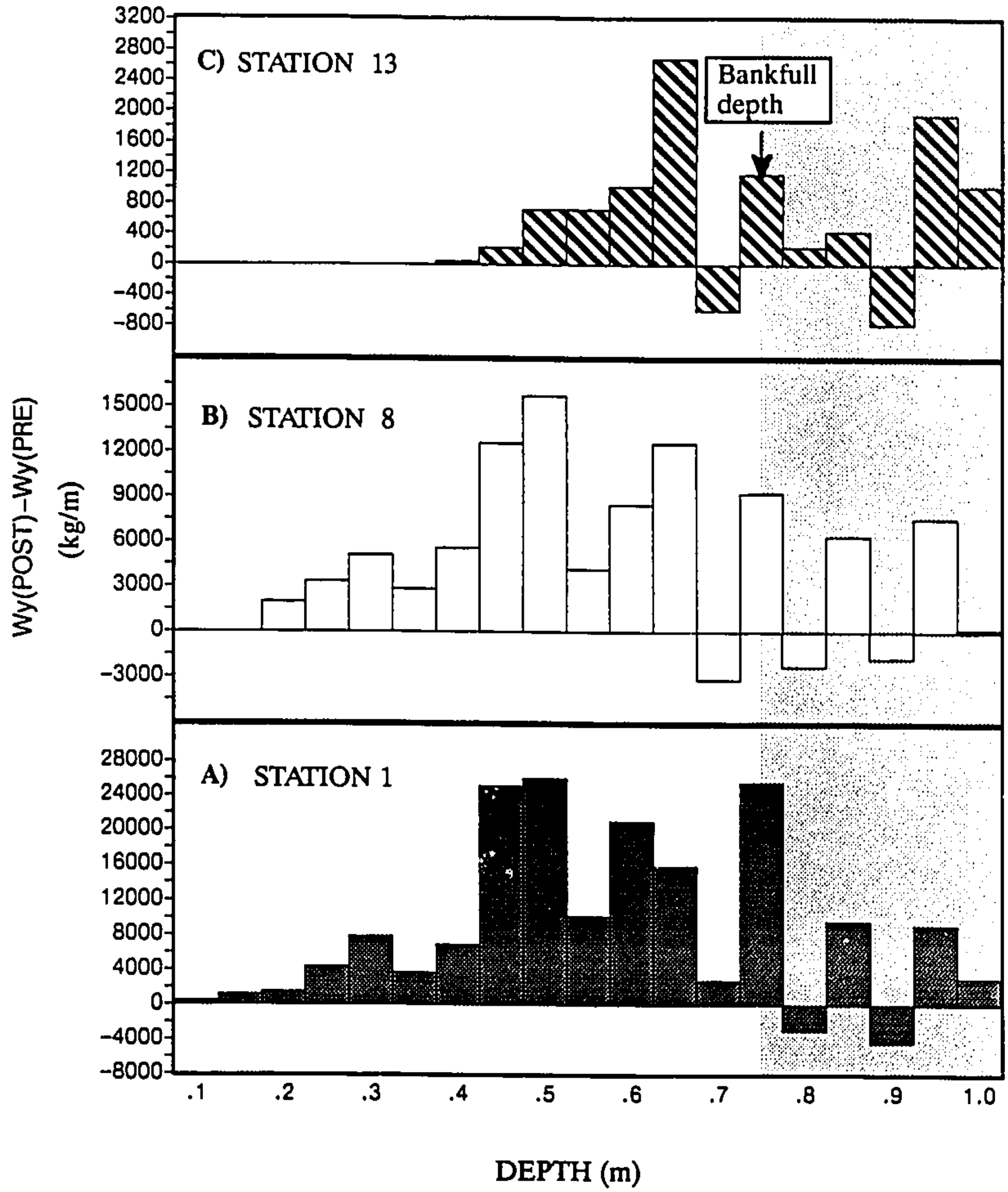

FIGURE 4.9 Post-Development Minus Pre-Development Cumulative Aggregate Sediment Transport Potential By Increment Of Depth

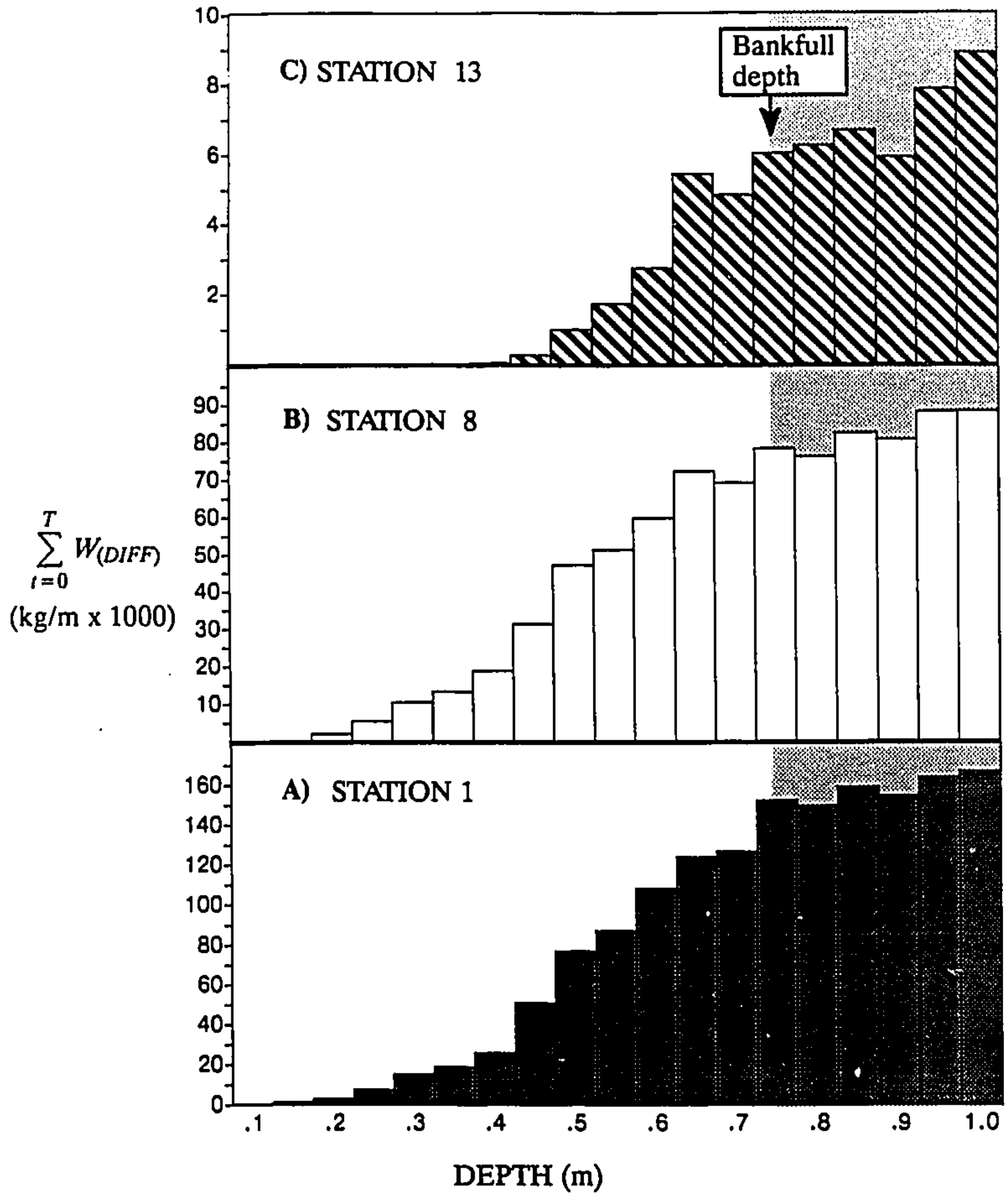

FIGURE 4.10 Cumulative Change In Cumulative Aggregate Transport Potential By Increment Of Depth

of cumulative aggregate sediment transport potential would suggest that moderate flow events become the dominant channel forming flows following urbanization in this case study. The implication on development of design criteria is that the focus of storage control should be on the control of flow geometry associated with these more frequent flow events.

TABLE 4.2

Summary of Cumulative Post- Minus Pre-Development Aggregate Sediment Transport Potential At Selected Boundary Stations (%)

STATION	$\Sigma[(W_y)_{POST} - (W_y)_{PRE}]$			
	$.5y_{BFL}$	$.66y_{BFL}$	$.75y_{BFL}$	$1.0y_{BFL}$
1	31	47	67	94
8	15	54	60	90
13	0	19	31	68

CHAPTER 5

THE IMPORTANCE OF THE BASAL STRATIGRAPHIC UNIT

5.1 Introduction

Data on bank stratigraphy and material characteristics from a field survey of urbanized streams are presented in this chapter. Trends from the empirical analyses of these data indicate that the resistance to scour of the stratigraphic unit in the bank toe region may be the dominant factor in the determination of channel response to an alteration in flow geometry. These analyses support field observations of the dominance of basal scour in channel formation and the need to address channel erosion potential on a point by point basis.

5.2 Background

Lee and Ham (1988) reported surveys of a number of recently urbanized and some non-urban streams in Surrey, British Columbia. Although parameters describing the bankfull hydraulic geometry of these streams was measured, bank material composition and structure were not recorded. Seven of these streams were re-surveyed as part of this research with the intention of characterizing stream bank material composition and stratigraphy. These streams were selected because they were all developed with 1:5 year storage facilities to control instream erosion. Survey methods and a summary of the resulting data are presented below.

5.3 Survey Methodology and Results

Seven of the Lee and Ham (1988) survey sites were re-located with the aid of one of the authors of the original survey (P. Ham, District of Surrey). Representative channel cross-sections are shown in Figures 5.1 (a) to (g). Information collected included,

a) mapping of bank stratigraphy,

b) sediment sampling by stratigraphic unit

c) mapping of plane form channel geometry approximately 50 m up and downstream of the survey section,

d) engineering survey of the hydraulic geometry at a representative site within the survey reach,

e) a description of riparian vegetation type and density,

f) in situ field measurement of bed material particle size,

g) classification of predominant channel forms, i.e. bar deposits, slides, slumps, tension cracks, flute marks (meso scale fluvial forms),

h) photographic documentation, and

i) simple field tests of bank material consistence.

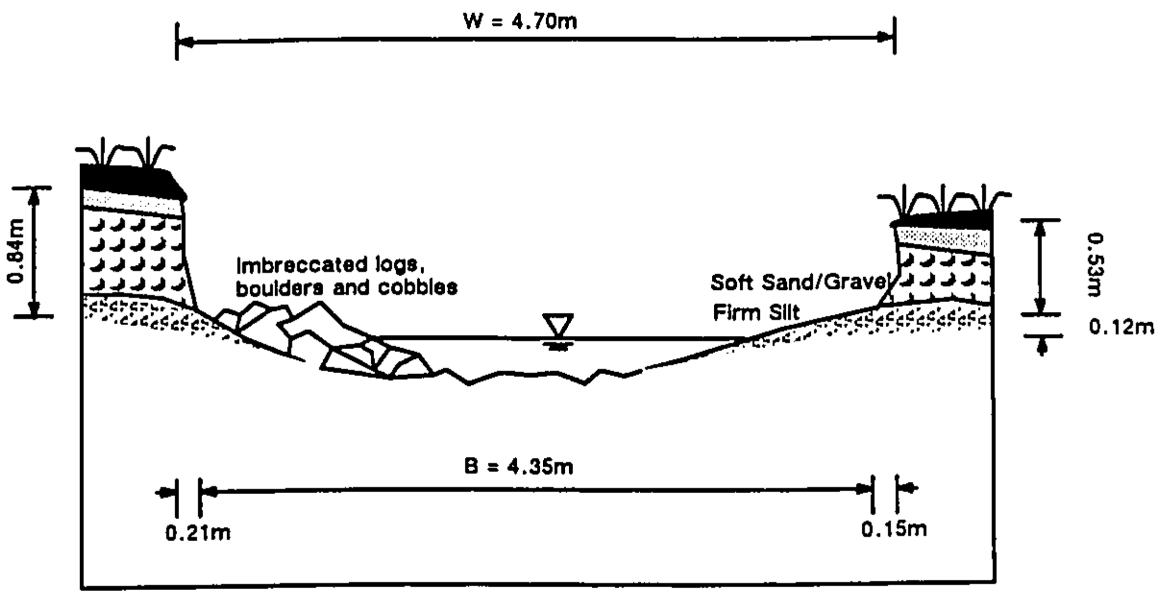

FIGURE 5.1a Representative Cross-Section through Reach A – Centennial Park Creek

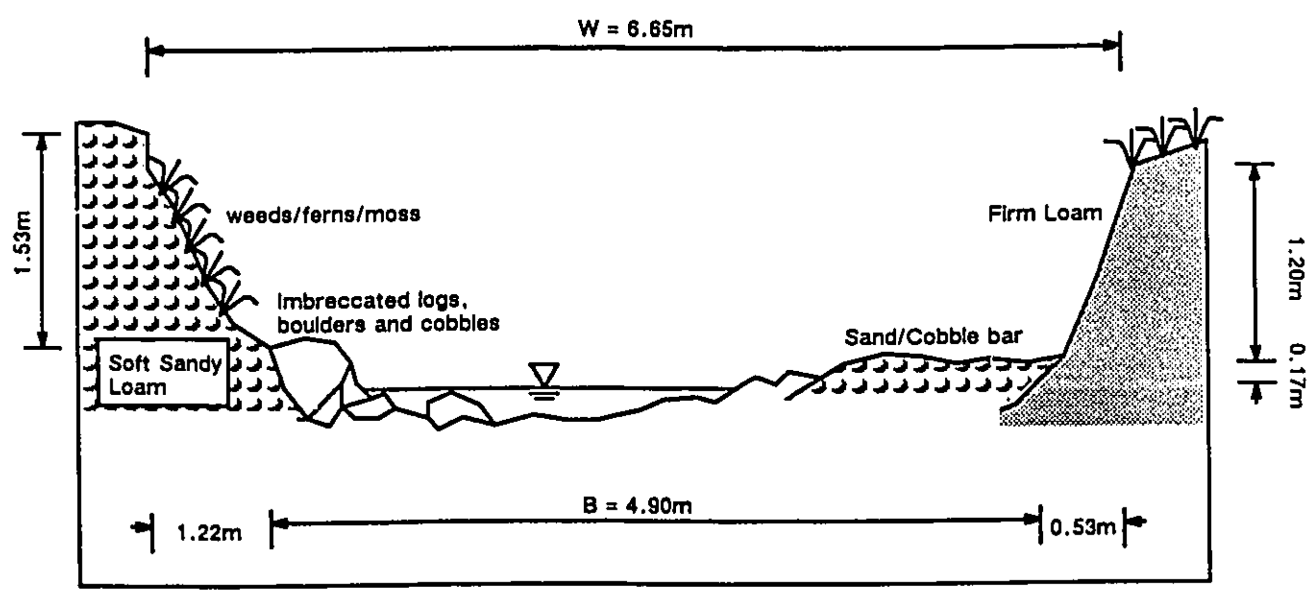

FIGURE 5.1b Representative Cross-Section through Reach B – Sunnyside Basin

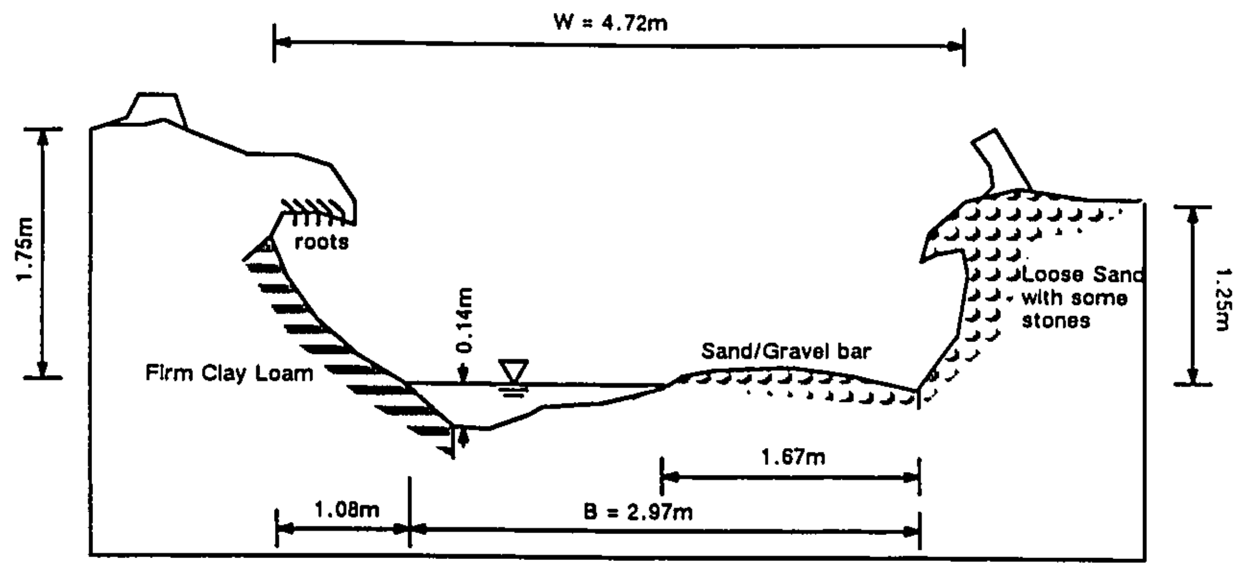

FIGURE 5.1c Representative Cross-Section through Reach C – Rita's Creek

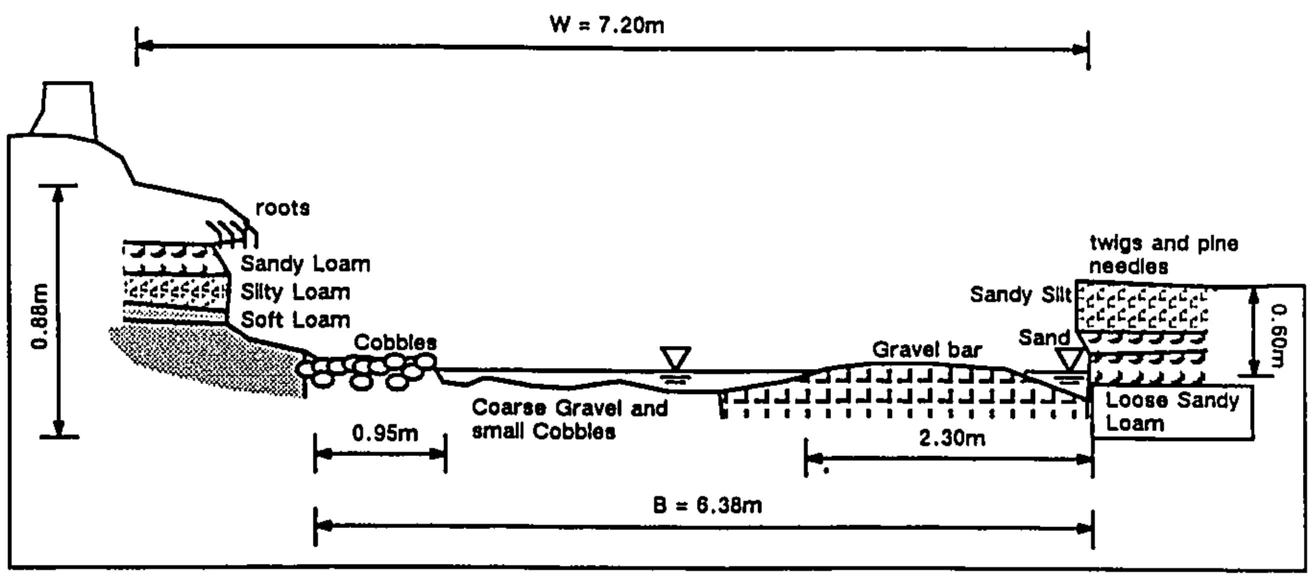

FIGURE 5.1d Representative Cross-Section through Reach D – North Branch of Mahood Creek

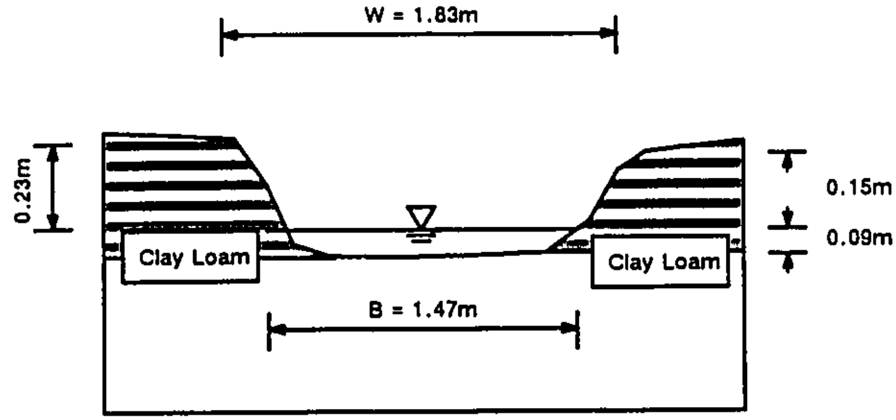

FIGURE 5.1e Representative Cross-Section through Reach E – Enver Creek

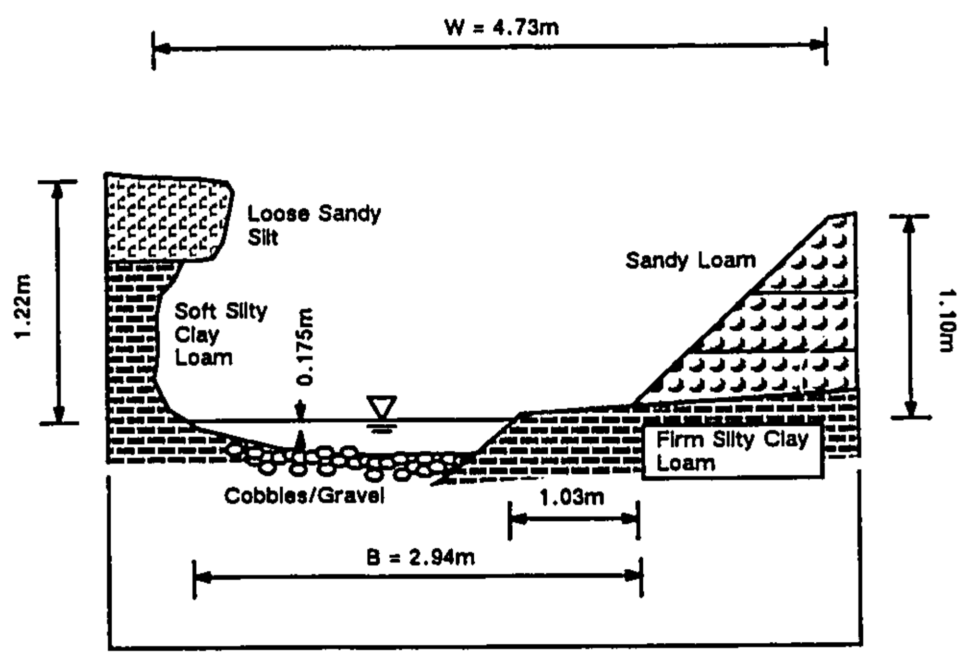

FIGURE 5.1f Representative Cross-Section through Reach F – Serpentine River

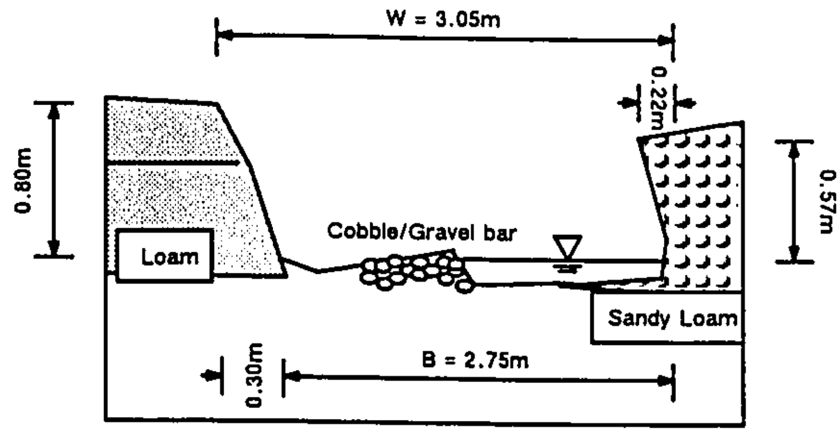

FIGURE 5.1g Representative Cross-Section through Reach G – Serpentine River

Field tests for consistence were as defined by Buol et al., (1973) and Holtz and Kovacs (1981). Standard field tests included:

I. Wet consistence - moisture content at or slightly above field capacity.
   A. Stickiness - quality of adhesion to other objects.
   B. Plasticity - capability of being moulded by hands near the plastic limit (Toughness).

II. Moist consistence - moisture content between dryness and field capacity.
   A. Dilatancy - reaction to shaking.
   B. Structure - structure and strength of aggregates.

III. Dry consistence - air-dry soil condition
   A. Structure - presence and crushing characteristics of aggregates.

Sediment samples were analyzed at the Royal Military College of Canada, Kingston, Ontario for textural class (particle size) and plastic index (PI) as defined by Atterberg limits using standardize liquid limit tests developed by Casagrande (Holtz and Kovacs, 1981). Textural classes were determined by wet sieving and hydrometer methods. A summary of field and laboratory data is presented in Table 5.1.

5.4 Analysis Of Field And Laboratory Data

The increase in the number of flow events which exceed τ_{CRT} results in an increase in the scour potential about the

TABLE 5.1

Summary Of Field And Laboratory Data

Description Watershed	Sample No.	Laboratory Data PLASTICITY LL	PL	PI	TEXTURE Cl	Si	Sa	SOIL CLASS	Field X1	X2	X3
Centennial	A1R*				Ah Horizon			O	-	-	-
	A2L*				<5	13	84	LSa	0	0	0
	A3L*				<7	<7	>85	GrSa	0	0	0
	A4L				11	82	7	Si	3	1	4
	A1R				Ah Horizon			O	-	-	-
	A2R*				<5	13	84	Lsa	0	0	0
	A3R*				<7	<7	>85	GrSa	0	0	0
	A4R[1]	40.0	34.0	8.5	11	82	7	Si	3	1	4
Sunnyside	B1L[1]	20.6	19.0	1.6	6	28	66	SaL	0	0	0
	B2L				14	36	50	L	2	2	3
Rita's Ck.	C1L	48.9	23.6	25.3	52	42	6	ClL	3	2	4
	C1R	43.3	40.8	2.5	3	7	89	Sa	0	0	0
Mahood	D1L*				7	23	70	SaL	1	0	0
(Bear) Ck.	D2L	48.8	46.0	2.0	8	57	35	SiL	1	0	0
	D3L	32.2	27.4	4.8	17	37	46	L	1	1	0
	D4L				17	37	46	L	0	1	0
	DR1	47.3	33.0	14.0	11	42	47	L	3	2	1
	D2R*					<13	87	Sa	0	0	0
	D3R	21.0	19.0	2.0		<33	67	SaL	1	0	0
Enver Ck.	E1L				29	40	31	ClL	2	3	4
	E2R	59.7	52.0	7.7	29	40	31	ClL	2	3	4
Serpentine	F1L	44.7	37.7	7.0	12	32	57	SaL	1	1	1
N. of 96	F2L	56.3	35.8	20.5	35	57	8	SiClL	3	2	2
Avenue	F1R*				<5	27	68	SaL	1	0	1
	F2R*				10	19	71	SaL	0	0	1
	F3R*				<5	23	72	SaL	0	0	1
	F4R				35	57	8	SiClL	3	1	3
Serpentine	G1L				18	42	40	L	2	2	1
South of	G2L	51.1	41.6	9.5	21	44	35	L	2	2	1
Freeway	G1R	37.5	31.0	6.5	13	19	68	SaL	3	1	0

* Insufficient sample passing No. 200 mesh sieve for PI test
1. Estimated from Figure 5.9 and Dunn, (1959).
X1 = Stickiness, X2 = Plasticity, X3 = Firmness
L = loam Cl = clay Si = silt
Sa = sand Gr = gravel O = organic

channel perimeter. However, bed and bank materials are often heterogeneous and structured as observed in the Surrey survey. Consequently, τ_{CRT} may vary significantly in the transverse direction depending upon the properties of the materials at each point about the channel periphery. The significance of bank structure was examined by comparing the least resistant bank toe stratigraphic unit in accordance with field classification of stickiness (X1), plasticity (X2), and firmness (X3) for the seven study reaches to the ratio of post- to pre-development bankfull channel width (W_R),

$$W_R = \frac{W_{POST}}{W_{PRE}} \qquad [5.1]$$

in which, W_{POST} = post-development bankfull channel width, and
W_{PRE} = pre-development bankfull channel width.

Stickiness, plasticity and firmness are separate qualitative measures of material consistence (Buol et al., 1973). The independence of these parameters was examined through a cross-correlation analyses of twenty-eight observations as presented in Table 5.2. The standard error of estimate in the regression coefficient ranged from 19.8 to 21.8 percent with a similar range in the error reported for the Y estimate. These statistics indicate that a correlation does exist between the variables, however, r^2 values (Table 5.2) indicate that the variation in any one variable explained by any one of the other two variables is poor.

TABLE 5.2

Cross-Correlation (r^2) Matrix of Stickiness (X1), Plasticity (X2), and Firmness (X3)

	X1	X2	X3
X1	1.000	0.494	0.488
X2		1.000	0.448
X3			1.000

Since standard soil classification procedures require all three parameters to characterize the consistence of a material a model which incorporates all three parameters should be considered. The following relation is one possible alternative,

$$W_R = m(SCORE) + b \qquad [5.2]$$

in which,

$$(SCORE) = (X1 + X2 + X3) \qquad [5.3]$$

where, SCORE = a composite measure of the resistance to scour
X1 = measure of wet consistence (stickiness),
X2 = measure of moist consistence (plasticity),
X3 = measure of dry consistence (firmness).

Sensitivity to scour is inversely proportional to material consistence as measured by plasticity and unconfined shear strength (ASCE, 1975) and hence to the value of SCORE. To provide a measure of the suitability of Eqn. 5.3 as a measure of material resistance to scour a number of other possible models based on various combinations of these parameters was examined using linear regression techniques. These models are,

$$W_R = m(X1) + b \qquad [5.4]$$

$$W_R = m(X2) + b \qquad [5.5]$$

$$W_R = m(X3) + b \qquad [5.6]$$

$$W_R = m_1(X1) + m_2(X2) + b \qquad [5.7]$$

$$W_R = m_1(X1) + m_2(X2) + m_3(X3) + b \qquad [5.8]$$

SCORE values were computed from field classifications of bank toe stratigraphic units ($SCORE_{TOE}$). The bank toe stratigraphic units receiving the lowest SCORE for each section were then compared with W_R, (Table 5.3).

Correlations derived for Eqn. 5.2 and 5.4 to 5.8 using linear regression analysis are presented in Table 5.4. Equations 5.4 to 5.6 present the correlation of W_R with the parameters X1, X2 and X3 independently. Plasticity (X2)

TABLE 5.3
Comparison Of W_R And Field Measures Of Stickiness (X1), Plasticity (X2), and Firmness (X3) For The Least Resistant Bank Toe Stratigraphic Unit

Sample No.	Field Description X1	X2	X3	SCORE (TOE)	W_R
E1R	2	3	4	9	1.02
F2L	3	2	2	7	1.63
A4R	3	1	4	8	1.96
G1R	3	1	0	4	2.03
D3R	1	0	0	1	2.56
C1R	0	0	0	0	3.05
B1L	0	0	0	0	3.80

explained 79.9 percent of the variation observed in W_R, with a standard error in the regression coefficient of SE = 22.5 percent. The proportion of variance explained by stickiness (X1) and firmness (X3) were .622 and .536 respectively.

TABLE 5.4
Proportion Of Variance (r^2) in W_R Explained By X1, X2, X3, and $SCORE_{TOE}$

Parameter	W_R	SE(%)
X1	.622	34.9
X2	.799	22.5
X3	.536	41.6
(X1,X2)	.885	58.1,33.1
(X1,X2,X3)	.886	69,51.9,592
$SCORE_{TOE}$	.815	21.3

Equations 5.7 and 5.8 present W_R as a linear function of (X1, X2) and (X1, X2, and X3) respectively. Parameter X3 in Eqn. 5.7 did not significantly increase the explanation of

variance in W_R. Removing X3 from the analysis yields Eqn. 5.8 which recorded a correlation coefficient of $r^2 = 0.885$.

The composite measure ($SCORE_{TOE}$) recorded an r^2 value of .815 with a standard error in the regression coefficient of 21.8 percent (Figure 5.2). Removal of X3 from $SCORE_{TOE}$ increase r^2 to .859. However, it is difficult to justify a specific model on the basis of these statistics alone given the size of the data base. These regression models however, do indicate that the composite parameter (SCORE) represents a measure of material resistance to scour.

Field designations of stickiness, plasticity and firmness as measured by SCORE were also compared against laboratory measurements of Plastic Index (Table 5.5). A simple linear regression analysis was performed on these data producing the relation,

$$PI = 2.81(SCORE)_{TOE} \quad r^2 = 0.88 \qquad [5.9]$$

in which, PI = Plastic Index.

FIGURE 5.2 Correlation between W_R and the Least Resistant Bank Toe Stratigraphic Unit

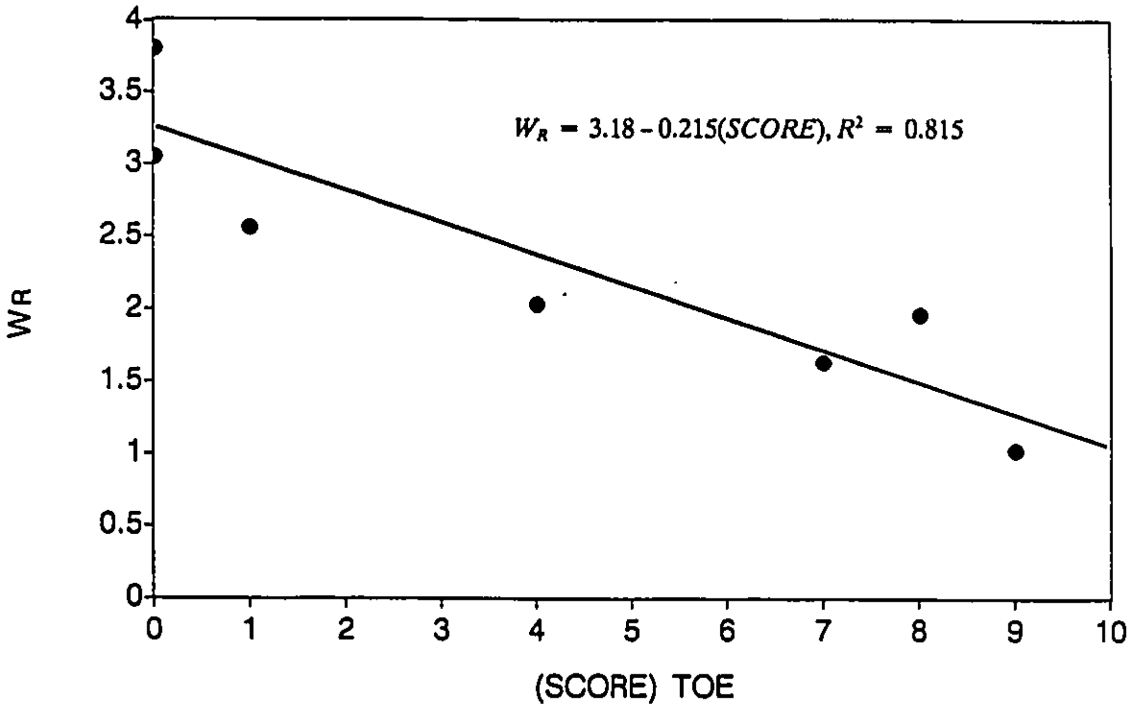

TABLE 5.5

Comparison of PI with Field Designations
Of Stickiness, Plasticity and Firmness

Sample No.	PI	X1	X2	X3	Score
C1L	25.3	3	2	4	9
C1R	2.5	0	0	0	0
D2L	2.0	1	0	0	1
D3L	4.8	1	1	0	2
D1R	14.0	3	2	1	6
D3R	2.0	1	0	0	1
E2R	7.7	2	3	4	9
F1L	7.0	1	1	1	3
F2L	20.5	3	2	2	7
G1R	6.5	3	1	0	4
G2L	9.5	2	2	1	5

X1 Stickiness
X2 Plasticity
X3 Firmness

A scattergram of these data and the regression line is shown in Figure 5.3. Also shown is sample point E1R which appears to be an outlier. An estimate of the population variance was obtained using the relationship,

$$Est.SD^2_{pop} = \frac{\sum (x_i - M_{samp})^2}{(n-1)} \qquad [5.10]$$

in which, Est.$(SD^2)_{pop}$ = the estimate of the population variance,

FIGURE 5.3 Comparison of Plastic Index with Field Designations X1, X2 and X3

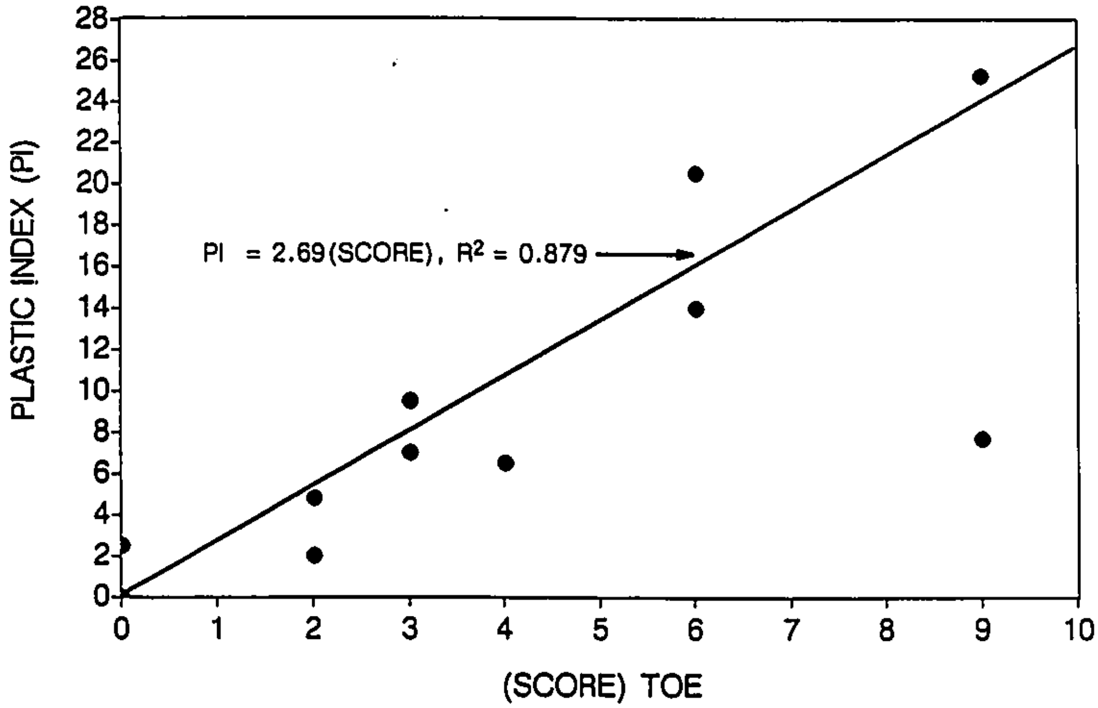

M_{samp}	=	the mean of the sample population, and
n	=	the number of observations in the sample.

Equation 5.10 was applied to the SCORE intervals 2, 3, 6, and 9 for which 2 observations existed in each interval. The approximated standard deviation (SD) was determined from the estimated variance and curves representing 1 SD departure from the regression line were fitted by eye. On this basis it was estimated that the sample point E1R lies beyond 2 standard deviations from the regression line and it was omitted from the regression analysis.

As a verification, three other methods were used to estimate PI for sample E1R. Firstly, sample E1R was classified as a clay loam of high plasticity (X2 = 3, LL = 59.7). According to the Unified Soil Classification System inorganic clays of high plasticity (LL > 50) are designated as CH on Cassagrande's plasticity chart (Holts and Kovacs, 1981). The plastic limit of soils in this category is described by the relation,

$$PI = 0.73(LL\text{-}20) \qquad [5.11]$$

where ($50 \leq LL \leq 100$). Using Eqn. 5.11, PI for E1R would be $PI_{E1R} = 29$.

Secondly, Plastic Limit values for the Surrey samples were correlated with percent clay, percent silt-clay, and percent silt resulting in r_2 values of .81, .57, and .16 respectively. These data are presented in Table 5.6. A scattergram showing PI as a function of percent clay and the fitted regression equation is provided in Figure 5.4. Using this relation PI_{E1R} = 14.8.

TABLE 5.6

Correlation Of PI With Textural Class Data

Sample No.	Clay Cl (%)	Silt Si (%)	SiCl (%)	PI
C1L	52	42	94	25.3
C1R	3	7	10	2.5
D2L	8	57	65	2.0
D3L	17	37	54	4.8
D1R	11	42	53	14.0
F1L	12	32	44	7.0
F2L	35	57	92	20.5
G2L	21	44	65	9.5
G1R	13	19	32	6.5

Finally values of PI and percent silt-clay collected by Dunn (1959) as presented in Vanoni (1975) report a value of PI=11.3 for a percent silt-clay of $\%Cl_{E1R}$ = 69. Percent silt-clay in the Surrey samples was poorly correlated (r^2=.57) with PI however, the estimated value is still approximately 47 percent larger than the laboratory value.

All four of the above methods indicate that the laboratory

FIGURE 5.4 Plastic Index as a Function of % Clay

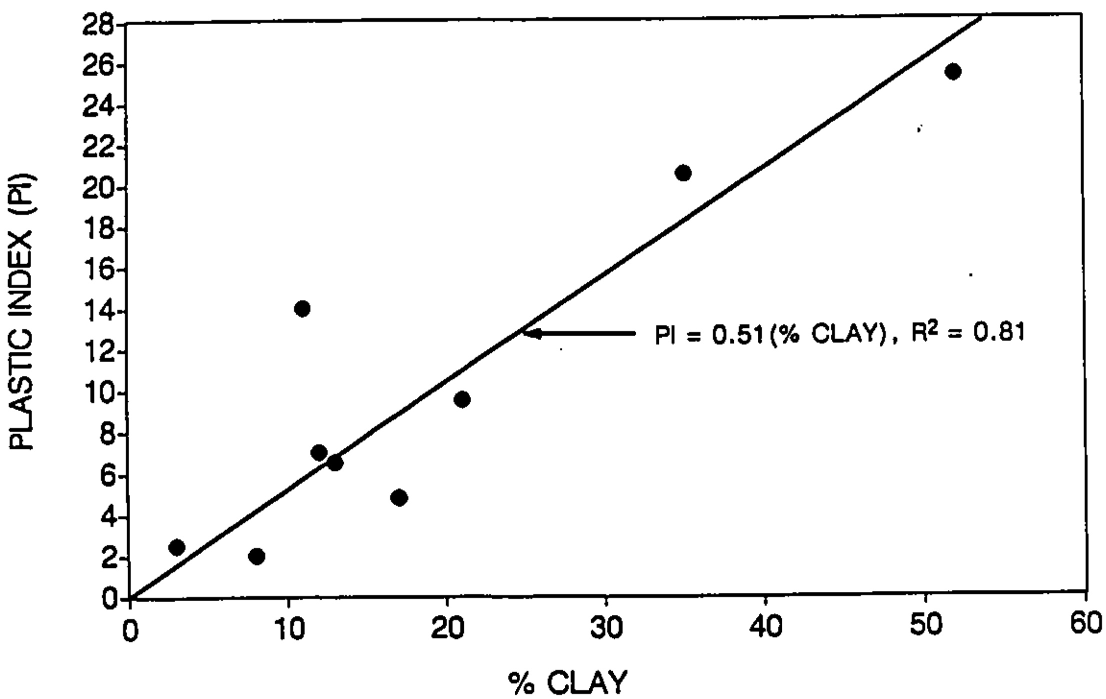

value of PI recorded for sample E1R is low and that it may be within the range $11.3 \leq PI_{E1R} \leq 29$. The value of PI_{E1R} as estimated from Figure 5.3 using values for SCORE falls within this range (PI_{E1R}=24).

The above analyses were performed to demonstrate that the parameter SCORE, which is a composite of field classifications of wet, moist and dry consistence, can be used as a measure of material resistance to scour. Accordingly, SCORE values may be used to compare the resistance to scour of bank stratigraphic units.

Using the SCORE parameter, correlations between W_R and the least resistant mid bank stratigraphic unit (Table 5.7) and composite bank samples (Table 5.8) were determined as,

$$(SCORE)_{BNK} = (X1 + X2 + X3)_{BNK} \qquad [5.12]$$

and

$$(SCORE)_{CMP} = (X1 + X2 + X3)_{CMP} \qquad [5.13]$$

in which, BNK = a subscript referring to the mid bank stratigraphic unit, and

CMP = a subscript referring to a composite sample comprised of all bank stratigraphic units.

The resulting correlation coefficients are compared to that obtained for $SCORE_{TOE}$ in Table 5.9. The relatively high correlation observed for $SCORE_{CMP}$ results from the overlap with bank toe stratigraphic units for unstratified banks (4 of the 7 cases). $SCORE_{CMP}$ for stratified banks was found to be a poor indicator of channel susceptibility to enlargement.

TABLE 5.7

Comparison Of The SCORE For The Least Resistant Mid Bank Stratigraphic Units With W_R

SAMPLE No.	W_R	FIELD DESCRIPTION MID BANK X1	X2	X3	SCORE MID BANK	RANK W_R	RANK MID
A3R	1.96	0	0	0	0	3	4
B1L	3.8	0	0	0	0	7	4
C1R	3.05	0	0	0	0	6	4
D2R	2.56	0	0	0	0	5	4
E1L	1.02	2	3	4	9	1	1
F3R	1.63	0	0	1	1	2	3
G2L	2.03	2	2	1	5	4	2

Table 5.9 indicates that the least resistant mid bank stratigraphic unit is not a good indicator of the susceptibility of the channel to enlargement in this case. A stronger correlation between channel response, as measured by W_R, was observed with the least resistant bank toe stratigraphic unit.

In Chapter 4 it was noted that urbanization produces a non-uniform increase in flow recurrence interval with the affect diminishing with return period. Further, the product of

TABLE 5.8

Comparison Of The SCORE For Composite Bank Samples With W_R

SECTION No.	W_R	FIELD DESCRIPTION COMPOSITE SAMPLE X1	X2	X3	SCORE (CMP)	RANK W_R	CMP
A	1.96	1.0	0.33	1.33	2.66	4	4
B	3.8	0.0	0.0	0.0	0.0	7	6
C	3.05	0.0	0.0	0.0	0.0	6	6
D	2.56	0.75	0.75	0.0	1.5	5	5
E	1.02	2	3	4	9	1	1
F	1.63	1.0	0.25	1.5	2.75	2	3
G	2.03	3	1	0	4	3	2

TABLE 5.9

Correlation Matrix Of W_R On SCORE Values For Least Resistant Bank Toe And Mid Bank Stratigraphic Units And Composite Bank Samples

SCORE	W_R (r^2)
TOE	.815
MID	.495
CMP	.743

frequency of occurrence and sediment transport rate indicates that the largest increase in effective work is for moderate flow events. These events reach depths of $y \leq .7\ y_{BNK}$ and consequently have less effect on mid bank stratigraphic units but a large impact on boundary materials in the bank toe region. This is consistent with the acceptance in the literature of basal scour as the dominate channel forming process and points to the relative importance of the bank structure in the determination of channel form and response. This suggests that a point by point examination of scour potential may be required to properly assess instream erosion hazard for channels formed in stratified deposits.

CHAPTER 6

PREDICTION OF CHANNEL RESPONSE

6.1 Introduction

An alluvial channel experiencing an alteration in the prevailing sediment and hydrologic regimes due to urbanization, may respond by,

a) altering roughness and thalweg alignment,
b) adjusting channel plane form geometry, and
c) downcutting (bed degradation).

Alteration of roughness and thalweg alignment are relatively rapid adjustments which tend to precede changes to channel hydraulic and plane form geometry. The later two responses tend to occur only after a twenty percent paving of the watershed and they also tend to occur simultaneously but on different temporal scales. Alteration of hydraulic geometry representing an intermediate channel response while changes in plane form geometry occur over the long term.

The actual response of the channel will vary with:

i) stream competence, as defined by the diameter of the largest particle transportable by the stream (ϕ_{MAX}), in relation to sediment supply and boundary material composition; and,

ii) the relative resistance of the bed and bank materials to scour.

In Chapter 5 the importance of the basal stratigraphic unit in the surveyed streams was discussed. It was also noted during the survey that the relative resistance of the bed and bank materials may control the initial response of the channel while ultimate channel form is controlled by stream competence in relation to sediment load characteristics.

Recall that Laursen (1952), expressed the rate of scour as the difference between the capacity for transport out of the scoured area and the influx or rate of supply to the area. This was written as,

$$\frac{df(B)}{dt} = g(q_S)_o - g(q_S)_I \qquad [6.1]$$

in which, $df(B)/dt$ = the change in bed geometry,
$g(q_s)_o$ = sediment transport out of a control section, and
$g(q_s)_I$ = sediment supply to the control section from upstream.

Three possible scenarios were identified using this model,

i) $df(B)/dt > 0$, bed scour (Erosion Patterns),
ii) $df(B)/dt = 0$, stable bed, and
iii) $df(B)/dt < 0$, aggrading bed (Sedimentation Patterns).

Equation 6.1 was developed from work on scour by jets and is essentially one-dimensional. However, it provides a useful basis from which to examine possible response scenarios for an alluvial channel with erodible banks. The following discussion is centred around the response of the stream to the cases of $df(B)/dt > 0$ (erosion by scour) and $df(B)/dt < 0$ (instability due to aggradation).

6.2 Erosion Patterns

In this discussion bank erodibility refers to the bank toe stratigraphic unit which is least resistance to scour. Bed erodibility refers to the resistance of the intact or armoured bed material. Bed forms composed of reworked (loose) alluvium overlying the intact bed materials are referred to as alluvial sediments.

In terms of the relative erodibility of the bank and intact bed materials three conditions may be considered,

i) CASE 1: $(q_S)_{BED} > (q_S)_{TOE}$,

ii) CASE 2: $(q_S)_{BED} = (q_S)_{TOE}$,

iii) CASE 3: $(q_S)_{BED} < (q_S)_{TOE}$

in which, $(q_S)_{BED}$ = the sediment transport potential associated with the intact or armoured bed material, and

$(q_s)_{TOE}$ = the sediment transport potential associated with the least resistant bank toe stratigraphic unit.

CASE 1 represents the condition where bed degradation (downcutting) exceeds bank retreat due to basal scour (undercutting). In CASE 2, the rate of undercutting and downcutting are balanced. While in CASE 3, undercutting predominates.

Each of these three cases may be further divided to account for bank structure. Since bank form is principally controlled by the bank toe stratigraphic unit (Chapter 3), the bank was divided into two units: one characterizing the bank toe and the other unit representing the remainder of the bank. From this structure three alternatives may be considered for each CASE,

a) $(q_s)_{TOE} < (q_s)_{BNK}$

b) $(q_s)_{TOE} \geq (q_s)_{BNK}$

c) $(q_s)_{TOE} > (q_s)_{BNK}$

where, $(q_s)_{BNK}$ = the sediment transport potential associated with the bank materials above the bank toe stratigraphic unit.

Table 6.1 summarizes the probable initial response of the stream channel, in terms of hydraulic geometry, to an increase in flow magnitude and frequency associated with urbanization for an horizontally bedded alluvial channel with erodible banks. These responses are schematically illustrated in Figures 6.1 (a) to (c) for CASEs 1 to 3 respectively. In those CASEs where the rate of bank toe recession controls bank stability, $(q_S)_{TOE} \geq (q_S)_{BNK}$, the bank toe stratigraphic unit is representative of the bank in general and $(q_S)_{BNK}$ need not be considered further.

CASE 1: $(q_S)_{BED} > (q_S)_{TOE}$ results in preferential degradation of the bed (downcutting), leading to a decrease in channel bed elevation ($Y_{ELV}\uparrow$) and subsequently, valley formation.

CASE 2: $(q_S)_{BED} = (q_S)_{TOE}$, initially width ($w\uparrow$) may increase and bed elevation may decrease simultaneously until the increase in width reduces flow depth ($y\downarrow$) and boundary shear stress on the bed to the point where degradation ceases.

CASE 3: $(q_S)_{BED} < (q_S)_{TOE}$, basal scour dominates resulting in an increase in channel width ($w\uparrow$). This initial response is illustrated diagrammatically in Figure 6.2.

Following this initial response, ultimate channel form is controlled by the characteristics of the sediment load relative to stream competence. Sediments transported into the

TABLE 6.1
Summary Of Probable Initial Channel For General Cases Of Bed Versus Bank Stability

Case	Scenario	Principal Form of River Development	Principal Bank Process
1	$(\tau_{CRT})_{BED} < (\tau_{CRT})_{BNK}$ — $(\tau_{CRT})_B < (\tau_{CRT})_C$; $(\tau_{CRT})_B > (\tau_{CRT})_C$; $(\tau_{CRT})_B \gg (\tau_{CRT})_C$	Valley Formation (downcutting)	Rate of Downcutting Controls Bank Stability - Slump, and Rotational Failure
2	$(\tau_{CRT})_{BED} \geq (\tau_{CRT})_{BNK}$ — $(\tau_{CRT})_B < (\tau_{CRT})_B$; $(\tau_{CRT})_B > (\tau_{CRT})_B$; $(\tau_{CRT})_B \gg (\tau_{CRT})_B$	Valley Formation (downcutting	Rate of Downcutting Controls Bank Failure, but intermediate bank forms are dependent on: $(\tau_{CRT})_B < (\tau_{CRT})_C$; $(\tau_{CRT})_B \geq (\tau_{CRT})_C$; $(\tau_{CRT})_B \gg (\tau_{CRT})_C$
3	$(\tau_{CRT})_{BED} \gg (\tau_{CRT})_{BNK}$ — $(\tau_{CRT})_B < (\tau_{CRT})_B$; $(\tau_{CRT})_B \geq (\tau_{CRT})_B$; $(\tau_{CRT})_B \gg (\tau_{CRT})_B$	Plane Form Alteration	Rate of Basal Scour Controls Bank Stability shear, beam tensile failure Cantilever overhangs

For a definition of subscripts B and C refer to Fig. 6.1 (a).

control reach or contributed through erosion of the boundary materials represent a range of particle sizes resulting in three probable scenarios:

a) Even though $df(B)/dt > 0$, a small but appreciable portion of the particle size distribution characterizing the sediments ($C_c\phi$ for cohesive materials in which C_c is the coefficient of coagulation) entering the control reach exceed $(\phi)_{CRT}$. These materials become part of the bed material component as alluvial sediments. Since scour of the bed materials tends to preferentially remove the finer particles then a veneer of coarser materials develops.

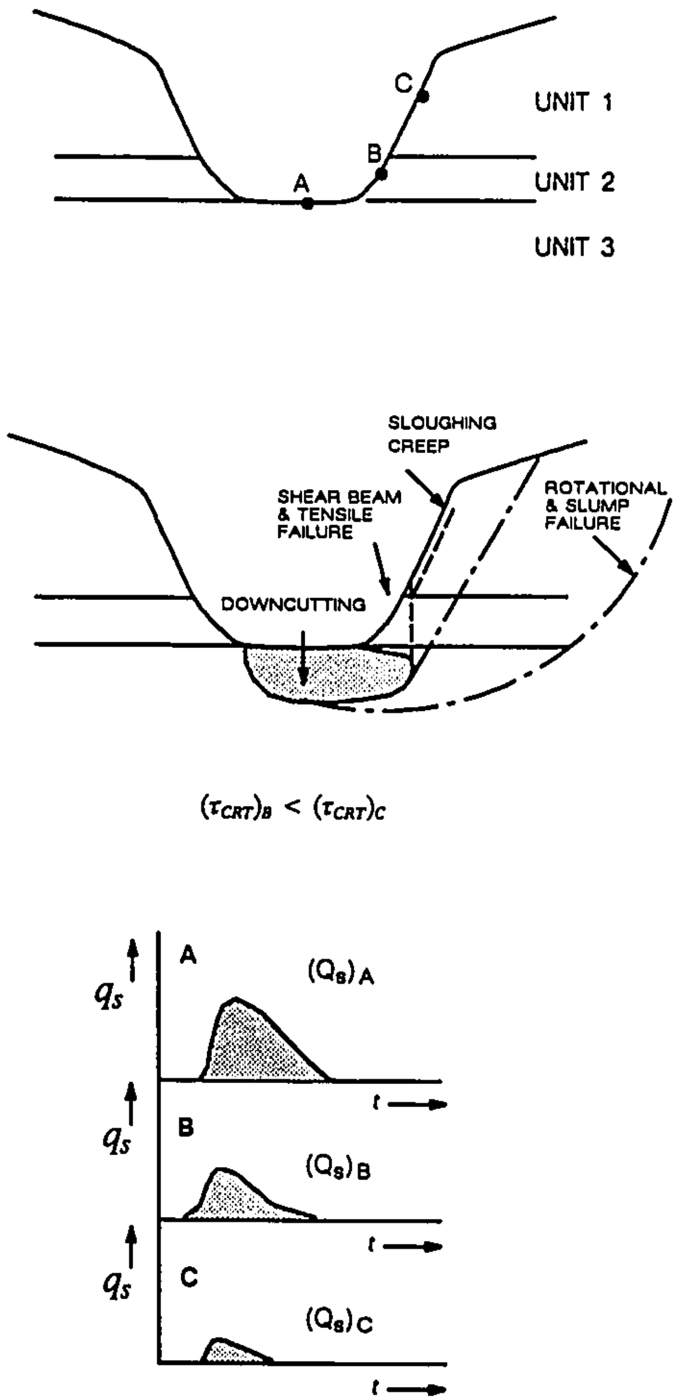

FIGURE 6.1a **CASE 1:** $(\tau_{CRT})_A < (\tau_{CRT})_{B,C}$ **For a Horizontally Bedded Alluvial Channel and Noting Disposition of Scour to Occur on One Side.**

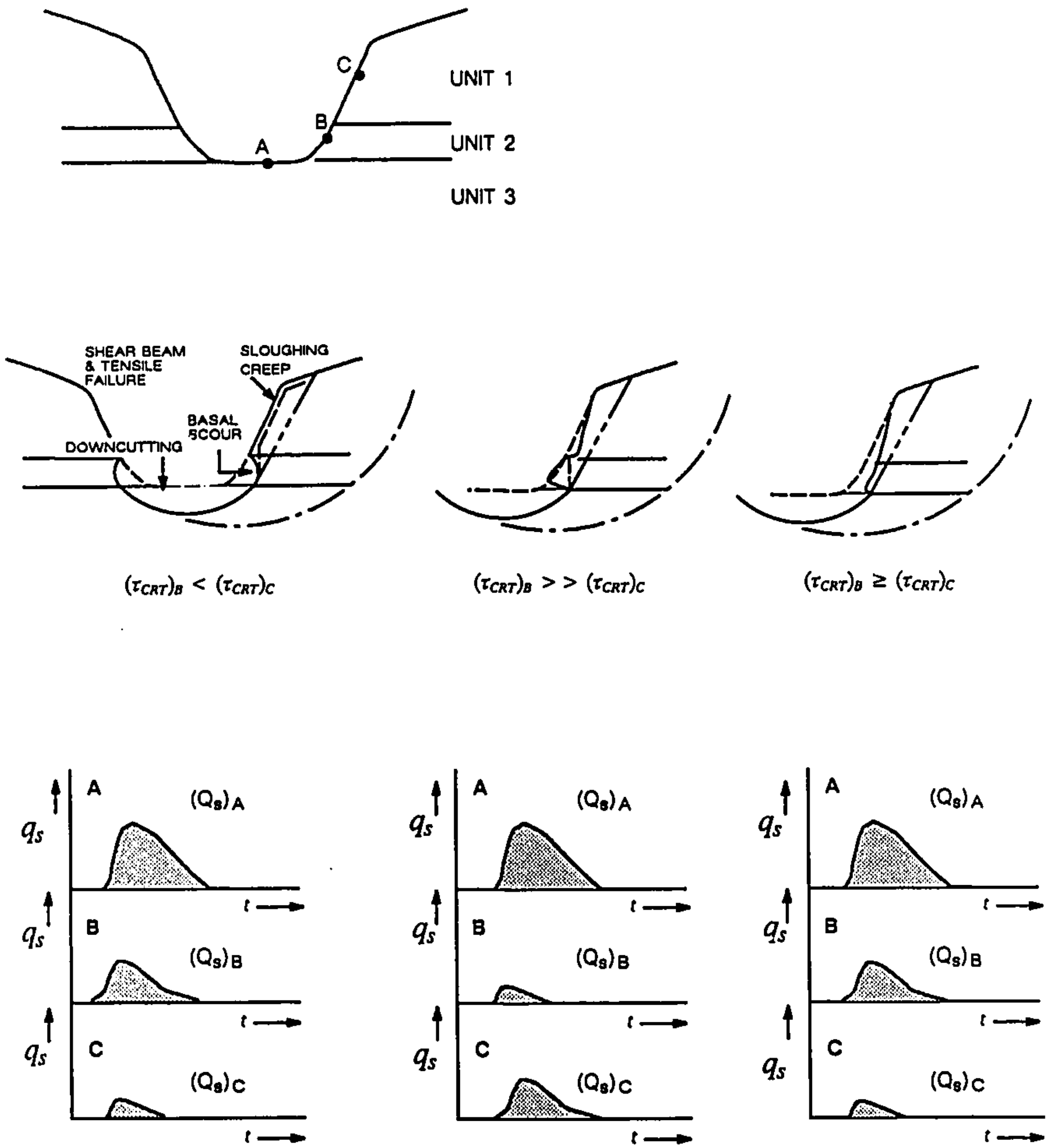

FIGURE 6.1b **CASE 2:** $(\tau_{CRT})_A \geq (\tau_{CRT})_{B,C}$ **For a Horizontally Bedded Alluvial Channel and Noting Disposition of Scour to Occur on One Side.**

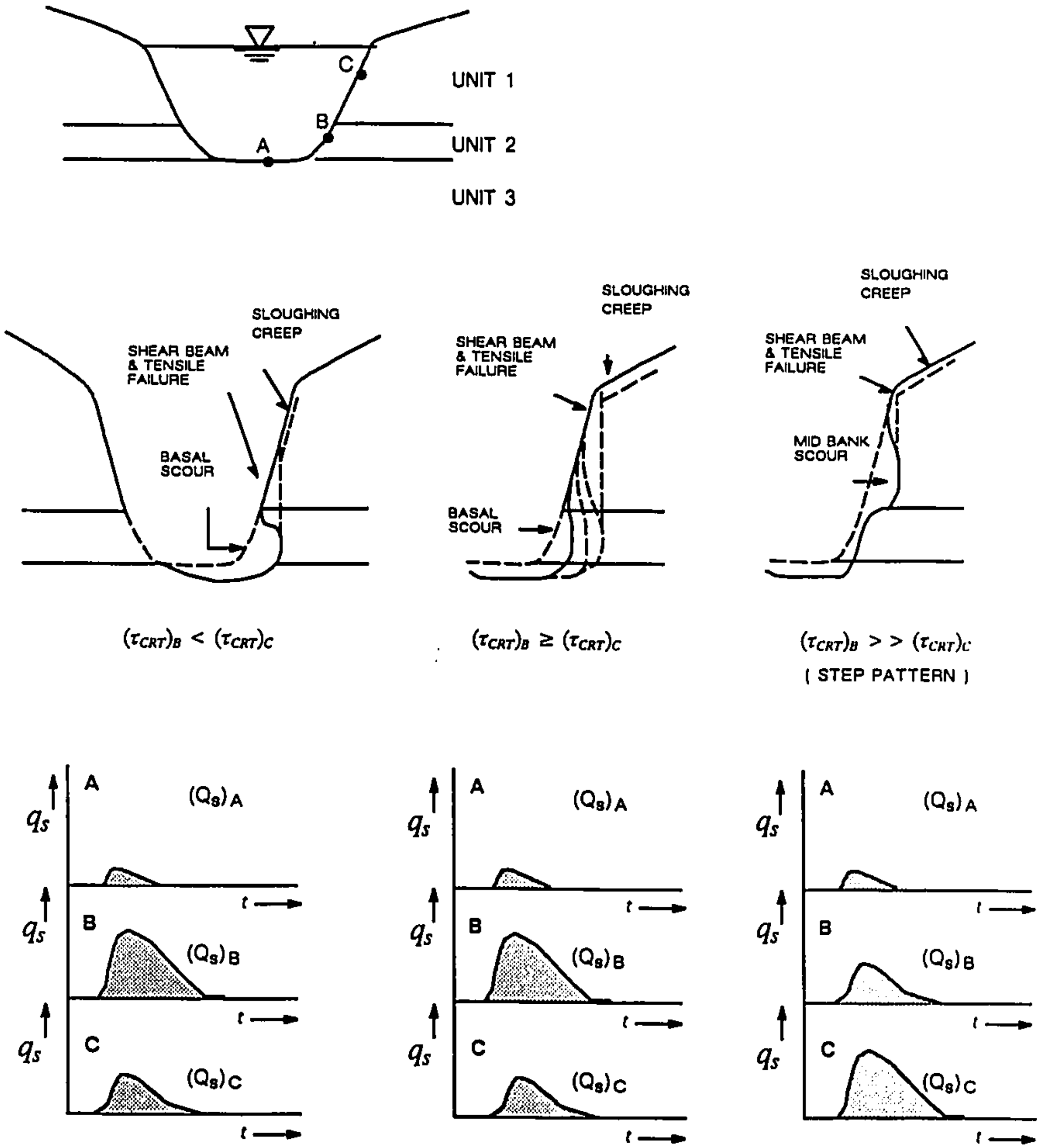

FIGURE 6.1c CASE 3: $(\tau_{CRT})_A >> (\tau_{CRT})_{B,C}$ **For a Horizontally Bedded Alluvial Channel and Noting Disposition of Scour to Occur on One Side.**

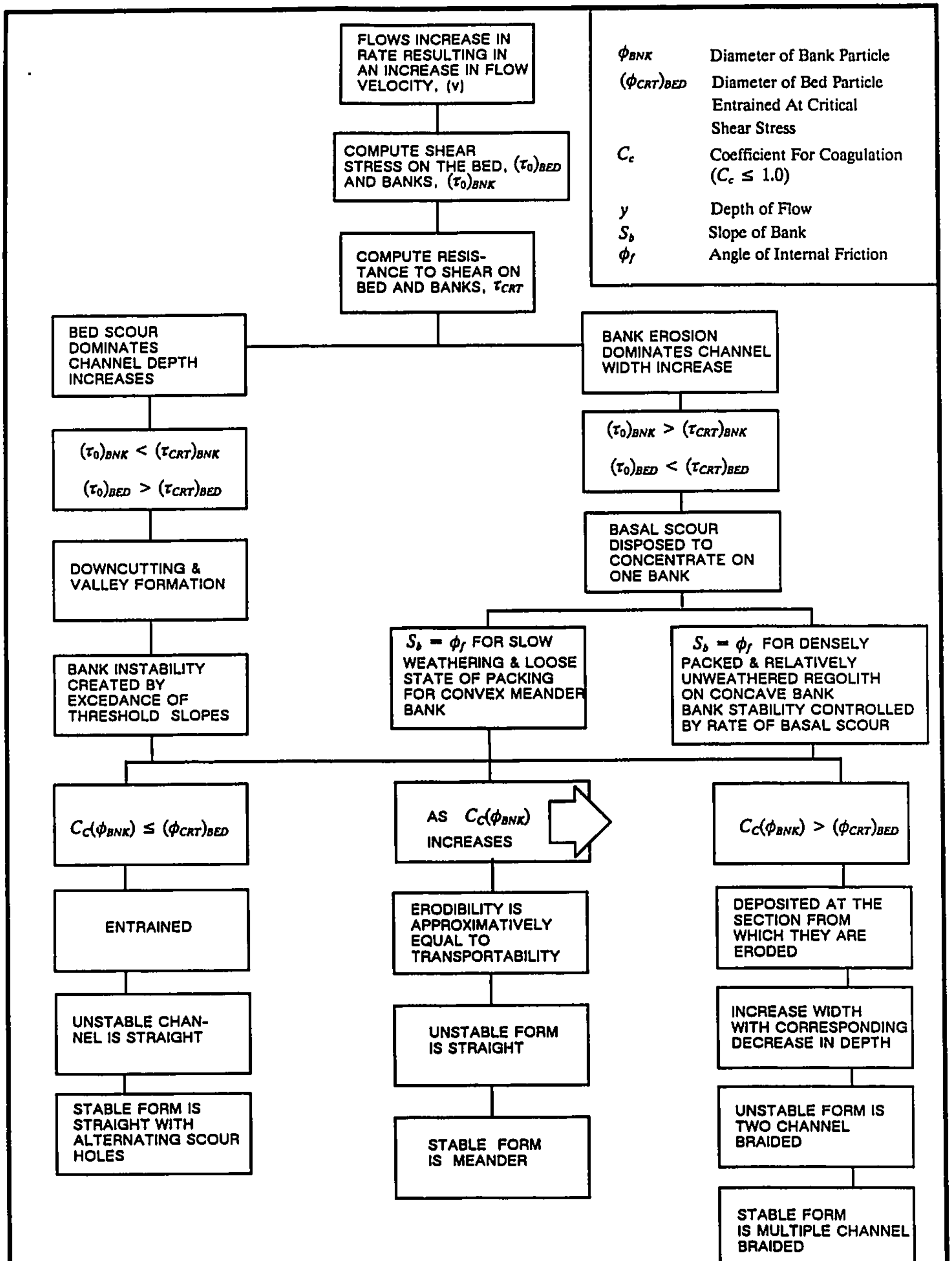

FIGURE 6.2 Erosion Patterns

b) The portion of the particle size distribution which exceeds ϕ_{CRT} is large and the volume of sediments is large then aggrading conditions would develop and sedimentation patterns would dominate (Section 6.3).

c) The portion of the particle size distribution exceeding ϕ_{CRT} is not appreciable and degradation of the bed would persist until an adjustment of the channel hydraulic and plane geometries, and/or a more resistant stratigraphic unit was encountered which were sufficient to reduce bed scour potential to $(q_S)_{BED} < (q_s)_{TOE}$.

These responses are also illustrated in Figure 6.2.

6.3 Sedimentation Patterns

Under aggrading conditions the influx of sediment exceeds the ability of the stream to transport the sediment out of the control reach. Under such circumstances there is an effective increase in the bed elevation $((y_{ELV})_{BED}\uparrow)$ and a concomitant increase in the flow elevation $((y_{ELV})_{FLW}\uparrow)$. The alteration of the flow field increases the scour potential incident on the bank materials while reducing the scour potential on the bed. The short term response of the channel is to adjust roughness and thalweg slope. This is followed by an increase in channel width $(w\uparrow)$ through bank erosion. This later response is represented diagrammatically in Figure 6.3.

Channel width may increase in one of two means,

a) where $\tau_o \geq (\tau_{CRT})_{BNK}$, the channel may increase in width directly through basal scour, and

b) where $\tau_o < (\tau_{CRT})_{BNK}$, channel width increases by scour and avulsion.

In the first instance, basal scour is the primary mechanism for bank failure. The bank sediments are added to the sediment load and depending upon the particle size distribution in relation to transport capacity, a balance between entrainment and deposition will occur. Two primary conditions are foreseeable,

i) where an appreciable quantity of the bank sediments contribute to the armouring process the channel bed elevation $((y_{ELV})_{BED}, \uparrow)$ will continue to increase with a resulting increase in channel width ($w\uparrow$) until flow depth ($y\downarrow$) and the associated scour potential decreases to $\tau_o < (\tau_{CRT})_{BNK}$, or

ii) where entrainment predominates and the portion of the bank sediments contributing to armouring is very small then width increase ($w\uparrow$) until $\tau_o < (\tau_{CRT})_{BNK}$. Bed elevation is unaffected by bank sediments.

These adjustments are to channel hydraulic geometry within the boundary of the control reach. The conditions which precipitated the increase in bed elevation are controlled by upstream sediment sources and sinks. They will remain operative until,

a) an adjustment in plane form channel geometry, i.e. an increase in channel slope ($S\uparrow$) with a commensurate increase in meander wavelength ($\lambda\uparrow$) and a decrease in sinuosity ($P_\lambda\downarrow$), is sufficient to produce the condition $\tau_o \approx (\tau_{CRT})_{BED}$, and/or

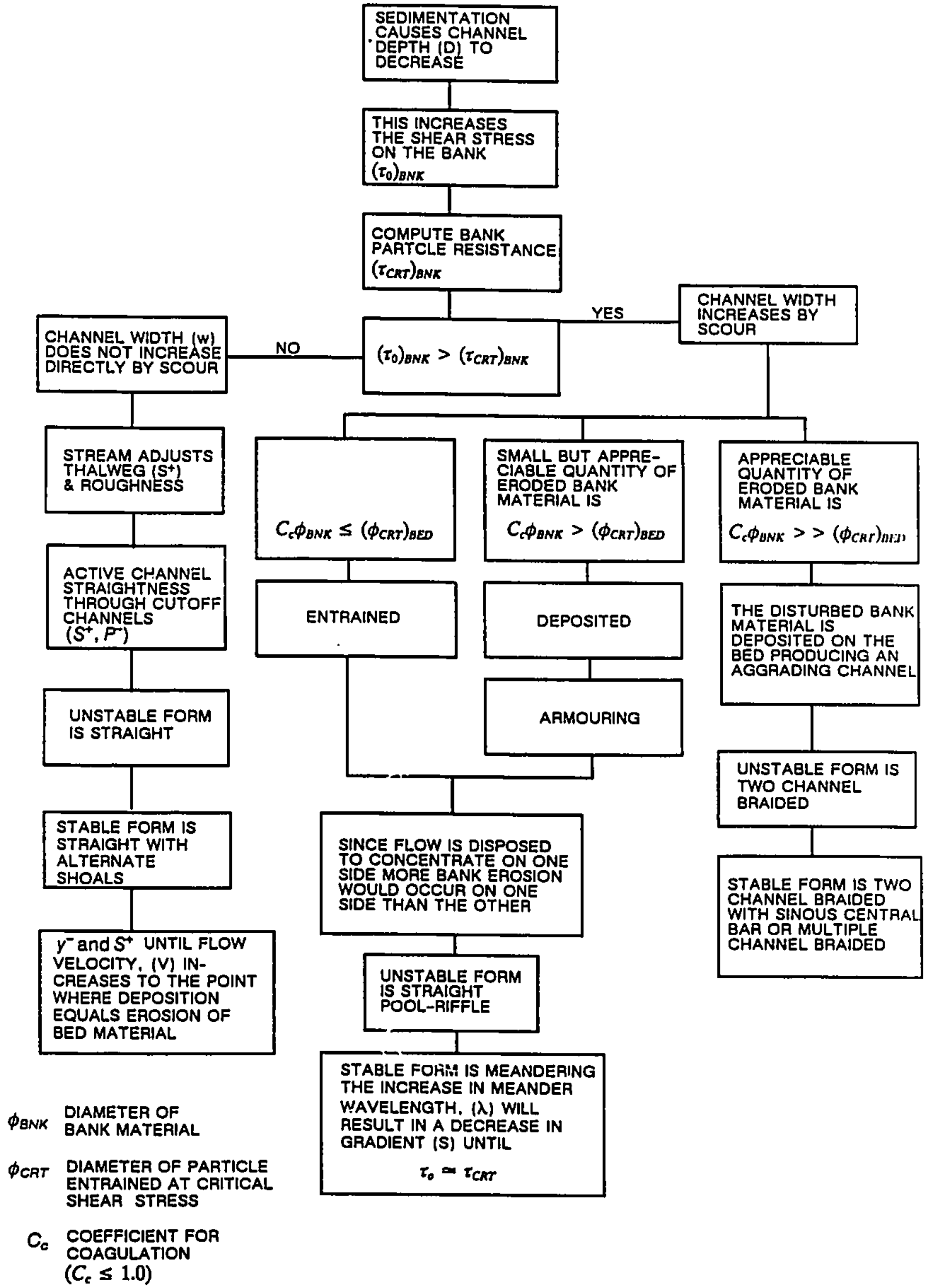

FIGURE 6.3 Sedimentation Patterns

b) there is a change in the independent variables, i.e. the upstream sediment load decreases ($Q_S\downarrow$) in relation to stream flow ($Q\uparrow$) approaching the condition $\tau_o \approx (\tau_{CRT})_{BED}$.

Avulsion represents a major change in channel direction and form due to scour in the overbank area by frequent overbank flows. The resulting formation of lateral channels and cutoffs eventually produces a wider and often straighter chanel. This was observed in a survey of Taylor Creek which is discussed in the following subsection.

6.4 Taylor Creek Survey

Taylor Creek downstream of St. Joseph Boulevard in Orleans, Ontario, is an example of stream responding to an alteration in the flow and sediment regimes in association with the development of the upper portion of the watershed. A qualitative assessment of channel stability was carried out in 1988, 2 years after large scale urbanization of the upland area was initiated (Figure 6.4). The stream represents a confined meandering system characterized by downstream migration of meanders and the resultant point-bar, pool-riffle morphology. Bank materials are typically fine grained and cohesive with some sand and gravel in alluvial deposits. Although the eroded materials are fine grained they are highly cohesive and tend to form aggregates ranging in diameter from a few millimetres to the size of a small stone.

A 5-year storage facility on Taylor Creek just upstream of the survey reach was constructed for flow control. It was also used to provide sediment control during the construction phase. However, high sediment loads frequently filled the pond and diminished its effectiveness as a routing element. This produces a scenario approximating Eqn. 2.7,

$$Q^{+}, L^{+} \approx w^{+},\ y^{\pm},\ \lambda^{+},\ S^{\pm},\ P_{\lambda}^{-},\ F^{+} \qquad [6.2]$$

However, the proportion of sediment being added to the bed and the magnitude of the sediment load is such that sedimentation patterns dominate (Figure 6.3). Consequently, the situation is more adequately represented by Eqn. 2.11,

$$Q^{-}, L^{+} \approx w^{\pm},\ y^{-},\ \lambda^{\pm},\ S^{+},\ P_{\lambda}^{-},\ F^{+} \qquad [6.3]$$

Bank materials are susceptible to scour as observed in the field (Figure 6.4). Consequently, the condition $\tau_o > (\tau_{CRT})_{BNK}$ results in expansion of channel width ($w\uparrow$) directly by scour. This process will continue until flow depth decreases ($y\downarrow$) and the condition $\tau_o \approx (\tau_{CRT})_{BNK}$ occurs.

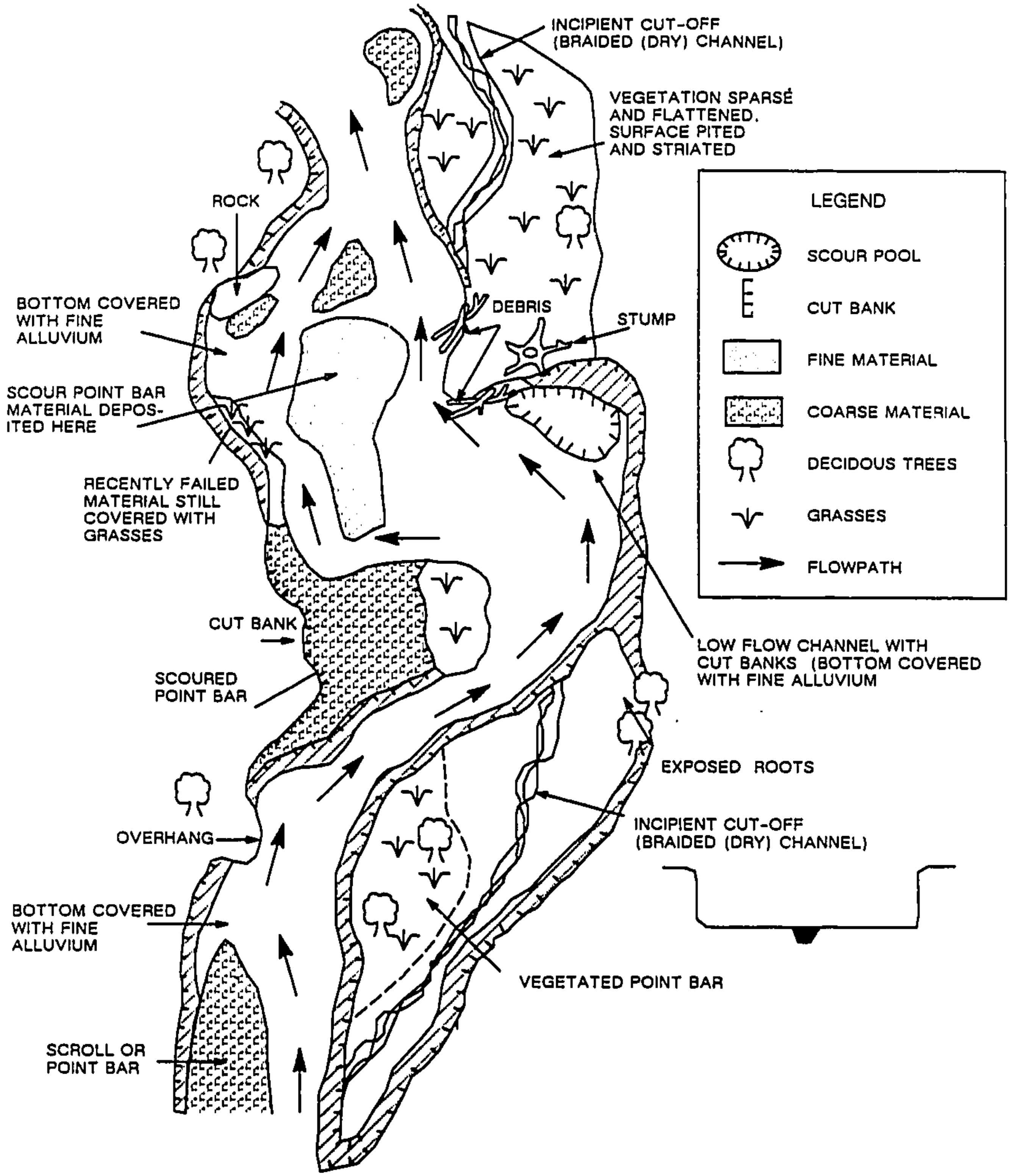

FIGURE 6.4 Schematic Showing a Channel in Apparent Transition as Suggested by Evidence of Undercutting and Avulsion Two Years After Urbanization.

The channel is also increasing slope ($S\uparrow$) through the short term adjustment of the thalweg. Avulsion, as seen in terms of incipient cutoff channels, will tend to straighten the channel and thereby increase slope. This process will continue until stream competence increase and the condition $\tau_o \approx (\tau_{CRT})_{BED}$ occurs.

Channel straightening also has the effect of reducing meander wavelength ($\lambda\downarrow$). Consequently, Eqn. 6.7 may be rewritten for Taylor Creek using the rational developed for sedimentation patterns as,

$$Q^+, L^+ \approx w^+,\ y^-,\ \lambda^+,\ S^+,\ P_\lambda^-,\ F^+ \qquad [6.4]$$

6.5 Summary

The response of a stream channel to an alteration in the independent variables of flow and sediment load may be interpreted in terms of the relative erodibility of bed and bank toe materials, and the characteristics of the sediment load in comparison to stream competence. Following adjustment of roughness and thalweg alignment, relative erodibility of bed and bank materials determines the initial channel response. Sediment characteristics relative to stream competence determines intermediate channel hydraulic geometry.

Long term channel geometry is determined by an adjustment of plane form and hydraulic geometry to stream competence and sediment load.

Figures 6.3 and 6.4 are proposed as systematic means for the interpretation of channel response to an alteration in the independent variables of flow and sediment load. The implication on the development of criteria for the design of erosion control facilities is the need to,

a) address the transverse variability in resistance to scour, and

b) the control of upland sediment supply.

CHAPTER 7

CONTROL PHILOSOPHY AND DESIGN APPROACH

7.1 Introduction

The general form of the proposed index for the measure of instream erosion potential is given is Eqn. 3.13 as,

$$(\Delta E_S)_P = \left[\int_0^T (f(q_S)_o - f(q_S)_I)dt\right]_{POST} - \left[\int_0^T (f(q_s)_o - f(q_s)_I)dt\right]_{PRE} \qquad [7.1]$$

where, $(\Delta E_S)_P$ = the change in scour potential at a point "P" about a channel perimeter,
T = the time interval,
$(q_s)_o$ = sediment transport rate into the control reach,
$(q_s)_I$ = sediment transport rate into the control reach from upstream sources,
POST = a subscript denoting post-development conditions, and
PRE = a subscript denoting pre-development conditions.

The transverse variation of the index is presented as a two-dimensional measure of the potential for channel deformation. The summation of the index about the channel perimeter yields an aggregate measure of the change in scour potential (Eqn. 3.14),

$$(\Delta E_S)_{AGG} = \int_0^{L_x} |(\Delta E_S)_P|\ dz \qquad [7.2]$$

where, $(\Delta E_S)_{AGG}$ = the aggregate change in scour potential

about a channel cross-section,
L_x = the length of the wetted perimeter, and
z = the transverse cross-sectional axis.

The control philosophy is predicated on the assumption that instream erosion potential will be minimized if the magnitude and transverse distribution of (ΔE_s) is held constant with pre-development conditions. This is represented by the condition $(\Delta E_s)_{AGG} \approx 0$ and represents a possible criteria for SWM design of storage facilities for instream erosion control.

7.2 Distributed Runoff Control

The magnitude and transverse distribution of (ΔE_s) is dependent on the degree of alteration of the flow field, the upstream sediment regime and the resistance and structure of the boundary materials. In terms of flow field alteration, the non-uniform increase in flood frequency causes the greatest increase in scour potential to occur for moderate flow events. The effect of the increase in scour potential associated with these events varies with the transverse distribution of material properties and bank structure.

A technique is proposed for the control of flow geometry which,

a) recognizes the contribution of the range of moderate through to bankfull flow events on channel form, and

b) distributes the degree of storage control by stage in proportion to the increase in scour potential.

The later point incorporates the transverse variation in bank material characteristics and bank structure. Consequently, the degree of storage control will vary from watershed to watershed depending upon the degree of alteration of the flow geometry and the structure and sensitivity of the bank materials to scour. Since the proposed technique considers the entire range of sub-bankfull flows and distributes storage control in a flexible manner, it is referred to as Distributed Runoff Control (DRC). The rational behind its application is demonstrated in the following general cases which cover a broad range of likely scenarios.

Figure 7.1 (b) is a schematic of the hypothetic distribution of (ΔE_S) under three general combinations of material resistance to scour in a channel formed in horizontally bedded material (Figure 7.1 (a)). Two bank stratigraphic units were considered as representative of bank erodibility (Chapter 6).

The first scenario satisfies the condition:

$$(\tau_{CRT})_{BNK} << (\tau_{CRT})_{TOE} << (\tau_{CRT})_{BED}.$$

In this scenario the greatest increase in (ΔE_S) is in the mid bank region. Control using the zero runoff increase stage-storage

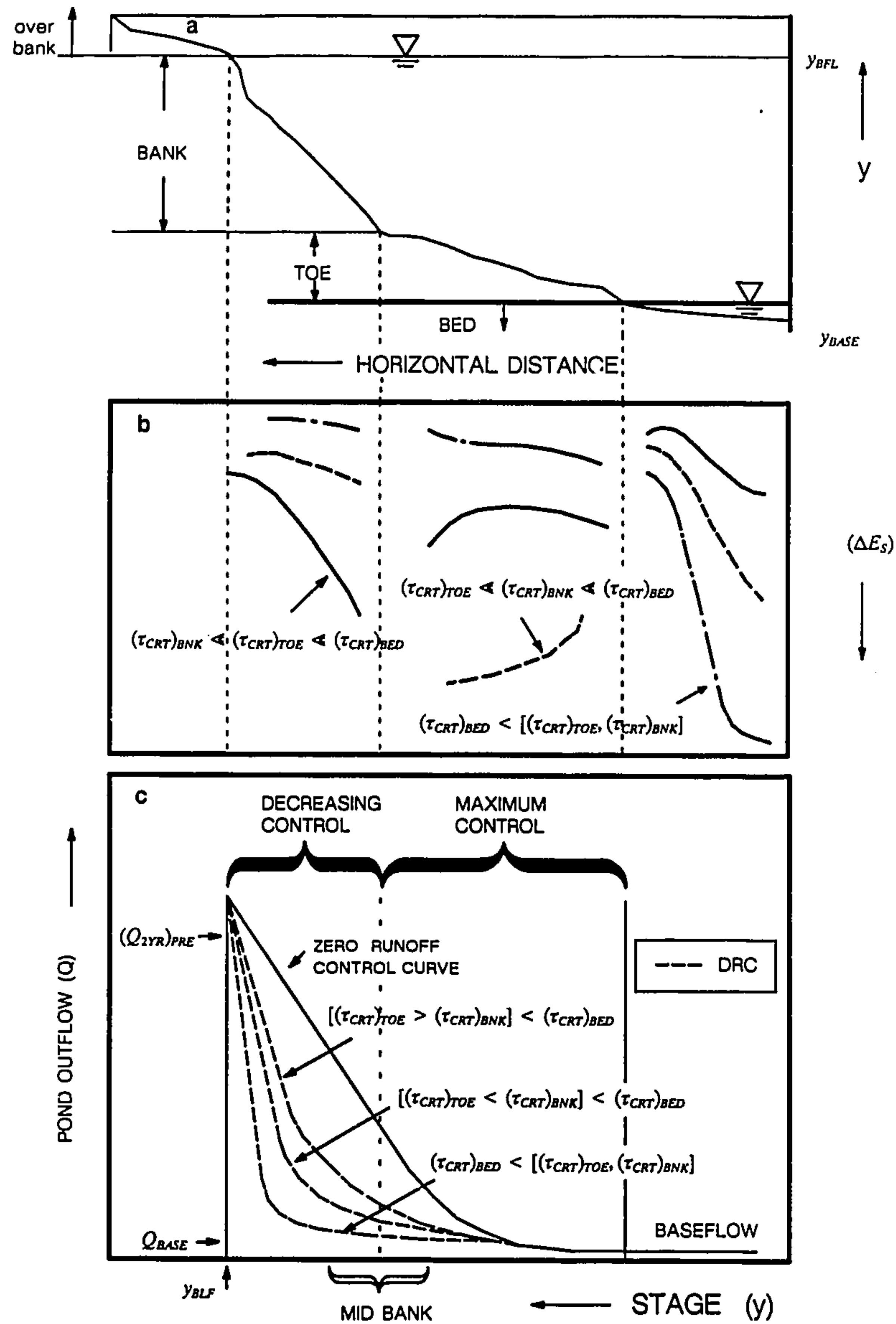

FIGURE 7.1 Schematic of Proposed Distributed Runoff Control (DRC) Approach.

curve is shown if Figure 7.1 (c). This curve is designed to match the pre- and post-development flood frequency curves but does not account for the increase in frequency or duration of flows. It consequently, under controls moderate flow events. To obtain the design condition $(\Delta E_S) = 0$, the degree of storage control must be increased for moderate flow events over that provided by the zero runoff increase curve. The greatest degree of control will now occur in the mid bank region then gradually decrease back to the zero runoff control curve for higher flow stages.

The second scenario describes the case:

$$(\tau_{CRT})_{TOE} << (\tau_{CRT})_{BNK} << (\tau_{CRT})_{BED}.$$

Maximum scour potential now occurs in the bank toe region. The greatest degree of control still occurs for mid bank flows, however, the degree of control will increase over the pre-development case (Figure 7.1 (c)), because the influence of moderate flows is more pronounced on the lower stratigraphic unit by virtue of the higher frequency and magnitude of inundation. The degree of control is then relaxed back to the zero runoff control curve for high stages.

The third condition:

$$(\tau_{CRT})_{BED} \leq [(\tau_{CRT})_{TOE}, (\tau_{CRT})_{BED}],$$

describes a relatively erodible bed material with resistant banks. Again the higher frequency and magnitude of inundation of the bed materials by moderate flow events will require a further increase in the degree of control for these events relative to the previous two cases (Figure 7.1 (c)). The degree of control is again relaxed back to the zero runoff control curve for higher stages.

These three scenarios serve to describe a basis for determining the slope of the maximum control portion of the stage-discharge curve. Bank structure determines where the zone of decreasing control begins (Figure 7.1(c)). The total amount of storage required will vary with the degree of alteration of the runoff regime. Control is affected through manipulation of the hydraulic performance of the storage outlet structure. Table 7.1 shows a comparison of this approach to those currently in use.

The proposed method is applied in Chapter 10 to a channel formed in cohesive materials.

7.3 Summary

A criteria for the control of flow geometry is proposed based on the maintenance of the pre-development magnitude and distribution of a scour index. A procedure, referred to as Distributed Runoff Control, for the application of the criteria is proposed. This procedure recognizes the contribution of the range of sub-bankfull to bankfull flows that determine channel form, but distributes storage control

TABLE 7.1
Comparison Of Current Instream Erosion Control Design Methods With The Proposed Approach.

	2YR	OC	ZASTI	DRC
FLOW RATE	o	o	o	o
FLOW VOLUME			o	o
SEDIMENT TRANSPORT RATE			o	o
DISCRETE EVENT	o	o	o	
MULTIPLE EVENT				o
1-D	o	o	o	
2-D				o
BANK STRUCTURE				o

2YR = Zero Runoff Control
ZASTI = Zero Aggregate Sediment Transport Increase
OC = Over Control
DRC = Distributed Runoff Control

in proportion to the change in scour potential following urbanization. The proposed design procedure is referred to as Distributed Runoff Control.

CHAPTER 8

DEVELOPMENT OF ANALYTICAL MODELS

8.1 Introduction

A quantitative tool was required for derivation of the two-dimensional excess boundary shear stress index. This was achieved in a two phase approach. The first step was to develop a computer model for the computation of boundary shear stress which would incorporate secondary currents and boundary effects. The model required the ability to determine boundary shear stress about the perimeter of an asymmetric channel of generally trapezoidal, rectangular or elliptical form, in any combination, in order to approximate natural channels. The output from this model was then used as input to an existing continuous hydrologic simulation model. This model was modified to determine the cumulative magnitude and transverse distribution of the index. The development of these models is described briefly in this charter. A more detailed description of the shear stress model is provided in Appendices B and C. The hydrologic model is described in Rowney and MacRae (1991 (a) and (b)). Specific modifications to the model are presented in Appendices D to G.

8.2 Determination Of Boundary Shear Stress

The transverse distribution of boundary shear stress for natural river sections is typically approximated by assuming a distribution derived from flume studies of prismatic channels or mathematical techniques which do not account for secondary currents. While many natural channels do approximate a trapezoidal configuration, urban streams often involve the study of small asymmetric channels where boundary and secondary current effects significantly modify the flow field.

A technique for the determination of shear stress based on a mathematical procedure for the computation of three-dimensional flow velocity and shear in open channels has been presented by Chiu and Chiou (1986). This technique was transformed into a computer language for application in this research.

The adopted approach has several advantages over current methods,

a) the three-dimensional distribution of flow velocity more accurately represents the flow field in a small urban channel,

b) it incorporates the affect of circulating "secondary" flow which operate in the transverse direction to the primary flow field, and

c) it allows for the modelling of the distribution of boundary shear stress over the entire perimeter of the active channel.

This representation of boundary shear stress is obtained through calibration of the model to an observed velocity field. Details concerning the modelling approach are described in Appendix B together with test applications. The User's Manual describing input requirements and output files is presented in Appendix C.

8.3 Continuous Simulation Modelling

There are several well conceived quantity/quality continuous hydrologic simulation models which have gained wide acceptance in the Canadian water resource community as planning level tools. However, QUALHYMO (Rowney and Wisner, 1985), was selected for development in this research for the following reasons,

a) it is suitable for the comparative evaluation of a large set of land use/storm water management/conservation practices in a thorough and systematic manner,

b) it employs a simplified approach while providing a level of analyses comparable to that obtained using more complex models for most applications, and

c) the pond routine was developed for the evaluation of Storm Water Management practices.

It was also written in modular form and suitable for modification and further development as a practical engineering tool.

8.3.1 Model Scope

For the purposes of this research the following major extensions were added to the model,

a) a routine (SHEAR1, Appendix D) for the determination of an index measuring scour potential.

b) a reduced heat budget technique for snowmelt computations (Appendix E),

c) a simplified energy budget approach for soil freeze-thaw modelling (Appendix F),

d) a groundwater recharge relation for frozen soil conditions (Appendix G), and

e) an algorithm to account for the effects of snow removal and disposal operations,

With the inclusion of these extensions the model now includes functional algorithms for the continuous simulation of,

- flow rate and volume (runoff from rainfall and snowmelt),
- sediment and constituent concentrations and mass,
- instream erosion potential,
- pond (reservoir) routing,
- stream routing, and
- baseflow from groundwater exfiltration.

These functions are grouped into various model commands as illustrated in Figure 8.1. The conceptual formulation of the model is shown in Figure 8.2. Testing and validation of the model is reported in Rowney and MacRae (1991 (b)).

8.3.2 Modelling Concept

In terms of hydrologic concept QUALHYMO is based on a lumped, hydrologic budget approach with unit hydrograph procedures for overland flow routing and hydrologic techniques for stream/reservoir routing. First order decay constituents are simulated using buildup-washoff or rating curve methods. Upland sediment generation is based on a rating curve approach. Instream erosion potential was addressed by incorporating the cumulative bedload transport function based on shear stress concepts described in Chapter 3. A comparison of QUALHYMO (Version 2.1, Rowney and MacRae, 1991 (a)), with other commonly used models is given in Rowney and MacRae (1991 (b)).

Function	Command	Description
INITIALIZE	START	Begin run, sets span of run, defines rain and flow input file numbers, and sets pollutant simulationon or off.
	FINISH	Terminates run.
	POLLUTANT RATE	Establishes pollutant source calculation method and sets parameters for pollutant source calculation
GENERATE	GENERATE	Causes the simulation of catchment runoff and, optionally, of pollutant load generation by runoff and/or snowmelt.
	STORE	Converts flow gauge records to internal model format.
	SHEAR1	Calculates an index of instream erosion potential.
ROUTE	POND	Routes flows and, optionally, pollutants through a detention storage pond.
	REACH	Routes flows and, optionally, pollutants through a river reach using finite difference approach.
	ADD SERIES	Sums two flow and pollutant series.
	SPLIT SERIES	Divides a flow and pollutant series into two parts.
OUTPUT	PLOT SPAN	Plots flow or pollutants for a specified short period.
	DUMP PLOT	Plots all flow or pollutant records for one or two series.
	PRINT SPAN	Prints flow or pollutant for a specified short period.
	DUMP PRINT	Prints all pollutant and flow records for one series.
	CALIBRATE	Calculates some basic statistics comparing two pollutant or flow series.
	EXCEEDANCE CURVES	Calculates number and duration of flow or concentration exceedances.
	MAXFLW	Calculates the maximum annual or monthly flow series.

FIGURE 8.1 Model Commands Grouped by Function Available in QUALHYMO Release 2.1

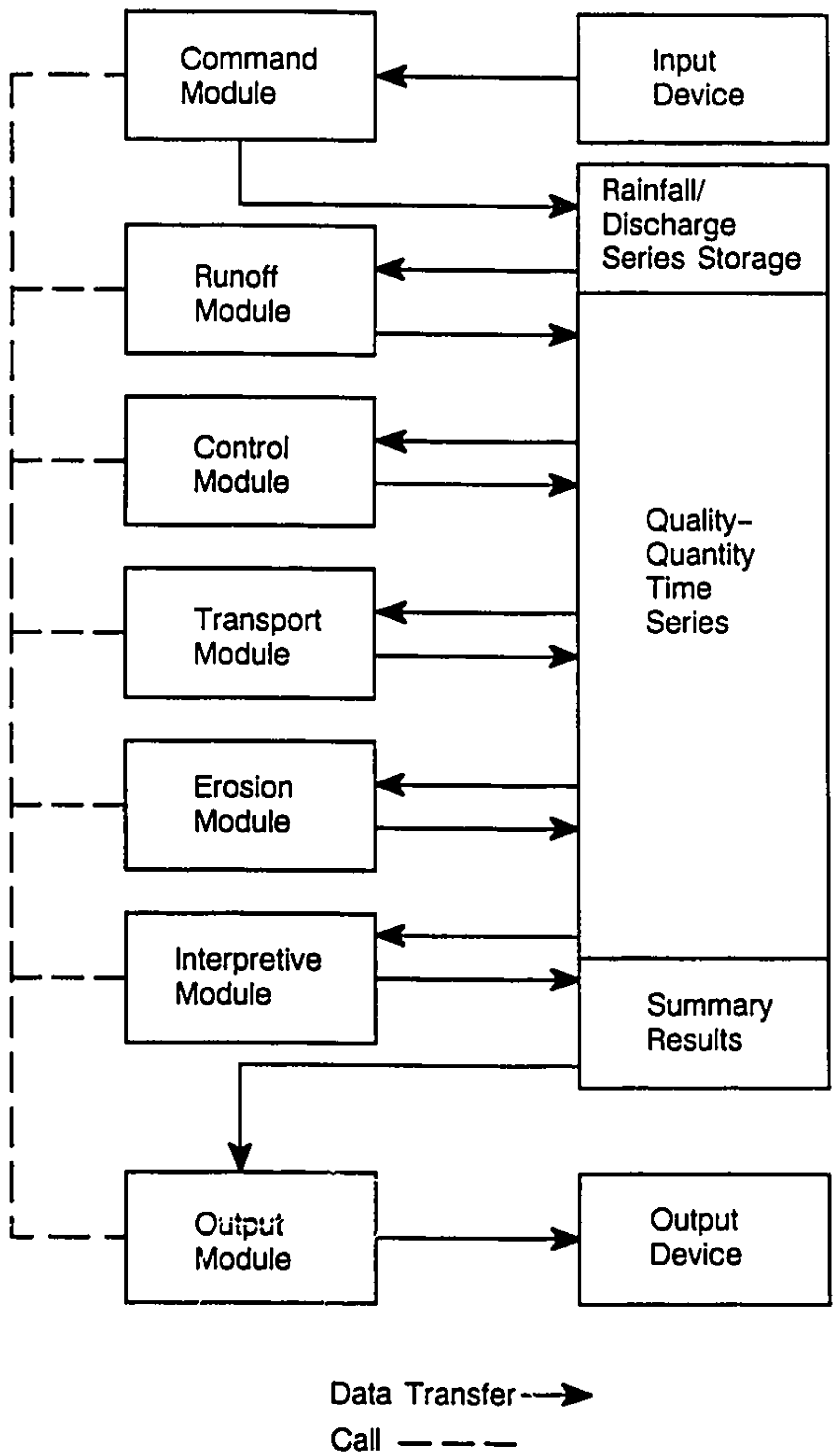

FIGURE 8.2 Conceptual Formulation of Program Components

CHAPTER 9

VALIDATION OF THE INDEX

9.1 Introduction

A change in flow characteristics resulting in a significant increase or decrease in the index should correspond to a real and parallel change in instream erosion hazard. To test the validity of the proposed index method MOBED was used to represent the real erosion hazard expressed in terms of change in bed elevation. If the indices provide a one to one mapping of index value with the magnitude of change of bed elevation than it may be deduced that the index approach provides a measure of boundary deformation for a one-dimensional case.

For this evaluation an explicit expression of the index was required. Several bedload sediment transport relations were considered and comparisons are reported below.

9.2 Relative Index Behaviour With Selected Sediment Transport Functions

The relative behaviour of the index was evaluated using four bed load sediment transport relations based on excess boundary shear stress (Eqns. 3.5 to 3.7 and 3.11). These transport functions were,

$$(EXTAU)_P : (q_S)_P = \int_0^T b_1 (\tau_e)_P \, dt \qquad (1)$$

$$(EVI)_P : (q_S)_P = \int_0^T b_2 (\tau_e)_P \tau_o \, dt \qquad (2)$$

$$(MPM)_P : (q_S)_P = \int_0^T m (\tau_e)_P^n \, dt \qquad (3)$$

$$(PWR)_P : (q_s)_P \propto (\Omega)_P = \int_0^T b_3 (\tau_e)_P \bar{v} \, dt \qquad (4)$$

in which,

EXTAU	=	excess boundary shear stress,
EVI	=	eroded volume indicator,
MPM	=	Meyer-Peter Muller bed load relation.
PWR	=	stream power relation,
τ_e	=	$(\tau_o - \tau_{CRT})$,
τ_o	=	instantaneous boundary shear stress at point P,
τ_{CRT}	=	critical shear stress,
b_1, b_2, b_3, m	=	empirically derived coefficients,
n	=	an empirically derived exponent,
v	=	average flow velocity,
Ω	=	stream power,

To evaluate these indices flow series were generated using the continuous hydrologic simulation model presented in Chapter 8. The model was set up for a hypothetical (51 ha) watershed. Land use was considered agricultural under pre-development conditions and mixed residential under future conditions (twenty percent paving of the basin). Hydrologic parameters were selected based on the calibration of QUALHYMO to urban watersheds (Rowney and MacRae, (1991(b)) and verified using relations developed by Leopold (1968) and Hollis (1975).

Four flow series were derived representing the following scenarios ,

a) present conditions (PRE),

b) future conditions without Storm Water Management (SWM) controls (POST w/o SWM),

c) 1:2 year pond control (2YR), and

d) 50 percent over control (50% OC).

The resulting hydrographs are illustrated in Figure 9.1. Pre-development flows represent the baseline condition. Post-development flows represent the alteration of the flow regime (Q^{+}) if no SWM controls for reduction of instream erosion protection are applied. The increase in Q_{2YR} was in the order of 3 times pre-development levels as expected for a twenty percent paving of the watershed (Hollis, 1975). The remaining two hydrographs represent conditions of reduced post-development peak flows with longer runoff durations.

A trapezoidal channel configuration (Figure 9.2) was adopted to be consistent with the MOBED analysis reported in Section 9.3. Shear stress distributions were determined using EROS1 which was calibrated using flume data, (Appendix B). The analysis was carried out for six flow depths (0.076 to 0.152

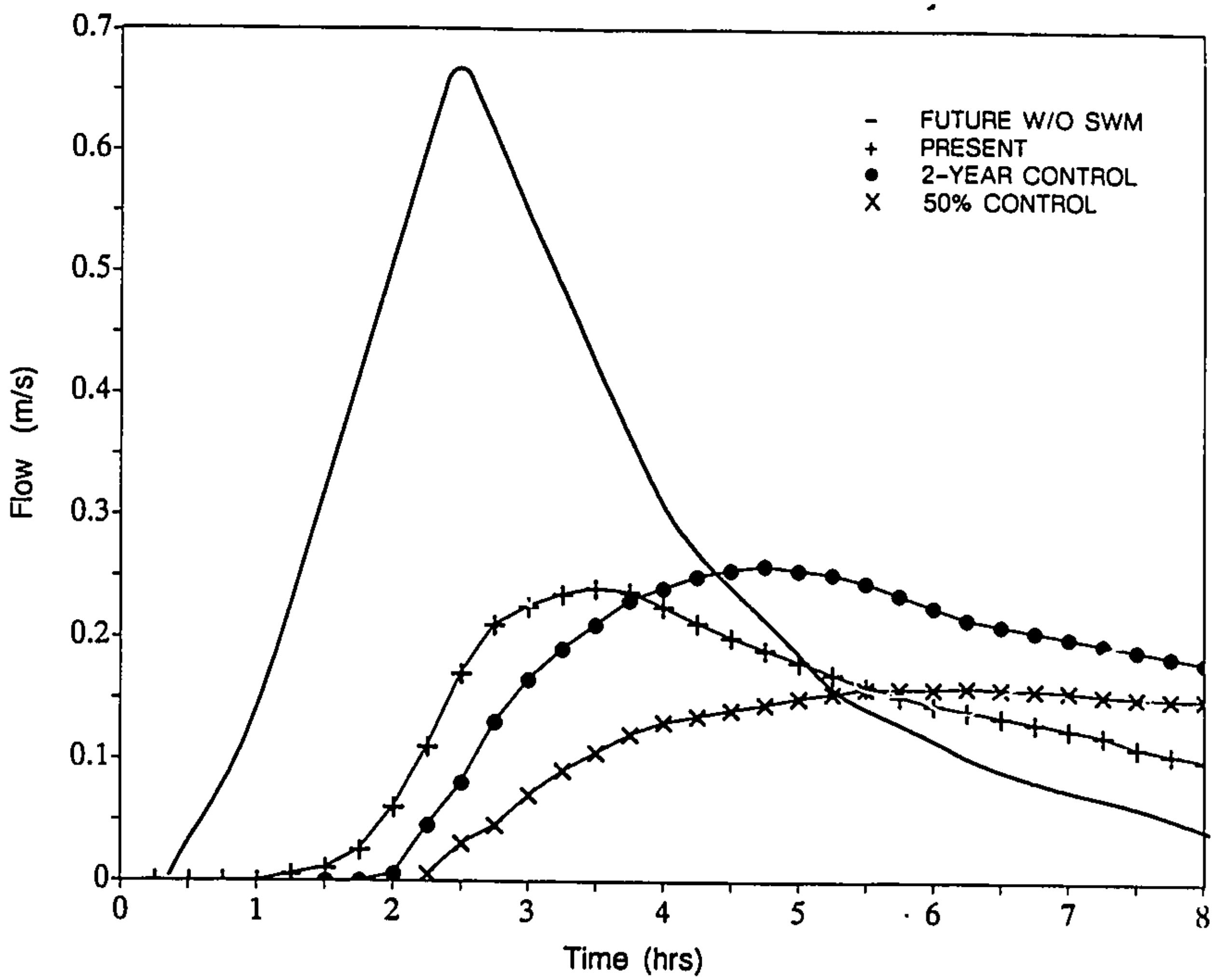

Figure 9.1 Selected Hydrographs for MOBED Analysis

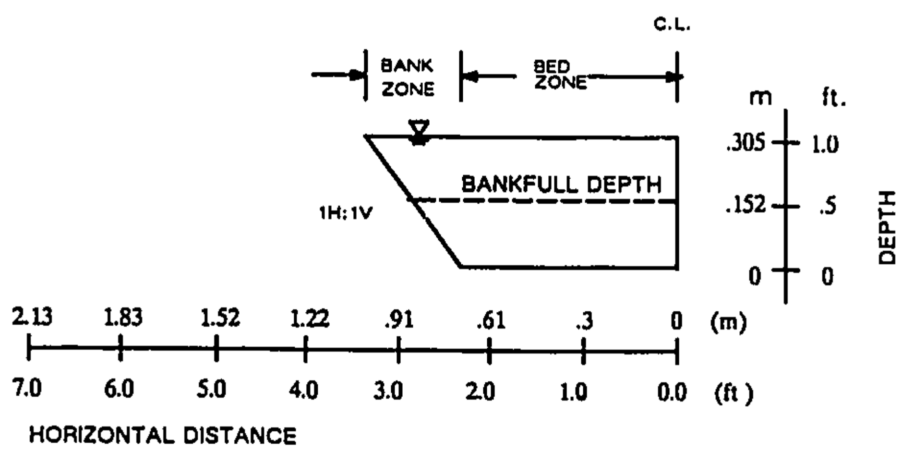

Figure 9.2 Idealized Trapezoidal Channel Semi-Perimeter with Completely Confined Overbank Area (1H:1V)

m). The resulting shear stress values are summarized in Table 9.1.

Table 9.1

Boundary Shear Stress Versus Depth For Selected Bed-Bank Stations In A Trapezoidal Channel

BED-BANK	DEPTH (m)					
STATION	0.152	0.137	0.122	0.107	0.091	0.076
1	5.621	4.908	4.324	3.739	3.184	2.671
3	5.310	4.711	4.175	3.629	3.103	2.605
5	4.300	3.969	3.572	3.174	2.758	2.317
7	1.590	1.776	1.643	1.571	1.393	1.082
8	0.991	1.092	0.915	0.771	0.589	0.254
11	1.121	2.006	1.805	1.523	1.331	1.087
13	2.787	2.610	2.413	2.102	1.896	1.657
15	3.361	3.103	2.849	2.490	2.193	1.906
17	3.687	3.285	2.921	2.452	1.992	1.599
19	3.610	2.973	2.437	1.896	1.302	0.938
21	3.117	2.298	1.618	1.135	0.752	0.000
23	2.308	1.417	0.982	0.795	0.000	
25	1.575	0.991	0.800	0.000		
FLOW (m^3/s)	0.245	0.205	0.169	0.135	0.104	0.077

These data were used to derive power functions of the form,

$$\tau_o = a(y-BED)^b \qquad (5)$$

in which, a = a coefficient,
b = an exponent,
YBED = the height on the bank/bank station, and
y = the depth of flow measured at the y-axis (Fig. 9.1).

The resulting relations are summarized in Table 9.2 and presented graphically for selected stations in Figure 9.3.

Table 9.2

Summary Of Boundary Shear Stress Relations for A Trapezoidal Channel (1H:1V)

BED-BANK STATION	a	YBED (m)	b	r^2
1	40.98	0.0	1.065	0.998
3	36.14	0.0	1.024	0.999
5	23.34	0.0	0.894	0.999
7	5.47	0.0	0.592	0.765
9	46.56	0.0	1.913	0.844
11	14.06	0.0	0.989	0.993
13	10.29	0.015	0.655	0.995
15	11.52	0.03	0.587	0.996
17	16.45	0.046	0.674	0.996
19	20.51	0.061	0.756	0.978
21	25.14	0.076	0.856	0.961
23	15.54	0.091	0.741	0.871
25	9.01	0.107	0.592	0.878

Terms are as defined for Eqn. 9.6 with the exception of r^2 which represents the square of the correlation coefficient.

Channel materials were specified as sand (diameter = 0.000944 m). Critical shear stress for cohesionless quartz particles in clear water is τ_{CRT}=0.48 Pa based on Shield's mean sediment size curve for uniform sand (Vanoni, 1975). The U.S. Bureau of Reclamation procedure gave values ranging from τ_{CRT}=1.92 Pa for clear water to τ_{CRT}=4.21 Pa for a high sediment load for the same particle size. The analysis was repeated using all three values of τ_{CRT}.

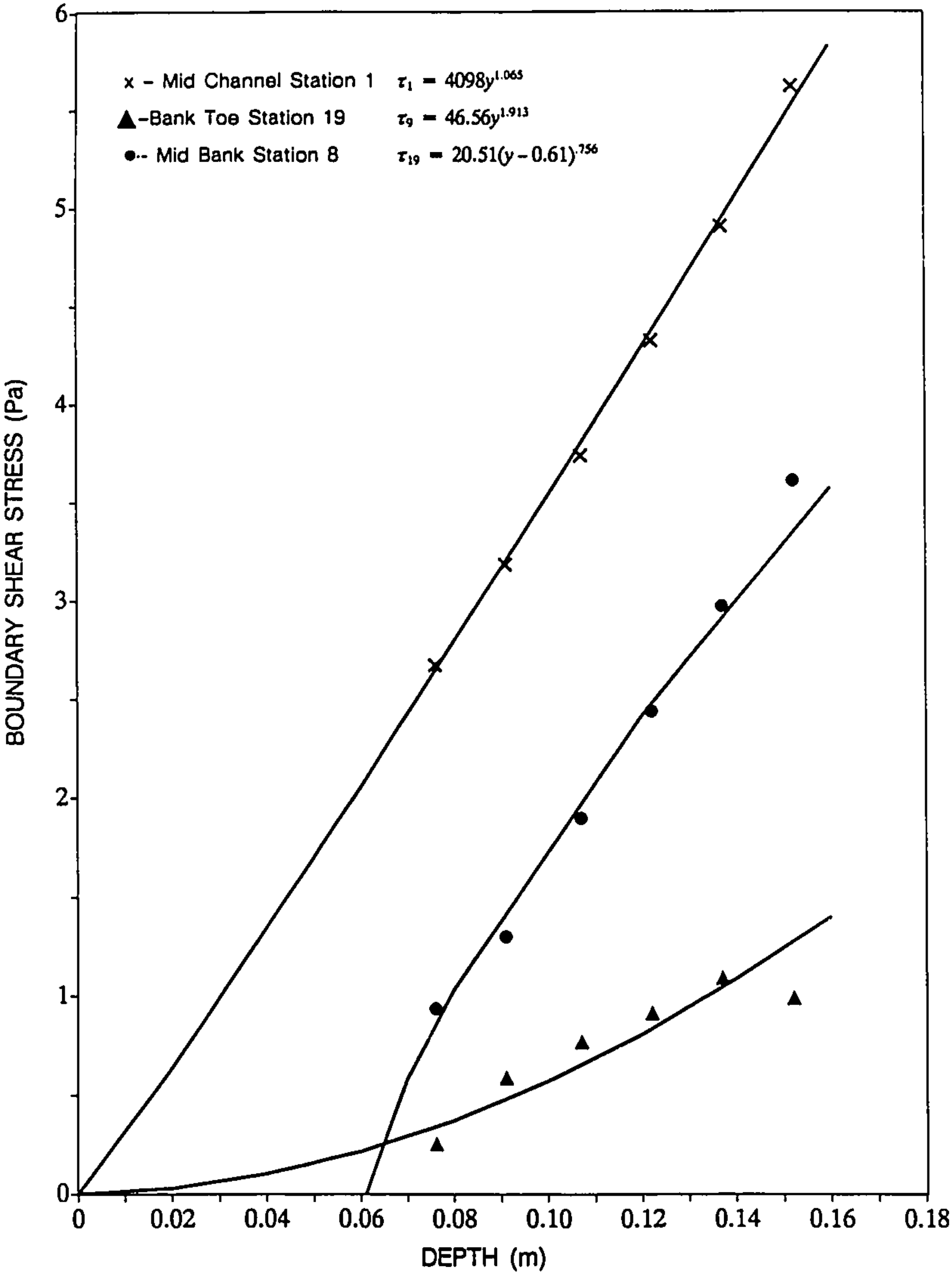

FIGURE 9.3 – Boundary Shear Stress Relations for Selected Depths for a Trapezoidal Channel (1H:1V)

Values for the index were computed for each flow series using the SHEAR1 Command in QUALHYMO. The distribution of the index across the trapezoidal section is shown for its semi-perimeter in Figures 9.4 and 9.5 and summarized in Table 9.3 and 9.4 for present and future land use scenarios respectively. Dimensionless plots were used to provide a better means of comparison of the behaviour of the index with its associated bed load sediment transport relation.

Table 9.3

Boundary Shear Stress Distribution For Present Land Use Conditions (τ_{CRT}=0.48 Pa)

BED-BANK	EXTAU		EVI		MPM		PWR	
STATION	(Pa)	(dim)	(Pa)	(dim)	(Pa)	(dim)	(Pa)	(dim)
1	164	1.0	549	1.0	260	1.0	109	1.0
3	161	.98	511	.93	248	.95	105	.96
5	146	.89	378	.69	199	.77	91	.84
7	52	.32	65	.12	43	.17	33	.3
9	10	.06	11	.02	8	.03	9	.08
11	42	.26	67	.12	43	.16	32	.29
12	75	.46	148	.27	89	.34	52	.48
14	84	.51	203	.37	113	.43	61	.56
16	67	.41	190	.35	101	.39	54	.49
18	50	.3	135	.25	73	.28	42	.38
20	32	.2	75	.14	43	.17	28	.26
22	18	.11	31	.06	20	.08	16	.15

The MPM and EVI measures of the index tend to place additional weight on higher flows. However, given that the indices share a common base (τ_e), it is not surprising that despite some minor differences they demonstrate very similar

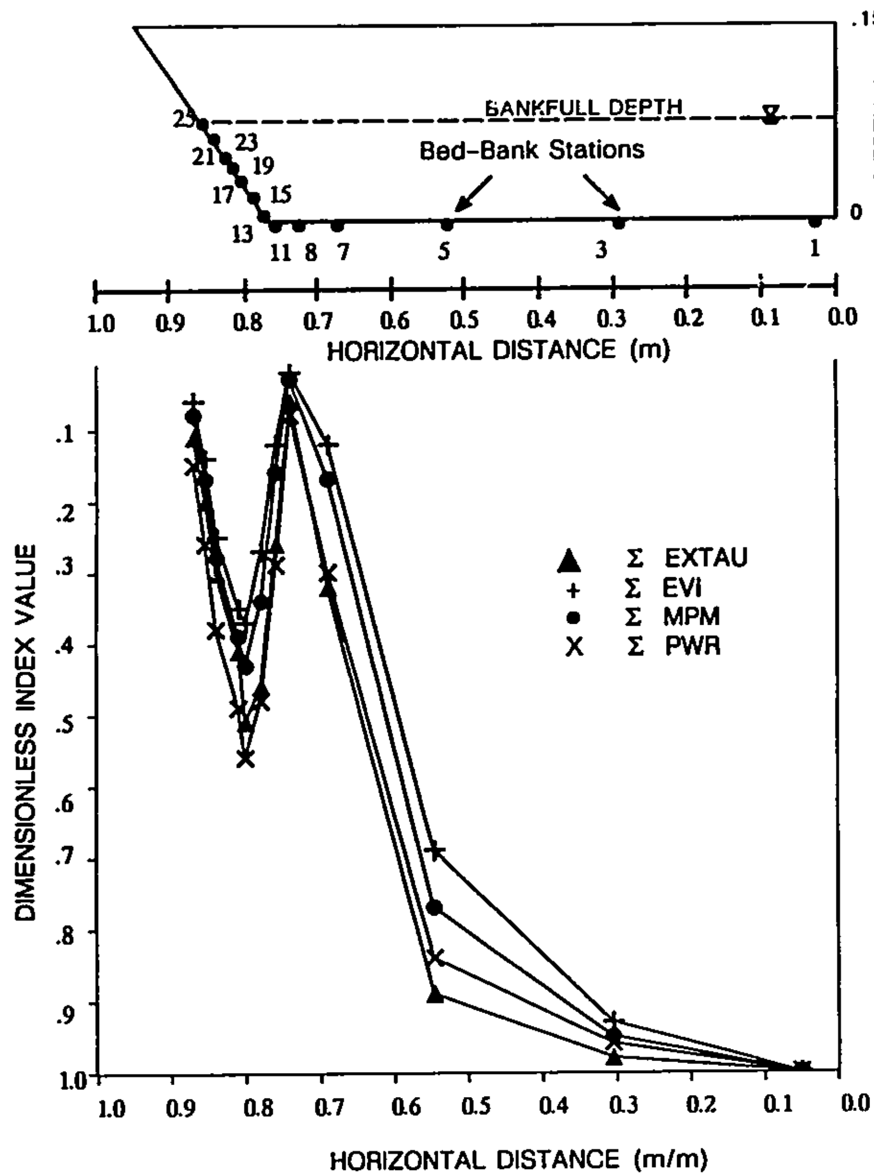

Figure 9.4 Comparison Of Selected Dimensionless Instream Erosion Indices for Pre-development (Non-urban) Land Use Conditions about a Confined Trapezoidal Channel Semi-Perimeter With a Sand Bed (ϕ = 0.000944 m)

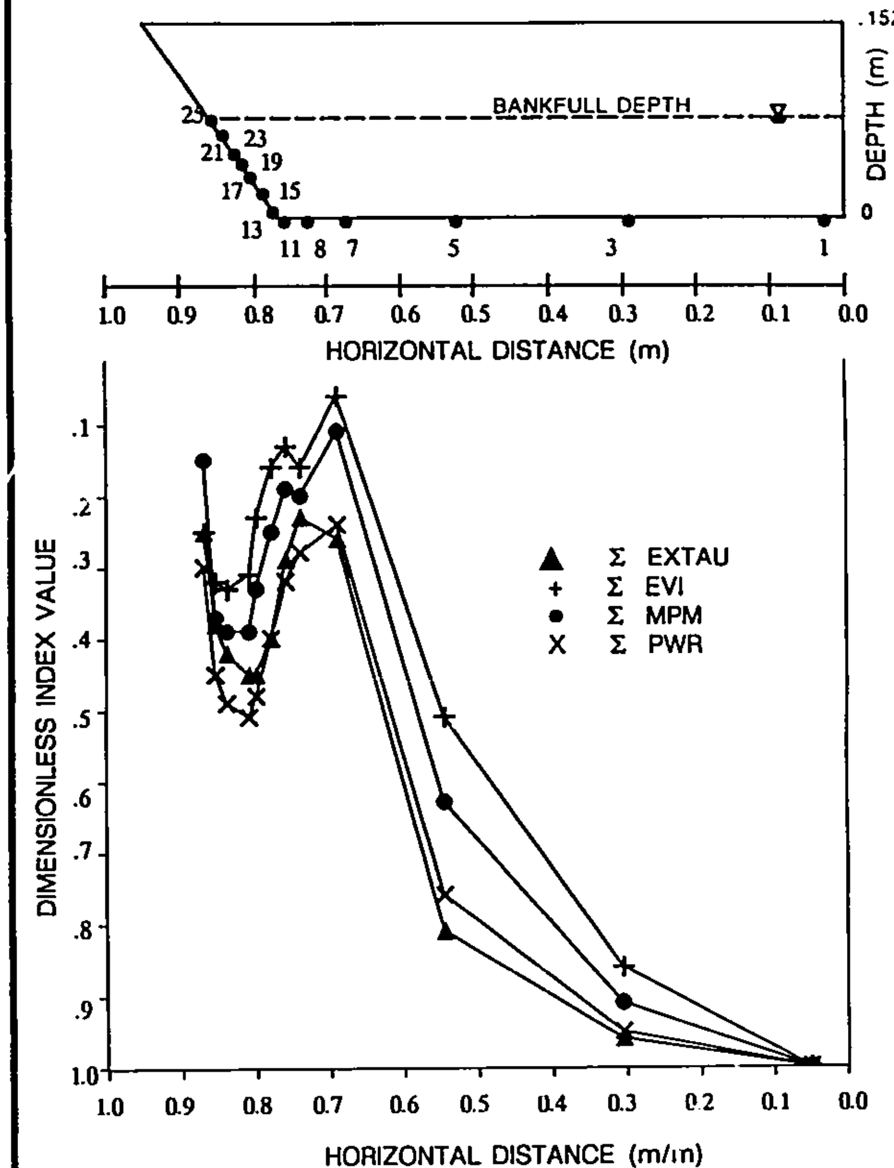

Figure 9.5 Comparison Of Selected Dimensionless Instream Erosion Indices for a Residential Land Use about a Completely Confined Trapezoidal Channel Semi-Perimeter With a Sand Bed (ϕ = 0.000944 m)

transverse profiles. Since the proposed technique employs a pre- versus post-development comparison, consistency in application of the selected transport function appears to be more important than the selection of the transport function itself. Consequently, the selection of the transport function will rest more heavily on the limitations imposed by its range in calibration and user familiarity with the function itself.

Table 9.4

Boundary Shear Stress Distribution For Future Land Use Conditions (τ_{CRT}=0.48 Pa)

BED-BANK STATION	EXTAU (Pa)	(dim)	EVI (Pa)	(dim)	MPM (Pa)	(dim)	PWR (Pa)	(dim)
1	228	1.00	1770	1.00	560	1.00	172	1.00
3	219	.96	1530	.86	507	.91	163	.95
5	185	.81	917	.51	351	.63	130	.76
7	60	.26	106	.06	62	.11	42	.24
9	53	.23	290	.16	114	.2	48	.28
11	66	.29	226	.13	107	.19	55	.32
12	88	.4	288	.16	141	.25	70	.4
14	103	.45	402	.23	182	.33	82	.48
16	102	.45	544	.31	217	.39	88	.51
18	97	.42	582	.33	220	.39	85	.49
20	88	.38	571	.32	208	.37	78	.45
22	57	.25	262	.15	112	.2	51	.3

dim = dimensionless

The various representations of the index also demonstrated a marked similarity in response to an alteration in the flow series as measured by the net change in aggregate sediment transport potential ($(\Delta E_S)_{AGG}$). The number of bed-bank stations (12) is evenly divided between the bed and bank segments of the channel boundary in this particular case. However, the ratio of length of bed to length of bank is 5:1. Consequently, $(\Delta E_S)_{AGG}$ is more sensitive to changes in the bank zone because of the lower density of bed stations per unit length of boundary. Although this particular distribution of stations is arbitrary, it is not unreasonable when consideration is given to the process of bed armouring and the effective decrease in τ_{CRT} along the bank due to weathering of bank materials.

Values of $(\Delta E_S)_{AGG}$, as determined for the trapezoidal test channel, are presented in Table 9.5(a), (b) and (c) for τ_{CRT}=0.48 Pa, 1.92 Pa and 4.31 Pa respectively. From this table it can be seen that the four representations of the index behave in a consistent and parallel manner with one exception as noted below.

For relatively low values of τ_{CRT} (Table 9.5(a): 0.48 Pa) the 50 percent over control option (50-OC) actually increases the aggregate net shear forces acting on the boundary as measured by EXTAU in comparison to the 2YR criterion. This is not reflected in the other indices because they place additional weight on the instream erosion potential of higher flows.

Table 9.5 (a)

Comparison Of $(\Delta E_S)_{AGG}$ For Selected Indices (τ_{CRT}=0.48)

SWM ALTERNATIVE	PRE	POST	2YR	50-OC
EXTAU	-	445	278	350
EVI	-	5114	938	570
MPM	-	1440	464	394
PWR	-	432	241	194

The performance of the various SWM options will be examined in Chapter 10.

Table 9.5 (b)

Comparison Of $(\Delta E_S)_{AGG}$ For Selected Indices (τ_{CRT}=1.92)

SWM ALTERNATIVE	PRE	POST[1]	2YR	50-OC
EXTAU	0	449	138	89
EVI	0	4458	172	129
MPM	0	1280	165	48
PWR	0	425	104	44

Table 9.5 (c)

Comparison Of $(\Delta E_S)_{AGG}$ For Selected Indices (τ_{CRT}=4.31)

SWM ALTERNATIVE	PRE	POST	2YR	50-OC
EXTAU	0	301	10	21
EVI	0	2972	50	110
MPM	0	681	9	20
PWR	0	269	9	19

Note: $(\Delta E_S)_{AGG}$=0 denotes a no scour condition.

9.3 Comparison With MOBED

The MOBED model was set up after consultation with the author (Krishnappan, Canada Center For Inland Waters (CCIW)), for the trapezoidal channel described in Section 9.2. This particular channel was adopted because of known hydraulic parameters and shear stress distributions measured in flume studies by Chiou and Lin (1983), and Ghosh and Roy (1970). The slope of the channel was reported to be S=0.003 m/m, with a roughness coefficient of n=0.015. A uniform particle diameter of ϕ=0.000944 m was assumed and the corresponding CONSTR value (constant in the determination of the energy grade line) was computed for conversion of the Kishi and Kuroki friction relations to a format consistent with Manning's relation, (Krishnappan, 1983).

The longitudinal profile of the study reach was described by twenty-one rectilinear cross-sections over a total reach length of 600 m (Figure 9.6). This configuration was designed to allow the model to dampen the effects of boundary conditions. The input hydrograph was discretized at 5 minute intervals over a time span of 15 hours. This time frame allowed for inclusion of the majority of the recession limb of the outflow hydrographs for the selected storage options. The input sediment concentration was zero representing clear water conditions.

A trial and error procedure was used to adjust DELTAX, the longitudinal channel length between successive cross-sections, until numerical stability was obtained. The resulting normalized longitudinal bed profile achieved for the selected storage options is illustrated in Figure 9.6. The predicted bed profile concavity agrees well with the parabolic configuration described for degrading beds by Torres and Jain (1984).

Since MOBED only accounts for bed degradation, $(\Delta E_S)_{AGG}$ was recomputed for each of the flow series presented in Section 9.2 for only the bed stations to provide a common basis for comparison. The revised $(\Delta E_S)_{AGG}$ values are listed in Table 9.6 against depths of degradation as measured using MOBED at XLENGH=118.8 m. Only the case of τ_{CRT}=1.92 Pa is reported because this condition (clear water - concentration of fine suspended solids is zero) best approximates the modeling assumptions used in the MOBED simulations.

An examination of Table 9.6 shows a one to one mapping of the rankings of the index values and degradation amounts. The uncontrolled future condition is clearly identified by both methods as having the greatest erosion potential.

TABLE 9.6

$(\Delta E_S)_{AGG}$ Versus Depth Of Degradation (cm)

INDEX	PRE	POST	2YR	50-OC
EXTAU	0.0	232.	97.2	61.6
EVI	0.0	905.	348.9	17.7
MPM	0.0	781.	122.8	4.2
PWR	0.0	230.	67.8	14.2
MOBED (cm)	0.0	5.0	2.8	1.1
INDEX RANK		3	2	1
MOBED RANK		3	2	1

9.4 Summary

The ability of the index to represent scour potential at a point about a channel perimeter was determined through a comparison with depths of degradation predicted using an established mobile bed sediment transport model. The model was used to determine the depth of scour associated with the passing of various forms of a 1:2 year design storm hydrograph through a trapezoidal channel formed in non-cohesive sediments. Measures of the proposed index were computed for the same conditions and summed only for the bed to provide a basis for comparison. The resulting ranking of index values

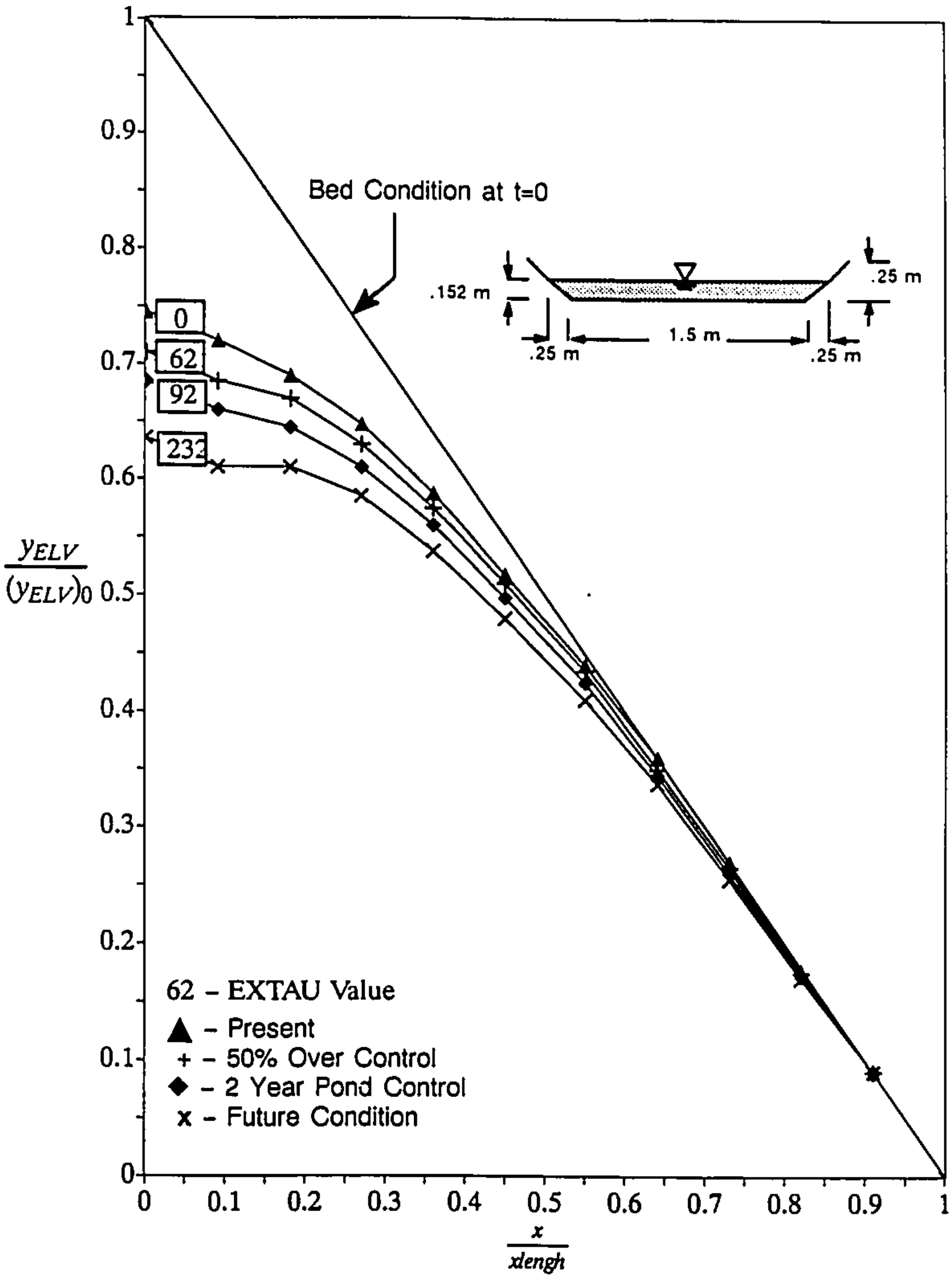

FIGURE 9.6 Normalized Bed Profile for Selected Storage Options Using MOBED (15 hour duration at 5 minute increments)

were found to compare on a one-to-one basis with a ranking of predicted depths of scour.

A sensitivity analysis was carried out on the index by using four common sediment transport functions. It was observed that the behaviour of these representations of the index was similar and that selection of the sediment transport relation was more dependent on limitations in calibration and user familiarity with the particular transport function selected.

CHAPTER 10

EVALUATION OF SELECTED STORAGE CONTROLS

10.1 Introduction

This chapter presents an evaluation of current storage control concepts and the concept of Distributed Runoff Control (DRC) as proposed in Chapter 7. The analysis was based on an evaluation of the magnitude and transverse distribution of a index of scour potential developed in Chapter 3. The analysis was carried out using both a discrete event approach and a continuous simulation techniques. The former approach was done for a hypothetical trapezoidal channel in noncohesive sediments and a case study involving an elliptical channel formed in cohesive sediments. The continuous simulation analysis was performed on the case study only. The sensitivity of the technique to the selection of τ_{CRT} was also examined.

10.2 Discrete Event Analysis

10.2.1 Hypothetical Trapezoidal Channel

The hypothetical watershed and trapezoidal channel describe in Chapter 9 was used for this portion of the analysis. QUALHYMO was used to generate the 1:2 year pre- and post-development hydrographs.

Consistent with the zero runoff increase concept,

$$(Q_{2YR})_{POST} = (Q_{2YR})_{PRE} \qquad [10.1]$$

where, (Q_{2YR}) = the peak flow rate of the 1:2 year recurrence interval design storm,
PRE = a subscript denoting pre-development conditions, and
POST = a subscript denoting post-development conditions.

Knowing the characteristics of the outlet structure, i.e. a rectangular weir, it is possible to construct a stage-discharge curve for 1:2 year control.

The 1:2 year storage pond was initially sized through conventional post- and pre-development 1:2 year hydrograph separation techniques. A stage-volume curve was established based on the geometry of river valleys in the Ottawa area. The initial stage-discharge and stage-volume curves were then entered into QUALHYMO which was set up for discrete event analysis by obtaining the soil moisture boundary condition from a continuous simulation analysis. The stage-volume curve was then adjusted by trial-and-error until the condition of $(Q_{2YR})_{POST} = (Q_{2YR})_{PRE}$ was satisfied. The resulting stage-discharge and stage-storage curves for zero runoff increase (2YR) method are illustrated in Fig. 10.1.

Having ascertained the dimensions of the 2YR control pond

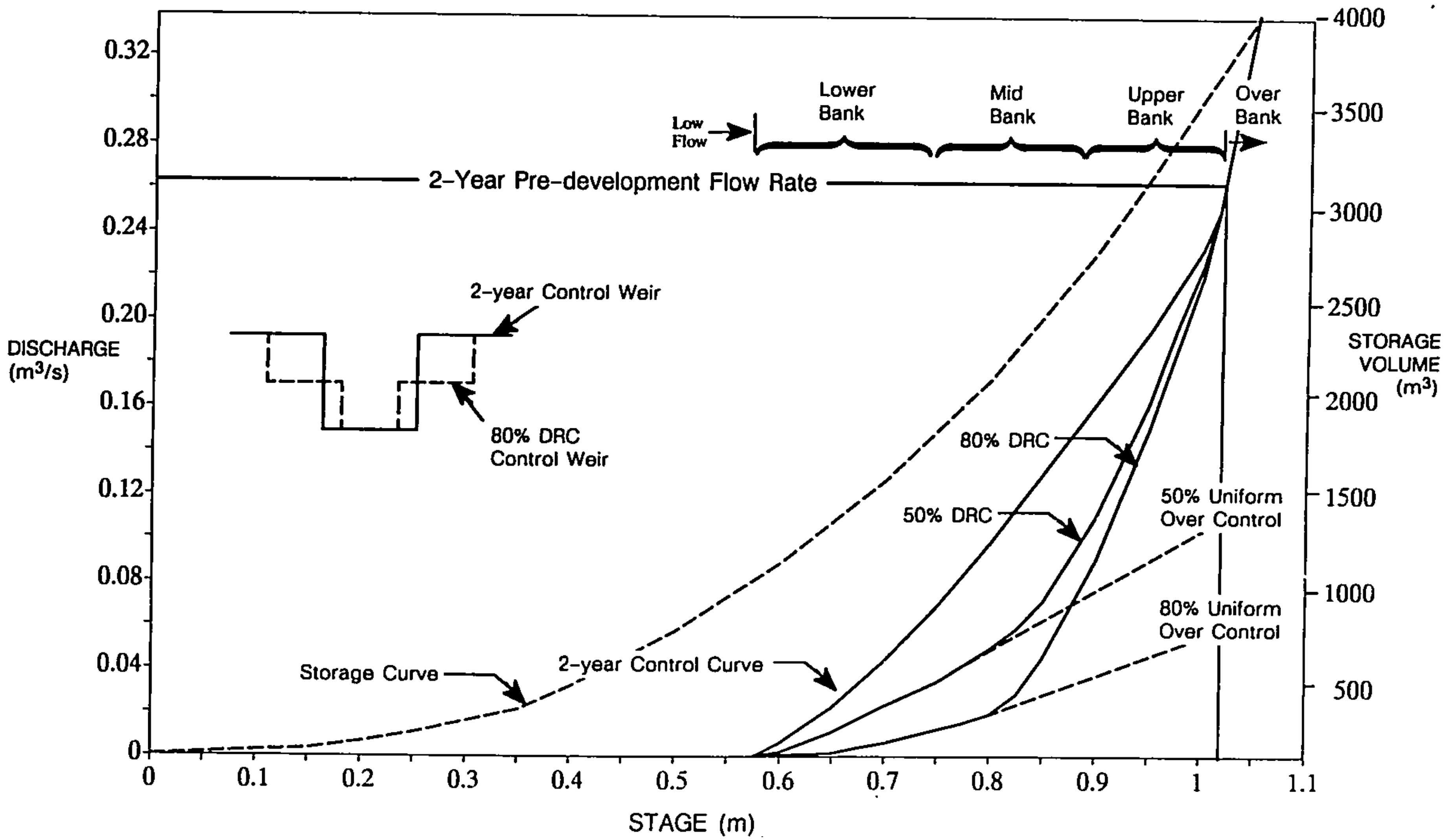

FIGURE 10.1 Stage-Discharge and Stage-Storage Curves for Selected SWM Controls for a Trapezoidal Channel (1H:1V)

QUALHYMO was then set up to calculate the shear stress indices for,

i) present conditions,
ii) future without Storm Water Management (SWM) control,
iii) future conditions with 2YR pond control,
iv) future conditions with over control, and
v) future conditions using DRC.

The simulations were based on a clear water condition as described in Chapter 9. Consequently, the $(q_s)_I$ terms in Eqn. 7.1 are equated to zero. Boundary shear stress relations of the form (Eqn. 9.6),

$$(\tau_o) = a(y-YBED)^b \qquad [10.2]$$

where, $(\tau_o)_P$ = the instantaneous boundary shear stress at point P,
y = the flow depth,
a = a calibration coefficient,
b = a calibration exponent, and
YBED = the height of the boundary station,

are as reported in Chapter 9.

The scour potential for the above flow conditions is summarized in Table 10.1 (τ_{CRT} = 1.92 Pa) and plotted in Figure 10.2 for the EXTAU representation of $(E_S)_P$. The change in erosion potential $(\Delta E_S)_P$, is reported in Table 10.2 and illustrated in Figure 10.3. In this particular case, a level of over control (OC) based on a 50 percent reduction in the 2YR control curve, gave the lowest value of $(\Delta E_S)_{AGG}$ for that option. Increasing the level of OC resulted in the prediction of aggradation while lower values of OC resulted in degradation. By adjusting the level of OC to minimize

Table 10.1

EXTAU Values (Pa) For A Trapezoidal Channel Semi-Perimeter (1H:1V) For Selected Flow Conditions And SWM Alternatives (τ_{CRT}=1.92 Pa)

STATION	PRE	POST	2YR	50-OC	80-DRC
1	64.8	138.0	95.2	80.7	70.9
3	60.1	127.0	88.4	75.1	65.8
5	42.4	88.4	62.6	51.7	46.4
7	0.0	8.1	0.0	0.0	0.0
9	0.0	32.6	0.0	0.0	0.0
11	2.1	27.0	3.1	0.0	2.6
12	11.5	34.1	17.4	7.9	13.1
14	22.2	48.5	33.2	23.0	24.6
16	23.8	62.1	35.6	19.4	26.6
18	16.5	62.7	24.9	5.7	19.1
20	7.7	59.0	11.3	0.0	9.3
22	0.6	32.5	0.5	0.0	0.9

$(\Delta E_S)_{AGG}$ this technique becomes the same as the zero increase in aggregate sediment transport method. The analysis was also repeated for several values of τ_{CRT} ranging from 0.48 Pa $\leq \tau_{CRT} \leq$ 4.31 Pa which corresponds to an increase in suspended sediment load (Prasuhn, 1987). The results of this sensitivity analysis are illustrated in Figure 10.4.

The following observations were drawn from this analysis:

a) All three control ponds reduced $(\Delta E_S)_{AGG}$ below that described for future conditions without SWM control.

b) Despite this reduction in erosion potential the transverse distributed of (E_S) noted a significant concentration in erosive potential in the mid channel and lower bank areas.

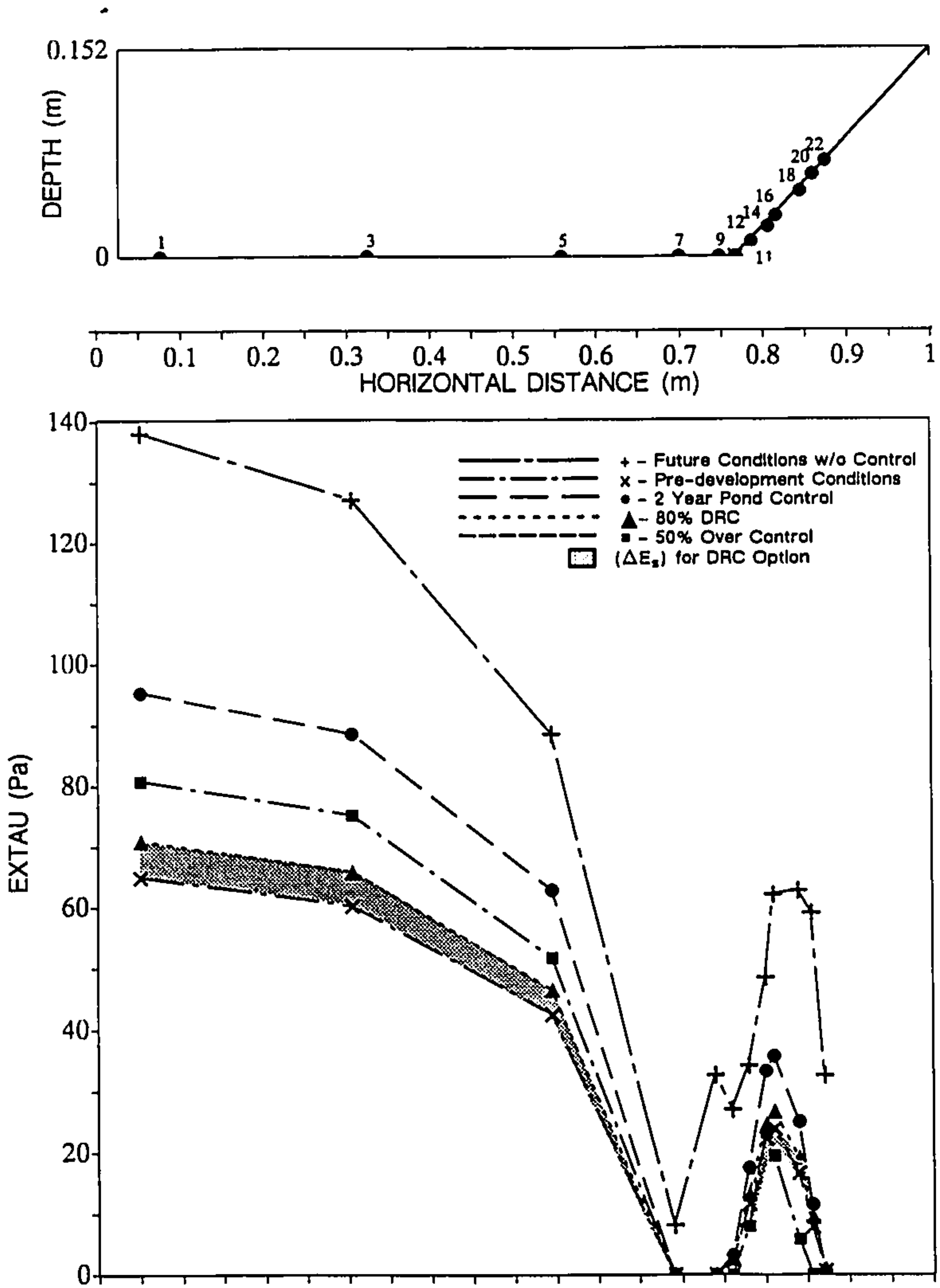

FIGURE 10.2 Transverse Distribution of EXTAU about a Trapezoida Channel Semi-Perimeter for Selected Flow Series

Table 10.2

Transverse Variation In $(\Delta E_S)_P$ For A Trapezoidal Channel Semi-Perimeter (1H:1V) For Selected SWM Options (τ_{CRT}=1.92 Pa)

STATION	PRE	POST	2YR	50-OC	80-DRC
1		73.2	30.4	15.9	6.1
3		66.9	28.3	15.0	5.7
5		47.0	21.2	10.3	5.0
7		8.1	0.0	0.0	0.0
9		32.6	0.0	0.0	0.0
11		24.9	1.0	2.1	0.5
12		22.6	5.9	3.6	1.6
14		26.3	11.0	0.8	2.4
16		38.3	11.8	4.4	2.8
18		46.2	8.4	10.8	2.6
20		51.3	3.6	7.7	1.6
22		31.9	0.1	0.6	0.3
$(\Delta E_S)_{AGG}$:		469	122	71	29

c) The DRC option recorded to lowest value of aggregate instream erosion potential $(\Delta E_S)_{AGG}$.

d) The effectiveness of the 2YR control pond increased with an effective increase in boundary material resistance to scour.

e) The effectiveness of the OC option decreases with an effective increase in boundary material resistance to scour.

f) The DRC option consistently provided the highest degree of control of instream erosion potential over the range in τ_{CRT} examined.

g) The degree of impact of flow alteration under uncontrolled conditions decreases with an effective increase in boundary material resistance to scour.

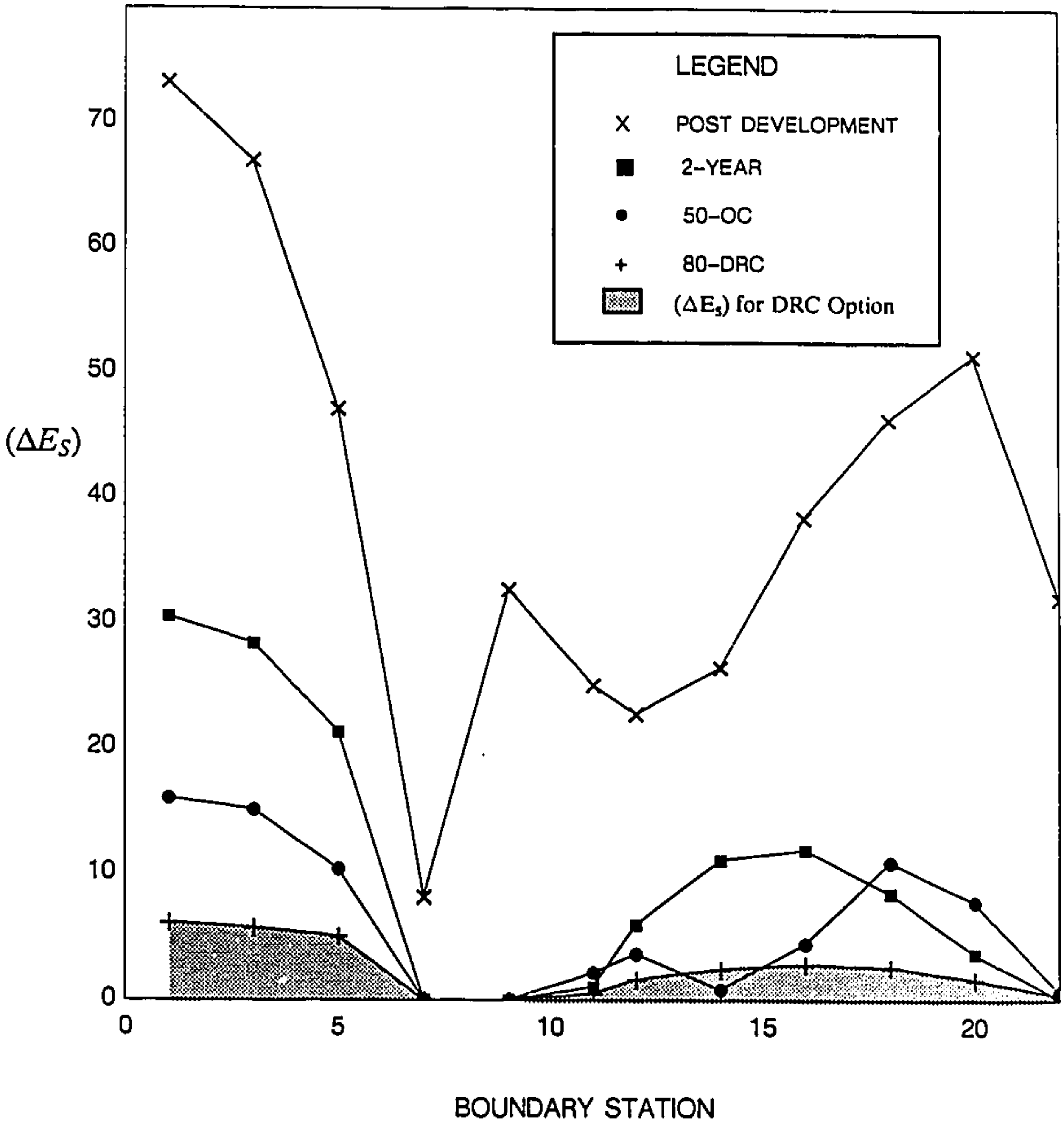

FIGURE 10.3 **Transverse Variation in (ΔE_S) For a Trapezoidal Channel Semi-Perimeter** (τ_{CRT} = 1.92Pa).

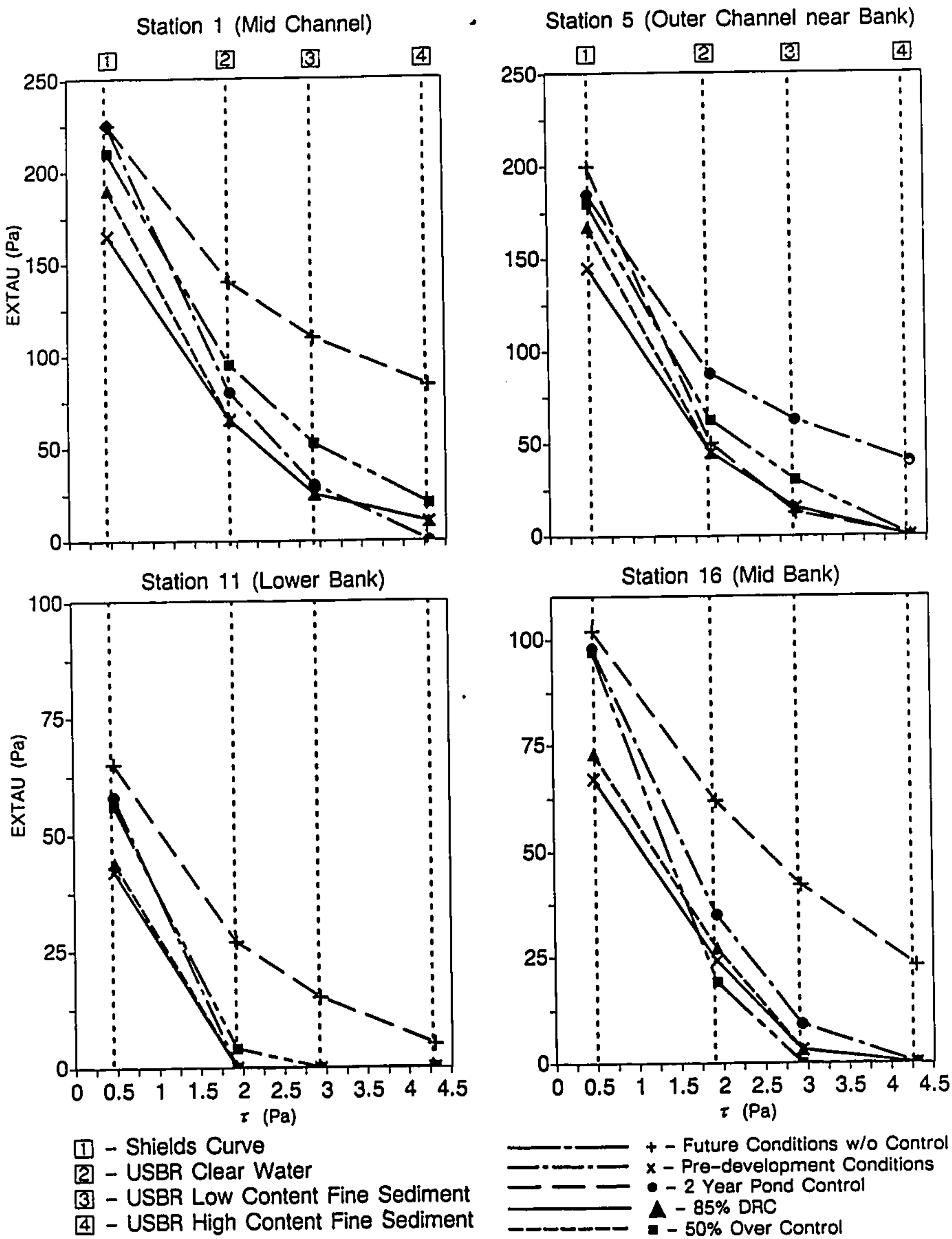

FIGURE 10.4 Performance of SWM Storage Options as Measured by EXTAU at Selected Bed–Bank Stations as a Function of τ_{CRT}

10.2.2 Bilberry Creek Case Study

An elliptical channel cross-section (Figure 10.5) surveyed in a stream near Ottawa, Ontario was adopted for evaluation of selected storage control options because of the availability of hydrologic, hydraulic and geotechnical data (CCL, 1986). Flows were generated using QUALHYMO based on a calibration to three Ottawa area urban watersheds (Rowney and MacRae, 1991(b)). A 2YR analysis was performed, as described in Section 10.2.1, to obtained the 2YR and OC control curves (Figure 10.5).

The effectiveness of the DRC criteria was evaluated for channel materials ranging from very soft to firm (Table 10.3).

Table 10.3

Values Of τ_{CRT} For Intact Cohesive Materials (Lefebvre, 1985)

Soft	3.0 Pa $\leq \tau_{CRT} \leq$ 12.0 Pa
Stiff	12.0 Pa $\leq \tau_{CRT} \leq$ 22.0 Pa
Very Stiff	22.0 Pa $\leq \tau_{CRT} \leq$ 140.0 Pa

The channel was divided into bed, lower bank, and upper bank zones to simulate the effect of a variation in material resistance to scour on control option performance. Four runs were made with varying degrees of material resistance (Table

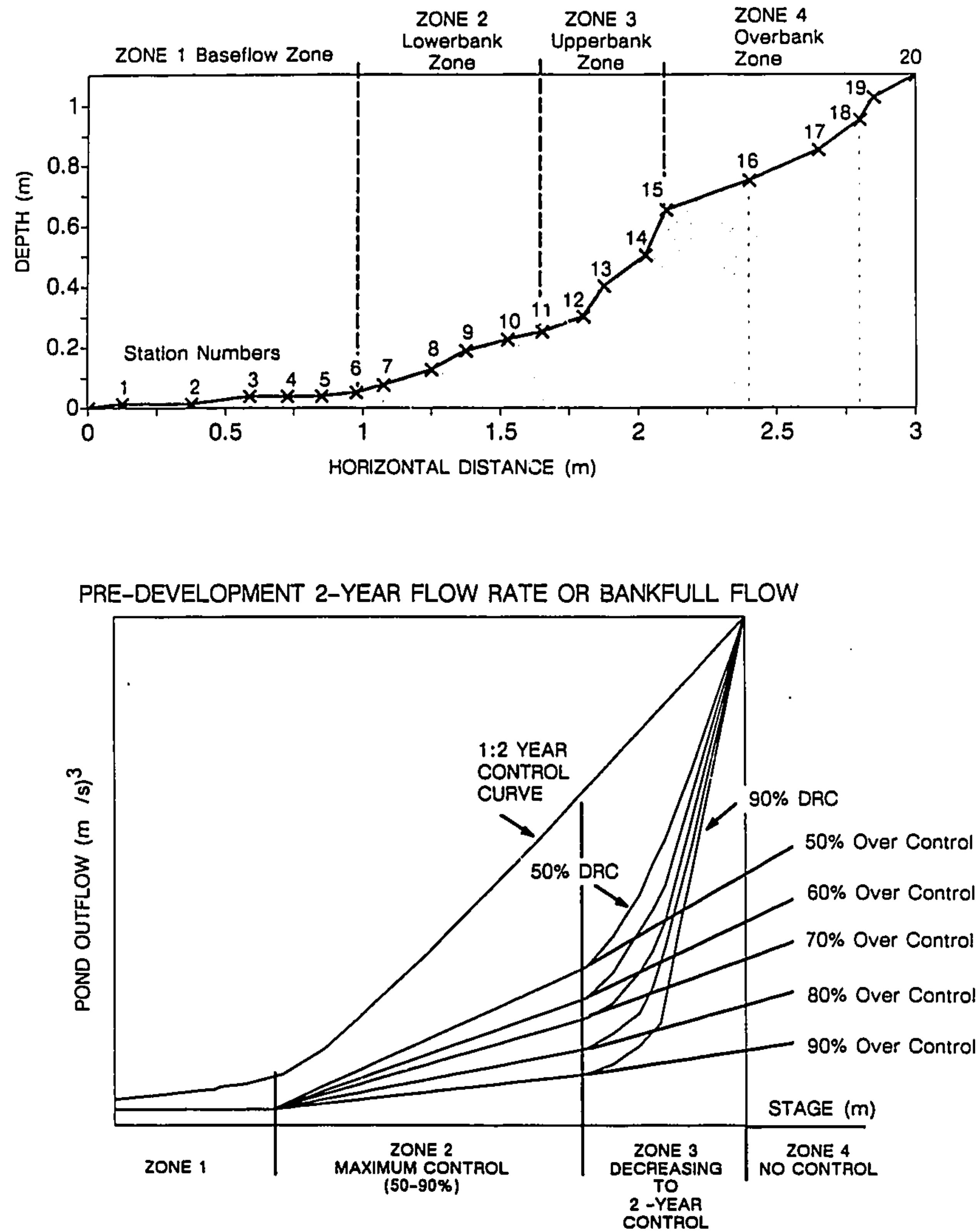

FIGURE 10.5 Classification of Bed–Bank Materials into Zones of Sensitivity to Scour and Corresponding Stage–Discharge Relations

10.4). Boundary shear stress relations (Eqn. 10.2) are reported in Table 10.5. The EXTAU values resulting from the QUALHYMO-SHEAR1 analysis are illustrated in Figures 10.6 (a) to (d).

The degree of DRC control was systematically increased from 70 to 90 percent as material susceptibility to scour

Table 10.4

Transverse Variation In Threshold Shear Stress Values For An Elliptical Channel In Cohesive Materials

ZONE	RUN 1	RUN 2	RUN 3	RUN 4	Geotechnical Parameters[1] SiCl (%)	cu (KPa)	wL	wP (%)	wn
1 Bed	12.0	9.0	6.8	5.1	95	7-10[2]	-	-	-
2 Lower Bank	8.0	4.5	3.4	2.6	90.5	38	70	33	58
3 Upper Bank	3.0	2.3	1.7	1.3	-	-	-	-	-

1. Test were performed by Golder Assoc. Ltd. and reported in CCL (1986).
2. Estimated from another station.

Definition of Terms:

SiCl = percent silt-clay content,
cu = cohesion measured as the undrained vane shear strength,
LL = Atterberg liquid limit,
PL = Atterberg plastic limit, and
wn = natural water content measured as the weight of water over the weight of the dry soil.

increased. The index $(\Delta E_S)_{AGG}$ was used to measure how well the transverse profile of (E_S) for each SWM option reproduced pre-development conditions, (Table 10.6).

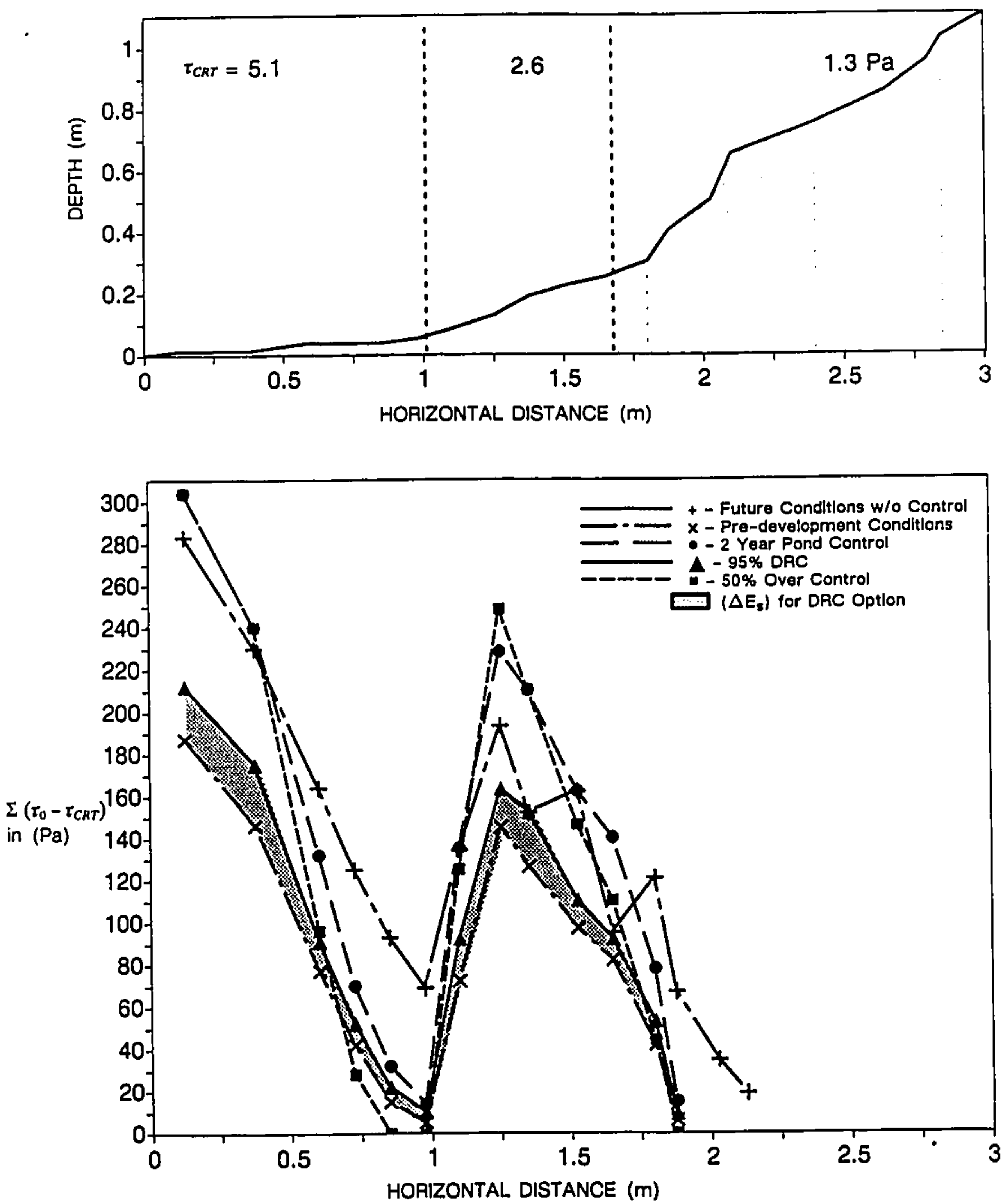

FIGURE 10.6a Transverse Distribution of EXTAU about an Elliptical Channel Semi-Perimeter for Selected SWM Storage Alternatives in very Soft Clay

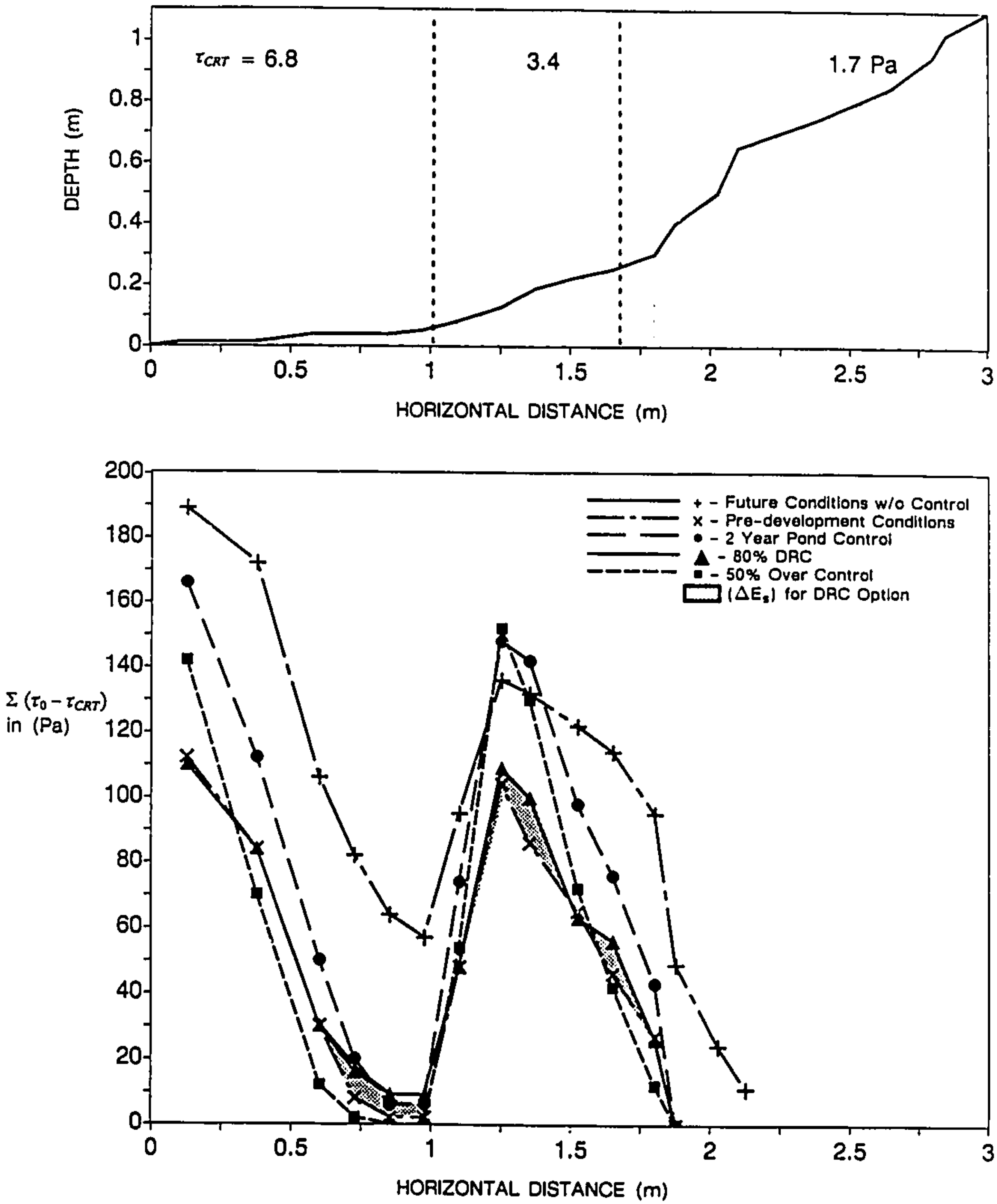

FIGURE 10.6b Transverse Distribution of EXTAU about an Elliptical Channel Semi-Perimeter for Selected SWM Storage Alternatives in Soft Clay

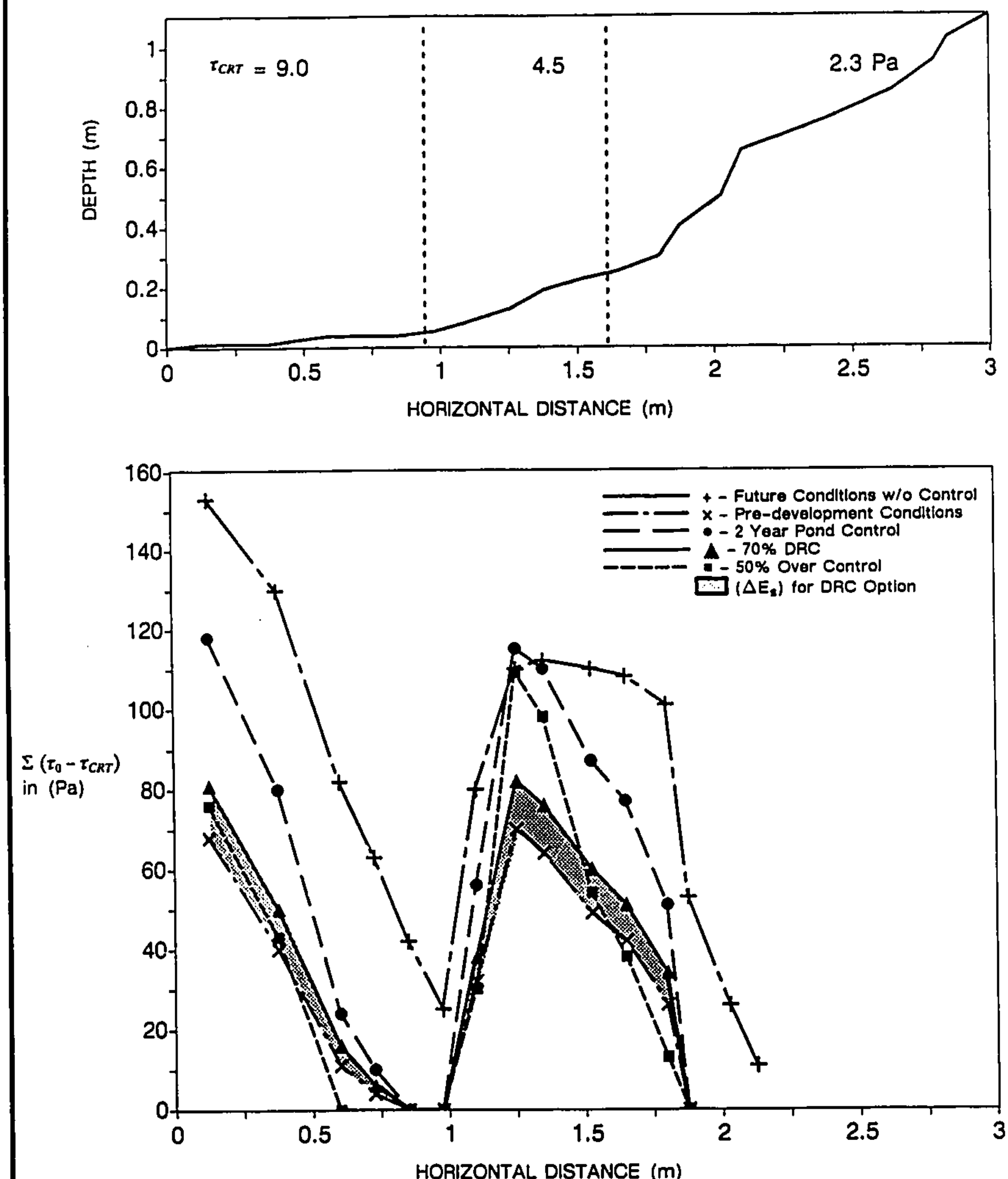

FIGURE 10.6c Transverse Distribution of EXTAU about an Elliptical Channel Semi-Perimeter for Selected SWM Storage Alternatives in Firm Clay

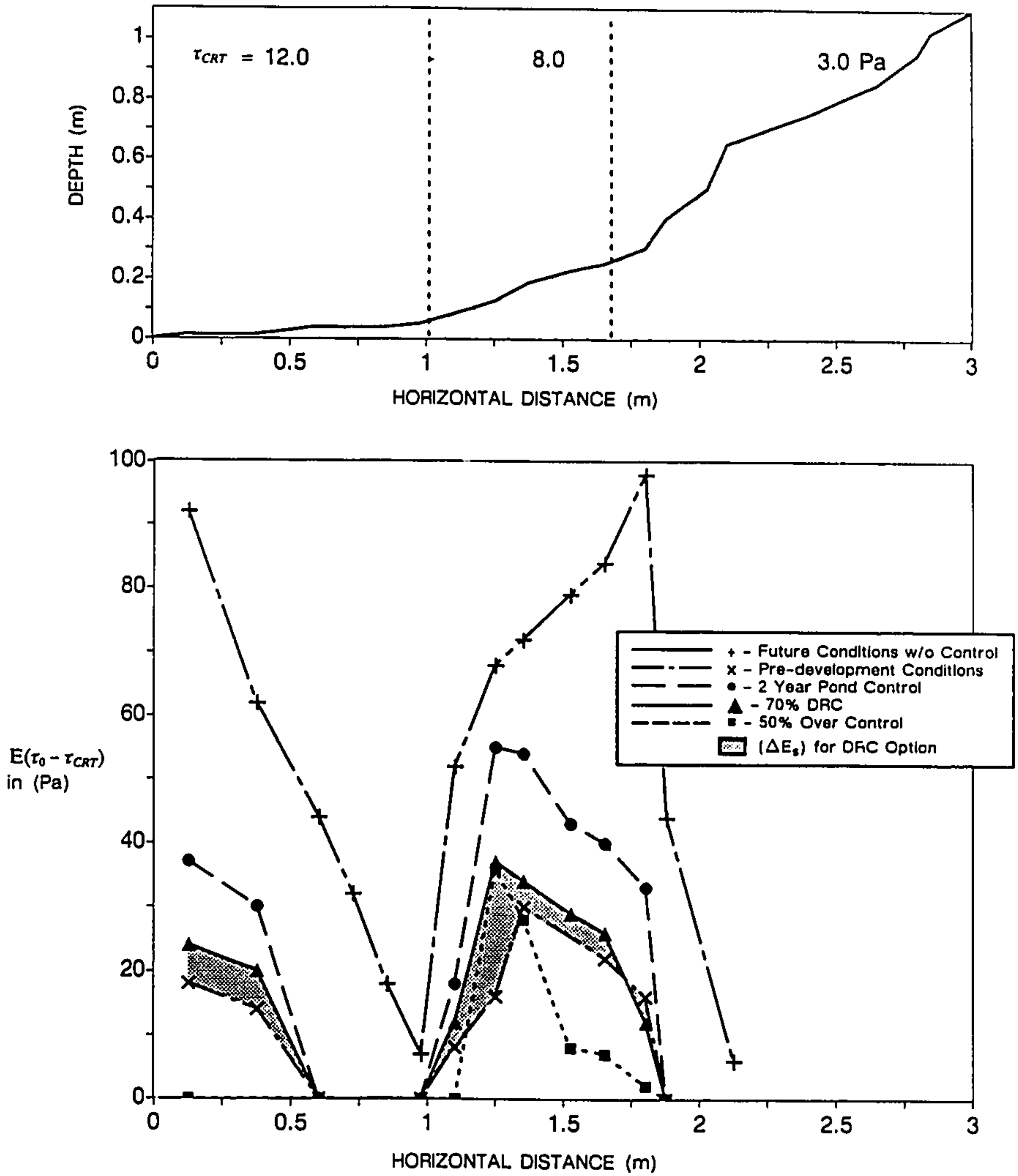

FIGURE 10.6d Transverse Distribution of EXTAU about an Elliptical Channel Semi-Perimeter for Selected SWM Storage Alternatives in Stiff Clay

Table 10.5

Boundary Shear Stress Relations For An Elliptical Channel

STATION	a	YBED (m)	b
1	20.8	0.	.43
3	17.8	0.	1.10
5	14.8	0.048	1.53
6	13.0	0.05	1.57
7	11.5	0.076	0.91
8	11.8	0.13	0.54
10	15.2	0.22	0.73
12	16.8	0.3	1.21
13	17.1	0.38	1.63
14	15.9	0.48	1.71
15	14.3	0.58	1.64

Table 10.6

$(\Delta E_S)_{AGG}$ For Selected Representations Of The Index And SWM Measures For An Elliptical Channel In Soft Cohesive Materials

INDEX	$(\Delta E_S)_{AGG}$				
	PRE	POST	2YR	50-OC	80-DRC
EXTAU	-	592	176	117	9
EVI	-	7988	1414	563	64
MPM	-	1768	321	138	12
PWR	-	817	172	90	7

Abbreviations are as defined in the text.

The general findings from this investigation are:

a) All four of the measures of the index consistently ranked the DRC option as preferable to the 2YR or 50-OC alternatives.

b) The impact of urbanization as measured by (ΔE_s) remained relatively constant with increasing boundary material resistance to scour.

c) All SWM pond control options tended to reduce scour potential in the bed zone with the degree of control increasing with increasing material resistance to scour.

d) However, the 2YR and OC pond options tended to aggravated erosion hazard in the lower bank area with the exception of stiff materials.

e) The OC option produced aggrading conditions for very resistant materials.

The above analysis demonstrates the plausibility of the proposed procedure for the design of control ponds for the reduction of instream erosion potential. This was achieved despite an increase in runoff volume of approximately 82 percent and an increase in peak flows of approximately three fold over pre-development conditions. According to Leopold (1968) this is equivalent to a 60 percent imperviousness with 45 percent of the area being served by sewers. More conservatively, Hollis (1975), estimates an equivalence to a 20 to 30 percent paving of the area which is consistent to a medium density single family development.

There are however, some questions concerning the applicability of the discrete event approach in the design of storage facilities, as identified above. Some of these aspects will be dealt with in the subsequent section concerning multi-event analysis.

10.3 Multi-Event (Continuous) Analysis

10.3.1 Introduction

The discrete event approach discussed above has become established as the basis for analysis of instream erosion potential primarily as an offshoot of flood hazard techniques. An inherent short coming with the discrete event approach is that it fails to account for the increased frequency of the occurrence of moderate to bankfull flows. Nor does it consider the affect of longer recession limbs on the stages achieved by succeeding events which occur prior to the emptying of the storage facility.

Snowmelt processes and/or multiple events may addressed through multi-event or continuous simulation methods. This section deals with the application of the proposed index method, using QUALHYMO, to the elliptical cross-section described in Section 10.2.2. The results are compared to those obtained using the discrete event approach reported in that Section.

10.3.2 The Role Of Snowmelt

The significance of snowmelt in terms of peak flow generation is known to vary with the size of the watershed, the perviousness of the soils, the degree and type of urban development, and the climatological characteristics of the region. Unfortunately, while much attention has been focused on the effects of urbanization on the translation of rainfall into runoff, comparatively little is understood about the affect of urban development on snowmelt. This may in part be due to the complications introduced by snow removal operations, the "heat island" effect and deicing compounds. Although, it is most likely related to the historically small scale of urban hydrologic investigations for which isolated but intense summer thunderstorms typically dominated peak flow generation. However, the trend toward broader watershed based Master Drainage plan studies has increased the spatial scale of hydrologic studies. As urban areas continue to expand and encompass larger drainage systems, the dominance of the flood frequency curve by snowmelt, snowmelt-rainfall, or rainfall generated peak flows becomes obscured. The effects of factors such as snow removal, deicing compounds, or the urban heat island phenomenon on snowmelt were not considered.

The QUALHYMO set up described in Section 10.2.3 was applied over the period of November 1, 1970 through January 1, 1973 inclusive. Snowmelt calibration is illustrated for the winter of 1970-71 in Appendix E. Infilling of the precipitation file obtained from AES for the Ottawa International Airport was required to obtain hourly precipitation increments. This procedure is described in Appendix I.

Snow pack accumulation over the winter of 1970-71 represented a maximum over the last twenty-five years. Melt rates however, were relatively low and of long duration. The winter of 1971-72 was more representative of an average accumulation and ablation year.

Indices and hours of exceedance for selected flow depths in the channel were computed for,

a) the entire simulation period of January 1, 1971 through to December 31, 1972, and

b) for selected months classified into climatological periods. These periods were described as,

   - o winter freeze-up which was observed to begin on or around December 1st and last until the end of February,

   - o spring snowmelt which was found to occur primarily between March 1st and April 30th,

   - o the summer period denoted by high evapotranspiration rates and intense convective as well as cyclonic thunderstorm activity. This period was considered to range from May 1st through to August 31st,

   - o the fall period, (September 1st to November 30th) begin characterized by lower intensity cyclonic activity and low evapotranspiration rates.

These dates were based on an examination of twenty years of precipitation and temperature data collected from the Ottawa International Airport, and flow simulation results using QUALHYMO. Specific meteorological events may vary around these dates however, in general they were found to provide a convenient means by which to compare the importance of snowmelt-rainfall processes versus rainfall events.

In the subsequent analysis an event was defined as any set of measurable precipitation not preceded or followed by any precipitation amount within 3 consecutive hours, or any precipitation amount exceeding 0.5 mm within 4 consecutive hours. A multiple event was defined as any event which occurred prior to 95 percent drawdown of the storage facility.

Figure 10.7 illustrates the hours of exceedance calculated by QUALHYMO under present land use conditions for melt and summer periods for the years 1971 and 1972. This figure demonstrates the importance of snowmelt in the contribution to flow in the lower and middle bank stages. The relative contribution of snowmelt versus rainfall in the upper bank region are more difficult to interpret because of the record snowpack depths recorded in 1971 and the occurrence of three large multiple rainfall events in 1972. The smallest of these events exceeded the historical 1:2 year design storm (31.5 mm)

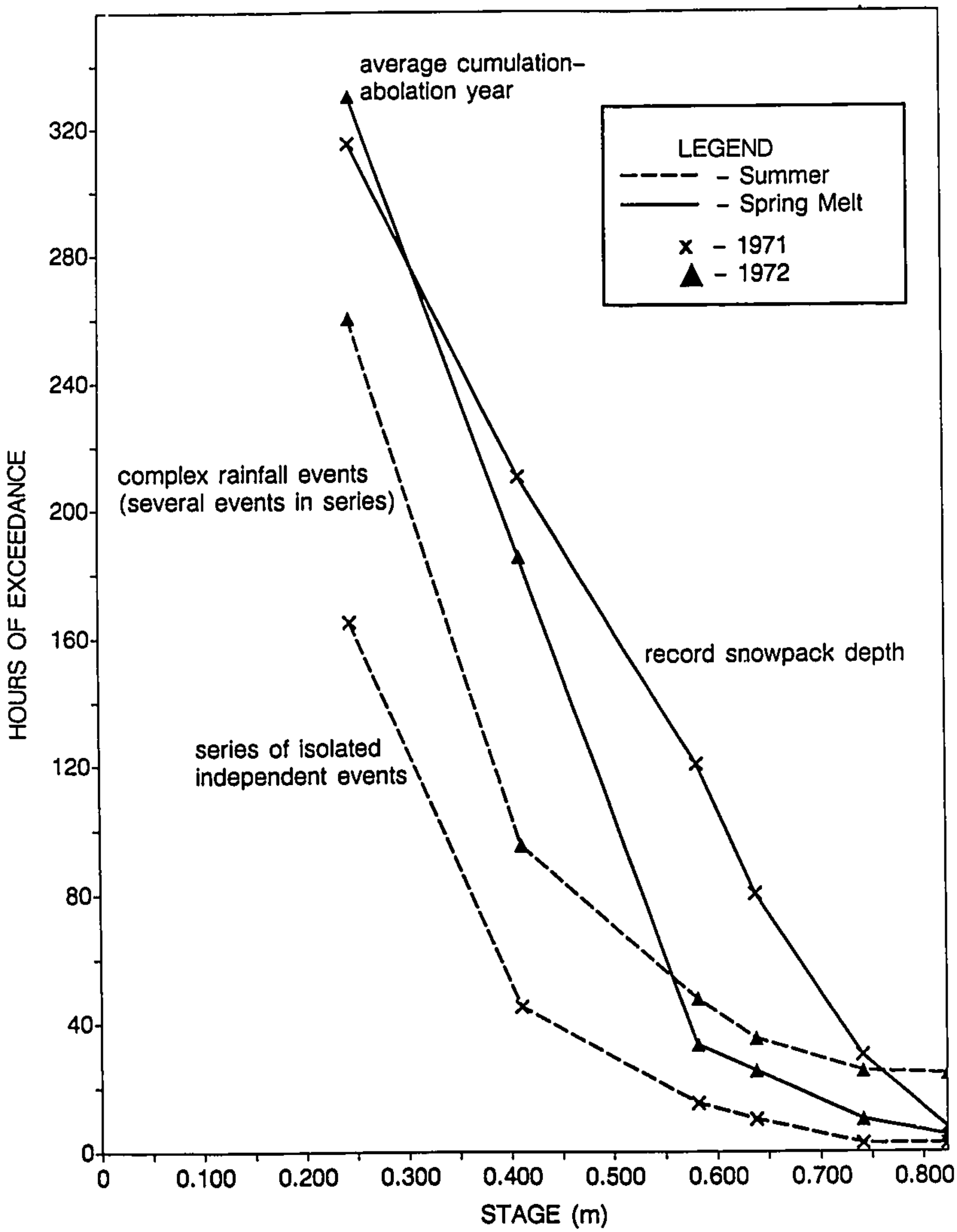

FIGURE 10.7 Mid Bank Exceedance Curves for Spring Melt and Summer Periods Under Present Land Use Conditions for the Years 1971 and 1972

in total rainfall by more then 70 percent. Some statistics for the major discrete as well as multiple events are provided in Table 10.7.

The significance of the dominance of the snowmelt-rainfall versus rainfall contribution to erosion potential was measured using EXTAU as a representation of the index. The distance (z-direction) weighted EXTAU values are reported in Table 10.8.

The summer period of 1971 tallied the lowest distance averaged value of EXTAU=84.1 Pa. This was despite the

Table 10.7
Summary Statistics For Major Summer Period Rainfall Events Recorded At Ottawa International Airport For the Years 1971 and 1972

DATE yr mo dy	TYPE	TOTAL PRECIP (mm)	DURATION (hr)	PEAK INTENSITY (mm/hr)	PEAK FLOW (m3/s)
71 06 07	discrete	20.1	3	15.5	2.35
71 07 17	"	33.8	8	13.7	2.77
71 08 10	"	36.8	4	24.6	4.97
71 09 13	"	19.5	8	9.9	1.82
72 05 30	"	17.4	10	4.6	1.17
72 06 21	multiple				
	- event 1	11.2	5	5.8	
	- event 2	43.2	19	9.1	4.36
72 07 12	multiple				
	- event 1	10.3	3	6.4	
	- event 2	5.4	4	4.6	
	- event 3	38.3	2	37.3	7.27
72 08 06	multiple				
	- event 1	1.6	3	1.0	
	- event 2	4.8	3	2.5	
	- event 3	2.7	5	0.8	
	- event 4	54.0	11	25.9	8.36

occurrence of two discrete rainfall events greater then the 1:2 year historical design storm event, and four near or greater then bankfull flow events. In contrast the average snowfall winter and multiple rainfall events in the summer of 1972 recorded values of 267 and 297, respectively. These periods represent instream erosion potential of more then 3-fold over that calculated for the summer of 1971. The record snowfall year of 1971, although melt rates were relatively low, produced a distance weighted average erosion potential of 471 Pa. This value represents an erosion potential of 5.6 times

Table 10.8
Distance Weighted (z-direction) EXTAU Values For The Spring Melt and Summer Periods For The Years 1971 and 1972

a) Actual EXTAU Values

STATION	WINTER 1971 (Pa)	SUMMER 1971 (Pa)	WINTER 1972 (Pa)	SUMMER 1972 (Pa)	ZDIST (m)
1	3300.	604.	2030.	1810.	0.360
3	891.	95.8	252.	686.	.360
5	109.	6.0	21.2	305.	.187
6	94.1	5.2	18.4	268.	.200
7	1440.	230.	728.	813.	.274
8	2990.	769.	2333.	1670.	.226
10	1890.	296.	907.	1050.	.250
12	794.	87.	228.	613.	.213
13	51.2	2.4	103.	213.	.187
14	0.0	0.0	0.0	65.4	.253
15	0.0	0.0	0.0	22.9	.125

Total Distance: 2.635

b) Distance Weighted EXTAU Values

STATION	WINTER 1971 (Pa)	SUMMER 1971 (Pa)	WINTER 1972 (Pa)	SUMMER 1972 (Pa)	ZDIST
1	171.1	31.1	105.3	93.8	0.137
3	46.2	5.0	13.1	35.6	0.137
5	2.9	0.2	0.6	8.2	0.071
6	2.7	0.1	0.5	7.7	0.076
7	56.8	9.1	28.7	32.1	0.104
8	97.3	25.0	75.9	54.4	0.086
10	68.1	10.7	32.7	37.8	0.095
12	24.4	2.7	7.0	18.8	0.081
13	1.4	0.1	2.8	5.7	0.071
14	0.0	0.0	0.0	2.4	0.096
15	0.0	0.0	0.0	0.4	0.047
Total	470.9	84.1	266.5	296.9	1.000

ZDIST is the distance between successive bed-bank stations.

the summer of 1971 and an increase of 1.6 times the summer period of 1972 which experienced several multiple rainfall-runoff events.

These findings serve as an indication of the relative importance of the snowmelt period and multiple rainfall events in the determination of instream erosion potential. The following analysis now examines the effectiveness of the various SWM storage alternatives over the same period in terms of the reduction in instream erosion potential.

10.3.3 Evaluation Of Storage Alternatives

The storage pond options,

a) 2YR control,
b) 50-OC control, and
c) 80-DRC control,

were evaluated for the period of November 01, 1970 through to January 01, 1973 using EXTAU as a measure of the index.

The transverse distribution of EXTAU for the elliptical channel semi-perimeter is illustrated in Fig. 10.8. A visual examination of this figure shows that the 70-DRC option provides the best control over instream erosion potential. It also recorded the lowest value of $(\Delta E_S)_{AGG}$ of the storage control options evaluated (Table 10.9, Figure 10.9).

An increase in the degree of control, i.e. 75-DRC did not improve the degree of control possibly because of the interaction of the longer recession limb with subsequent runoff events. Similarly, a further reduction in the degree of control i.e. 65-DRC, also resulted in an increase in instream erosion hazard. This implies that there exists some optimal solution between the degree of control and the residual effects of the reservoir on peak flows from subsequent events. This apparent relationship would probably vary from watershed to watershed depending upon the geometry of the basin,

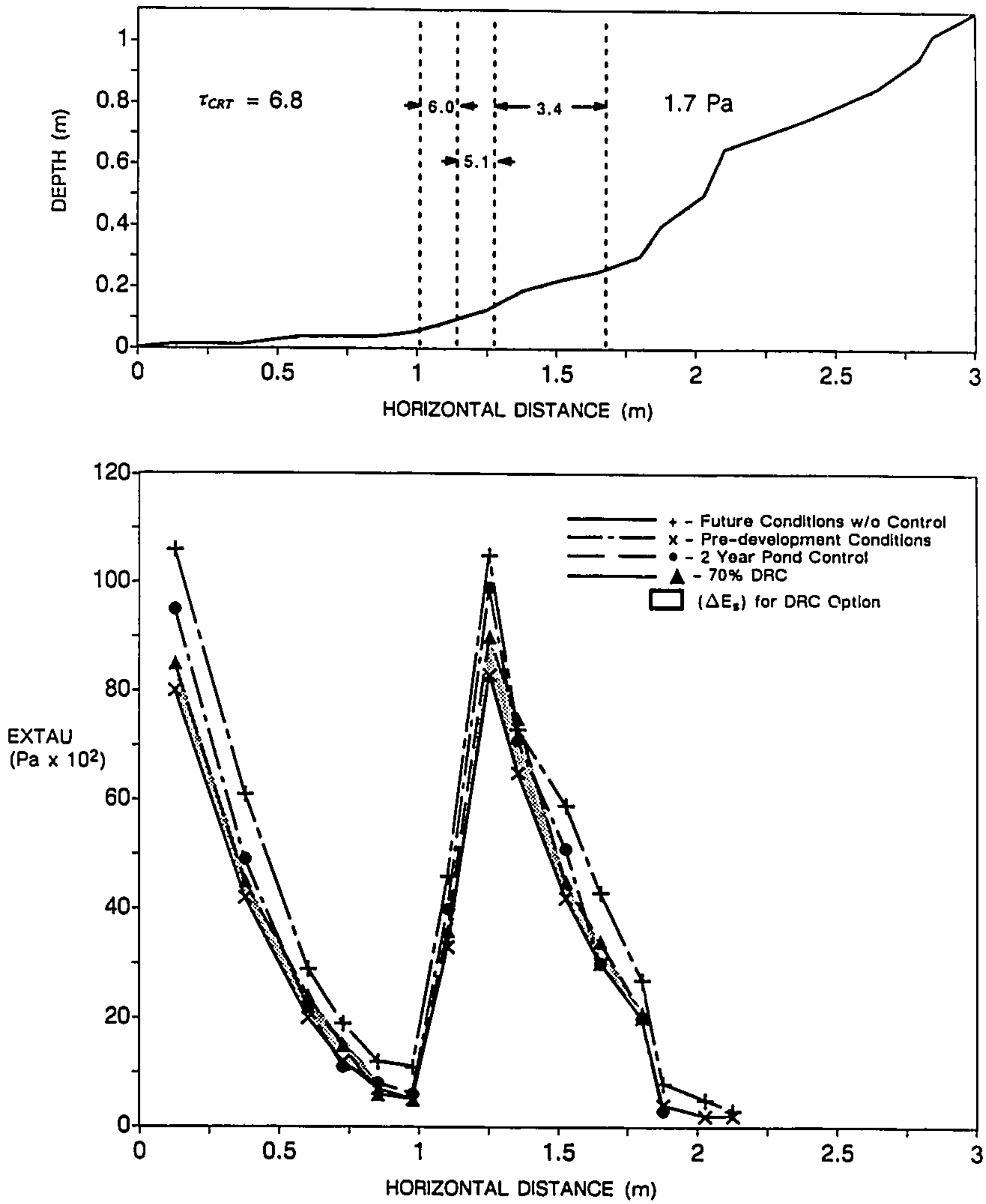

FIGURE 10.8 Transverse Distribution of EXTAU for an Elliptical Channel Semi-Perimeter Using Continuous Simulation for the Years 1971 and 1972

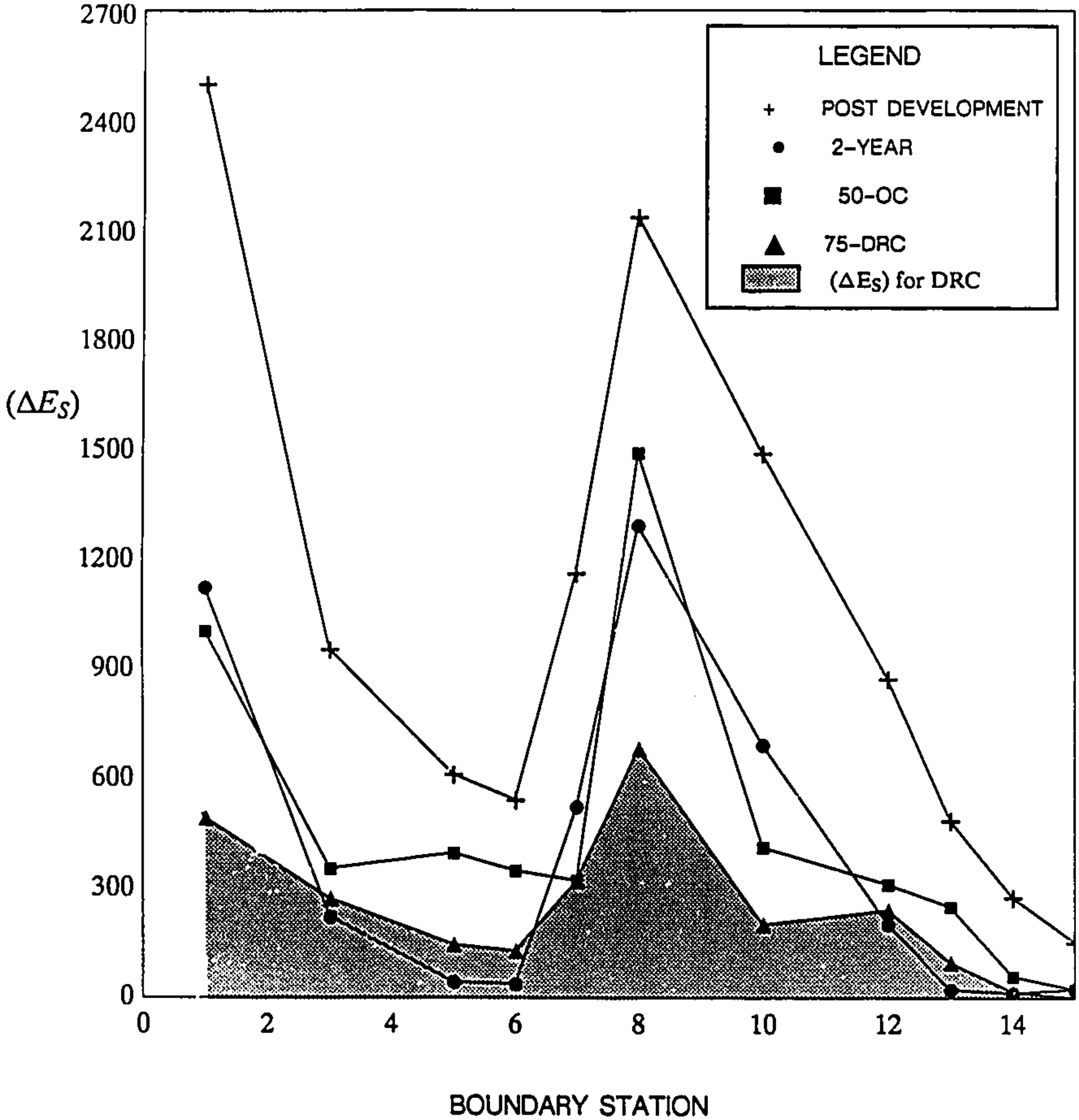

FIGURE 10.9 **Transverse Variation in (ΔE_S) About an Elliptical Channel Semi-Perimeter for Selected Sum Control : Two Year Simulation Period (1971-1972)**

drainage network, boundary material properties, and precipitation characteristics.

Table 10.9

Transverse Distribution Of (ΔE_s) For A Two Year Continuous Simulation (1971-1972)

STATION	PRE	POST	2YR	50-OC	70-DRC
1	-	2510	1120	1000	490
3	-	950	220	352	270
5	-	609	42	395	144
6	-	539	36	346	126
7	-	1160	520	320	320
8	-	2140	1290	1490	680
10	-	1490	690	410	200
12	-	870	200	310	240
13	-	484	21	248	96
14	-	274	12	58	15
15	-	152	22	22	0

A comparison between Figs. 10.6 (a) to (d) and 10.8 shows the similarity in the behaviour of the storage options under discrete event and continuous simulation approaches. The analysis was also repeated using other representations of the index, the results of which support the above findings (Table 10.10).

Table 10.10

$(\Delta E_S)_{AGG}$ Analysis For Continuous Simulation Approach For Selected Representations Of The Scour Index

INDEX	PRE	POST	2YR	50-OC	80-DRC
EXTAU	0	11178	4733	5435	2601
EVI	0	125482	34826	32379	23940
MPM	0	27326	7671	7439	5409
PWR	0	12890	4289	4555	2872

10.4 Conclusions

Discrete event and continuous simulation analyses were performed using the SHEAR1 Command in QUALHYMO to evaluate the performance of the 2YR, OC and DRC control options. The analysis was carried out using a hypothetical trapezoidal channel formed in non-cohesive sediments and for an elliptical channel formed in cohesive materials. In both cases τ_{CRT} was varied to simulate very soft (loose) to stiff conditions. The DRC option was consistently identified as the preferred SWM storage alternative as measured by the transverse distribution and magnitude of the scour index (ΔE_S).

The role of snowmelt and the significance of multiple rainfall events was also addressed. It was found that these two factors comprised the greatest contribution to erosion potential as measured by EXTAU over a two year simulation period. Despite the apparent significance of these two factors, the basic conclusions concerning the effect of uncontrolled flows and the effective control obtained through the DRC option remained fundamentally the same as that described for the discrete event approach.

From these analyses it was concluded that with proper design, storage controls can effectively reduce possible morphological alteration of the urban stream channel following development. However, more research is required into snowmelt-rainfall processes and the significance of multiple rainfall events before their role in the determination of channel form can be more fully assessed. Finally, the index method as proposed, provides a practical and effective means by which to design and compare SWM storage alternatives.

CHAPTER 11

CONCLUSIONS

11.1 General

A number of critical points have been concluded by inference from the literature:

a) An alteration in the independent variables of flow and sediment load following urbanization alters channel hydraulic geometry;

b) The objective of Storm Water Management (SWM) is to prevent, in so much as possible, disruption of the natural pre-development stream channel form;

c) Current SWM methods have employed concepts of retention and detention primarily through the use of storage ponds to correct for the modification to natural watershed storage associated with land use alteration and drainage improvements;

d) These methods employ hydrologic criteria or one-dimensional sediment transport models based on the 1:2 year design storm;

e) Current design methods have met with limited success and in certain instances they resulted in the aggravation of instream erosion hazard.

11.2 Findings From This Research

It has been demonstrated in this research that:

a) The largest increase in sediment transport potential following urbanization may be associated with moderate flow events, (RI < 1:1.5 years). The effect of this increase is to shift channel forming dominance away from bankfull flows toward moderate flow events. The implication on design criteria is the need to use a continuous simulation approach to account for the non-uniform alteration in the flood frequency curve associated with urbanization.

b) Correlations were cbtained relating the increase in post development channel width to the resistance to scour of the least resistant bank toe stratigraphic unit. Composite representations of bank resistance and the mid bank stratigraphic unit were weakly correlated with the increase in stream channel width. This observation points to the need to address scour potential on a point by point basis about the channel periphery.

c) Channel response scenarios were developed to explain initial and intermediate channel forms observed following development. Intermediate channel response is determined by the characteristics of the sediment load relative to stream competence.

d) An index of scour potential was proposed based on a pre- versus post-development comparison of sediment mass balance at a point about the channel perimeter. The index was validated through comparison with a mobile bed sediment transport model. It was concluded that the index represents a measure of the scour potential at a point. Temporal alteration of the flow field was incorporated into the index by integration with respect to time. Transverse variations in boundary material resistance to scour was addressed by integrating the index across the wetted perimeter.

e) A design criteria was proposed based on maintaining the pre-development value of the index at a point about the channel perimeter. It follows that channel erosion is minimized if the alteration in the transverse distribution of the index is maintained constant with pre-development values.

f) A method for the application of the proposed criteria was developed which distributes storage utilization through manipulation of the hydraulic performance of the outlet structure to minimize the value of the index.

This work integrates existing sediment transport theory with incites into the morphological response of a stream channel to develop a comprehensive approach to the design of storage facilities for the control of instream erosion.

11.3 Future Research

The proposed models, their functional algorithms and the analytical approach, should receive further testing. This should involve a wider range of channel configurations and boundary materials. The technique developed in this research was designed for application to small urban streams formed in intact clay materials or armoured beds of low mobility. For application to mobile bed channel systems the role of bed forms on flow geometry must be addressed.

There is a general lack of case studies documenting the effectiveness of SWM measures on channel form. Monitoring of shear stress distributions and erosion processes in streams with and without SWM controls should receive a high priority.

There is no method available, except through field trials, to test the validity of the proposed design procedure. Toward this end a number of agencies have been approached with regard to the establishment of a demonstration case and a long term monitoring program.

APPENDIX A

FIELD IDENTIFICATION OF EROSION PROCESSES FROM FLUVIAL FORMS

A1.0 Field Identification Of Erosion Processes From Fluvial Forms

Floodplain morphology as described by macroforms, mesoforms and microforms and their activity rates may be used to identify the dominant erosion mechanisms controlling channel form. Lewin (1978) provides a description of these forms which have been summarized in the following table.

Table A1

Floodplain Morphology after Lewin, (1978)

Macroforms	Mesoforms	Microforms
1. Floodplain dimensions and relief	Channel dimensions	Plane beds
2. Channel patterns (single, braided)	Longitudinal bars	Ripples
3. Activity pattern (rotation, aggradation, translation, etc.)	Transverse bars	Dunes
4.	Point bars	Current lineations
5.	Levée	Flute marks
6.	Crevasse channels and splays	Avalanche faces
7.	Dead or flood channels	Silt-clay deposits
8.	Bar surfaces and swales	Shrinkage cracks
9.	Floodbasins, and backswamps	Rainprints etc.
10.	Exogenic forms etc.	

These forms represent three scales in time of evolution and relative size. Macroforms represent the largest scale, that of the floodplain and its river channel pattern. Mesoforms represent an intermediate scale which operate in the order of the active channel and represent its major components. The third and smallest scale is represented by the microforms. These forms relate to the perturbations in the primary flow or secondary current patterns. As the size of the sedimentary forms decrease their susceptibility to short term fluctuations in sediment and water flows increases. This differential in the time of response and scale of feature should be considered in the interpretation of former flow patterns and erosion mechanisms.

A2.0 Field Classification Of Shear Dominated Fluvial Forms

In the case of homogeneous bank materials the dominance of corrasion, which includes the forces of shear, abrasion and lift may be reflected in:

1. Smoothed banks remaining after flood passage;
2. Frequent overhangs along the length of the channel. These overhangs are typically bound by roots in the vegetative layer;
3. Surficial slumping of large blocks which topple or slide forward into the stream channel or to the base of the bank slope but remain largely intact with the original vegetation, typically grasses, continuing to grow on the side; and,
4. Relatively straight tension cracks in the table land near

and roughly parallel to the top of the bank.

A3.0 Field Classification Of Fluvial Features Related To The "Falling Stage" Phenomena.

Fluvial forms related to the falling stage phenomena in homogeneous materials are unique from corrasion dominated forms in several discernible ways:

1. Deep seated failures, typically rotational slumps;
2. Arc shaped tension cracks in the table land near the top of the channel bank but set back further from the edge of bank than noted for surficial failures; and,
3. The failed material often transforms into a slurry thereby losing its original form.

Generally a stream reconnaissance is required along each water course to characterize the dominant failure mechanisms because of the uniqueness and variability of riverine sediments and bed-bank conditions. Although the above classification system is highly qualitative and not exhaustive it may be useful as a guide to the identification of dominate erosion mechanisms from geomorphic evidence.

APPENDIX B

MODELING APPROACH AND VERIFICATION

B.1 Modeling Approach

B.1.1 Primary Flow Isovels

Liggett et al. (1965), and Chiu (1967) set up a curvilinear coordinate system of ξ- and η-curves as illustrated in Figure B.1. These were expanded by Shen and Komura (1968) and subsequently adopted by Chiu and Hsiung (1978, 1981) and Chiu and Lin, (1983). The later authors suggested that a three-dimensional flow distribution as defined by a coordinate system of primary flow isovels (equi-velocity curves) may be represented by,

$$\xi = Y(1-Z)^{\beta} \exp(\beta Z - Y + 1) \qquad [B.1]$$

in which,

$$Y = \frac{y+\delta Y}{D+\delta Y+\epsilon} \qquad [B.2]$$

and,

$$Z = \frac{ABS(z)}{BI+\delta I} \qquad [B.3]$$

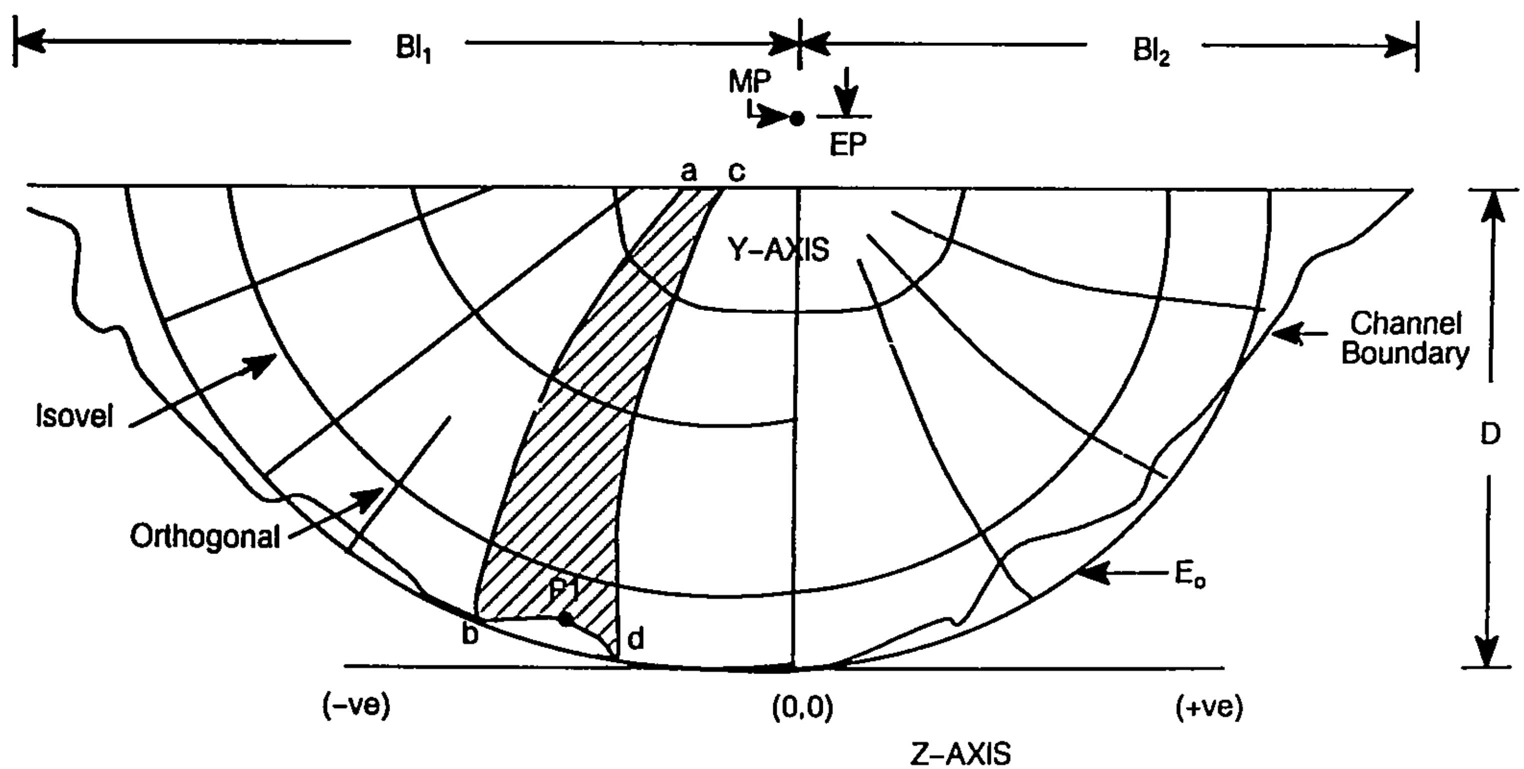

FIGURE B.1 Definition Sketch for 3-D Velocity Field

where, ξ is a variable defined by a logarithmic velocity distribution law,

$$u = (\frac{v*}{k}) \ln(\frac{\xi}{\xi_o}) \qquad [B.4]$$

In reference to Figure B.1, D = the water depth at the y-axis which runs through the point of maximum primary flow velocity (MP) in the cross-section; BI for i=1 or 2 for the right and left sides of the y-axis respectively, represents the channel top width at depth D; z = the coordinate in the transverse direction from the y-axis; y = the coordinate in the vertical direction; v* is the (cross-sectional) mean shear velocity; u = the primary flow velocity (in the x-direction) at some point (z,y); finally, δY, δI, β, ξ_0, k, and ϵ are coefficients characterizing the velocity distribution of the primary flow.

B.1.2 Determination of ξ-curve Coefficients

The model coefficients are determined by first selecting a point (Zb,Yb) on each bank and fitting a zero-velocity isovel, ξ-curve through these points and the origin (y=0 and z=0). This isovel is used to approximate the channel boundary and may be initially estimated as,

$$\xi = \left[\frac{\delta Y}{(D+\delta Y+\epsilon)}\right] \exp\left(1-\left[\frac{\delta Y}{(D+\delta Y+\epsilon)}\right]\right) \qquad [B.5]$$

To force the isovel through these points the slope of the ξ-curve at [Zb,Yb] is set equal to the slope of the bank at that point using the following relation,

$$S_\xi = \frac{dy}{d(ABS(z))} = \frac{\beta(D+\delta Y+\epsilon)}{(BI+\delta I)} \frac{(Y*Z)}{(1-Y)(1-Z)} \qquad [B.6]$$

The coefficients are then determined through an iterative process as follows:

a) Given (S_ξ) and ϵ (assume a value if unknown), assume a value for δY. Substitute into Eqn. B.7,

$$\beta = S_\xi\left(\frac{BI+\delta I}{D+\delta Y+\epsilon}\right)\left[\frac{(D+\epsilon-Y_b)(BI+\epsilon-Y_b)(BI+\delta I-ABS(Z_b))}{ABS(Z_b)(YB+\delta Y)}\right] \qquad [B.7]$$

to express ß as a function of only δI and substitute this expression into Eqn. B.8 and solve for δI.

$$\xi_o = \left(\frac{Y_b+\delta Y}{D+\delta Y+\epsilon}\right)\left[1-\frac{ABS(Z_b)}{BI+\delta I}\right]^\beta \exp\left[\beta\frac{ABS(Z_b)}{BI+\delta I} - \frac{Y_b+\delta Y}{D+\delta Y+\epsilon}+1\right] \qquad [B.8]$$

b) Substitute ϵ, δI, and δY into Eqn. B.7 and solve for ß.

c) Calculate the ξ-value for all observed primary flow velocities

d) Using the method of least squares determine k and ξ_0 in

Eqn. B.3 from the linear regression of u/u* with $\ln(\xi)$ as computed above for each observed velocity, where,

$$k = 1/b \qquad [B.9]$$

and,

$$\xi_o = e^{(-a/b)} \qquad [B.10]$$

(a is the y-intercept, b is the slope of the regression line, k is a calibration coefficient, and ξ_0 is the true zero velocity ξ-value).

e) Determine the standard deviation σ given by the regression line for the predicted values of u.

f) Repeat the above steps for different values of δY and compare σu to select the best set of model coefficients.

The curve $\xi=\xi ó$ is an approximation of the channel boundary (including banks) which should coincide relatively closely with $\xi=\xi_0$ which represents the zero u-curve. The $\xi ó$-curve was introduced as a guide to the parameter estimation procedure so that the effect of the actual cross-section could be incorporated into the simulated isovels.

B.1.3 Orthogonal Trajectories

Using rectilinear coordinates, i.e. $u = u(z,y)$ the velocity gradient is expressed as the partial derivative,

$$du = (\partial u/\partial z)\,dz + (\partial u/\partial y)\,dy \qquad [B.11]$$

However, the advantage of using a curvilinear coordinate system is that the velocity relation reduces to $u = u(\xi)$, which simplifies the equations of motion and continuity. It is therefore, practical to undergo a coordinate transformation from the rectilinear to curvilinear system.

Following previous developments by others, Chiu and Lin (1983) developed a family of orthogonal trajectories to the isovels as described by Eqn. B.1,

$$\eta = \pm\frac{1}{Z}\left(ABS(1-Y)\right)^{\beta\left[\frac{D+\delta Y+e}{BI+\delta I}\right]^2}\exp\left[Z+\beta\left(\frac{D+\delta Y+e}{(BI+\delta I)}\right)^2 Y\right] \qquad [B.12]$$

Equation B.12 is derived from Eqn. B.1 and is only negative when $(1-Y)<0$, or $y>(D+\epsilon)$ and $\epsilon<0$, that is the point of maximum primary flow velocity, MP is below the water surface.

Equation B.12 follows naturally from the vector transformation of the Jacobians. The transformation equations,

$z = f(\xi,\eta)$, $y = g(\xi,\eta)$, and $x = x$ (where it is assumed that f and g are continuous, having continuous partial derivatives and a single-valued inverse) establish a one to one correspondence between the points in the (x,y,z) and (x,ξ,η) coordinate systems. Since the x-direction does not undergo transformation it will be left out of the following discussion.

Using vector notation the transformation can be written,

$$r = zi = yj = f(\xi,\eta)i + g(\xi,\eta)j \qquad [B.13]$$

A point P can now be defined by both rectangular as well as curvilinear coordinates, (ξ,η). From Eqn. B.13,

$$dr = \frac{\partial r}{\partial \xi} d\xi + \frac{\partial r}{\partial \eta} \qquad [B.14]$$

If η is held constant, then as ξ varies r describes a curve which is called the ξ-coordinate curve. Similarly, if ξ is held constant, then as η varies r describes the η-coordinate curve. The vector $\partial r/\partial \xi$ is tangent to the ξ-coordinate curve at P. Letting $\mathbf{e}_1$ be a unit vector at P in this direction, then

$$\frac{\partial r}{\partial \xi} = h_\xi \, \mathbf{e}_1 \qquad [B.15]$$

where,

$$h_\xi = \frac{\partial \mathbf{r}}{\partial \xi}$$

In a similar manner,

$$\frac{\partial \mathbf{r}}{\partial \eta} = h_\eta \, \mathbf{e}_2 \qquad [B.16]$$

in which,

$$h_\eta = \frac{\partial \mathbf{r}}{\partial \eta}$$

Subsequently, Eqn. B.13 can be expressed as,

$$dr = h_\xi \, d\xi \, \mathbf{e}_1 + h_\eta \, d\eta \, \mathbf{e}_2 \qquad [B.17]$$

where the quantities h_ξ and h_η are referred to as the scale factors. These quantities were derived by Chiou and Lin (1983) from Eqns. B.1 and B.6,

$$h_\xi = \frac{(D+\delta Y+e)\,Y(1-Z)}{\xi\sqrt{\left([(1-Y)(1-Z)]^2+\left[\beta\left(\frac{D+\delta Y+e}{(BI+\delta I)\,YZ}\right)^2\right]\right)}} \qquad [B.18]$$

and,

$$h_\eta = \left(\frac{BI+\delta I}{D+\delta Y+e}\right)\left(\frac{\xi}{\eta}\right)\left[\frac{Z(1-Y)}{Y(1-Z)}\right]h_\xi \qquad [B.19]$$

The three-dimensional structure of primary flow velocity may now be reproduced through a convenient network of ξ- and

η-curves.

B.1.4 Shear Stress Distribution

The momentum equation in the x-direction (longitudinal direction) in the (ξ,η) coordinate system can be obtained from the coordinate transformation of this equation in the (x,y,z) system (Shen and Komura, 1968; Chiou and Lin, 1983),

$$\rho\left(\frac{\partial u}{\partial t}+u\frac{\partial u}{\partial x}+\frac{V_\xi}{h_\xi}\frac{\partial u}{\partial \xi}\right)=-\frac{\partial}{\partial x}(p+\rho gH)+\frac{\partial \sigma_x}{\partial x}+\frac{1}{h_\xi}\frac{\partial \tau_{\xi x}}{\partial \xi}+\frac{1}{h_\xi h_\eta}\frac{\partial h_\eta}{\partial \xi}\tau_{\xi x} \qquad [B.20]$$

The terms in Eqn. B.20 are defined as, ρ = fluid density: V_ξ is the ξ component of secondary flow velocity: 'p' represents hydrostatic pressure: 'g' is the force of gravity: and σ_x is the normal stress in the x-direction excluding pressure. Equation B.20 may also be rearranged and written in the form of a differential equation,

$$\frac{\partial \tau_\xi}{\partial \xi}+\left(\frac{1}{h_\eta}\frac{\partial h_\eta}{\partial \xi}\right)\tau_{\xi x}=h_\xi F \qquad [B.21]$$

where,

$$F=\rho\left[\frac{\partial u}{\partial t}+u\frac{\partial u}{\partial x}+V_\xi\frac{1}{h_\xi}\frac{\partial u}{\partial \xi}\right]+\left[\frac{\partial(p+\rho gH)}{\partial x}\right]-\frac{\partial \sigma_x}{\partial x} \qquad [B.22]$$

Since normal stress is relatively small it may be neglected and the solution to Eqn. B.21 may be expressed as,

$$\tau_{\xi x}(\xi,\eta) = \frac{-1}{h_\eta}\int^{\xi_{MAX}(\eta)} h_\xi h_\eta F d\xi + \tau_{\xi x}[\xi_{max}(\eta),\eta] \qquad [B.23]$$

where, $\xi_{MAX}(\eta)$ is the maximum value of ξ on the η-curve. However, for steady uniform flow in the x-direction du/dt=0, du/dx=0, and dp/dx=0. Consequently, Eqn. B.21 may be expressed as,

$$F = \rho g\left(\frac{\partial H}{\partial x}\right) + \rho\ V_\xi \frac{1}{h_\xi}\frac{\partial u}{\partial \xi} = \rho g S_f + V_\xi \frac{1}{h\xi}\frac{\partial u}{\partial \xi} \qquad [B.24]$$

where, S_f = the channel slope.

Similarly Eqn. B.23 may be written as,

$$\tau_{\xi x}(\xi,\eta) = \frac{\rho\ g S_f}{h_\eta}\int_\xi^{\xi_{MAX}\eta} h_\xi h_\eta d\xi - \rho\int_\xi^{\xi_{MAX}\eta} h_\eta V_\xi \frac{\partial u}{\partial \xi} d\xi] \qquad [B.25]$$

The first integral represents the effect of gravity with a mean value over the entire wetted perimeter of ρgRS, where R is the hydraulic radius. Using a method developed by Graf (1971), Chiu and Chiou (1986) showed that this term may be numerically integrated to yield a value of boundary shear equivalent to ρgSA divided by the length of the segment bd (Fig. B.1), where A is the area between successive η-curves.

The second integral in Eqn. B.25 represents the affect of secondary velocities. This term has a mean value of zero and is used to modify the distribution of shear resulting from the first term. However, the solution of Eqn. B.25 requires knowledge of the secondary flow component V_ξ, which in turn requires knowledge of $\tau_{\xi x}(\xi,\eta)$ and consequently, it can not be used to compute shear stress.

If the wind effects are neglected the shear stress on the water surface may be assumed to be zero. Similarly, where the N-curves originate (MP), $\xi = \xi_{max}(\eta) = 1$. The velocity gradient at this point in $(1/h_\xi)(\partial u/\partial \xi) = 0$ (as $h\xi \to \infty$)and hence $\tau_{\xi x} = 0$. These two cases describe the complete boundary conditions for the third term in Eqn. B.19. Consequently, the third term may be ignored.

Recognizing that $\tau_{\xi x}(\xi,\eta)$ is a function of ξ and η, which vary with the difference, $[\xi_{MAX}(\eta)-\xi]$ on any N-curve, Chiu and Hsiung, (1981) expanded the solution of Eqn. B.21 into the form of a polynomial in $[\xi_{MAX}(\eta)-\xi]$, which may be written as,

$$\tau_{\xi x}(\xi,\eta) = a_0+a_1[\xi_{MAX}(\eta)-\xi]+a_2[\xi_{MAX}(\eta)-\xi]^2 \qquad [B.26]$$

in which, $0<=[\xi_{MAX}(\eta)-\xi]<1$, and a_0, a_1, and a_2 are coefficients. Eqn. B.26 represents an alternate solution to Eqn. B.25 and an approximation of Eqn. B.21.

The η-curves originate from the point of maximum primary flow velocity, MP. At this point $\xi = \xi_{MAX} = 1.0$ and the velocity gradient $(1/h\xi)\partial u/\partial\xi = 0$ (as $h_\xi \to \infty$), and hence the shear stress $\tau_{\xi x} = 0$, and consequently,

$$a_0 = 0 \qquad [B.27]$$

The first term in Eqn. B.26 corresponds to the first integral in Eqn. B.25, that is, it represents the shear stress distribution without consideration of the effect of secondary currents and other factors. Consequently, from Eqns. B.23 and B.25,

$$\tau_{\xi x}(\xi,\eta) = \frac{\rho g S_f}{h_\eta}\int_{\xi}^{\xi_{MAX}\eta} h_\xi h_\eta d\xi = a_1[\xi_{MAX}(\eta)-\xi] \qquad [B.28]$$

in which, $a_1 = \tau_{\xi x} / \partial\xi$ is constant along any η-curve. This coefficient may be determined at the boundary condition $\xi = \xi_0$ as,

$$a_1 = \left[\frac{\rho g S_f}{h_{\eta\xi_o}}\int_{\xi_o}^{\xi_{MAX}\eta} h_\xi h_\eta d\xi\right]\left(\frac{1}{[\xi_{MAX}(\eta)-\xi_o]}\right) \qquad [B.29]$$

The value of a_2 can now be found for each value of η at any bed-bank station, (the integral term being estimated through numerical integration along the η-curve).

Secondary flow and other effects are considered in the second term in Eqn. B.26, which is referred to as the "residual" term. The value of the coefficient a_2 may be determined by using Eqns. B.21 and B.26 at the boundary condition, $V_\xi=0$ at $\xi=\xi_0$;

$$a_2 = \left[\frac{-h_\xi F_o - a_1 \{1-(\frac{1}{h_\eta}\frac{\partial h_\eta}{\partial \xi})\,[\xi_{MAX}(\eta)-\xi_o]\}}{[\xi_{MAX}(\eta)-\xi_o]\ \{2-(\frac{1}{h_\eta}\frac{\partial h_\eta}{\partial \xi})\,[\xi_{MAX}(\eta)-\xi_o]} \right] \qquad [B.30]$$

where, $h_\eta/\partial\xi$, h_η, and h_ξ are evaluated at each bed-bank station.

The above technique for the calculation of shear was translated into a computer simulation model under the acronym of EROS1. The model was developed for the derivation of the boundary shear stress distribution in nonuniform natural channels as a basis for the evaluation of the impact of urbanization on instream erosion potential. The FORTRAN 77 source code, a users manual and example input and output files are provided in Appendix C. The advantages and limitations of the proposed technique are discussed in the users manual.

B.2 Model Verification

Verification of the model is reported in this subsection in two parts. The first application is to a velocity and boundary shear stress distribution observed for a prismatic laboratory channel. The second application is toward the reproduction of a velocity profile observed in a natural channel.

B.2.1 Application To A Prismatic Laboratory Channel

Direct measurement of boundary shear, even in laboratory flumes, is very difficult to obtain. This is especially true near the channel side walls. Consequently, indirect measurements are usually made using Preston tube estimates,

$$\tau_o = b(P_S - P) + (4a\ \rho\ \epsilon_K{}^2)/\log d^2 \qquad [B.31]$$

in which, b is the slope of the calibration curve relating the quantity τ_o to measurements of the change in static and stagnation pressure along the channel boundary (P_S-P), a is the y-intercept of the calibration curve, ρ (the fluid density), ϵ_K (the fluid viscosity), and d (the diameter of the tube opening).

A second indirect measurement technique is based on measurements of the logarithmic velocity profile. Ghosh and Roy, (1970) presented boundary shear stress distributions for various prismatic channel configurations and bed roughness using both techniques. To provide a demonstration of EROS1 modeling capabilities a trapezoidal channel semi-perimeter of 1H:1V was selected for comparison with Ghosh and Roy values. A depiction of the channel is provided in Figure B.2 (a) together with a comparison of isovels derived from observed

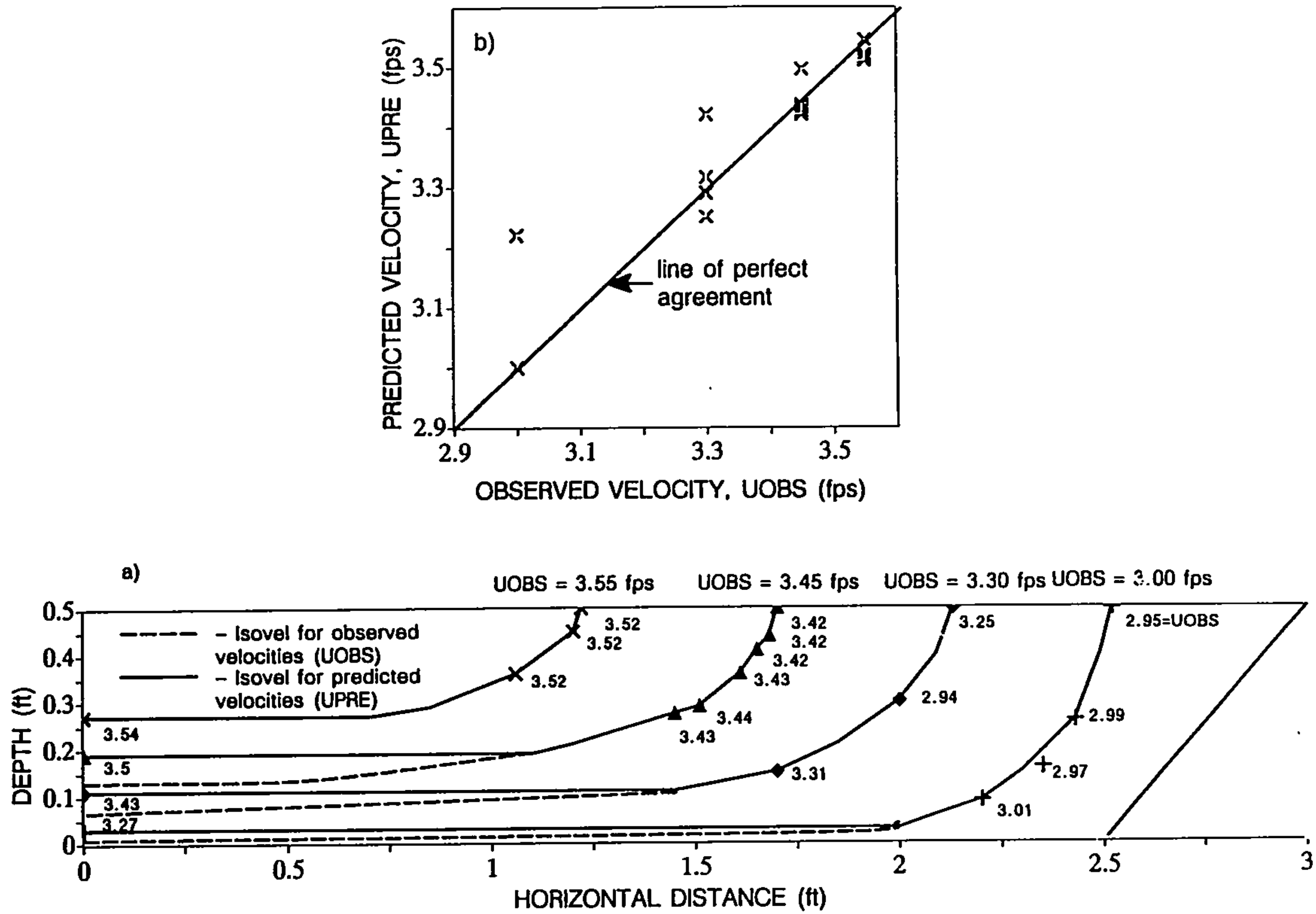

FIGURE B.2 Comparison of Observed versus Predicted Velocities for a Trapezoidal Channel Semi-Perimeter

primary velocities and predicted velocity. Figure B.2 (b) provides a plot of predicted versus observed velocities. The regression coefficient of 0.77 was obtained indicating good agreement. Examination of Figure B.2 (a) indicates that the model provides an good reproduction of primary flow velocities in the boundary and upper portions of the flow field. The agreement was poorest in the lower depths of the flow field in the central portion of the channel. The statistics for the analysis are provided as a sample output file in Appendix C.

Figure B.3 shows a PLOTSEC2 display of predicted isovels and the shear stress ratio for comparison with indirect measurements of boundary shear as reported by Ghosh and Roy. Shear stress ratio is defined as the instantaneous shear divided by the average shear. It can be seen from this figure that the predicted distribution of boundary shear stress is generally in good agreement with the observed distribution obtained from indirect measurements. The minimum shear stress value appears to be shifted slightly toward the channel center for predicted conditions. This is associated with the approximation of the channel boundary using EPRIME. Regardless, both the magnitude and transverse distribution exhibited by the predicted values is considered to be in good agreement with published observations.

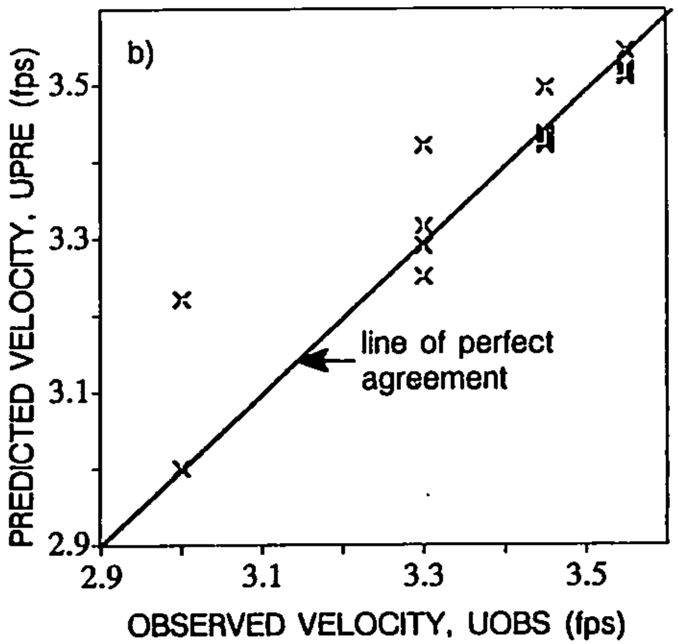

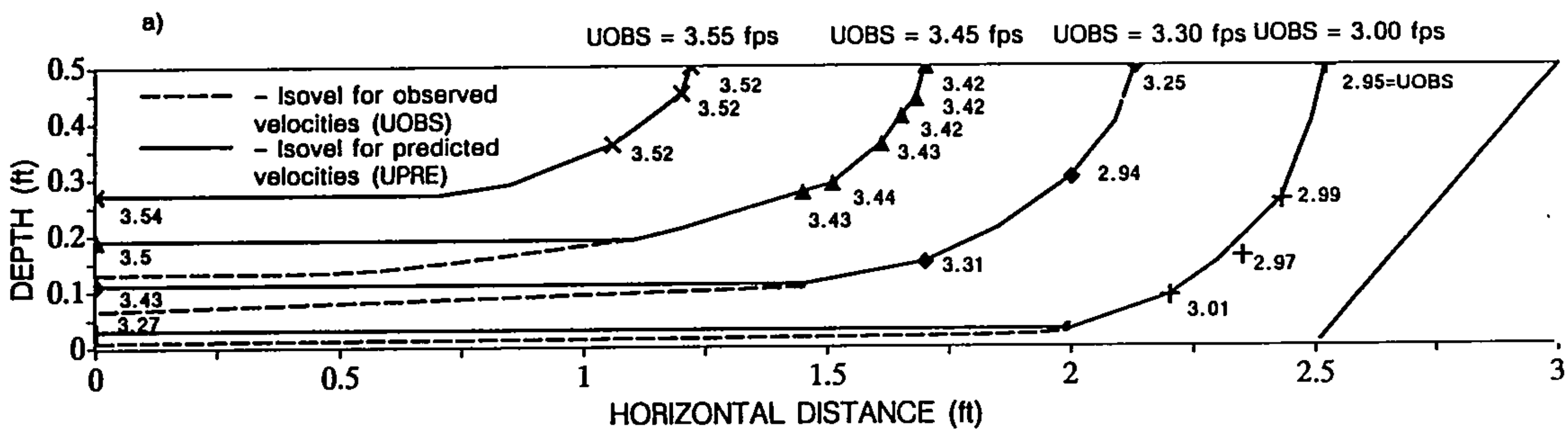

FIGURE B.2 Comparison of Observed versus Predicted Velocities for a Trapezoidal Channel Semi-Perimeter

B.2.2 Application To Rideau River

For verification of the models ability to reproduce the velocity profile observed in a natural channel a section of the Rideau River at Lees Avenue, Ottawa, Ontario was selected for study. The study section is located approximately 4.5 m downstream of Lees Avenue bridge. Velocity profiles were measured at this section on March 20, 1987 at eight transects located along the section at intervals of approximately 10 m, (McGuire, 1987). Although the flow was affected by the presence of river ice, for the calculation of boundary shear only the lower portion of the velocity profile was considered as proposed by Coleman, (1981). The cross-section configuration and observed velocities for the channel semi-perimeter are presented in Figure B.4 (a) and (b) respectively.

Using the Prandtl-Von Karmon logarithmic velocity law was fitted to the data for comparison with the EROS1 distribution. This was done by first writing the logarithmic velocity

equation as,

$$\frac{v(k)}{v*} = \ln(y) + C$$

$$e^{(vk/v*)} = e^{(lny+C)} = e^{(lny)}e^{C} \qquad [B.32]$$

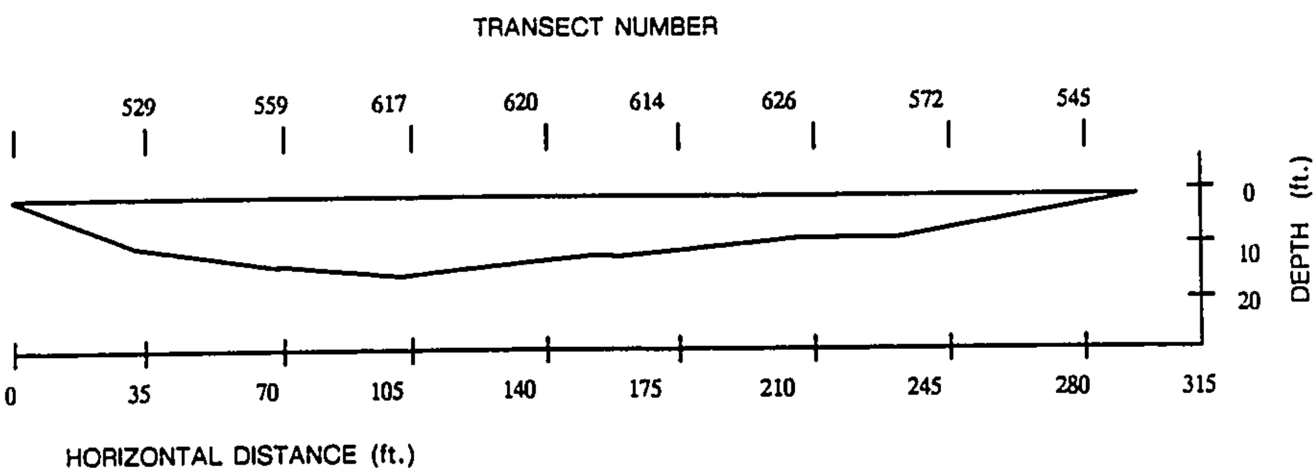

a) Cross-Section Configuration

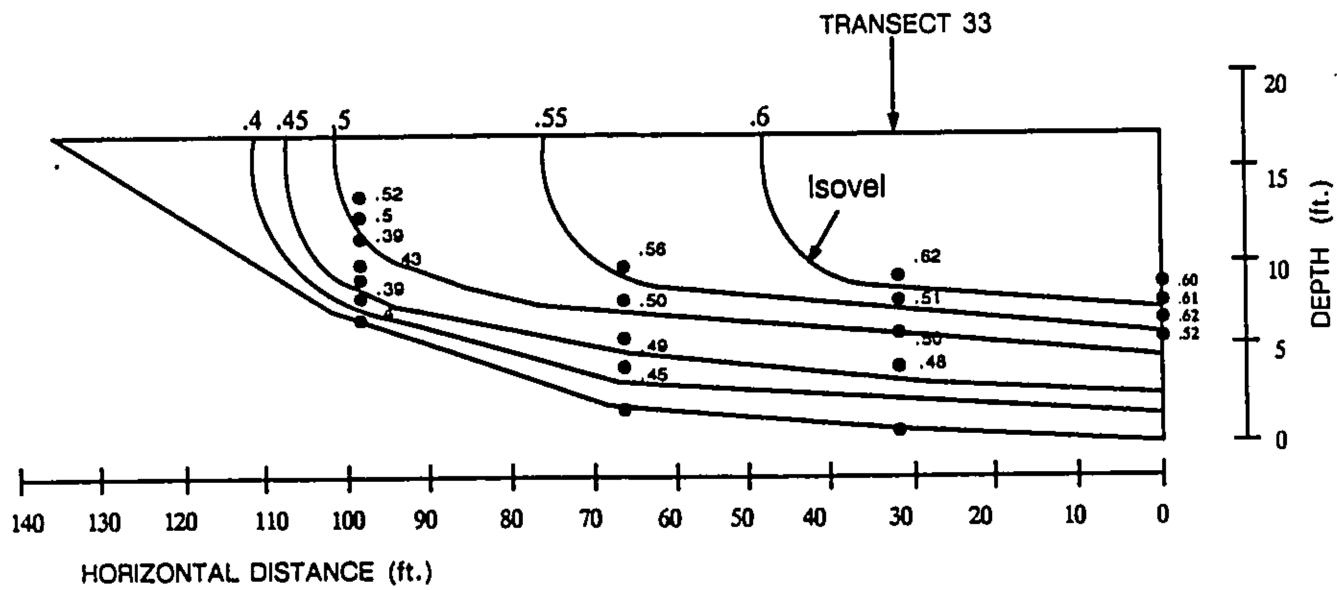

b) Observed Velocities

FIGURE B.4 Field Observations of the Rideau River at Lees Avenue, Ottawa, Ontario, (McGuire, 1987)

Since, e^c = constant, then let the constant be denoted by "a", hence,

$$e^{(vk/v_*)} = ay \qquad [B.33]$$

Solving for "a" yields,

$$a = \frac{e^{(vk/v_*)}}{y} \qquad [B.34]$$

Using the velocity profile observed at z = 33 ft (Figure B.4 (b)), Table B.1 was constructed to solve for "a".

TABLE B.1

Solution For The Constant In The Prandtl-Von Karmon Logarithmic Velocity Profile

y (ft)	v (fps)	k	v (fps)	$e^{(vk/v_*)}$ dim	a (ft^{-1})
4.16	0.475	0.4	0.0384	141.4	34.0
5.16	0.503			189.4	36.7
7.16	0.572			388.8	54.3
9.16	0.617			621.5	67.8

dim = dimensionless

Having obtained "a" for various flow depths (y), it is now possible to derive a relationship as shown in Figure B.5.

$$a = 7.114(y) + 2.608, \quad R = 0.993 \qquad [B.35]$$

where, R = the correlation coefficient.

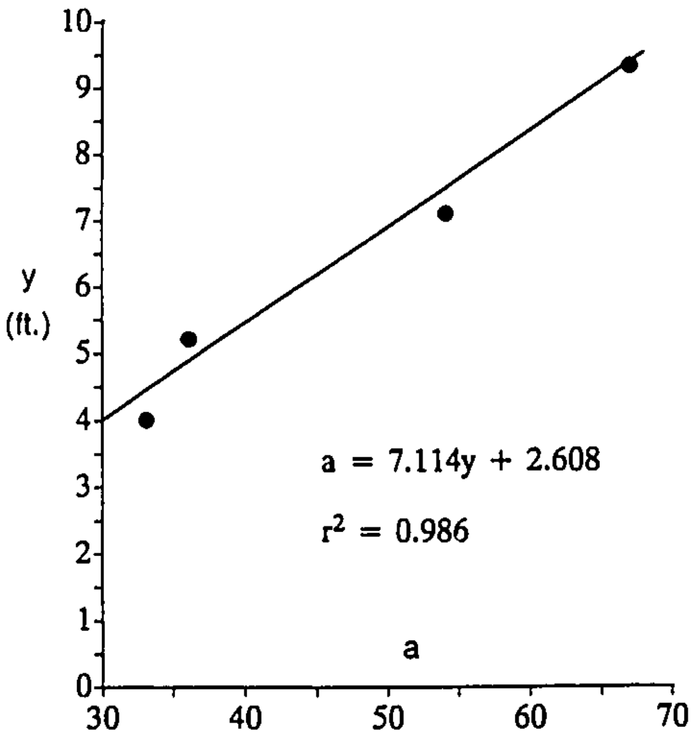

Figure B.5 Constant in the Prandtl–Von Karmon Logarithmic Velocity Profile for the Rideau River at Lees Avenue (Transect 33)

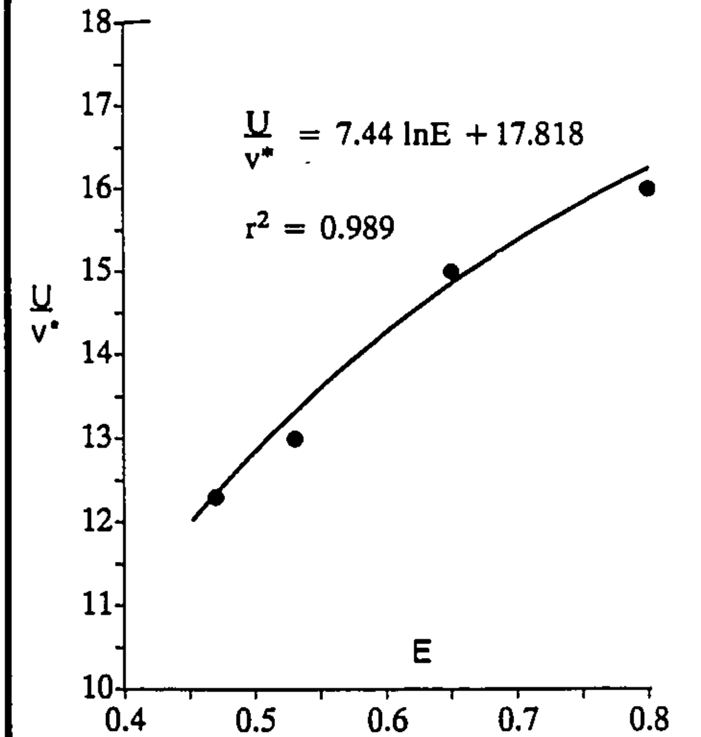

Figure B.7 E – Curve Values as a Function of U/v*

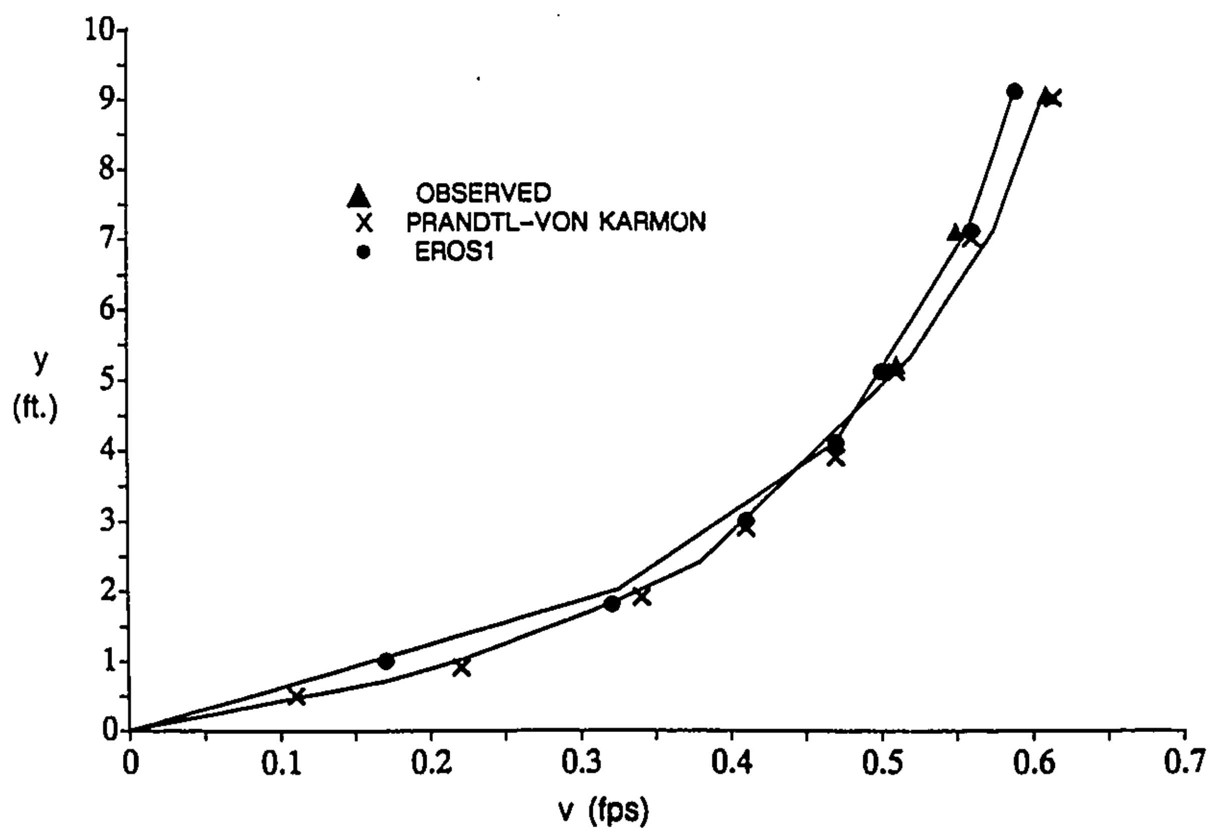

Figure B.6 Observed and Simulated Velocity Profiles for the Rideau River at Lees Avenue (Transect 33)

Rearranging Eqn. B.33 to isolate "v", and substituting for "a" yields,

$$v=\frac{v*}{k}[\ln(7.114(y)+2.608)+\ln(y)] \qquad [B.36]$$

This relation may be simplified to give,

$$v=\frac{v*}{k}[\ln(7.114(y^2)+2.608(y))] \qquad [B.37]$$

Solving for "v" for any depth yields the predicted velocity profile which is plotted in Figure B.6 against observed values. It can be seen from this figure that the Prandtl-Von Karmon logarithmic velocity profile closely approximates the observed velocity profile.

Velocity data for all of the transects shown in Figure B.4 (b) were entered into the EROS1 model. The model was calibrated to a flow of 44,5 m^3/s (1571 cfs) for the entire cross-section as computed from the velocity transects. Based on a total cross-sectional area of 287 m^2 (3087 ft^2), the average velocity was found to be 0.157 m/s (0.516 fps) with a longitudinal slope of 0.00000384 m/m at a Manning's roughness value of n = 0.03. A summary of the ξ-coefficients is provided in Table B.2.

These values were obtained with a rough calibration of the model. A detailed calibration was then performed to determine ξ_o and k for the desired transect (z = 10 m, or 33 ft).

Table B2

Summary Of ξ-Coefficients For The Rideau River At Lees Avenue

Parameter	Value(ft)
β	5.215
δi	1.39
δy	0.26
ϵ	0.105

Since z is held constant, and only y is allowed to vary, the shape in the z-direction is a constant value of Z=0.244. Further, β is also constant, therefore, Eqn. B.3 reduces to,

$$\xi = Y(1-.244)^{5.215} e^{(5.215(.244)-Y+1)} = 0.233(Y)\, e^{(2.271-Y)} \qquad [B.38]$$

It is now possible to solve for ξ for any depth and plot the function u/v* = $f(\xi)$ as illustrated in Figure B.7. A regression analysis of this plot gave the following expression,

$$\frac{u}{v*} = 7.414\ln(\xi)+17.818,\ r=0.995 \qquad [B.39]$$

in which r is the correlation coefficient.

Rearranging Eqn. B4.4 gives,

$$\frac{u}{v*}=\frac{1}{k}\ln\left(\frac{\xi}{\xi_o}\right) \qquad [B.40]$$

Expanding Eqn. B.40 yields,

$$\frac{u}{v*}=\frac{1}{k}\ln(\xi)-\frac{1}{k}\ln(\xi_o) \qquad [B.41]$$

By equating Eqn. B.41 with the general form of the linear regression equation,

$$y=bx+a \qquad [B.42]$$

where y = the y-axis value, x = the x-axis value, b = the slope of the line, and a = the y-axis intercept, it can be seen that,

$$y=\frac{u}{v*} \qquad [B.43]$$

$$b=\frac{1}{k} \qquad [B.44]$$

$$x=\ln(\xi) \qquad [B.45]$$

$$a=-(\frac{1}{k})\ln(\xi_o) \qquad [B.46]$$

From Eqn. B.39, values can be assigned to Eqns. B.44 and B.46 yielding, k=0.135 and ξ_0=0.0904. By substituting these values into Eqn. B.40 the logarithmic velocity profile can be obtained form the following calibration relation,

$$u=0.284\ln\left[\frac{\xi}{0.0904}\right] \qquad [B.47]$$

$$u=0.284\ln\left[(0.233Y)\frac{e^{(2.271-Y)}}{0.0904}\right]$$

in which Y is given in Eqn B.2.

The resulting velocity gradient is illustrated in Figure B.6 in comparison with that derived using the Prandtl-Von Karmon method and observed velocities. This comparison is summarized in terms of percent error in Table B3.

Table B3

Comparison Of Prandtl-Von Karmon and EROS1 Logarithmic Velocity Curves Against Observed Velocities for Rideau River at Lees Avenue

Y (ft)	OBSERVED VELOCITY (fps)	PREDICTED VELOCITIES PRANDTL (fps)	EROS1 (fps)	PERCENT ERROR PRANDTL	EROS1
4.16	0.475	0.470	0.471	-1.05	-0.84
5.16	0.503	0.510	0.511	1.39	1.59
7.16	0.572	0.571	0.565	-0.17	-1.22
9.16	0.617	0.617	0.597	0.00	-3.24

Both the Prandtl-Von Karmon and EROS1 methods appear to reproduce the observed velocity profile well. The slightly poorer fit by the EROS1 model for the EROS1 model for higher flow depths reflects the assumption that the point of maximum primary flow velocity occurs above the water surface (ϵ=0.105 ft). One of the effects of ice cover is that this point occurs within the flow field. However, near bed velocities are of more importance in the determination of scour.

APPENDIX C

A Boundary Shear Stress Distribution Model: EROS1

C1.0 Introduction

C1.1 Background

The concept for EROS1 originated from the need to develop a methodology and a tool for the evaluation of the effectiveness of storm water management measures (SWM) toward the mitigation of increased erosion potential associated with the process of urbanization. Current methods based on hydrologic methods do not adequately account for the resistance of the channel materials. More sophisticated mobile bed degradation models, while accounting for the physical processes of sediment transport require field data for calibration and verification of model parameters and do not adequately address bank stability. Further, these techniques may not be applicable in small channel where boundary effects from banks significantly modify the primary flow field.

EROS1 was developed based on the computerization of the technique developed by Chiu and Lin (1983) for the mathematical modeling of non-uniform and non-symmetric 3-D flow in a manner practicable to the practicing water resources specialist. This technique is capable of simulating various patterns of primary flow velocity distribution and incorporates the affect of circulating secondary currents to determine the associated boundary shear stress at any point along an irregular channel perimeter. The resulting shear values and distributions may then be related through principles of fluvial geomorphology, river engineering, and slope stability to channel form to provide an index of channel stability.

C1.2 Modeling Approach

A brief description of the governing equations is presented in Appendix B. For a complete theoretical discussion of the technique the reader is referred to Chiu and Chiou, (1985), Chiu and Lin, (1983), Chiu and Hsiung, (1981), Chiu and Lin, (1978), Chiu et al., (1976), and Ghosh and Roy, (1970).

C2.0 MODEL STRUCTURE

C2.1 Computer System Requirements

The model code is written in Microsoft FORTRAN (MS-FORTRAN) which includes extensions to the subset language and some of the features of full ANSI standard, (FORTRAN 77). No unusual

FORTRAN extensions were employed, however some conventions, particularly file handling statements may not be applicable directly to all computer systems.

The model requires nominal storage and operating space allocations and should run easily on any IBM or compatible PC system. The model has been successfully tested on the IBM-PC, KAYPRO 286i (AT), and the ZENITH-PC.

The code itself consists of a main program (MAIN) which invokes six subroutines in a predetermined manner, (Figure C1). The only flexibility provided to the user in the nature or sequence in which the commands are issued is in the manner in which the ξ-coefficients are determined and the number of depths for which shear will be simulated, (Section C3.1.1).

The operations performed by each subroutine and MAIN are summarized below.

ROUTINE	FUNCTION
MAIN	* assigns variable names * calls subroutines * determines hydraulic geometry parameters * computes a rating curve * closes files
FILES	* opens input and output files
READER	* reads input file and stores input data in an array
ECOEF	* fits a logarithmic velocity profile to velocity

	data * determines ξ-coefficients, YDELTA, IDELTA, BETA, and EP
ORTHO	* transposes curvilinear to cartesian coordinates * numerically integrates up each η-curve to determine its length and the rate of change of the ξ-curve. * calls subroutine NEWT
NEWT	* determines the curvilinear coordinates of selected points along each η-curve
TAUBED	* calculates shear stress at each bed-bank station * determines average shear for the channel section

C2.2 Model Execution

To execute the model type "EROS1". The user will be prompted for the name of the input file. The file name entered must be that of an existing file in the form "file.dat". If the file does not exist the model will inform the user and send a prompt for another file name.

Following the successful entry of the input file the user is prompted for an output file name. The file name entered may be in the general form "file.out" or any arbitrary nomenclature acceptable to the operating system. The model inquires as to the status of the designated file. If it already exists the user is asked if they wish to over-write the file or if they would prefer to enter an alternative file name. If the designated file does not exist a new file is created automatically and assigned the name entered.

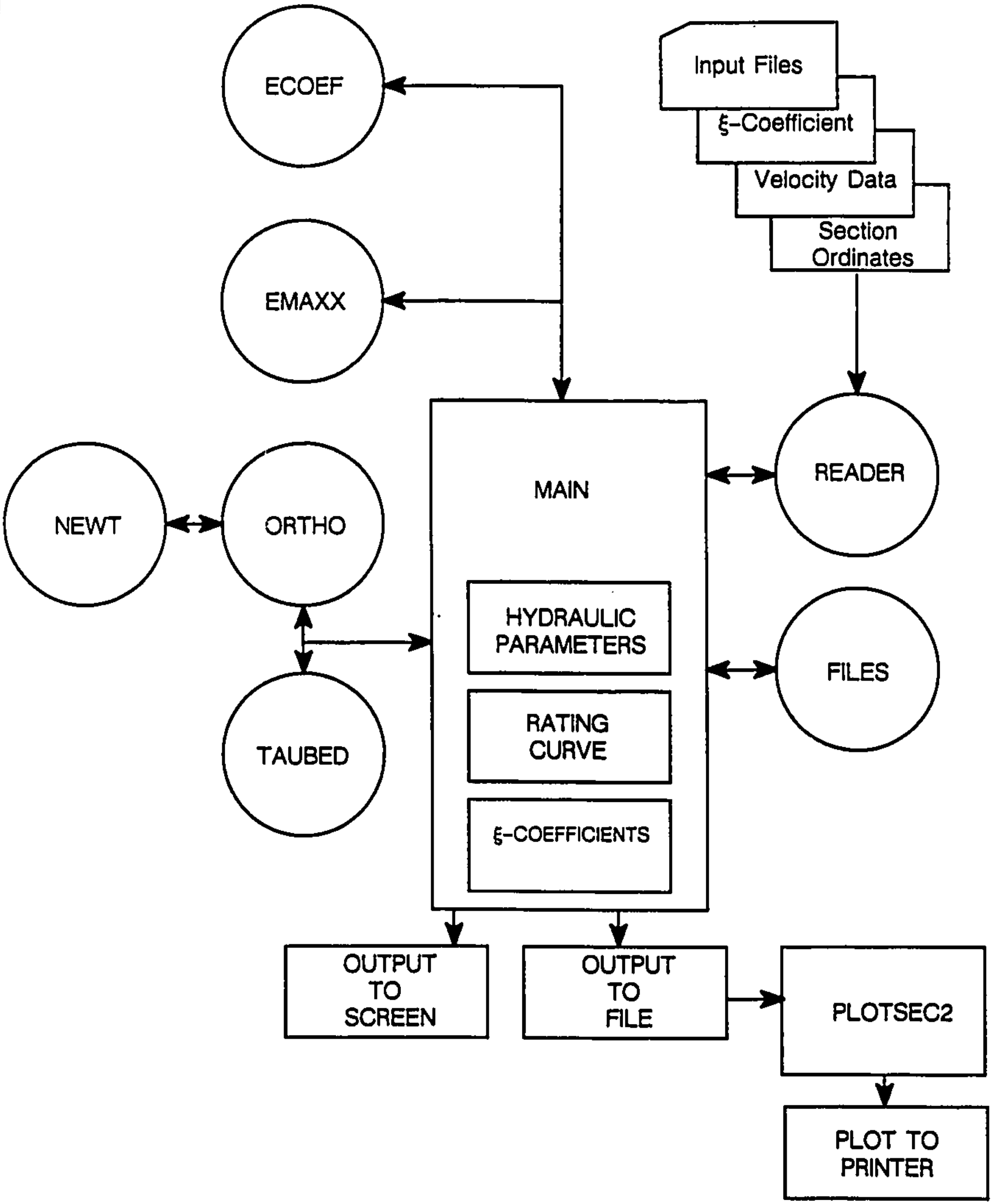

FIGURE C.1 EROS1 Model Organization

Upon satisfaction of these prompts the model will begin execution and will continue to run to completion if uninterrupted. If interrupted by a "Ctrl C" or a "Ctrl Break" the run will be terminated and the output erased.

C3.0 MODEL INPUT REQUIREMENTS

This section describes the functions and data input requirements for EROS1 release 1.0 and PLOTSEC2 release 1.0.

C3.1 EROS1

C3.1.1 ξ-COEFFICIENT CARD

The ξ-COEFFICIENT card is used to initialize the major controlling variables in the determination of the isovel curves, orthogonal trajectories and key flow and hydraulic characteristics for the subject cross-section.

PARAMETER	DIMENSION	DESCRIPTION
TITLE		Optional user documentation
SECNO		Cross-section designation number, (0 <= SECNO <= 99999)
SIDE(I)		Side refers to the right or left sides of the y-axis where I is either 1 or 2, (designation is arbitrary).
BI(SIDE)	feet	BI is the top width (feet) at depth D for SIDE=1 or 2.
D	feet	The water depth at the y-axis which runs through the point of maximum primary flow velocity, (M). D must be the same for both I=1 and 2.

YB	feet	The y-coordinate of a point on the bank through which the isovel at zero velocity is forced.
ZB	feet	The z-coordinate of a point on the bank through which the isovel at zero velocity is forced. Note ZB < 0.0 for SIDE = 1.
DMIN	feet	The minimum depth for which the isovel curves will be generated for the calculation of shear stress.
YDELTA	feet	If > 0, a coefficient characterizing the primary velocity distribution in the y-direction. If ≤ 0, an empirical relation will be used to estimate YDELTA.
EP	feet	Distance from the water surface to the point of maximum primary flow velocity (M). If M > D then EP > 0.0, or if M <= D then EP <= 0.0.
SLPB	dim*	The slope of the isovel at the bank station (ZB,YB).
SLPF	dim	The longitudinal channel slope.
MANN	dim	Manning's roughness coefficient.
JFLAG		If = 1. The simulation will proceed automatically for all depths (bed-bank stations) over the range DMIN < D < DMAX. If = 0. The simulation will terminate after the first depth, D=DMAX.
YFLAG		If = 1. IPARM(5)=EPRIME If = 2. IPARM(5)=YDELTA
METHOD		If = 1. The regression method is used to derive E-coefficient values for all depths. If = 2. The extrapolation method is used to interpolate E-coefficient values for all depths between calibration depths.

NCALIB	<=7	If METHOD=2 enter number of depths for which E-coefficients are provided. If METHOD=1 Omit.

------------------ If METHOD =1 then repeat ----------------
------------------ the following sequence ----------------
------------------ for IPARM = 1,6 ----------------

IPARM(I) — Variable identifier according to the following convention (1=1,6).
IPARM(1)=YB
IPARM(2)=ZB
IPARM(3)=BETA
IPARM(4)=EP
IPARM(5)=EPRIME or YDELTA according to value selected for YFLAG
IPARM(6)=SLPB

IEQN(I) — Equation type identifier according to the following convention, (I=1,4).
IPARM(I)=SLPM(I)*D+BCEPT(I)
IPARM(I)=EXP(SLPM(I)*D+BCEPT(I))
IPARM(I)=SLPM(I)*LN(D)+BCEPT(I)
IPARM(I)EXP(SLPM(I)*LN(D)+BCEPT(I))

SLPM(I) — Slope of the line in the regression equation IEQN(I). An arbitrary value may be supplied if JFLAG = 1, (I=1,4).

BCEPT(I) — Y-intercept of the regression equation IEQN(I). An arbitrary value may be supplied if JFLAG = 1, (I=1,4).

-------------------- End of Sequence ------------------

--------------- If METHOD=2 --------------
--------------- repeat the following sequence --------------
--------------- NCALIB times --------------

PTABLE(NCALIB,I) — Calibration depth, D(I)
Corresponding YB value
" ZB "
" BETA "
" EP "
" EPRIME " if YFLAG=1
" YDELTA " if YFLAG=2
" SLPB "

If JFLAG=1 then NCALIB=1 and one row in the PTABLE matrix must be entered although dummy values may be used.

--------------------- End of Sequence -------------------

* dim = dimensionless

Notes: The first 20 fields on each card may be used to document the code for ease of reference with fields 21-80 representing the active input field. Parameters are entered without omission in the order as listed. The model reads only numeric, decimal and negative declarants, (the later must be preceded by a space). Alpha characters may be used freely to document the input parameters anywhere in the eighty column field.

The depth D is the depth at which calibration of the model is desired which usually but not necessarily corresponds to the bankfull stage. DMIN is determined as the depth of flow below which the assumed logarithmic velocity distribution used for calibration is no longer representative of the prevailing velocity distribution. This may be estimated from consideration of channel geometry, eddy viscosity, the Reynold's number, and the height of the roughness elements.

C3.1.2 VELOCITY DATA

Observed or derived primary flow velocities are used to calibrate the logarithmic velocity distribution equation.

PARAMETER	DIMENSION	DESCRIPTION
TITLE		Optional user documentation. Not used by the model.
NUOBS		The number of point velocities to be read, (NUOBS <= 50).
YOBS(I)	feet	The y-coordinate of the point velocity in the (z,y) plane, I=1,NUOBS.
ZOBS(I)	feet	The z-coordinate of the point velocity in the (z,y) plane. I=1,NUOBS. Note ZOBS < 0.0 if SIDE=1.
UOBS(I)	fps	The point flow velocity in the x -direction, I=1,NUOBS.

------------ Repeat (YOBS,ZOBS, UOBS) NUOBS times. ---------

Notes: If observed primary flow velocities are not available for the subject reach a derived flow velocity distribution may be used. In this case it is suggested that the average flow velocity be computed using Manning's formula and an assumed logarithmic velocity profile be fitted along the y-axis by assuming that 0.4D <= v <= 0.6D according to the roughness and hydraulic geometry of the subject cross-section. At least three point velocities along the y-axis are required for the operation of the model. It is not necessary to input point velocities within the flow field for values of z > 0.0. However, to obtain proper calibration flow velocity measurements through the entire water column are required.

This is for two reasons:

1) Two provide a check on the flow computations,
2) for the proper estimate of the effect of secondary currents on boundary shear stress, and

However, when calibrating to measured shear stress data only the velocities measured in the near bank zone are valid because of Prantl's assumption of constant internal shear stress over the entire flow depth, (Vetter, 1986). It is recommended therefore, that the pseudo Von Karman constant (k) reported in the output be calibrated to a value calculated from the slope of the logarithmic velocity distribution in the lower part of the flow depth, (Coleman, 1981).

C3.1.3 Cross-Section Ordinates

The cross-SECTION ORDINATES card describes the channel boundary. A maximum of twenty bed-bank stations may be used to define a channel semi-perimeter.

PARAMETER	DIMENSION	DESCRIPTION
TITLE		Optional user documentation. Not used by the model.
NUMB		The number of bed-bank stations to be read, (NUMB ≤ 20).
YBED(I)	Feet	The y-coordinate of the bed-bank station in the (z,y) plane, (I=1,NUMB).

ZBED(I)	Feet	The z-coordinate of the bed-bank station in the (z,y) plane, (I=1,NUMB). If SIDE=1, ZBED < 0.0, If SIDE=2, ZBED > 0.0 by convention.

----------- Repeat [YBED(I), ZBED(I)] pairs -------------
----------- NUMB times -------------

Notes: The η-curve is undefined at the y-axis, therefore by definition the bed-bank station at the origin (0,0) MUST NOT be included in the list of ordinates. Shear stress is calculated at each bed-bank station. The resulting shear stress distribution is than used to derive average shear, TAUBAR. TAUBAR may then be compared with the average shear stress value TAUAVE, as computed by Du Boys' relation, to calibrate the model, (see Section C4.0). To obtain a representative shear stress distribution it is generally desirable to use a minimum of 10 bed-bank stations.

C3.2 PLOTSEC2

PLOTSEC2 is a graphics package written in BASIC. It is designed to plot cross-section coordinates, the isovels and the orthogonal trajectories describing the primary velocity distribution. In addition the program outputs a plot of the boundary shear stress distribution expressed as a ratio of instantaneous shear stress to average shear stress.

MENU COMMAND	DESCRIPTION
R (READ)	The user is prompted for the EROS1 output file as input to PLOTSEC2. Upon entry of the appropriate file name the file is scanned and a plot of the channel cross-section semi-perimeter and shear stress distribution will appear on the screen.
P (PLOT)	This command will result in the plotting of the isovels and orthogonal trajectories. The isovels are plotted in increments of $0.1(\xi)$ over the interval $0.2 <= \xi <= 0.9$. The estimated zero velocity isovel EPRIME is also plotted. The user is also prompted for the number of orthogonal trajectories to be plotted.
S (SKIP)	When in the P mode the S command may be used to abort the plotting of the current isovel. The plot routine immediately skips to the beginning of the next isovel where it resumes plotting. The "/" key may be used at any time to terminate the isovel or orthogonal plot commands.
T(TITLE)	The T command enables the user to enter a discretionary title at the top of the plot.
H(HARD COPY)	The H command allows the user to clear the menu line from the screen in preparation for the generation of a hard copy of the plot.
CLS (CLEAR)	The C command enables the user to completely clear the screen.
MD (EDIT)	This command allows the user to change a parameter value and re-compute the isovel and orthogonal curves. The new curves may then be replotted using the above commands.
Q(QUIT)	Allows the user to return to DOS.

Notes: Even if JFLAG=0 a plot will only be generated for the first depth simulated. Since the plot routine scans the entire file before execution considerable time may be saved if the

EROS1 run is aborted after completing calculations for the first depth, (JFLAG=1).

To obtain a hard copy of the graphics displayed on the screen a system equipped with a printer and graphics card is required. The DOS GRAPHICS command should be executed before the PLOTSEC2 is called. The program is not designed for interface with a plotter.

The plotted isovels may be converted to units of (fps) using the calibrated logarithmic velocity distribution equation, (Eqn. 5.6) for comparison with observed flow velocity data.

C4.0 CALIBRATION PROCEDURE

This section describes a suggested calibration procedure for EROS1 which may be carried out in two parts. The first stage involves the matching of observed or derived instantaneous discharge and average primary flow velocity at depth D with those generated by the model. This is achieved through manipulation of the parameters for longitudinal channel slope, (SLPF) and Manning's roughness coefficient, (MANN). This phase may be completed with only a gross calibration of the isovel coefficients.

The second stage involves the refinement of the estimation of the isovel coefficients. The process is schematized in Figure C2 and describe below with an example run provided in Section C5.

C4.1 Calibration to Flow Data

STEP 1 - Using observed values of UOBS, YOBS, and ZOBS for depth D plot the logarithmic velocity profile for the primary flow velocity through the point of maximum flow velocity (M) along the (z=0,y) axis. If observed flow velocities are unavailable than use observed or derived instantaneous discharge, Qat depth D to compute channel cross-sectional area, A and the average flow velocity, (v= Q/A). Fit an assumed logarithmic velocity profile to v by assuming 0.4(D) <= v <= 0.6(D) according to channel roughness and hydraulic geometry. Using the fitted profile determine a minimum of three point velocities along the y-axis for use in the simulation.

STEP 2 - From the logarithmic velocity distribution estimate EP. If EP is indeterminate than set EP within the range 0.15(D) as an initial estimate and refine through calibration as described below.

STEP 3 - Determine BI for the desired semi-perimeter at depth

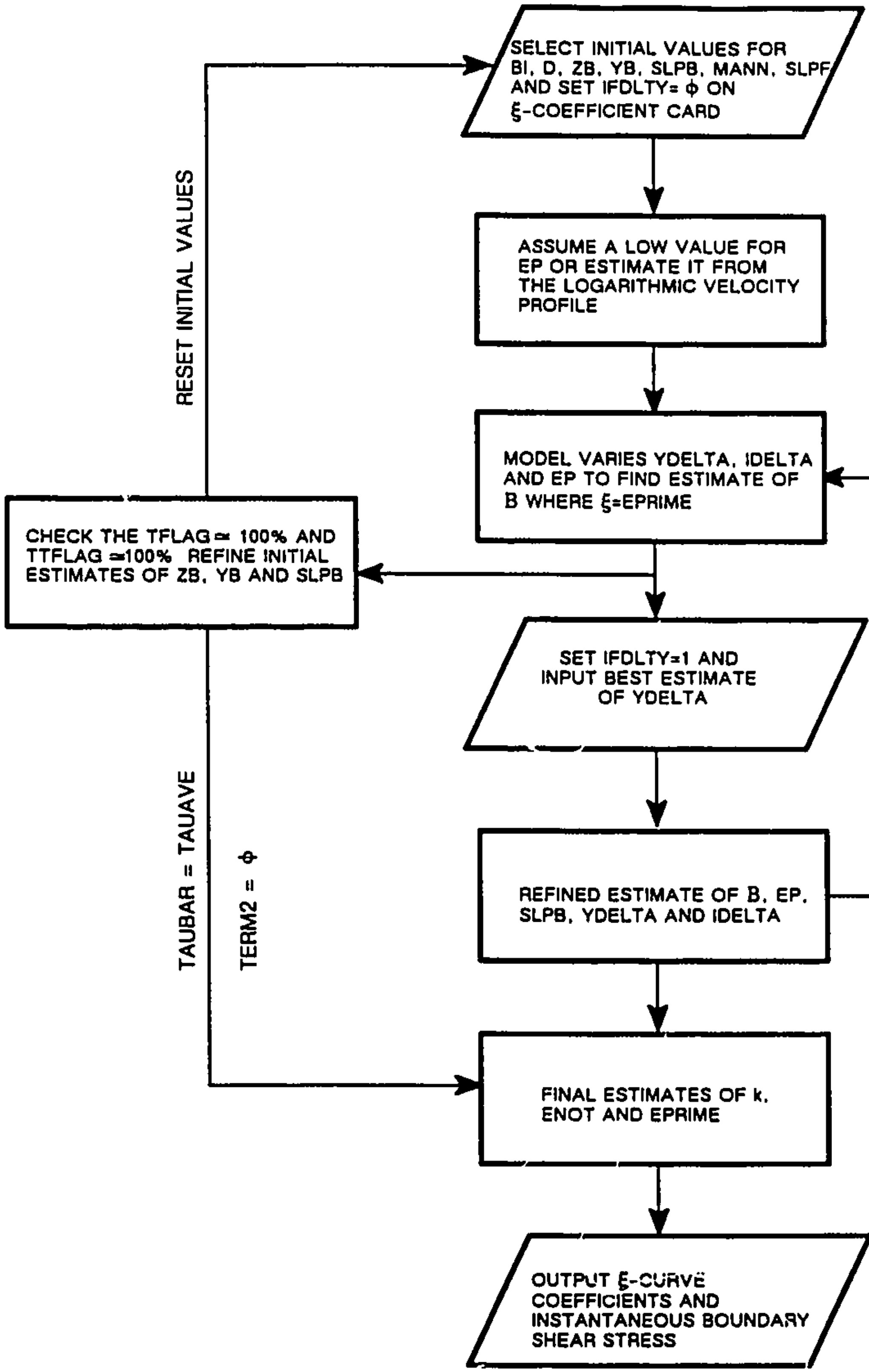

FIGURE C.2 ξ–Curve Calibration Procedure

D from the cross-section hydraulic geometry.

STEP 4 - Select a bed-bank station (ZB,YB) through which the zero velocity isovel will be forced. As a first estimate select a point on the boundary where $0.05(y) \le YB \le 0.2(y)$. Generally, the more circular or elliptical the channel shape the greater the value of YB.

STEP 5 - Set the initial value of (SLPB) as a representative bank slope through the point (ZB,YB) as determined from cross-section geometry.

STEP 6 - Use an observed or estimated value for longitudinal channel slope, (SLPF).

STEP 7 - Determine Manning's roughness coefficient, (MANN) from published tables, or alternatively from experimental or field observations.

STEP 8 - As a first approximation set YDELTA=0 in the input deck and allow the model to quantify the parameter from an empirical relation of the form, YDELTA = 0.0048(D)**2.

STEP 9 - Set up the EROS1 input file using up to twenty bed-bank stations. A minimum of ten stations is suggested.

STEP 10 - Run EROS1 for the first depth, D. This is achieved by setting JFLAG = 1. Note that if JFLAG = 0 than the model will automatically proceed to attempt to compute shear for a second depth at some increment of D. To abort the run type "Ctrl Break". Failure to terminate the run at this point may result in a "run-time" error and loss of the output file.

STEP 11 - Examine the output file dumped to the screen. Note the value of the parameter EDIF which is a measure of the discrepancy between the estimated and target value of the zero velocity isovel. Vary SLPB until the model converges to a solution ($\xi \approx$ETARGET) then vary ZB until DELTAI < 0.02(BI). Continue this procedure until the model is able to converge to a value of BETA within ICOUNT = 100 (iterations).

STEP 12 - If the value of BETA > 30 than the model may generate an error related to the size of the exponential argument. The value of BETA may be reduced by decreasing SLPB and/or selecting a lower bed-bank station, (ZB,YB).

STEP 13 - Examine the model output sent to file for predicted flow rate, Q and average velocity, v. If these do not match observed values vary SLPF and/or MANN appropriately until the desired Qand v are obtained.

C4.2 Calibration of the Isovel Coefficients

Once the model has been calibrated to observed flow data, SLPF and MANN are considered to be fixed. This reduces the number of degrees of freedom within the model and it is now easier to refine the estimate of the isovel coefficients DELTAY, and DELTAI through manipulation of EP, SLPB, YB and ZB.

STEP 1 - Re-run the model and examine the output file dumped to the screen for values of TAUBAR, TAUAVE, TERM1 and TERM2. The objective of the calibration is to satisfy the following criteria as closely as possible;

a) TERM1 + TERM2 = TAUBAR = TAUAVE

b) TERM2 = 0.0

c) the resulting shear stress values TAU and TRATIO should reproduce the desired shear stress distribution.

In regular prismatic channels (trapezoidal and rectangular) the shear distribution is relatively well known from field and laboratory studies, (Ghosh and Roy, 1970). These may be used as a guide if observed shear stress values are not available for the subject channel. Unfortunately, there is a scarcity of published data available for irregular natural channel cross-sections and user discretion and experience is required to obtain the best fit.

STEP 2 - Assume SLPB and EP to be fixed and vary (ZB,YB) until the above criteria are approximated as closely as possible. This procedure is valid within limits because as ZB increases relative to YB, the line of estimated zero velocity moves beyond the channel boundary. Secondly, as the value of YB increases the minimum shear stress value moves toward the center of the channel. Consequently, these values can only vary as long as the gross shape of the boundary shear stress distribution continues to resemble the desired configuration.

STEP 3 - Replace YDELTA=0 with the estimated value from the previous step and refine the estimates of SLPB and EP, (first one and then the other) by improving the approximation of the above criteria.

STEP 4 - Repeat STEPS 2 and 3 until further refinement of the calibration parameters does not significantly improve or the desired shear stress distribution is obtained.

Note that similar shear stress distributions may be obtained with various combinations of (ZB,YB), SLPB, and EP. Consequently, it is recommended that the user follow a well defined calibration procedure.

STEP 5 - If the shear stress distribution is desired at a number of depths then the following steps may be considered to avoid having to calibrate the model in detail for each depth. Select a minimum of two more depths, i.e DMIN and a representative stage intermediate between D and DMIN. Repeat the above procedure for each depth. It is advisable to start with DMIN. Having obtained the calibration parameters (YB, ZB, BETA, EP, SLPB) for D and DMIN plot these values and use a linear extrapolation technique to estimate parameter values for intermediate depths.

STEP 6 - Calibrate the model for the intermediate depths by refining the initial estimates obtained above.

STEP 7 - Plot the following relations;

a) IPARM(1) = YB = f(D)

b) IPARM(2) = ZB = f(D)

c) IPARM(3) = BETA = f(D)

d) IPARM(4) = EP = f(d)

e) IPARM(5) = EPRIME = f(D)

f) IPARM(6) = SLPB = f(D)

STEP 8 - Fit regression equations of the following type to the above parameters, (IPARM(I)),

a) IEQN(1): IPARM(I) = SLPM(I)*D+BCEPT(I)

b) IEQN(2): IPARM(I) = EXP(SLPM(I)

c) IEQN(3): IPARM(I) = SLPM(I)*LN(D)+BCEPT(I)

d) IEQN(4): IPARM(I) = EXP(SLPM(I)*LOG(D)+BCEPT(I))

STEP 8 - Select the equation of best fit for each parameter and set up the following table for input into EROS1,

PARAMETER	IPARM	IEQN	SLPM	BCEPT
YB	1	1,4	a1	b1
ZB	2	1,4	a2	b2
BETA	3	1,4	a3	b3
EP	4	1,4	a4	b4
EPRIME	5	1,4	a5	b5
SLPB	6	1,4	a6	b6

STEP 9 - Input the values from the above table into the EROS1 input file and set JFLAG=0.

STEP 10 - Rerun the model and examine the output file dumped to the screen. Evaluate the performance of the simulated shear stress parameters for each depth increment. If the results are unsatisfactory the user may discard the results obtained for the uncalibrated depths or refine the estimates of the calibration parameters and repeat the analysis.

C5 Sample Input And Output Files

A sample EROS1 input file is presented in Table C1 for a trapezoidal channel semi-perimeter with a 1H:1V side slope.

This particular input deck has selected the regression method (METHOD=1) to determine boundary shear stress distributions for depths ranging from 0.25≤D≤0.5 feet. However, by setting JFLAG=0, the run will be terminated after the first depth has been analysed.

Table C1

EROS1
TRAPEZOIDAL SEMI-PERIMETER INPUT FILE

```
E-COEFFICIENT        SECNO=100 SIDE=1
                     BI=3.0    D=0.5      YB=0.1070    ZB= -2.615
                     DMIN=0.25 DELTAY=.001784  EP=0.104
                     SLPB=1.0  SLPF=0.0031     MANN=0.015
                     JFLAG=0   YFLAG=1         METHOD=1
                     IPARM=1 IEQN=4 SLPM=  0.611  BCEPT= -1.813
                     IPARM=2 IEQN=3 SLPM=  0.065  BCEPT=  2.660
                     IPARM=3 IEQN=3 SLPM= -3.643  BCEPT=  0.752
                     IPARM=4 IEQN=3 SLPM= -0.0287 BCEPT=  .0603
                     IPARM=5 IEQN=4 SLPM=  3.3445 BCEPT= -2.422
                     IPARM=6 IEQN=1 SLPM=  0.0    BCEPT=  1.0
VELOCITY DATA        NUOBS=20
                        Y       Z    UOBS     Y      Z    UOBS
                       0.03   -0.00  3.00    0.11 -0.00  3.30
                       0.08   -2.20  3.00    0.18 -0.00  3.45
                       0.16   -1.70  3.30    0.15 -2.40  3.00
                       0.27   -0.00  3.55    0.26 -1.45  3.45
                       0.25   -2.45  3.00    0.31 -1.50  3.45
                       0.30   -2.00  3.30    0.36 -1.05  3.55
                       0.36   -1.60  3.45    0.41 -1.65  3.45
                       0.46   -1.20  3.55    0.46 -1.68  3.45
                       0.50   -1.22  3.55    0.50 -1.70  3.45
                       0.50   -2.15  3.30    0.50 -2.54  3.00
SECTION ORDINATES    NUMB=20
                        YBED      ZBED         YBED        ZBED
                        0.000    -0.125        0.000      -0.500
                        0.000    -1.000        0.000      -1.500
                        0.000    -1.750        0.000      -2.000
                        0.000    -2.250        0.000      -2.400
                        0.000    -2.425        0.000      -2.450
                        0.000    -2.500        0.050      -2.550
                        0.100    -2.600        0.150      -2.650
                        0.200    -2.700        0.250      -2.750
                        0.300    -2.800        0.350      -2.850
                        0.400    -2.900        0.500      -3.000
```

Execution of the model results in the generation of two output files. The first file, generally labled "file.out", provides the user with a hard copy of the model coefficients and associated shear stress values for the selected bed-bank stations. A sample of this hard copy output file is provided in Table C2.

The second output file is labled "file.plt" (plt being a notation for plot). This file is ready by PLOTSEC2 to generate a graphical display of the cross-section and the boundary shear stress distribution. An illustration of a PLOTSEC2 output is given in Figure C3.

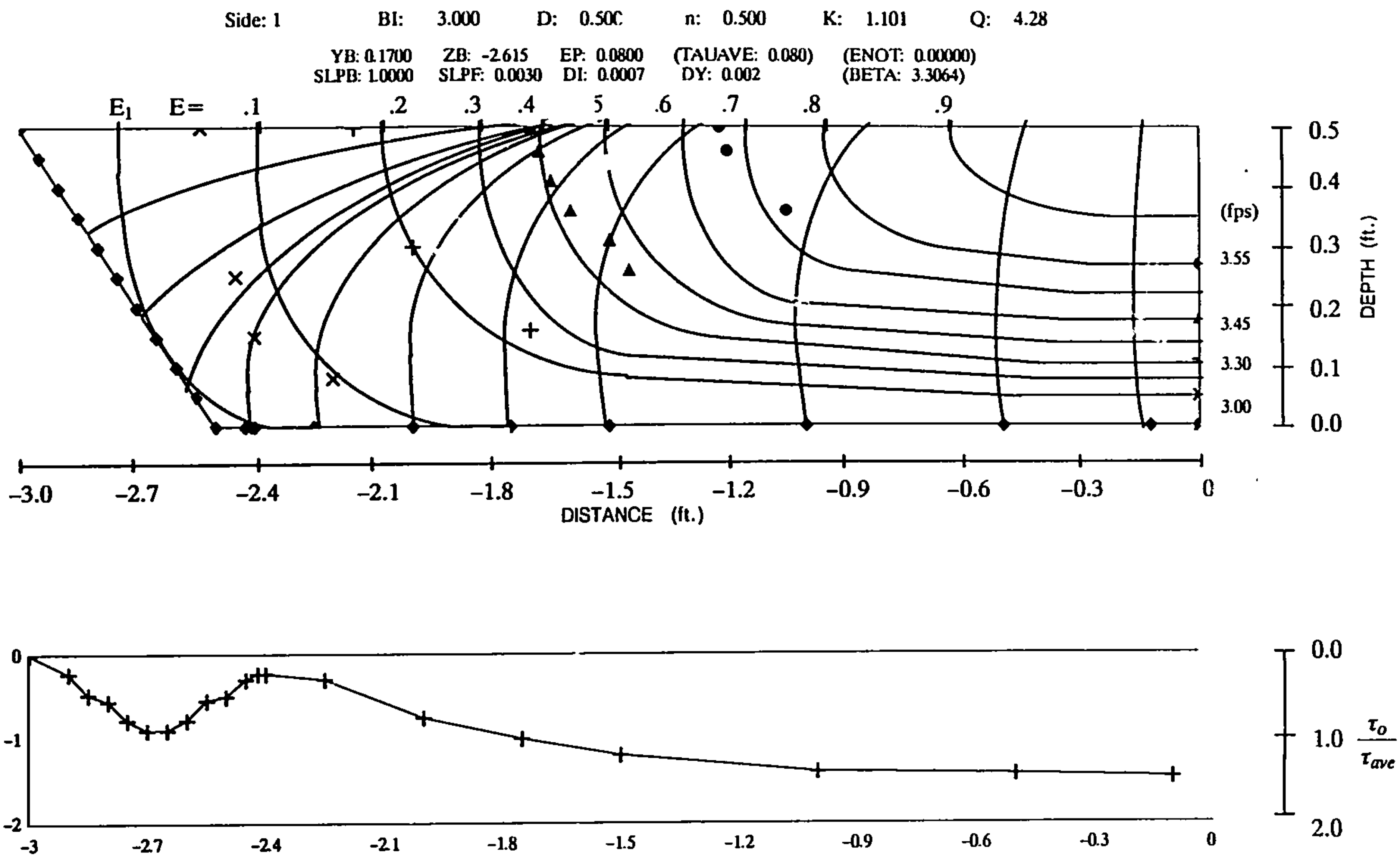

FIGURE C.3 EROS1 Predicted Velocity Field and Boundary Shear Stress Values for a Trapezoidal Semi-Perimeter

Table C2
EROS1
HARD COPY OUTPUT FILE

```
************* E R O S 1 ***********

BY C. R. MACRAE

DECEMBER 1986
SHEAR STRESS MODEL FOR NONUNIFORM
& NONSYMMETRIC 3-D FLOW
RESEARCH VERSION NOT FOR GENERAL USE


SECNO:     100        SIDE:         1        BI:    3.000
    D:       .500       YB:       .107       ZB:   -2.615
 DMIN:       .250   YDELTA:       .002       EP:    .104
 SLPB:   1.000000     SLPF:    .003100     MANN:    .015

JFLAG: 0    YFLAG:  1     METHOD: 1

I: 1   IPARM:  1  IEQN:  4    SLPM:   .611000   BCEPT: -1.8130
I: 2   IPARM:  2  IEQN:  3    SLPM:   .065000   BCEPT:  2.6600
I: 3   IPARM:  3  IEQN:  3    SLPM:-3.643000    BCEPT:   .7520
I: 4   IPARM:  4  IEQN:  3    SLPM:  -.028700   BCEPT:   .0603
I: 5   IPARM:  5  IEQN:  4    SLPM:  3.344500   BCEPT: -2.4220
I: 6   IPARM:  6  IEQN:  1    SLPM:   .000000   BCEPT:  1.0000

NUOBS: 20
YOBS:      .0300    ZOBS:       .0000   UOBS:      3.0000
YOBS:      .1100    ZOBS:       .0000   UOBS:      3.3000
YOBS:      .0800    ZOBS:     -2.2000   UOBS:      3.0000
YOBS:      .1800    ZOBS:       .0000   UOBS:      3.4500
YOBS:      .1600    ZOBS:     -1.7000   UOBS:      3.3000
YOBS:      .1500    ZOBS:     -2.4000   UOBS:      3.0000
YOBS:      .2700    ZOBS:       .0000   UOBS:      3.5500
YOBS:      .2600    ZOBS:     -1.4500   UOBS:      3.4500
YOBS:      .2500    ZOBS:     -2.4500   UOBS:      3.0000
YOBS:      .3100    ZOBS:     -1.5000   UOBS:      3.4500
YOBS:      .3000    ZOBS:     -2.0000   UOBS:      3.3000
YOBS:      .3600    ZOBS:     -1.0500   UOBS:      3.5500
YOBS:      .3600    ZOBS:     -1.6000   UOBS:      3.4500
YOBS:      .4100    ZOBS:     -1.6500   UOBS:      3.4500
YOBS:      .4600    ZOBS:     -1.2000   UOBS:      3.5500
YOBS:      .4600    ZOBS:     -1.6800   UOBS:      3.4500
YOBS:      .5000    ZOBS:     -1.2200   UOBS:      3.5500
YOBS:      .5000    ZOBS:     -1.7000   UOBS:      3.4500
YOBS:      .5000    ZOBS:     -2.1500   UOBS:      3.3000
YOBS:      .5000    ZOBS:     -2.5400   UOBS:      3.0000
```

```
NUMB: 20
YBED:      .0000     ZBED:       -.1250
YBED:      .0000     ZBED:       -.5000
YBED:      .0000     ZBED:      -1.0000
YBED:      .0000     ZBED:      -1.5000
YBED:      .0000     ZBED:      -1.7500
YBED:      .0000     ZBED:      -2.0000
YBED:      .0000     ZBED:      -2.2500
YBED:      .0000     ZBED:      -2.4000
YBED:      .0000     ZBED:      -2.4250
YBED:      .0000     ZBED:      -2.4500
YBED:      .0000     ZBED:      -2.5000
YBED:      .0500     ZBED:      -2.5500
YBED:      .1000     ZBED:      -2.6000
YBED:      .1500     ZBED:      -2.6500
YBED:      .2000     ZBED:      -2.7000
YBED:      .2500     ZBED:      -2.7500
YBED:      .3000     ZBED:      -2.8000
YBED:      .3500     ZBED:      -2.8500
YBED:      .4000     ZBED:      -2.9000
YBED:      .5000     ZBED:      -3.0000

     HYDR:  .4287     BI:      3.000    VBAR:     3.145
   USHEAR:  .2068   AREA:      1.375    DBAR:      .458
        Q:  4.324

SUMMARY OF E-COEFFICIENT ANALYSIS

                                                  BEST      LAST
     VELOCITY PARAMETERS                        ESTIMATE  ITERATION

A) REGRESSION COEFFICIENT:                        .7666     .7669
B) SUM OF UOBS MINUS UPRED:                       .8277     .8262
C) STANDARD DEVIATION OF UPRED:                   .1953     .1953
D) CALIBRATION COEFFICIENT (K):                  1.1054      N/A


       ECOEFFICIENT PARAMETERS

     BETA: 3.333     YDELTA:  .0017787
       EP:  .105     IDELTA:  .0002174
   EPRIME:.00796       ENOT: .4615E-08


          PREDICTED VERSUS OBSERVED VELOCITIES

I:  1     UOBS: 3.000     UPRED: 3.217    UDIFF: -.217
I:  2     UOBS: 3.300     UPRED: 3.427    UDIFF: -.127
I:  3     UOBS: 3.000     UPRED: 3.011    UDIFF: -.011
I:  4     UOBS: 3.450     UPRED: 3.496    UDIFF: -.046
I:  5     UOBS: 3.300 .   UPRED: 3.313    UDIFF: -.013
```

I: 6	UOBS: 3.000	UPRED: 2.967	UDIFF: .033
I: 7	UOBS: 3.550	UPRED: 3.544	UDIFF: .006
I: 8	UOBS: 3.450	UPRED: 3.430	UDIFF: .020
I: 9	UOBS: 3.000	UPRED: 2.987	UDIFF: .013
I: 10	UOBS: 3.450	UPRED: 3.437	UDIFF: .013
I: 11	UOBS: 3.300	UPRED: 3.285	UDIFF: .015
I: 12	UOBS: 3.550	UPRED: 3.519	UDIFF: .031
I: 13	UOBS: 3.450	UPRED: 3.427	UDIFF: .023
I: 14	UOBS: 3.450	UPRED: 3.423	UDIFF: .027
I: 15	UOBS: 3.550	UPRED: 3.515	UDIFF: .035
I: 16	UOBS: 3.450	UPRED: 3.422	UDIFF: .028
I: 17	UOBS: 3.550	UPRED: 3.516	UDIFF: .034
I: 18	UOBS: 3.450	UPRED: 3.419	UDIFF: .031
I: 19	UOBS: 3.300	UPRED: 3.248	UDIFF: .052
I: 20	UOBS: 3.000	UPRED: 2.946	UDIFF: .054

TAUAVE: .0828 lb/ft² TAUBAR: .0842 lb/ft² TFLAG: 98.29 (%)

TERM1: .0793 lb/ft² TERM2: .0001 lb/ft² TTFLAG:104.2963 (%)

TTOTAL: .0794 lb/ft²

SECNO: 100 SIDE: 1 DEPTH: .500 FEET

	BED-BANK STATION		SHEAR STRESS (TAU)		
No.	YBED (ft)	ZBED (ft)	TAU (lb/sqft)	TAU (Pa)	TRATIO (dim)
1	.000	-.125	.1174	5.622	1.4183
2	.000	-.500	.1153	5.519	1.3924
3	.000	-1.000	.1109	5.312	1.3401
4	.000	-1.500	.1005	4.811	1.2138
5	.000	-1.750	.0898	4.298	1.0842
6	.000	-2.000	.0700	3.351	.8455
7	.000	-2.250	.0332	1.590	.4011
8	.000	-2.400	.0207	.992	.2503
9	.000	-2.425	.0241	1.154	.2911
10	.000	-2.450	.0296	1.415	.3570
11	.000	-2.500	.0443	2.123	.5356
12	.050	-2.550	.0582	2.785	.7027
13	.100	-2.600	.0702	3.360	.8477
14	.150	-2.650	.0770	3.684	.9295
15	.200	-2.700	.0754	3.612	.9112
16	.250	-2.750	.0651	3.119	.7868
17	.300	-2.800	.0482	2.309	.5826
18	.350	-2.850	.0329	1.577	.3980
19	.400	-2.900	.0212	1.016	.2564
20	.500	-3.000	.0000	.000	.0000

APPENDIX D

QUALHYMO - SHEAR1 COMMAND

D1.0 SHEAR1 Command Input Requirements

This appendix provides a description of functions and input requirements for the SHEAR1 COMMAND available in QUALHYMO release 2.1. The theory and capabilities of QUALHYMO are presented else where, (Rowney and MacRae, 1991(a) and (b)).

D2.0 Purpose

The SHEAR1 command allows the user to generate four shear stress related indices based on cumulative excess shear (EXTAU). These parameters are considered to be indicators of instream erosion potential. A discussion of the theory and exact mathematical description of the indices is provided in Chapter 3.0.

The user may select from three options to compute instantaneous shear stress from a specified flow series generated by or supplied to QUALHYMO. These options are as follows,

a) The model will compute the indices from cross-section ordinates, selected hydraulic parameters and a matrix of depth versus shear stress for up to twelve bed-bank stations. The model will automatically compute a rating curve from the supplied hydraulic and cross-section data, then assign a depth corresponding to any flow in the flow series specified for analysis. Having determined the depth the model will "look up" (assign or extrapolate) the appropriate shear stress value for each depth.

b) The model will compute the indices from cross-section ordinates, selected hydraulic parameters and a power function relating shear stress to flow depth. A rating curve is computed as above however, shear stress is determined directly from the shear-depth function for up to twelve bed-bank stations.

c) The model will compute the indices directly from a power relation expressing shear stress as a function of flow as provided by the user for up to twelve bed-bank stations. Cross-section ordinates and hydraulic characteristics are not required for this computation.

Having determined the instantaneous shear stress value for a specified flow at some time step δt, the model then proceeds to compute the indices. This is achieved by summing the instantaneous index value over the course of the flow series.

Four representations of the index are built into the model and computed automatically. These are,

a) EXTAU: $(q_s)_p = \int b_1(\tau_o - \tau_{CRT})_p \, dt$

b) EVI: $(q_s)_p = \int [b_2(\tau_o - \tau_{CRT})_p]\tau_o \, dt$

c) MPM: $(q_s)_p = \int [m(\tau_o - \tau_{CRT})_p]^n \, dt$

d) PWR: $(q_s)_p = \int [b_3(\tau_o - \tau_{CRT})_p]v \, dt$

D3.0 Input Format

Parameter	Description
ID	Identification number of the flow series for which the indices are to be determined.
ISER	Series number for ID (dummy variable).
SECNO	Cross-section designation number.
IOPT	Flag designating the desired option. If = 1, option a) is selected, If = 2, option b) is selected, If = 3, option c) is selected.
NSTAT	The number of bed-bank stations for which shear stress indices will be determined, (1 <= NSTAT <= 12).
ISTAT(1)	Nominal value assigned to first bed-bank station considered for analysis.
...	
ISTAT(NSTAT)	Nominal value assigned to last bed-bank station considered for analysis.

------- Omit the next three parameters --------
------- if IOPT = 1 --------
------- Otherwise repeat sequence NSTAT times --------

Parameter	Description
ACOEF(ISTAT)	Coefficient in power function
XMIN(ISTAT)	Minimum depth (IOPT=2) or minimum flow (IOPT=3).
AEXPO(ISTAT)	Exponent in power function.

-------- Omit next three parameters --------
-------- if IOPT = 2 or 3 --------
-------- Otherwise repeat sequence NDEPTH times --------

NDEPTH	Number of depths in the shear-depth matrix (2 <= NDEPTH <= 20).
XDEPTH(1)	First depth (m),
...	
XDEPTH(NDEPTH)	Last depth, (m).
XTAU(1,1)	Shear stress value for first depth (XDEPTH = 1) at the first bed-bank station (ISTAT = 1),
...	
XTAU(NSTAT,NDEPTH)	Shear stress value for last depth (XDEPTH = NDEPTH) at the last bed-bank station, (ISTAT = NSTAT).

----------- Repeat following 10 parameters once ----------
----------- for each side ----------
----------- Otherwise omit if IOPT = 3 ----------

---------- Hydraulic parameters ----------

SIDE	Nominal value indicating channel side, If = 1, left side when looking upstream, If = 2, right side looking downstream.
BI(SIDE)	Top width (m) of the active channel for the given side.
DMAX	The maximum water depth at the y-axis (m), including overbank flow.
SLPF(SIDE)	The longitudinal channel slope for the given side.
SMANN(SIDE)	Manning's roughness coefficient for the appropriate side.
SMANOB(SIDE)	Manning's roughness coefficient for the overbank flow for the given side.
DTOB(SIDE)	Depth (m) of top of bank of active channel. *** DTOB(1) must equal DTOB(2) ***

---------- Cross-section Ordinates ----------
---------- repeat YBED(I) and ZBED(I) pairs ----------
---------- for I = 1,NUMB ----------
---------- Omit if IOPT = 3 ----------

NUMB	Number of bed-bank stations, (10 <= NUMB <= 20)
YBED(I)	The y-coordinate (m) of the bed-bank station in the (z,y) plane, (YBED(SIDE) = 0).
ZBED(I)	The corresponding z-coordinate (m) in the (z,y) plane, (ZBED(SIDE,1) = 0).

---------- The following Parameters ----------
---------- must be included for all options ----------

TAUCRT(I)	The critical shear stress at ISTAT(1), (Pascals).
...	
TAUCRT(NSTAT)	The threshold shear stress at ISTAT(NSTAT) in Pascals.
KCOEF	The coefficient in DuBoy's relation.
BCOEF	The coefficient in Meyer-Peter Muller relation.
BEXPO	The exponent in the Meyer-Peter Muller relation.
IAYR	The beginning year of computation period.
IAMO	The beginning month of computation period.
IADY	" " day " " "
IBYR	" ending year " " "
IBMO	" " month " " "
IBDY	" " day " " "

Notes:

The **SHEAR1** command does not directly compute shear stress values at each bed-bank station from channel geometry, and flow hydraulics. It relies on the user to provide shear stress values for each station as either a function of depth, as in IOPT=1 or 2, or as a function of flow, (IOPT=3). To derive shear stress values at each station the user may use a variety of methods from simplified manual calculations to more sophisticated model applications such as EROS1, (Appendix C).

```
---------------------------------------------------------------
SHEAR1          ID=1 ISER=103  SECNO=595  IOPT=2
                NSTAT=11 ISTAT=1 3 5 6 7 8 10 12 13 14 15
                COEFFICIENTS FOR TAU VERSUS DEPTH RELATIONS
                     ACOEF   XMIN   AEXPO
                     20.75   0.020  0.861
                     17.83   0.045  1.091
                     14.81   0.048  1.532
                     12.95   0.050  1.573
                     11.55   0.076  0.102
                     11.84   0.130  0.538
                     15.16   0.220  0.732
                     16.84   0.300  1.206
                     17.15   0.380  1.629
                     15.88   0.480  1.710
                     14.30   0.580  1.638
                SIDE=1
                     BI=3.0          DMAX=2.51       SLPF=.0023
                     SMANN=0.025     SMANOB=0.045    DTOBL=1.11
                NUMB=20
                     YBED  ZBED   YBED  ZBED   YBED  ZBED
                     .000 0.000   .020  .125   .040  .375
                     .045  .601   .048  .850   .050  .975
                     .130 1.250   .220 1.524   .272 1.646
                     .300 1.701   .380 1.875   .480 2.024
                     .580 2.143   .740 2.399   .850 2.649
                     .960 2.801  1.018 2.865  1.110 3.000
                    1.510 4.470  2.510 5.940
                SIDE=2
                     BI=2.13         DMAX=2.51       SLPF=.0023
                     SMANN=0.025     SMANOB=0.045    DTOBR=1.11
                NUMB=17
                     YBED  ZBED    YBED  ZBED    YBED  ZBED
                     .000  0.000   .001   .200   .010   .400
                     .050   .600   .125   .725   .200   .850
                     .250  0.980   .300  1.100   .400  1.200
                     .540  1.275   .680  1.350   .775  1.475
                     .870  1.600   .980  1.850  1.110  2.130
                    1.510  3.740  2.510  7.400
                TAUCRT= 16 16 16 16 12 12 12 8 8 8 8
                DUBOY'S RELATION          KCOEF=1.0
                MEYER PETER MULLER        BCOEF=1.0  BEXPO=1.5
                BEGINNING DATE   81 06 15
                ENDING DATE      81 06 16
---------------------------------------------------------------
```

In this example the investigator has requested that shear stress indicators be determined for eleven points (NSTAT=11 bed-bank stations). In this particular case all eleven stations are on one side of the channel starting with station one at the channel centerline and ending with station 15 near the top-of-bank of the active channel. Option two (IOPT=2) was selected requires the entry of the coefficients, parameters, and exponents for the power relations derived previously by the user for each bed-bank station. The threshold shear (TAUCRT) is highest for the intact stiff cohesive materials along the channel bottom and diminish up the bank with exposure of bank materials and degree of weathering.

APPENDIX E

QUALHYMO - Snowmelt Routine

E1.0 Introduction

As depicted in Figure E.1 the snowmelt module modifies the precipitation input prior to the computation of effective precipitation or runoff volume and infiltration. If snowmelt is requested the model checks a concurrent temperature file between the months of November and May inclusive for violation of a base temperature criteria BASET as specified by the user on the GENERATE command. If the ambient temperature for the current time step is less then the base temperature then the precipitation is assumed to fall as snow. One of two temperature index methods as specified by the user is then called to update the snow pack and the precipitation value is set to zero and sent back to the GENERATE command.

When the ambient air temperature equals or exceeds the base temperature precipitation falling during that time increment is assigned as rain. If the snow pack is not zero melt is calculated using the appropriate melt routine and added to the rainfall. The modified rainfall amount is then sent back to the GENERATE command.

As noted above two temperature index methods are available

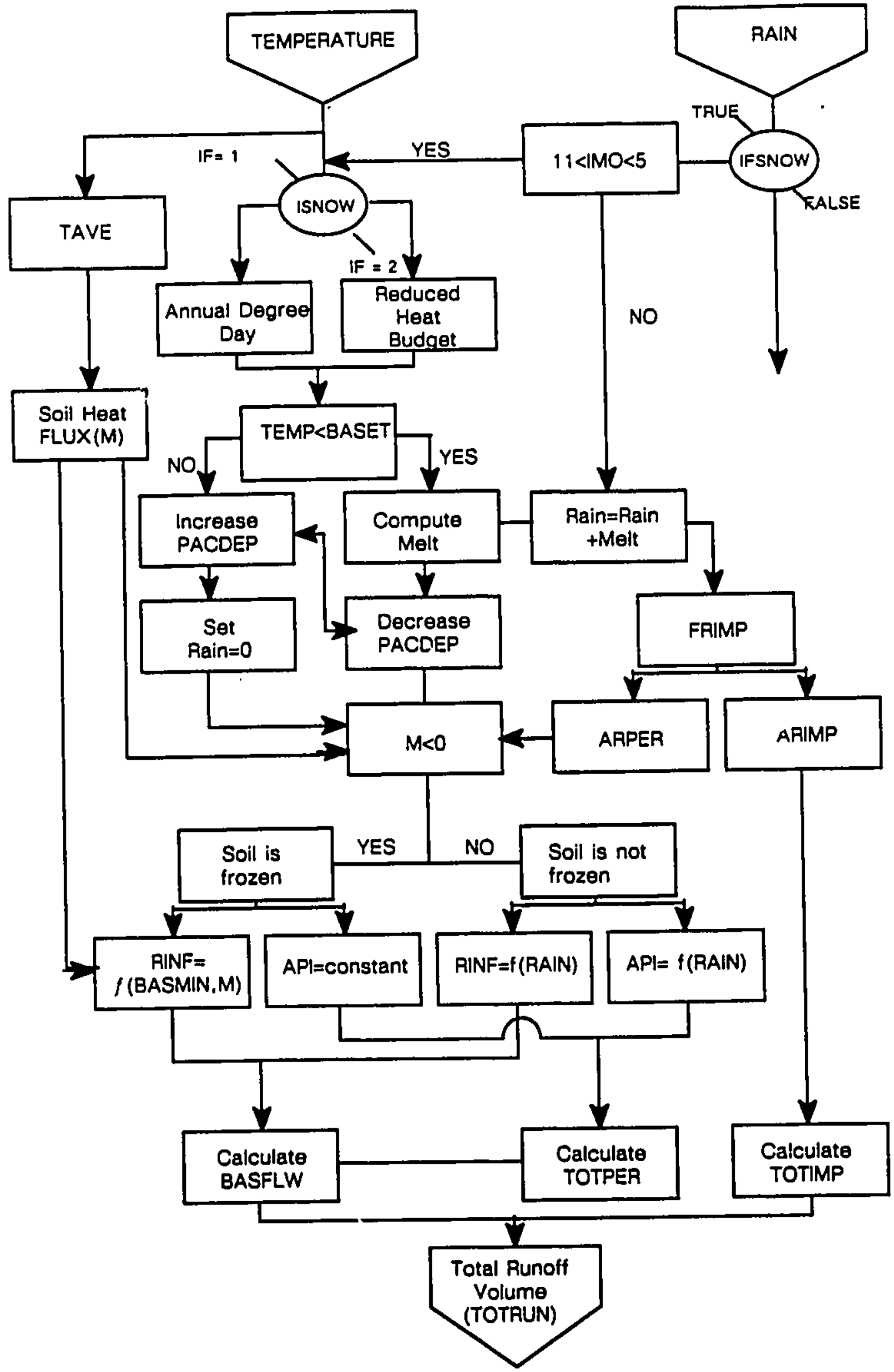

FIGURE E.1 Systems Diagram of Snowmelt and Soil Freeze –Thaw Algorithms in Upland Generation in QUALHYMO

in QUALHYMO. Temperature indices are commonly use in hyrologic modeling for three primary reasons,

a) atmospheric temperature data is an indicator of the energy input to the snowpack,
b) it is generally the only readily available meteorologic parameter, and
c) temperature indices are relatively simple, easily understood, and often provide snowmelt estimates comparable to that obtained using more sophisticated energy balance concepts, (U.S. Army Corps of Engineers, 1956; Anderson, 1973).

The degree day method has been found to provide good estimates of snow pack accumulation an ablation in areas covered by a dense forest canopy. In such areas the ambient air temperature provides a close approximation of the long-wave radiation exchange between the vegetation cover and the snow surface. Except in the rare case of high geothermal inputs long-wave radiation is the most important heat flux in a forested area. A more significant departure between the degree day method an a more elaborate technique may be expected for large open areas, and areas having high variations in aspect and elevation. In these cases short-wave radiation, latent and sensible heat fluxes which are not directly related to air temperature can vary widely. However, for the most applications envisioned during the development of the model a modified degree day method provides a most acceptable approach consistent in sophistication and accuracy with a planning level analysis.

E2.1 The Annual Degree Day Method

For preliminary or screening level analyses the user may desire to use the degree day method adopting an annual snowmelt coefficient. This method is one of the simplest and most widely used snowmelt modeling techniques available. In its general form snowmelt may be estimated as,

$$TMELT = SNOFAC\ (TMEAN) \qquad [E1]$$

where,
TMELT = snowmelt in water equivalents per time step, (mm),
SNOFAC = an annual snowmelt factor determined by trial-and-error, and
TMEAN = the mean temperature per time step, (°C).

Unfortunately no global or universal value for the snowmelt factor exists. Rather the value for the factor is unique to the region for which it was derived. It has also been found to vary seasonally and with meteorologic conditions. Eggleston et al., (1971) suggested the following relation,

$$snofac = k_m k_v R_I (1-alb) \qquad [E2]$$

where,
km = proportionally constant,
k_v = vegetation transmission coefficient for radiation,
R_I = solar radiation index, and
alb = snow albedo.

For wet weather (rainy days) the melt factor was adjusted as follows,

$$SNOFAC = SNOFAC + 0.00126(precip) \qquad [E3]$$

where PRECIP is the total precipitation per time increment.

Equation E3 reflects the net effect of precipitation as rain and the associated prevailing meteorologic conditions on the melt process. According to Anderson (1973) cloud cover has the effect of reducing the energy flux to the snow pack. He accounted for this reduction by reducing ambient air temperature by 0.8°C on overcast days. However, rain reduces the albedo or reflectivity of snow to approximately 0.4 in comparison to a value of 0.8 for fresh snow. Further, the rain itself accounts for a positive heat flux to the snow pack. The net effect of these factors is an increase in the melt factor.

The seasonality of the snow factor was demonstrated by Gray (1970) and Anderson, (1973). The proposed the use of a sinusoidal curve to represent the seasonal variation in the melt factor as represented by the variable ZMELTF in Figure E.2. The maximum and minimum values of ZMELTF coincide with the summer solstice (June 21st) and the winter equinox (December 21st) respectively. However, experience with a similar model calibrated to fourteen small (less then 1 km^2)

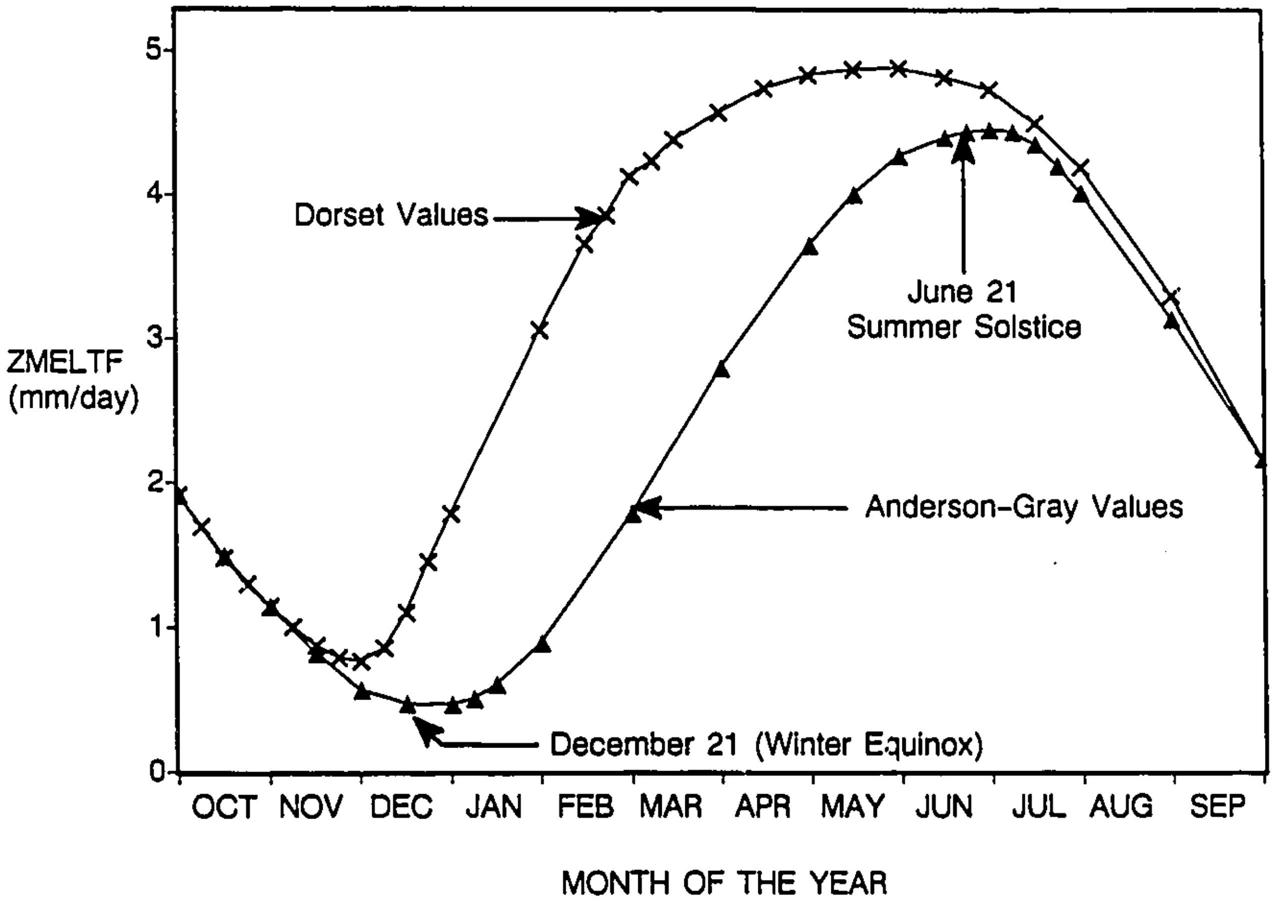

FIGURE E.2 Seasonal Variation of Melt Factor ZMELTF (CCL, 1984)

watersheds near Dorset, Ontario (CCL, 1984) indicated that a shift in the curve may be expected with the maximum value of ZMELTF occurring in late March or early April.

This method was developed for the estimation of daily snowmelt, although Anderson's method was based on 6-hourly time increments. For small watersheds smaller time increments may be used to simulate runoff processes. Although QUALHYMO allows the user to specify any time increment, melt is essentially computed as the average hourly amount divided by the number of time steps per hour. The user should not confuse the smaller time step with increased accuracy of snowmelt simulation.

This is in part because the snow pack itself tends to filter out nonuniformities in the thermal inputs into the melt process as follows,

a) the cold storage or "negative heat" in the snowpack must be satisfied,

b) if the snow pack is dry some melt most occur to bring the liquid content of the pack above the irreducible value, and

c) a time lag occurs due to percolation of the melt water through the snowpack.

Given these considerations the computation of melt for time increments of less then one hour may be questionable even for more sophisticated energy balance methods. Secondly, the melt factor is a climatic parameter by its very derivation as the average value over a number of melt seasons and its relative insensitivity to short term meteorologic conditions. Modeling of snowmelt induced runoff with a short time resolution (one hour) would require the inclusion of other factors influencing melt rates such as wind speed, vapor pressure gradients, air pressure, albedo and short wave radiation. The inclusion of these factors would however, necessarily increase the complexity of the model and the input requirements. There is therefore a need to balance an adequate accounting of the runoff process consistent with user requirements and the associated computational and input requirements.

As input requirements increase the model becomes more cumbersome to use. There is also the problem of the availability and accuracy of some input parameters. The physical dimensions of current hardware also place some limitations on the number of computational steps that can be performed while still maintaining a practical and useful planning level simulation tool with extended modeling capabilities. In this regard temperature index methods readily lend themselves to computer applications with relatively modest input and computational requirements.

Based on the above considerations a modified degree day method and a reduced heat budget technique were included in QUALHYMO to simulated snowmelt. The modified heat budget technique involves the incorporation of a base temperature term (BASET). A degree day is defined as a deviation of 1° from a given datum temperature (base temperature) over a twentyfour hour period. This base temperature, above which melt will occur is commonly defined as 0°C. However, snowmelt has been observed to lag behind ambient air temperature due in part to the reflection of short wave insolation and the thermal storage capacity of the snowpack. Gray (1970) incorporated the base temperature term into Eqn. E1 to account for this apparent discrepancy resulting in the following expression,

$$TMELT = SNOFAC\ (TMEAN - BASET) \qquad [E4]$$

The exact value of BASET, although typically close to zero must be determined by trial-and-error. The U.S.Army Corps of Engineers Snow Laboratories reported values of -2.8°C for open sites and 5.6°C for forested areas. These values were derived for use with maximum daily temperatures and an assumed melt factor of 1.83 mm/(°C.d).

E2.2 Reduced Heat Budget

In Eqn. E4 the melt factor, SNOFAC is a constant value throughout the year. Based on research by Gray, (1970) and Anderson, (1973) a variable melt factor and a wet-dry day criteria were adopted to account for the dispersive effects of cloud cover on insolation and the thermal energy contained in the precipitated water.

For dry days the resulting equation may be expressed as,

$$TMELT = ZMELTF\ (TMEAN - BASET) \qquad [E5]$$

The specific shape of the curve must be defined for each distinct climatic region. Consequently, QUALHYMO provides the user with the choice of providing their own values for ZMELTF or selecting either the Anderson-Gray or Dorset values as default. Values for ZMELTF are provided in TABLE E1.

Table E1

ZMELT Values For Reduced Heat Budget Technique

DATE	ZMELTF (mm/dy)	
	Anderson-Gray	Dorset
Nov 1	1.143	1.143
Dec 1	0.559	0.762
Jan 1	0.457	1.778
Feb 1	0.889	3.048
Mar 1	1.778	4.064
Apr 1	2.794	4.572
May 1	3.632	4.826

As noted above however, Eqn. E5 was found to be less representative of melt on days recording more than a trace amount of precipitation, i.e. "wet days". Gray (1970) put forward a wet day relation based on a reduced heat budget equation to account for the heat content of the rain which has been slightly modified to include the variable melt factor as follows,

$$TMELT = [ZMELTF+COEFD(PTOT)](TMEAN-BASET)+COEFE \qquad [E6]$$

in which COEFD is a coefficient reported by Gray, PTOT is the total precipitation per time increment, and COEFE is used to represent the effect of rain on the albedo of the snow pack.

The differentiation of the melt process into "wet" and "dry" periods is useful to better approximate the unique set of meteorological conditions that prevail during these two distinct periods. Since the meteorological conditions are relatively uniform within the prevailing period the distinction has been found to be convenient and consistent with field observations.

The criteria for the distinction between periods is based on the magnitude of PTOT. The following criteria proposed by Anderson (1973) was adopted in QUALHYMO,

a) WET DAY: PTOT >= 0.42 mm/hr, and

b) DRY DAY: PTOT < 0.42 mm/hr.

The use of this criteria reduces the effect of trace amounts of precipitation on melt computations by assuming that a simple temperature index or dry day conditions prevail on those days. While this is not completely true it is considered to be a reasonable approximation for a planning level analysis.

E3.0 Test Application

The ability of the two snowmelt procedures was tested by comparing predicted snow accumulation and ablation rates with measured snow depth. Snow depth, reported in water equivalents is routinely collected by the Atmospheric Environment Service, (AES). In Ottawa the AES surveys a designated snow course located in a field near the Ottawa International Airport. Snow samples are taken by core sampler at intervals along the snow course. The samples are then analyzed and averaged to determine the water equivalent of the snow pack at the point in time. These readings are routinely collected on the 1st, 8th, 15th and 22nd day of each month.

Along with the snow course data, hourly precipitation and air temperature data were collected from AES for the airport for input into QUALHYMO. Default "Dorset" values were selected for the variable snowmelt coefficient when using the reduced heat budget approach. Other parameters were set at COEFD=0.0012, and COEFE=0.05 while the precipitation correction factors were turned off (CFACTR=1.0, and CFACTS=1.0). This left BASET as the only calibration coefficient for this technique. Calibration parameters for the annual heat budget method are the annual melt coefficient and BASET.

Snow pack accumulation and ablation was simulated for the winters of 1970-71 and 1982-83. These winters were selected because they represent the greatest and least snow depths recorded at the Ottawa International Airport over the period of 1967 to 1987, respectively. Both of the snowmelt models were found to provide the best fit with BASET=0.5°C.

The annual snowmelt coefficient method (SNOFAC=0.15) reproduced the snow pack accumulation period in early winter in a manner virtually identical to the reduced heat budget method, (Figure E3). Both methods tended to underestimate during this period for the 1971-72 data. However, good agreement was obtained with the 1982-83 winter measurements using the reduced heat budget method. No analysis was performed for the winter of 1982-83 using the annual degree day method.

Differences between the two methods began to appear in the mid winter period and gradually increased toward spring. The

fig E.3

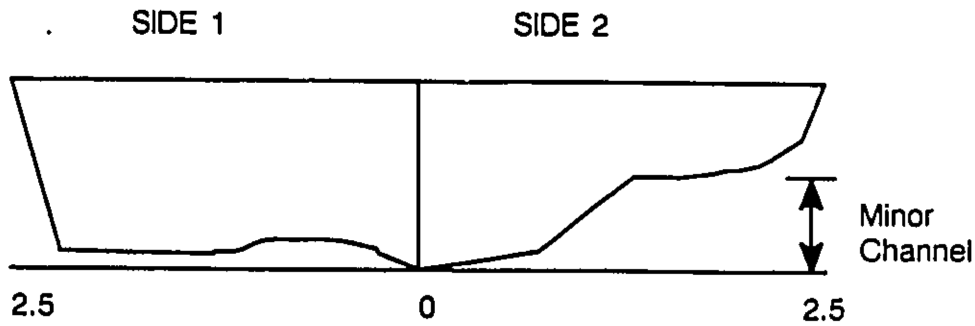

FIGURE I.2 Section A: Hydraulic Geometry

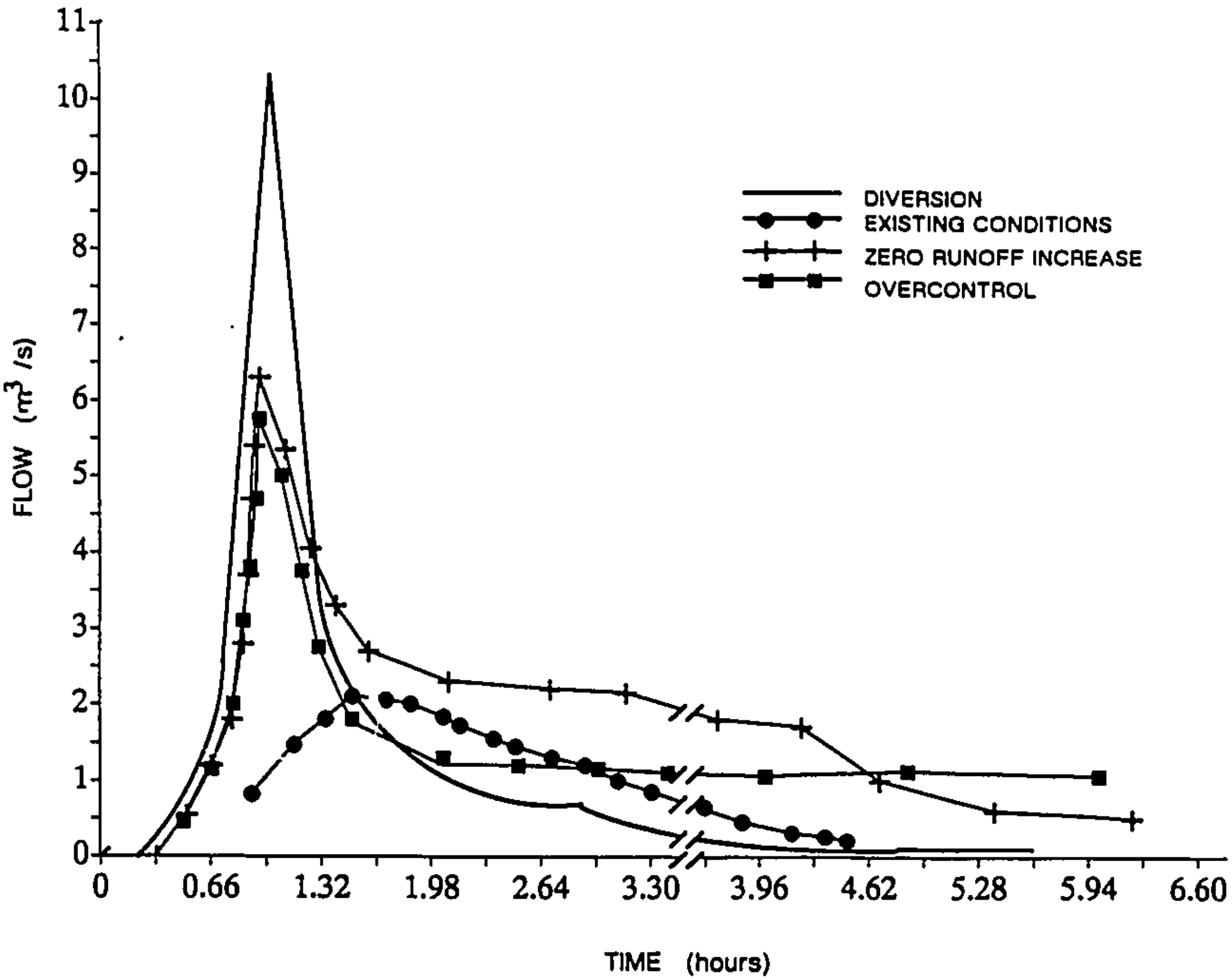

FIGURE I.3 Hydrographs for the 5-Year Design Storm

reduced heat budget method provided a good reproduction of maximum snow pack depths and ablation rates for both winter periods. The 1970-71 winter representing a calibration run and the winter of 1982-83 representing a verification year. These two years together represent record maximum and minimum snowfall years respectively.

The predicted disappearance or final day of measurable snow cover was also in close agreement with recorded values. The annual coefficient method slightly over estimated snow pack depth for the winter of 1971-72. Further, ablation rates were slightly lower resulting in significantly lower melt runoff volumes. Never-the-less, the two methods were considered to have performed well, particularly the reduced heat budget method. Further, the good calibration and verification of the reduced heat budget method over such extremes is very encouraging.

APPENDIX F

QUALHYMO - SOIL FREEZE-THAW ROUTINE

F1.0 Introduction

Soil ice effects infiltration and hence recharge to the groundwater reservoir. This has two important hydrologic implications,

a) increased apparent surface imperviousness and hence increased runoff volumes during snow melt and rainfall conditions, and
b) decreased recharge to the groundwater reservoir which is manifested in lower groundwater outflow rates.

The following discussion concerns the surface runoff computations in QUALHYMO and the role of soil freezing.

F2.0 Surface Runoff Volume

QUALHYMO has two methods for determining runoff volume. One method (for pervious areas) is based on the SCS method (Soil Conservation Service, 1972) and the other (for small impervious areas) uses a volumetric coefficient approach. The later method assumes a constant runoff coefficient and therefore is unaffected by changes in hydrologic conditions brought on by soil freezing. Consequently, this discussion will focus on the influence of soil freezing on the SCS method.

F2.1 Runoff Volume - Pervious Areas

As noted in the User's Manual the model reads hourly rainfall records in either Atmospheric Environment Service (AES) condensed format or HEC "STORM" format. Excess rainfall in pervious areas is calculated by the model using the SCS relation:

$$Q = \frac{(P - ABSPER)^2}{(P - ABSPER + SSTAR)} \qquad [F1]$$

where,
Q = cumulative depth of runoff (mm),
P = cumulative depth of precipitation (mm),
$ABSPER$ = initial abstraction (mm), and
$SSTAR$ = loss parameter (mm).

SSTAR and ABSPER are updated by the model for each event, to provide an accounting for initial moisture conditions as described below.

F2.2 Soil Moisture Accounting

In the case of SSTAR, this is accomplished by expressing SSTAR as a function of a variable Antecedent Precipitation Index, the API. In essence, API is a number which can be used to provide an indication of soil moisture conditions prior to a storm and is determined from the following relation:

$$API_2 = APIK(API_1) + P_1 \qquad [F2]$$

where, $APIK$ = coefficient,
P_1 = precipitation in the previous time step,
API_1 = condition at the beginning of the time step,
API_2 = condition at the end of previous time step.

The coefficient APIK is a constant parameter with a value typically taken as 0.9 (it is always a positive number less than 1). As a result, the API tends to increase with rainfall, and always decreases during dry periods. At any time a high API indicates relatively moist antecedent conditions, and a low API indicates relatively dry conditions. It can be interpreted therefore, that the API attempts in a simple way to account for previous rainfall conditions, with the parameter APIK determining the 'memory' of the system. Further, an inverse relationship exists between SSTAR and the API, since moist soil conditions imply a smaller SSTAR value than average, and dry conditions imply a larger SSTAR value than average.

QUALHYMO employs an empirical function relating SSTAR and API,

$$SSTAR = SMIN + (SMAX - SMIN)e^{SK(API)} \qquad [F3]$$

where, $SMIN$ = minimum value of SSTAR,
$SMAX$ = maximum value of SSTAR, and
SK = a calibration parameter.

Use of the API as a means of adjusting the SCS loss parameter has been investigated and tested in the IMPSWM program, (Wisner et al., 1983). However, the procedure implies that API recharge occurs solely through rainfall, (Eqn. F2). Modification of this technique or a parallel algorithm is required for frozen soil and snow conditions.

F2.3 Initial Abstraction, Absper

The second adjustment made in QUALHYMO to provide a continuous capability relates to the value of the available initial abstraction, ABSPER. The user inputs a maximum value of the ABSPER to the model, and this is thereafter adjusted automatically by the model. It is not influenced by soil freezing and therefore will not be considered further.

F3.0 Infiltration

QUALHYMO employs a simple algorithm for the computation of infiltration into the soil column,

$$RINF = RAIN_i - VOLAVE_i - ABSAVE_i \qquad [F4]$$

where, RINF = area weighted infiltration, (mm)
RAIN = total precipitation in the time step, (mm)

$$VOLAVE = \frac{VOLPER(ARPER) + VOLIMP(ARIMP)}{ARPER + ARIMP} \qquad [F5]$$

and,

$$ABSAVE = \frac{ABSI(ARIMP) + ABSP(ARPER)}{ARIMP + ARPER} \qquad [F6]$$

in which, VOLAVE = the area weighted runoff depth , (mm)
ABSAVE = area weighted initial abstraction, (mm)
VOLPER = depth of runoff from pervious areas, (mm)
VOLIMP = impervious area runoff depth, (mm)
ABSI = impervious area initial abstraction, (mm)
ABSP = pervious area initial abstraction, (mm)
ARIMP = impervious land area, (ha),
ARPER = pervious land area, (ha), and
i = the ith time step.

Using Eqn. F4 infiltration is found for each successive time step for which rainfall occurs. For weather conditions through the months of November to May inclusive, in which ambient air temperature falls below a user specified base temperature (BASET) all precipitation is assumed to occur as snowfall and rain is set to zero. Consequently, no infiltration occurs and hence according to Eqn. F4 there is no recharge to the groundwater reservoir, (SVOL). For extended cold periods (i.e. several consecutive months) there is a possibility of creating artificially low groundwater storage levels. However, some recharge does occur although the mechanism of recharge from basal melt of the snow pack through frozen soils is not well understood.

For above freezing temperatures or as described by the user through the BASET parameter in the GENERATE command, all precipitation plus all snowmelt (if a snow pack exists) is assumed to occur as RAIN. This value is then sent to the GENERATE command where runoff volume and losses are determined, and subsequently infiltration amounts are quantified.

It should also be noted that interception and evaporation losses are not considered in the model except implicitly through initial abstraction.

F4.0 Soil Freeze-Thaw Theory

Cary et al., (1978) simplified the analysis of soil freezing and thawing by considering only the net daily heat flow across the soil surface. It was argued that when about the top 30 cm of the soil is cooled to near 0°C, essentially all further heat loss for this strata comes from the freezing of water. This is because the latent heat of freezing far exceeds the heat stored in the soil. Cary et al., deduced that at this temperature the daily net heat flux into and out of the soil may be interpreted as the freezing or thawing of water.

Following this rational, when the sum of the daily heat flows is negative then water in the soil will freeze. Conversely, when the heat flow is positive the soil is considered to be unfrozen. Cary et al., stated this concept as,

$$M = \sum_{n=1}^{n} (G_n + UP_n) \qquad [F7]$$

in which, M = the cumulative heat flux through the soil at soil temperatures less then or equal to zero,

G_n = the daily average soil heat flux downward across the soil surface, and

UP_n = the daily average soil heat flux upward from soil sublayers into the frost susceptible layer.

These heat fluxes may be evaluated using energy balance methods. However, these methods require knowledge of the heat flux from net radiation, the heat associated with the evaporation of water, and the sensible heat exchange between the soil surface and the air. Simulation of these fluxes and processes requires a level of sophistication which is considered to be beyond the scope of a planning level model.

Values of UP_n as determined from measurements of thermal conductivity and soil temperature gradients are relatively small and were expressed in an empirical relation by Cary et al.,

$$UP_n = 2.5 \sin(J+80) \qquad [F8]$$

in which J is the Julian date, and UP_n is given in W/m^2. This relation reproduced observed values well and given the relatively small magnitude of UP_n to G_n it was considered a reasonable approximation at a planning level analysis.

To avoid using the complex energy exchange method, Cary et al., proposed a second method based on the determination of the heat conducted across the soil surface. This could be approximated by,

$$G_n = (k/l)(T_s - T_o) \qquad [F9]$$

where, T_s = the average soil temperature,
T_o = average soil temperature at some shallow depth l,
k = the average soil thermal conductivity over l.

Following a rational similar to the degree day method employed for snowmelt simulation, Cary et al., suggested a simple method for the estimation of daily soil heat flux from daily mean temperature records and snow pack depths. At some shallow depth the thermal insulation of the upper soil layers is sufficient to create a lag in the response of the soil at this depth to current diurnal temperatures. Consequently, at this depth the average daily soil temperature (T_o), which may be a few centimeters below the soil surface, is proportional to the previous day's surface temperature. Noting that,

$$T_o = (T_{s-1} - \delta T_{-1})B^{-1} \qquad [F10]$$

Cary et al., then proposed the following relation for Eqn. F9,

$$T_s - T_o = (T_s - \delta T) - \left(\frac{T_{a-1} - \delta T_{-1}}{B}\right) \qquad [F11]$$

in which, δT = the difference between the soil surface temperature and the temperature of the air at a height of 2 m above the soil surface,

B = is a proportionality constant,

T_{a-1} = the average daily air temperature for the previous day, and

δT_{-1} = the value of δT for the previous day.

Assuming that the quantity $(\delta T - \delta T_{-1}) \approx 0$, and B is near unity, then Eqn. F9 may be approximated by,

$$G_n = \frac{k}{l}\left(T_s - \frac{T_{a-1}}{B}\right)\left(1 - \frac{PACDEP}{PACDEP + N}\right) \qquad [F12]$$

where, the last term is the dampening term to account for snow pack (PACDEP).

F4.1 Model Algorithms

The above soil freeze-thaw method was then incorporated into a algorithmic language in QUALHYMO. A schemetization of the algorithm is illustrated in Figure F.1 and its connectivity within the GENERATE COMMAND in QUALHYMO is shown in Figure E.1.

The surface temperature of the soil is considered near zero when the average daily ambient air temperature for the

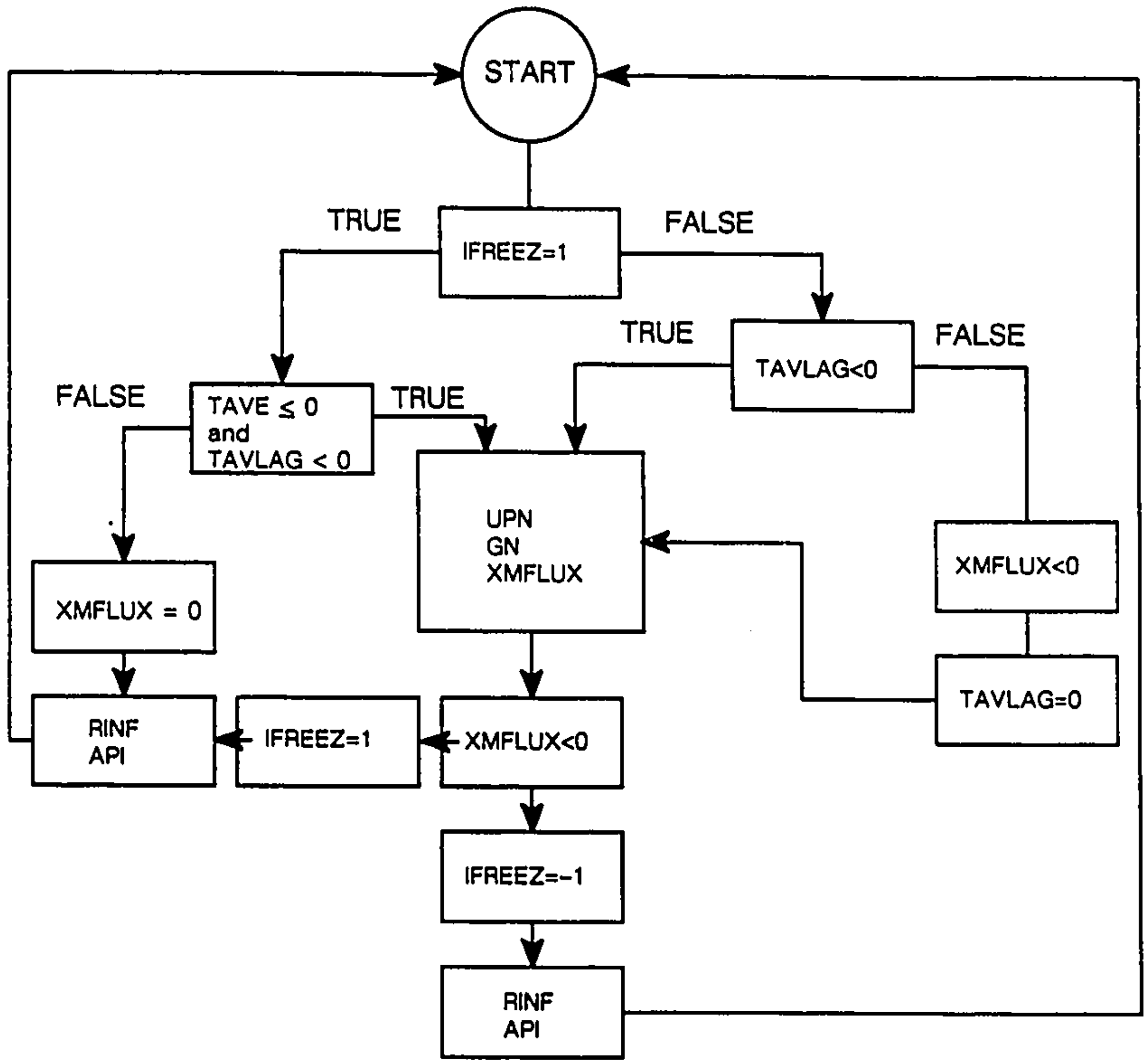

FIGURE F.1 Flow Diagram for Cary, et al., (1978) Soil Freeze –Thaw Process

previous day (TAVLAG) is less then zero and that for the current day (TAVE) is equal to or less then zero. The cumulative heat flux through the soil (XMFLUX) is then determined, and if found to be less then zero the soil is considered frozen. Once frozen, API is set equal to SMAX (a soil moisture corresponding to an AMC III condition as defined by the Soil Conservation Society, (SCS, 1973). Infiltration is also computed using a functional relation with BASMIN and MXFLUX as the primary variables as discussed in Appendix E. The soil is considered unfrozen when TAVLAG > 0.0 and XMFLUX ≥ 0.0.

F4.2 Test Application

Cary et al., reported weather station data for a site in eastern Washington State. They also reported the observed frost depth and the sum of the soil heat deficits (XMFLUX) for several sites including a stubble plot as presented in Figure F2. Figure F2 also shows a plot of the soil heat deficits predicted by QUALHYMO for comparison. The difference observed between the Cary et al., estimates and those obtained using QUALHYMO are due to differences in boundary conditions. Never-the-less, the reproduction of the Cary et al. estimates, particularly the critical periods of freezing and thawing were considered reasonable.

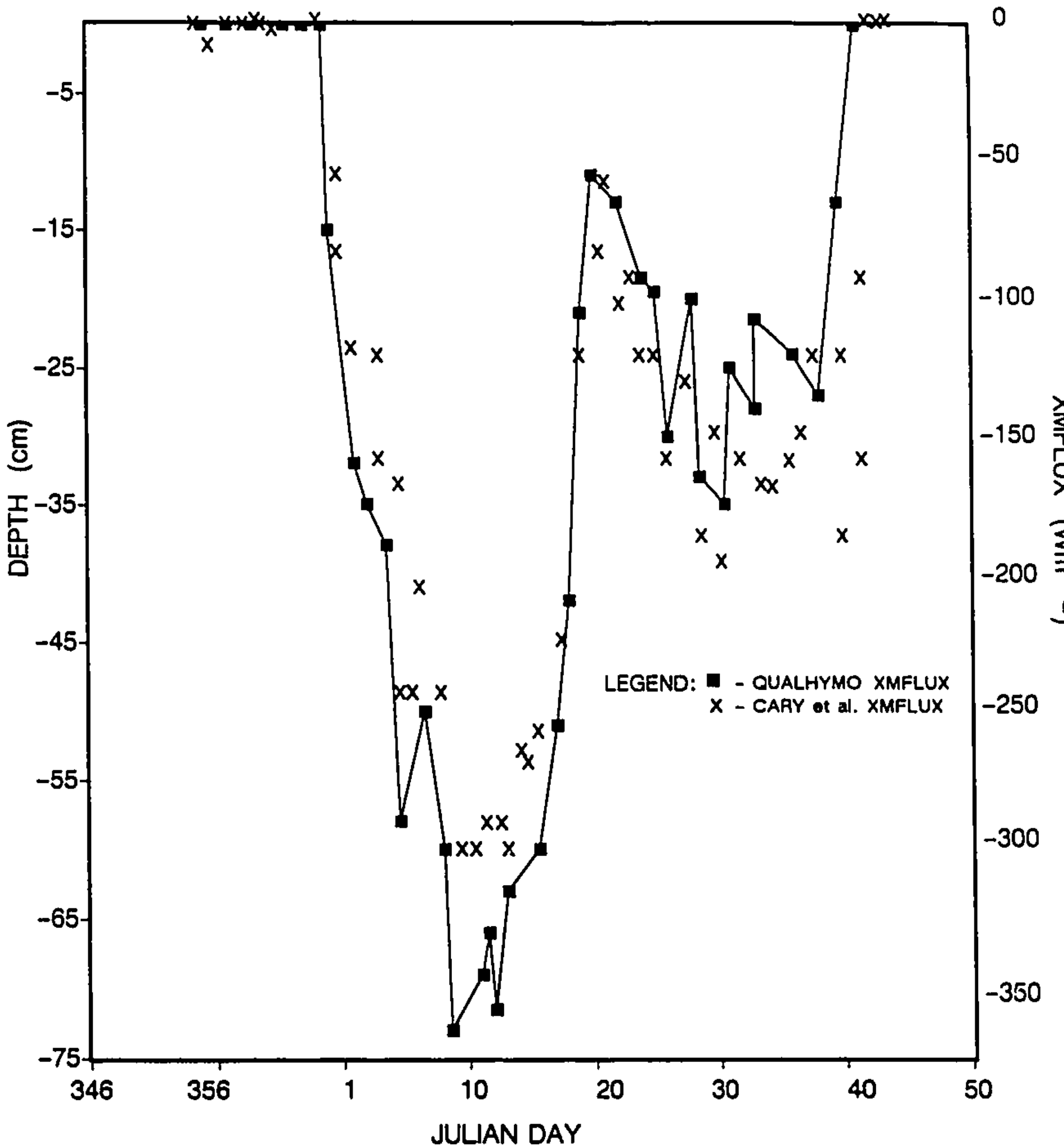

FIGURE F.2

Comparison of Values of XMFLUX from Cary et al., (1978) and QUALHYMO

APPENDIX G

QUALHYMO - Recharge Relation

G1.0 Introduction

The current version of QUALHYMO employed a simple relation to update the groundwater reservoir. This was achieved by assuming that the portion of rainfall not translated into overland flow or stored as initial abstraction, infiltrated into the soil reservoir, (SVOL). This relation is expressed as,

$$RINF = RAIN(I) - VOLAVE - \left(\frac{ABSI*ARIMP+ABSP*ARPER}{ARIMP+ARPER}\right) \quad [G1]$$

where, RINF = portion of rainfall infiltrated into the soil reservoir, (mm)
RAIN(I) = the rainfall amount in the current time step,
VOLAVE = the area weighted average runoff volume,
ABSI = the initial abstraction for impervious surfaces,
ABSP = the initial abstraction for previous surfaces,
ARPER = total amount of previous land area, (m^2), and
APIMP = total amount of impervious land area, (m^2).

This relation however, is not applicable during extended periods in which the ground is considered frozen or for which precipitation occurs primarily as snowfall. It was necessary, therefore when implementing snowmelt and soil freeze-thaw capabilities into the model that a recharge relation be developed which is suitable for "winter periods". Since QUALHYMO employs two baseflow routines which differ significantly, it was necessary to develop two separate but compatible infiltration relations. The development of these relations is discussed below.

G2.0 Recharge For A Single Linear Reservoir

For the single linear reservoir option, baseflow is expressed as,

$$BASFLO = SVOL2*BFAC3+BASMIN \qquad [G2]$$

in which, BASFLO = the baseflow rate, (m^3/s)
BASMIN = the minimum baseflow rate, (m^3/s),

$$SVOL2 = (SVOL*BFAC1+RINF)*BFAC2 \qquad [G3]$$

,and

$$BFAC3 = SLOSK1*SLOSK2*DA(ID)/1000, \qquad [G4]$$

where, SVOL = the soil reservoir volume in the previous time step, (mm)
BFAC1 = (1.0-SLOSK1*DT(ID)*1800)
BFAC2 = 1.0/(2.0-BFAC1)
SLOSK1 = the baseflow recession constant, (mm/s/mm)
SLOSK2 = a loss parameter, (dimensionless)
DA(ID) = drainage area for the selected area, (m^2),
DT(ID) = the time increment, (hrs).

In Eqn. G2, BASMIN is a quantity defined by the user as a calibration parameter. It is not accounted for in the watershed water balance. It may therefore, be removed form the relation resulting in the expression,

$$\text{BASFLO} = \text{SVOL2*BFAC3} \qquad [G5]$$

We may now re-introduce BASMIN as the value of BASFLO observed at the beginning of winter freeze-up. This period being defined as that period during which precipitation occurs primarily as snow and the soil is considered frozen such that recharge from rainfall is negligible. During this period it is assumed that,

$$\text{BASFLO} = \text{BASMIN} \qquad [G6]$$

Expanding Eqn. G5 under the above assumption yields,

$$\begin{aligned} \text{BASMIN} &= \text{SVOL2*BFAC3} \qquad [G7] \\ &= [(\text{SVOL*BFAC1+RINF})\text{*BFAC2}]*\left[\frac{\text{SLOSK1*SLOSK2*DA(ID)}}{1000}\right] \end{aligned}$$

In this relation, BASMIN, SLOSK1, SLOSK2, DT(ID) and DA(ID) are user defined values. The constants BFAC1, BFAC2, and BFAC3 are all determined from these values and the variable quantities SVOL and SVOL2 are updated internally by the model from an initial user defined value. This leaves RINF as the only unknown quantity.

Rearranging Eqn. G7 and solving for RINF, we have,

$$RINF = \frac{BASMIN}{BFAC3*BFAC2} - SVOL*BFAC1*BFAC2 \qquad [G8]$$

In this relation recharge through RINF is exactly offset by losses resulting in a constant baseflow of rate equal to BASMIN. This however, does not reflect field observations in which, the long term average groundwater flow rate typically declines over the winter period in a very gradual manner. This gradual recession of groundwater flows may be related to the depth of frost penetration into the soil mantle and to the quantity of water temporarily lost from the groundwater reservoir in the form of ice. Using the soil heat flux parameter XMFLUX as an indicator of these processes the following relation is proposed,

$$RINF=[\frac{BASMIN}{BAFC3*BFAC2} - SVOL*BFAC1*BFAC2]*[1.0 - \frac{XMFLUX}{XMFLUX+ALPHA1}] \qquad [G9]$$

in which, the term

$$[1.0 - \frac{XMFLUX}{XMFLUX+ALPHA1}] \qquad [G10]$$

represents a correction factor to account for frost penetration and the loss of free groundwater to ice formation. ALPHA1 is a calibration parameter.

G3.0 Recharge For Multiple Linear Reservoirs

An equivalent expression quantifying RINF was developed for use with the multiple linear reservoir option in QUALHYMO. This relation may be written as,

$$RINF=\left[\frac{BASMIN*DT(ID)*3600*COEFA}{DA(ID)}\right]*\left[1.0-\frac{XMFLUX}{XMFLUX+ALPHA1}\right] \qquad [G11]$$

in which, COEFA = a proportionality constant, (2435).

APPENDIX H

Precipitation Infilling Technique

Hourly rainfall data are collected using automated typing-bucket rainfall gauges. These instruments are however, only effectively operate during above zero temperatures. For freezing conditions the AES employs daily manual measurements using a variety of methods including standard rain gauges or snow depth measurements. Consequently, hourly rainfall data are primarily available for the Ottawa International Airport meteorological office for the period of April 01 through to November 30th. Only total daily precipitation being available from December 1st through to March 31st.

QUALHYMO however, accepts only one specified format for any START Command. Although the START Command could be issued separately for winter and summer periods, it was felt that daily totals averaged uniformly over the sub-hour time step of the model would severely dampen any flows occurring from snowmelt-rainfall events during this period. Consequently, it was necessary to transform the daily totals into estimated hourly amounts.

The development of a suitable infilling technique is obviously important to the generation of peak flows. As such a number of alternative schemes were considered. One of the most common and simple approaches is to assume a uniform hourly distribution, wherein each hourly increment equals 1/24th of the daily total. This method solves the problem of how to distribute the hourly amounts but it is essentially the same as a separate issue of the START Command with daily totals as described above. Consequently, this method was not considered appropriate.

A variation of this technique is to assume a uniform hourly distribution over some time period less than twenty four hours. This period typically being defined by a statistical analysis of the duration of winter storm events. While this method represents a significant improvement, the assumption of uniform intensity does not represent a real storm distribution. There is also the problem of when during the twenty four hour period to center the storm event. This difficulty could be solved in part by referring to synoptic journals published by AES. This option was not pursued however, because of the laborious nature of the task when dealing with multi-year simulations. Although this may be simplified by a screening of possible significant events.

A third method is based on the derivation of a dimensionless rainfall distribution from a statistical analysis of major rainfall events. The daily totals are then redistributed according to this "representative" distribution and the timing of the event within the day is established from temperature variations denoting the occurrence of a frontal system.

Such an analysis was performed for a ten year period, 1974-1983 using Ottawa International Airport data. Thirty nine major rainfall events ranging from 7.7 mm $\leq$ PTOT $\leq$ 109.1 mm in total precipitation were identified. The cut off at a minimum value of PTOT = 7.7 mm was arbitrary, however, it was reasoned that smaller events are unlikely to result in a major flood flow event even with snowmelt.

Of the 39 events identified, only one event occurred in the March-April snowmelt period, (Fig. H.1). This event recorded 16.4 mm of rainfall over a 3 hour period producing a maximum intensity of 11.4 mm/hr. Given the insufficient number of observed rainfall events during this period an average distribution utilizing all 39 events was derived. The resulting distribution is illustrated in Fig. H.2.

From Fig. H.2 it can be seen that 75 percent of the rainfall mass occurs within the first 3 hours of the event, and 97 percent occurs within the first 7 hours. This distribution reflects the relatively short duration of the major events. Only 5 of the 39 events exceeded 8 hours in duration.

The dimensionless rainfall distribution was applied to the

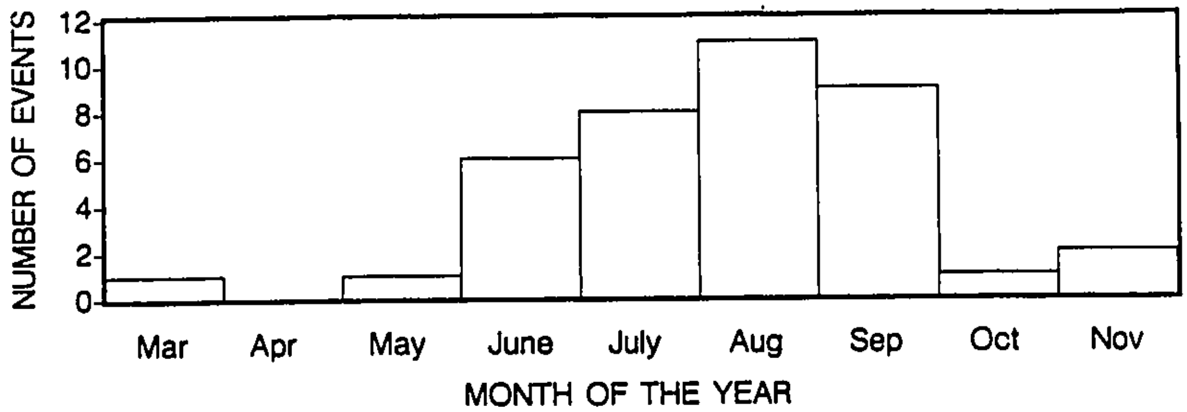

FIGURE H.1 Distribution of Major Rainfall Events for the Months of March through November (Ottawa International Airport, 1974–1983)

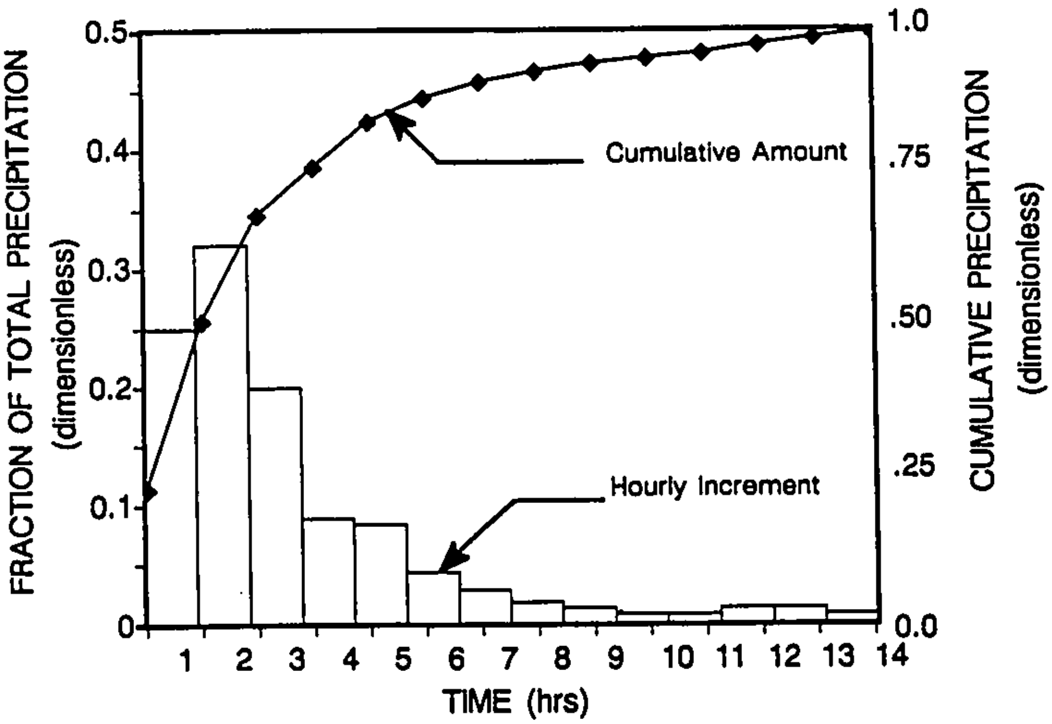

FIGURE H.2 Dimensionless Distribution of Hourly Rainfall Amounts based on AES Data from 1974–1983 (Ottawa International Airport)

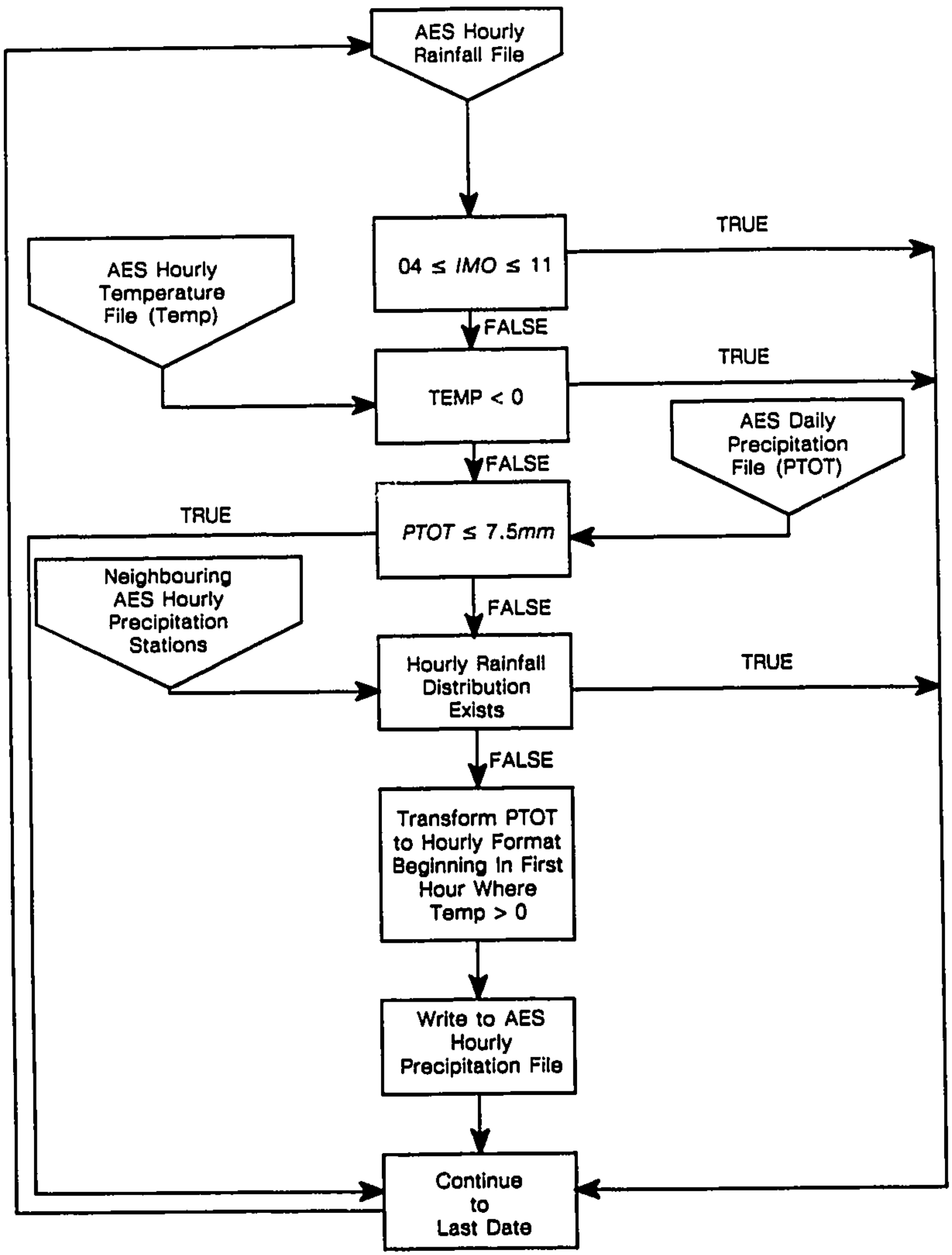

FIGURE H.3 Decision Making for Infilling AES Hourly Precipitation Files

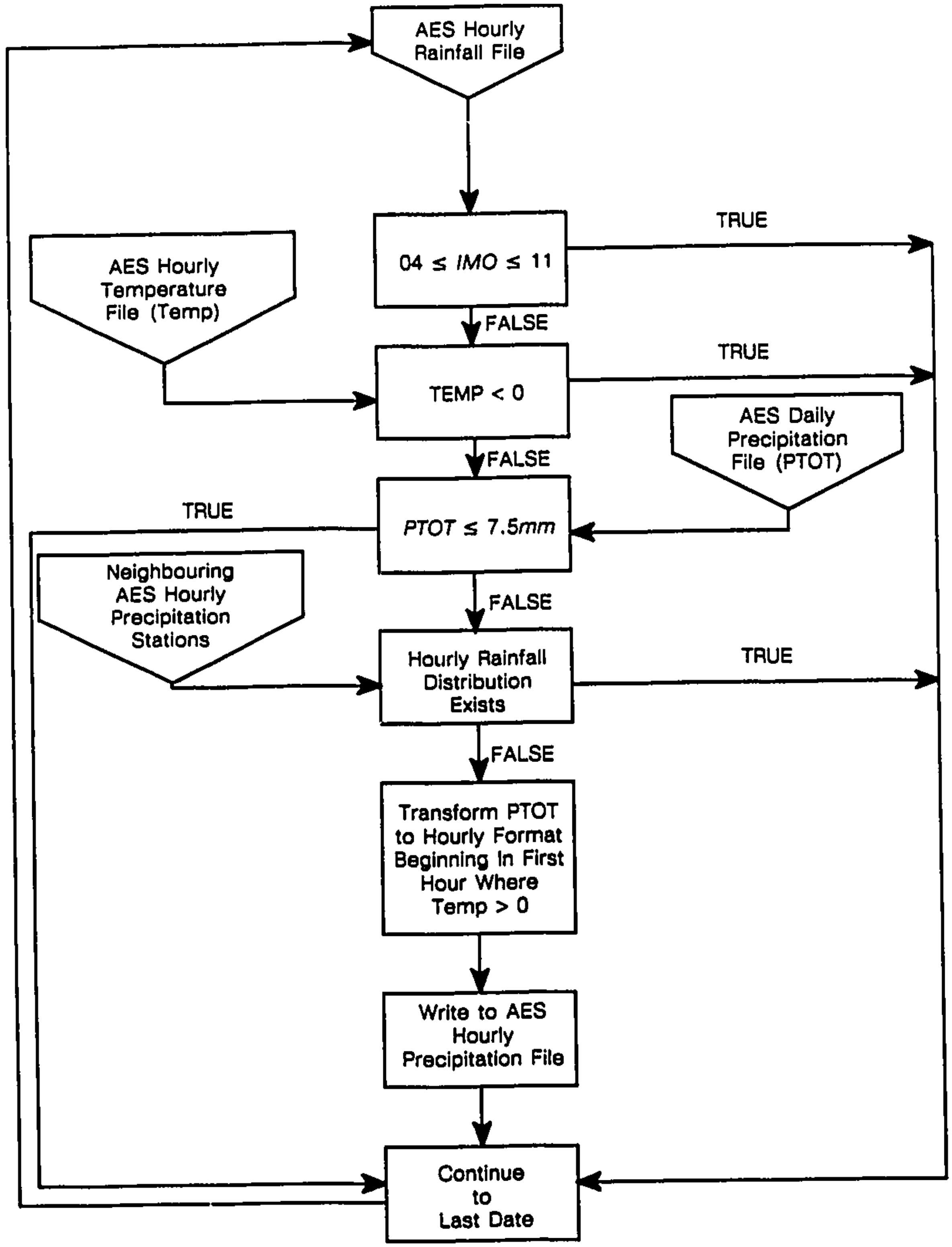

FIGURE H.3 Decision Making for Infilling AES Hourly Precipitation Files

intense during the critical spring snowmelt period, the "rate" of snowmelt takes on additional importance. Fortunately, the majority of melt was found to occur in April for which hourly rainfall amounts are available from AES.

APPENDIX I

CASE STUDY

This appendix deals with the application of the models and procedures presented in the previous Sections. This is achieved through a case study which represents a real situation although the name of the creek is fictitious. It is felt that such an application will help demonstrate the concepts applied in this research and illustrate how some of the difficulties in the proposed approach may be addressed in practice.

I.1 Testville Creek

I.1.1 Introduction

Testville Creek is a small watershed (220 ha) located near Toronto, Ontario. Under existing conditions approximately 25 percent of the watershed, in the lower third of the basin, is urbanized (Figure I.1). Development of a tract of land in the centre of the watershed is currently in progress. This new development was approved without consideration of instream erosion. Development of the remainder of the watershed has been proposed by several proponents.

The lower reach of the creek drains through a deeply incised

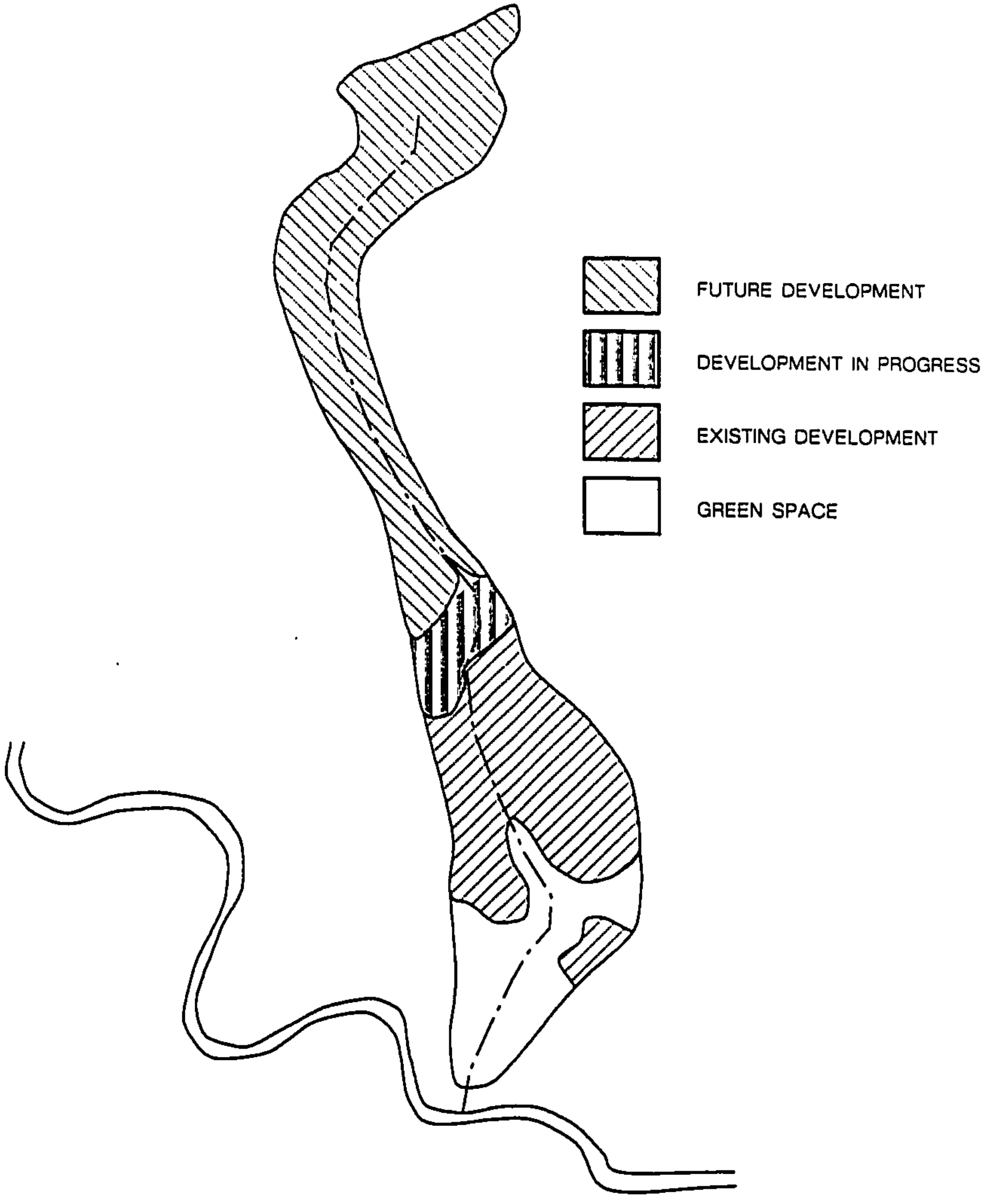

FIGURE I.1 Study Watershed - Future Land Use Conditions

wooded valley cut into shale bedrock and is considered to be a local amenity. The stream channel through this reach is rectangular to trapezoidal in shape (Figure I.2). A minor channel can be identified (Figure I.2) which has a flow capacity of approximately a 1:2 year recurrence interval flow under pre-development conditions.

The shale, when exposed to the air and allowed to dry, quickly fractures and disintegrates into blocky fragments in a silty clay matrix. The bed and banks appear to represent various degrees of weathering probably directly related to extent of exposure and the number of cycles of wetting and drying. The weathering products range from coarse material and fractured shale in the mid bank area to almost complete disintegration of the shale material in the upper bank area. The bed materials consist of intact shale or large plates of fracture shale partially covered by smaller plates and shale fragments. The gradation in boundary material characteristics important in determining the response of the stream channel to an increase in flow rate and duration because of the susceptibility of these weathering products to scour.

The increase in storm water runoff associated with urbanization has raised concerns about the impact of the proposed developments on the stability of the active stream channel. Enlargement of the stream channel may cause severe

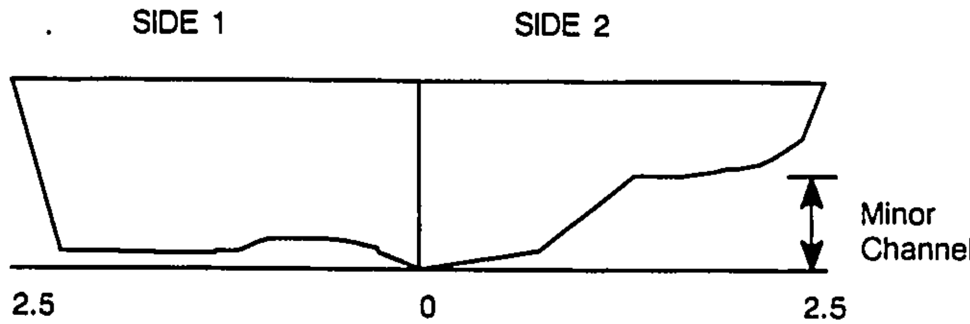

FIGURE I.2 Section A: Hydraulic Geometry

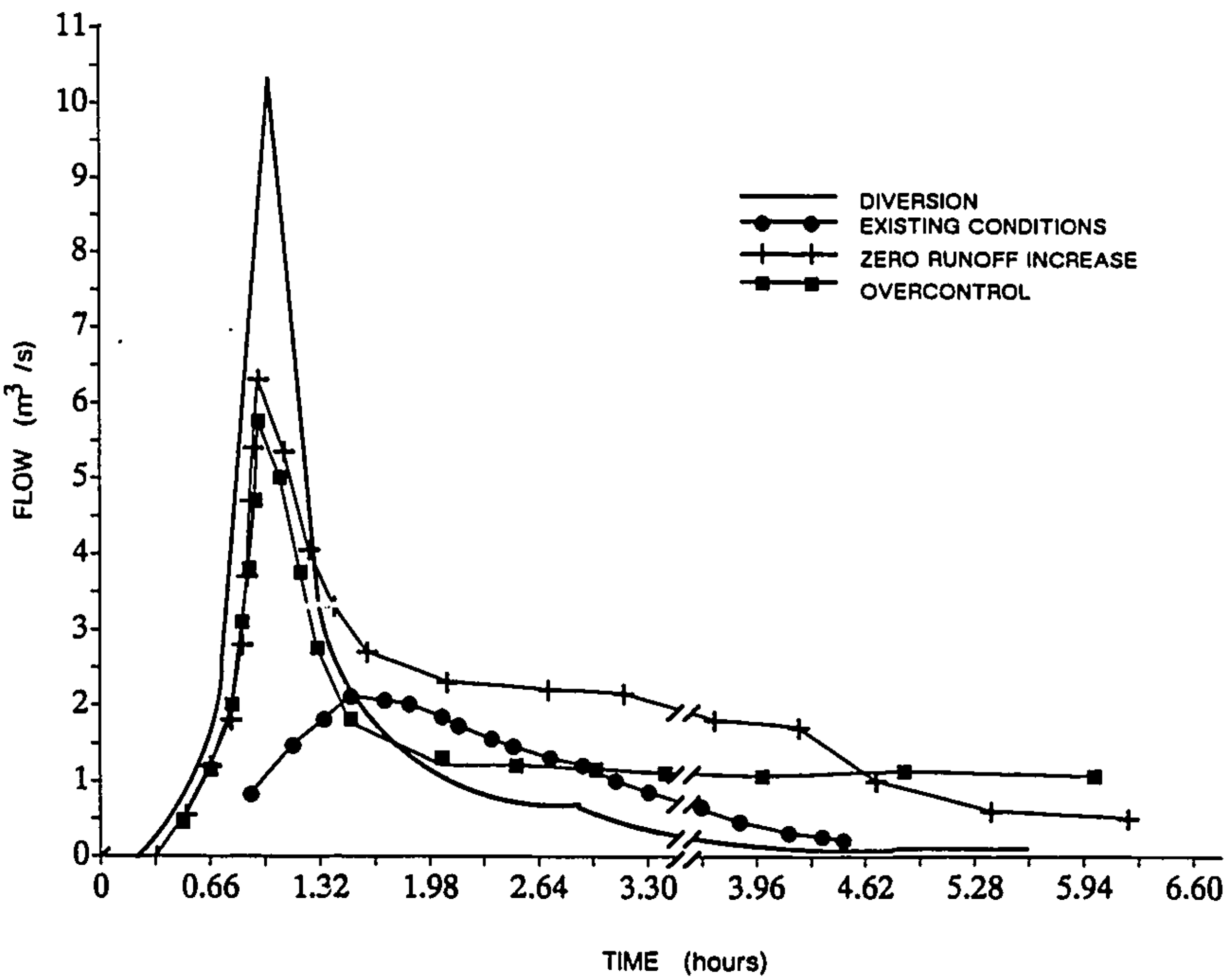

FIGURE I.3 Hydrographs for the 5-Year Design Storm

aesthetic degradation of the ravine and loss of tableland through over steepening of the valley banks and subsequent headwall retreat. The agencies responsible for approving the development required that the proponent demonstrate that the development would not increase erosion hazard in the stream channel through the ravine reach. A study was then commissioned to develop a number of drainage control alternatives to minimize erosion potential.

The study was organized into three phases:

a) conceptual design phase;

b) planning level design phase; and,

c) detailed design phase.

The conceptual design phase deals with the development of a board range of possible alternatives. Models are set up using existing data, if available, and literature values for parameter estimation. The objective of this phase is to reduce the number of alternatives to those which are the most feasible and practicable in terms of control and cost of implementation. It also establishes the protocol for data collection in the planning level design phase. The following test case deals with the application of the index method developed in this work to the conceptual design phase. Application at the planning level phase would be similar to that described in Chapter 10.

I.1.1 Storm Water Management Alternatives

Current storm water management (SWM) policy for instream erosion control commonly requires control of the 1:2 year post-development peak flow rate to the pre-development level, (Hawley and McCuen, 1987). This is referred to as the zero runoff increase concept.

The proponent proposed several storm water management options:

Alternative A: Diversion of minor flows up to and including the 1:5 year design storm event from all new developments (Figure I.1). The remainder of the watershed has already been developed or is approved for development and retrofitting of SWM controls to these areas was not considered practical.

Alternative B: Application of zero runoff control to all approved and future developments in the watershed with all flows being discharged to the study creek.

Alternative C: Application of the concept of over control (50 % reduction in the 1:2 year peak flow rate) to all approved and future developments in the watershed with all flows being discharged to study creek.

The first option, diversion, would route flows up to the 1:5 year flow to a larger creek. This would require the construction of a large interceptor sewer which would add thousands of dollars to the cost of each home. It is also represents a potential transfer of the problem to another drainage system. The later two options represent detention schemes which would permit the release of storm water to the receiver at a reduced flow rate. By constructing an in-line pond within the approved but as yet unconstructed portion of the uncontrolled development in the central are of the basin, some of the flows from this tract of land could also be controlled. These storage alternatives could also be implemented at a lower cost, and consequently, would be preferable if the level of environmental protection offered was considered satisfactory. The decision maker was faced with the task of evaluating the merits of these options. In this regard the index method was proposed as a means of aggregating and summarizing the analytical data as an aid to the interpretation and evaluation process. The following analysis was proposed:

a) develop the explicit form of the index and note the simplifying assumptions;

b) determine τ_{CRT};

c) determine the change in the flow regime;

d) compute the index value at selected boundary stations;

e) compare and evaluate the proposed alternatives; and,

f) recommendation a preferred set of alternatives.

These activities are summarized below.

I.1.2.1 Index Method And Simplifications

The functional form of the index is introduced in Chapter 3 as,

$$(\Delta E_S)_P = \left(\left[\int_0^T f(q_S)_O dt - \int_0^T f(q_S)_I dt\right]_{POST} - \left[\int_0^T f(q_S)_O dt - \int_0^T (q_S)_I dt\right]_{PRE} \right)$$

[I.1]

where, $(E_S)_P$ = the scour potential at point P about the channel perimeter,
$(q_S)_O$ = the sediment transport potential out of the control reach,
$(q_S)_I$ = the potential sediment influx from upstream of the control reach,
PRE = a subscript denoting pre-development conditions, and
POST = a subscript denoting post-development conditions.

The explicit form of Eqn. I.1 was derived by computing (q_S) using the relations,

$$(EXTAU)_P:\ (q_S)_P = \int_0^T b_1(\tau_e)_P\, dt$$

,and

$$(EVI)_P:\ (q_S)_P = \int_0^T b_2(\tau_e)_P \tau_o\, dt$$

in which, $\tau_e = (\tau_o - \tau_{CRT})$, and
b_1, b_2 = calibration coefficients.

The pre-development land use was cash crop and dairy farming which dedicated large tracts of land to pasture and the remaining land to corn and alphafa. A dairy operation was located at the most downstream point of the proposed development. A large instream pond had been excavated for a water supply on this property. The pond operated in a manner similar to the proposed control ponds. Consequently, with the implementation of on-site sediment controls during construction, sediment yields following development will approximate pre-development levels downstream of the control pond. Equating, $[(q_S)_I]_{POST} \approx [(q_S)_I]_{PRE}$, Eqn. I1 reduces to,

$$(\Delta E_S)_P = \left(\left[\int_0^T f(q_S)_O dt\right]_{POST} - \left[\int_0^T f(q_S)_O dt\right]_{PRE} \right)$$

Equation I.4 represents a comparison of pre- versus post-development scour potential at a point about the channel perimeter. Evaluation of Eqn. I.4 at selected points about the perimeter will provide a measure of the potential increase in stream instability.

I.1.2.2 Estimation Of τ_{CRT}

Allen and Larramore (1985) established a relationship between channel enlargement and the degree of urbanization for shale and chalk bed rock controlled streams in Texas. Using hydraulic geometry relationships and flow characteristics describe in their research it was possible to estimate an average shear stress value (τ_{AVE}) of approximately 30 Pa for a stable pre-development bankfull condition. Bed shear stress using EROS1 was found to be in the order of 1.45 to 1.55 times τ_{AVE}. On this basis, $(\tau_{CRT})_{BED}$ was estimated to be 45 Pa. However, the Texas shales as described by Allen and Larramore (1985) appear to be completely unconsolidated unlike that observed for the Testville Creek shales. Based on a depth of 0.5 m at Section A (Figure I.2), which corresponds to a 1:2 year recurrence interval flow, a shear stress of 100 Pa was determined for the bed according to EROS1 simulations. Using the existing channel to represent a stable case, a critical shear stress of 45 Pa $\leq (\tau_{CRT})_{BED} \leq$ 100 Pa was selected for this analysis.

EROS1 was set up for the reach in question using engineering survey data of channel form and longitudinal channel slope. Velocity data were established for the cross-section by prorating laboratory measurements for a trapezoidal channel (Ghosh and Roy, 1970) using Manning's formula.

Bank materials above the minor channel (0.5 to 1.1 m) consist of smaller gravel sized shale and silt stone fragments in a clay-silt matrix. This is more typical of the description provided for the Texas shales. Consequently, $(\tau_{CRT})_{UPP}$ was estimated to be less then or equal to 50 Pa for the upper bank material. A value of τ_{CRT} between the values reported for the bed and upper bank (45 Pa $\leq (\tau_{CRT})_{BNK} \leq$ 75 Pa) was selected for the bank of the minor channel.

A range of values for τ_{CRT} were used to provide an estimate of the sensitivity of the analysis to the selection of the threshold value.

I.1.2.3 Hydrology

The proposed method is applicable to both discrete event and continuous simulation approaches using QUALHYMO, (Rowney and MacRae, 1991(a)). However, for a preliminary screening, OTTHYMO (Wisner et al., 1983), a discrete event unit hydrograph model was employed to determine peak flow rates and runoff volumes. Modelling was carried out for the 1:2 year design storm event. A comparison of peak flow rate at the study section for the three alternatives is given in Table I.1.

TABLE I.1

Comparison Of Peak Discharges For The Selected SWM Alternatives

Alternative	1:2 year (m^3/s)
Diversion	4.9
Zero Runoff Increase	3.6
Over control[1]	3.3

1. Outflow form the controlled developments is set at 50 percent of the pre-development peak flow rate for the 1:2 year design storm for proposed developments.

The storage volumes required to effect the above reductions in instream erosion potential were determined using the reservoir routing routine in OTTHYMO. The analysis indicated that four ponds were required totalling 8,100 m^3 and 10,000 m^3 of storage for the zero runoff increase and over-control options respectively for the 1:2 year event.

The peak flow rate for the diversion scheme is higher then those associated with the storage options because the approved developments in the central portion of the watershed are without any control. However, a comparison of the hydrographs for these alternatives shows that the duration of flows associated with the diversion option is significantly shorter than that obtained using either storage control method (Figure I.3). This is because of the smaller runoff volumes routed to the stream after diversion of up to the 1:5 year flow from the upper watershed. All three alternatives were found to be preferable to development without any runoff control. Reduction of the post-development hydrograph peak flow rate to pre-development 1:2 year levels could not be achieved without retrofitting the entire uncontrolled development area.

I.1.2.4 Estimation Of The Index Value

The 1:2 year hydrograph was discretized at 6 minute intervals. The resulting flows were then used to calculate instantaneous shear stress using simplified relations of shear stress versus discharge developed using EROS1 (Figures I.4 and I.5). The corresponding index values were obtained using a finite difference form of Eqn. I.4. A summary of the results is presented in Table I.2 for the 1:2 year event.

TABLE I.2

Summary Of Shear Stress Indices For The 1:2 Year Event

Alternative	EXTAU Bed	EXTAU Lower Bank	EXTAU Upper Bank	EVI Bed	EVI Lower Bank	EVI Upper Bank
	($\times 10^3$ Pa)			($\times 10^3$ Pa)		
Diversion	113	49	87	17.69	8.22	6.18
Zero Runoff Increase	46	7	17	6.07	0.72	1.16
Over Control	30	2	10	3.94	0.18	0.58

$$(TAU_{CRT})_{BED} = 100 \text{ Pa}$$
$$(TAU_{CRT})_{BNK} = 50 \text{ Pa}$$

For ease of presentation the data was reported in terms of relative differences between the alternatives of storage and diversion. Consequently, the reduction of the erosion indices is presented as a factor of the index value recorded for the diversion option (Table I.3). From this table it can be seen that the zero runoff increase option reduced EXTAU by 1.7 to 7.0 times diversion values for EXTAU. The over control reduced the indices from 1.4 to 24.5 times diversion values for EXTAU. Slightly greater reductions were observed using

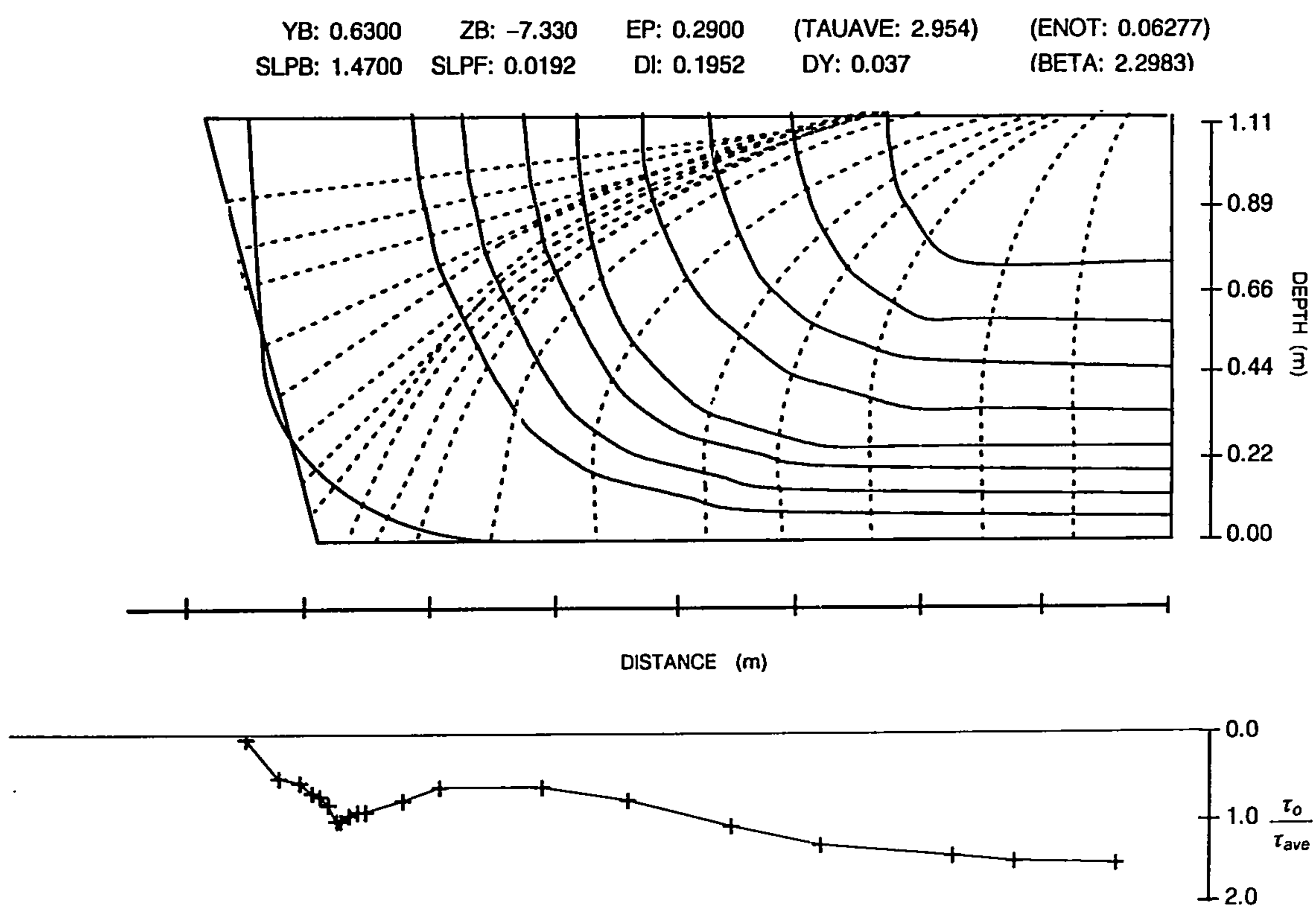

FIGURE I.4 Boundary Shear Stress Distribution for Testville Creek Channel Semi-Perimeter – Section A

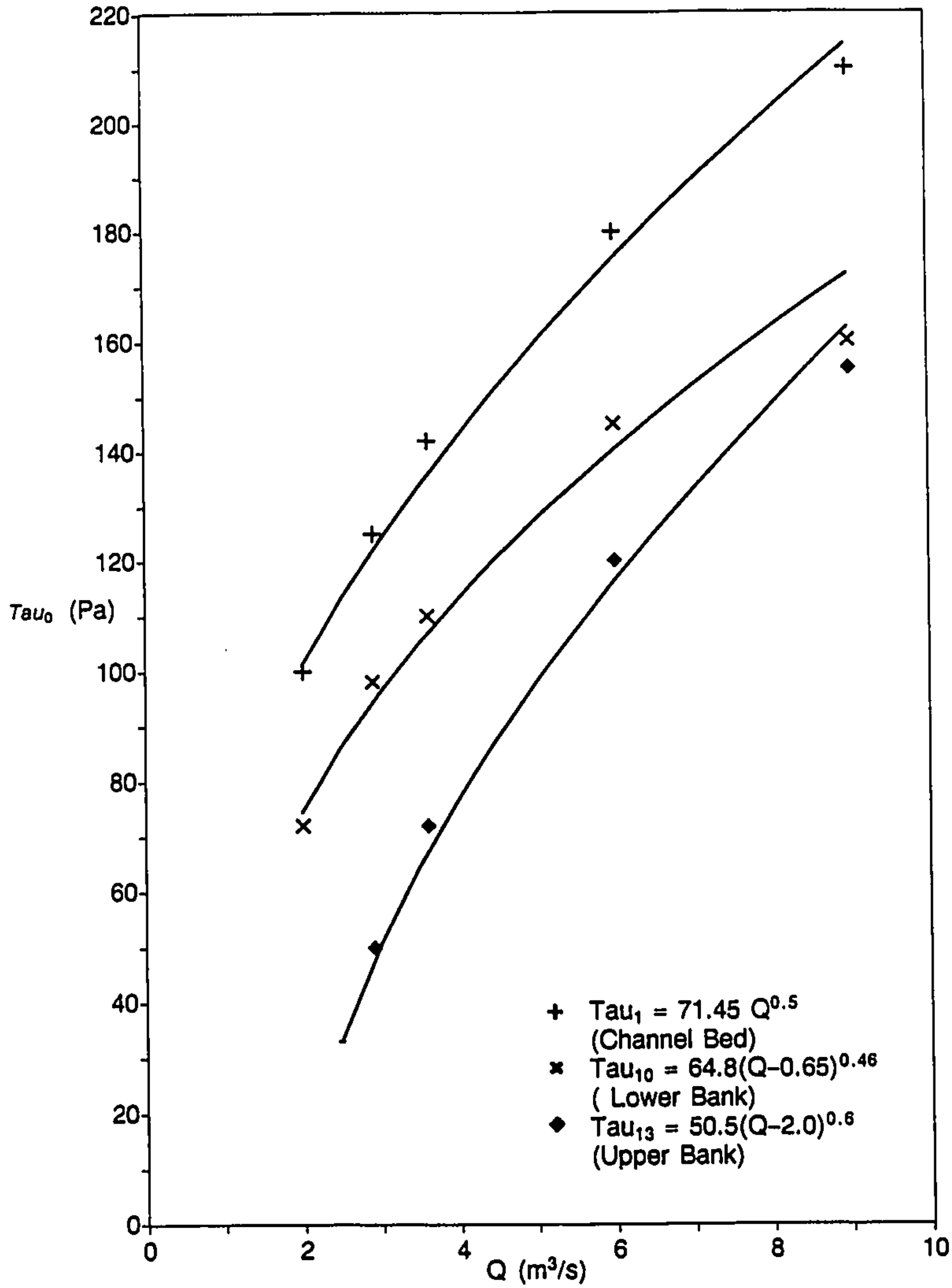

FIGURE I.5 Simplified Boundary Shear Stress Relation for Testville Creek – Section A

the EVI representation of the index.

A sensitivity analysis was conducted by comparing index values using values of τ_{CRT} of 50 Pa, 75 Pa and 100 Pa for the minor channel bank. The storage options tend to become more attractive as τ_{CRT} increases in magnitude for the 1:2 year event regardless of the index used. However, for $(\tau_{CRT})_{BNK}$ = 50 Pa the diversion option provided the lowest index value.

TABLE I.3

Reduction Of Shear Stress Indices For Storage Alternatives In Comparison To Diversion

Storage Alternative	Location	τ_{CRT} (Pa)	EXTAU (%)	EVI (%)
Zero	Bed	100	1.7	2.9
Runoff	Lower Bank	100	7.0	11.7
Increase	Upper Bank	50	1.2	5.2
Over	Bed	100	1.4	4.5
Control	Lower Bank	100	24.5	41.0
	Upper Bank	50	8.7	10.3

Terms are as described in Table I.2.

I.1.4 Conclusions

From the above analysis it was concluded that SWM control through the use of runoff storage appears can be used to control instream erosion as an option to the diversion of flows out of the watershed. The next phase of the investigation will require the design and implementation of a monitoring program. This program would collect flow data, including velocity profiles at selected cross-sections through the reach of interest.

Various storage options based on the zero runoff increase, over control and distributed runoff control criteria would be designed. An analysis, similar to that described in Chapter 10, would then be carried out to select a preferred storage control option.

The use of a two-dimensional index based on excess shear and integrated with respect to time provides a more comprehensive approach to the evaluation erosion phenomena then that provided by current practice. The methodology based on this index, as presented in this work, provides a systematic procedure for the evaluation and design of runoff storage facilities for instream erosion control.

REFERENCES

Ackers, P. and White, R. (1973). "Sediment Transport: New Approach and Analysis," Journal of the Hydraulics Division, ASCE, 99, HY11, pp. 2041-2060.

Allen, P.M. and Narramore, R. (1985), "Bedrock Controls On Stream Channel Enlargement With Urbanization, North Central Texas," Water Resources Bulletin, 21, 6, pp. 1037-1048.

Anderson, E.A. (1973), "National Weather Service River Forecast System - Snow Accumulation And Ablation Model," NOAA Technical Memmorandum NWS HYDRO-17.

Andrews, E.D. (1979), "Hydraulic Adjustments Of The East Fork River, Wyoming To The Supply Of Sediment," In: Adjustments of the Fluvial System, D.D. Rhodes and G.P. Williams eds., Kendall/Hunt Publ. Co., Dubuque, Iwoa, pp. 69-94.

ASCE (1982), "Relationship Between Morphology Of Small Streams And Sediment Yield," Journal of the Hydraulics Division, American Society of Civil Engineers, 108, HY11, pp. 1328-1365.

Barishnikov, N.B. (1967), "Sediment Transport In River Channels With Flood Plains," Berne Symposium, International Association For Scientific Hydrology, 75, pp. 404-413.

Bathurst, J.C. (1982), "Distribution Of Boundary Shear Stress In Rivers," In: Adjüstments of the Fluvial System, D.D. Rhodes and G. Williams ed., Kendall Hunt Dubuque, Iowa, pp. 333-350.

Benson, M.A. and Thomas, D.M. (1966), "A Definition Of Dominant Discharge," Bulletin of the International Association for Scientific Hydrology, 11, pp. 76-80.

Bishop, R. and Mather, C. (1990), "The Rouge River Watershed Management Study: The Technical Background Studies," Proceedings, 43rd Annual Conference of the Canadian Water Respources Association, Pentiction, British Columbia, May 16-18, pp. 133-140

Blench, T. (1951), "Regime Theory For Self-Formed Sediment Bearing Channels," Hydraulics Division, ASCE, 77.

Blench, T. (1957), "Regime Behaviour Of Canals And Rivers," Butterworths Sci. Publ., London, Eng., pp 2-3.

Blench, T. (1966), "Mobile Bed Fluviology," University of Alberta Press, 300 pp.

Bogardi, J. (1974), "Sediment Transport In Alluvial Streams," Akadémiai Kiadó, Budapest, Hungary.

Brotherton, D.I. (1979), "On The Origin And Characteristics Of River Channel Patterns," Journal of Hydrology, 44, 3/4, pp. 211-230.

Bryan, K. (1927), "Channel Erosion Of The Rio Salado, Socorro County, New Mexico," Contributions to the Geography of the United States, Bulletin 790, U.S. Geologicl Survey, Washington D.C., pp. 17-19.

Buol, S.W., Hole, F.D., and McCracken, R.J. (1973), "Soil Genesis And Classification," The Iowa State Univ. Press, Ames, Iowa, 360 pp.

Burkham, D.E. (1972), "Channel Changes Of The Gila River In Safford Valley, Arizona 1846-1970," Professional Paper 655-G, U.S. Geological Survey, Washington D.C.

Burkham, D.E. (1981), "Uncertainties Resulting From Changes In River Form," Journal of the Hydraulics Division, ACSE, pp. 593-610.

Carlston, C.W. (1965), "The Relation Of Free Meander Geometry To Stream Discharge And Its Geomorphic Implications," American Journal Of Science, 263, pp. 864-885

Cary, J.W., Campbell, G.S. and Papendick, R.I. (1978), "Is The Soil Frozen Or Not? An Algorithm Using Weather Records," Water Resources Research, 14, 6, pp. 1117-1122.

CCL (1984), "TVA Hydrologic Modelling Of The Dorset Area Watersheds," Report by Cumming-Cockburn Ltd. for The Ontario Ministry of the Environment.

CCL (1986), "Billberry Creek: Storm Water Management and Erosion Control Study," Report by Cumming-Cockburn Ltd., to the Rideau Valley Conservation Authority.

Chang, H.H. (1982), "Mathematical Model Of Erodible Channels," Journal of Hydraulic Engineering, 108 (HY5), pp. 678-689.

Chang, H.H. (1984), "Modelling Of River Channel Changes," Journal of Hydraulic Engineering, 99 (HY11), pp 157-172.

Chang, H.H. (1985), "River Morphology And Thresholds," Journal of Hydraulic Engineering, ASCE, 111, 3, pp. 503-519.

Chang, Y.C. (1983), "Lateral Mixing In Meandering Channels," in River Mechanics, Proceedings of the Conference Rivers '83, ASCE, N.Y., pp. 598-610.

Chen, Y.H. (1973), "Mathematical Modelling Of Sediment Routing In Natural Channels," Ph.D. Thesis, Colorado State University, Fort Collins, Colorado.

Chiu, C.C. (1967), "Factors Determining The Strength Of Secondary Flow," Journal of the Engineering Mechanics Division, ASCE, 93, EM4.

Chiu, C.C., Lin, H. and Mizumura, K. (1976), "Simulation of Hydraulic Processes In Open Channels," Journal of the Hydraulics Division, ASCE, 102, HY2, pp. 185-206.

Chiu, C.C., Hsiung, D.E., and Lin, H. (1978), "Three-dimensional Open Channel Flow," Journal of the Hydraulics Division, ASCE, 104, HY8, pp. 1119-1136.

Chiu, C.C. and Hsiung, D.E. (1981), "Secondary Flow Shear Stress and Sediment Transport," Journal of the Hydraulics Division, ASCE, 107, HY7, pp. 879-898.

Chiu, C.C. and Lin, G. (1983), "Computation of a 3-D Flow and Shear In Open Channels," Journal of the Hydraulics Division, ACSE, 109, 11, pp. 1424-1440.

Chiu, C.C. and Chiou, J. (1986), "3-D Structure of Flow In Rectangular Open Channels," Journal of the Hydraulics Division, ASCE, 112, 11.

Chorley, R.J., Schumm, S.A. and Sugden, D.E. (1984), "Geomorphology," Methuen, New York, New York, 605 pp.

Colby, B.R. (1964), "Discharge Of Sands And Mean Velocity Relationships In Sand-Bed Streams," Professional Paper 462-A, U.S. Geological Survey, Washington, D.C.

Coleman, N.L. (1981), "Velocity Profiles With Suspended Sediment," Journal of the Hydrauics Division, ASCE, 19, 3, pp. 211-229.

Collins, S.F. and Schalk, M. (1937), "Torrential Flood Erosion In The Connecticut Valley, March 1936," American Journal of Science, 234, pp. 293-307.

Costa, J.E. (1974), "Reponse And Recovery Of Piedmont Watershed From Tropical Storm Agnes, June 1972," Water Resources Research, 10, pp. 106-112.

Craig, R.F. (1987)," Soil Mechanics (Fourth Edition)," Van Nostrand Reinhold (UK) Co. Ltd., 410 pp.

Davies, T.R.H. (1987), "Channel Boundary Shape - Evolution And Equilibrium," In: River Channels - Environment And Process, K.

Richards ed., Basil Blackwell Ltd., pp. 228-248.

Dawdy, D.R. and Vanoni, V. A. (1986), "Modelling Alluvial Channels," Water Resources Research, 22, 9, pp. 71S-81S.

Day, T. (1989), "Sediment/Water Quality Interactions," Presented at the Non-Point Source Pollution Workshop, Canadian Water Resources Association and Soil Conservation Society, Carleton University, Ottawa, Ontario.

Dunn I.S. (1959), "Tractive Resistance Of Cohesive Channels," Journal of the Soil Mechanics and Foundation Division, ASCE, 185, SM3, pp. 1-24.

Dury, G.H. (1973), "Magnitude Frequency Analysis And Channel Morphology," Proceedings, 4th Geomorphology Symposium, Binghamton, New York, New York, pp. 91-122.

Einselle, G., Overbeck, R., Schwarz, H.U. and Unsold, G. (1974), "Mass Physical Properties Sliding And Erodibility Of Experimentallt Deposited And Differently Consolidated Clayey Muds," Sedimentology, 21, pp. 339-372.

Eggleston, K.O., Israelsen, E.K. and Riley, J.P. (1971), "Hydrid Computer Simulation Of The Accumulation And Melt Processes In A Snowpack," Utah Water Research Laboratory, PRWG 65-1, Utah State University, Logan.

Flaxman, E.M. (1963), "Channel Stability In Undisturbed Cohesive Soils," Journal of the Hydraulics Division, ASCE, 89, HY2, pp. 87-96.

Gardner, J.S. (1977), "Some Geomorphic Effects Of A Catastrophic Flood On The Grand River, Ontario," Canadian Journal of Earth Science, 14, pp. 2294-2300.

Gray, D.M. (1973), "Handbook On The Principles Of Hydrology," Secretariat, Canadian National Committee for the International Hydrologic Decade, Water Information Center, Inc., New York.

Ghosh, S.N. and Roy, N. (1970), "Boundary Shear Distribution In Open Channel Flow," Journal of the Hydraulics Division, ASCE, 96, HY4, pp. 967-994.

Gibbs, H.J. (1969), "Discussion," Proceedings, Expansive Soils and Moisture Movement in Partly Saturated Soils, Seventh International Conference on Soil Mechanics and Foundation Engineering, Mexico City, Mexico.

Graf, W.H. (1971), "Hydraulics Of Sediment Transport," McGraw-Hill.

Graf, W.L. (1975), "The Impact Of Suburbanization On Fluvial Geomorphology," Water Resources Research, 11, 14, pp. 690-692.

Gregory, K.J. and Walling, D.E. (1973), "Drainage Basin Form and Process, A Geomorphological Approach," Edward Arnold Ltd., London, 456 pp.

Guy, H.P. and Ferguson, G.E. (1962), "Sedimentation In Small Reservoirs Due To Urbanization," Journal of the Hydraulics Division, ACSE, 88, HY2, pp. 27-31.

Hack, J.T. and Goodlett, J.C. (1960), "Geomorphology And Forest Ecology Of A Mountain Region In The Central Appalachians," Professional Paper 347, U.S. Geological Survey, Washington D.C., pp 48-51.

Hagerty, D.J., Spoor, M.F. and Kennedy, J.F. (1986), "Interactive Mechanics Of Alluvial-Stream Bank Erosion," Proceedings, 3rd International Symposium On River Sedimentation, S.Y. Wang, W.H. Shen and L.Z. Ding, (ed.), Univ. of Mississippi, pp. 1160-1168.

Hammer, T.R. (1972), "Stream Channel Enlargement Due To Urbanization," Water Resources Research, 8, pp. 1530-1537.

Harvey, A.M. (1969), "Channel Capacity And The Adjustment Of Streams To Hydrologic Regime," Journal of Hydrology, 8, pp. 82-96.

Harvey, A.M. (1975), "Some Aspects Of The Relations Between Channel Characteristics And Riffle Spacing In Meandering Streams," American Journal of Science, 275, pp. 470-478.

Harvey, A.M., Hitchock, D.H. and Hughes, D.J. (1979), "Event Frequency And Morphological Adjustment Of Fluvial Systems In Upland Britain," In: Adjustments Of The Fluvial System, D.D. Rhodes and G. Williams ed., Kendall Hunt Dubuque, Iowa, pp. 139-167.

Harvey, M.D. and Watson, C.C. (1986), "Fluvial Processes And Morphological Thresholds In Incised Channel Restoration," Water Resources Bulletin, 22, 3, pp. 359-368.

Hawley, M.E. and McCuen, R.H. (1987), "Elements Of A C Comprehensive Storm Water Management Plan," Journal Water Resources Planning And Management, ACSE, 113(6), pp. 793-809.

HEC (1977), "HEC-6, Scour And Deposition In Rivers And Reservoirs, User's Manual," Hydraulic Engineering Center, U.S. Army Corps of Engineers.

Henderson, F.M. (1966), "Open Channel Flow," The MacMillan

Co., New York, New York, 522 pp.

Hitchcock, D.H. (1977), "Channel Pattern Changes In Divided Reaches: An Example In The Coarse Bed Material Of The Forest Bowland," In: River Channel Changes, K.J. Gregory ed., John Wiley & Sons, Inc., New York, pp. 207-220.

Hollis, G.E. (1975), "The Effect Of Urbanization On Floods Of Different Recurrence Interval," Water Resources Research, 11, 3, pp. 431-435.

Hollis, G.E. and Luckett, J.K. (1976), "The Response Of Natural River Channels To Urbanization: Two Case Studies From Southwest England," Journal of Hydrology, 30, pp. 351-363.

Holtz, R.D. and Kovacs, W.D. (1981), "An Introduction To Geotechnical Engineering," Prentice-Hall Inc., Englewood Cliffs, New Jersey,

Hooke, J.M. (1979), "An Analysis Of The Processes Of River Bank Erosion," Journal of Hydrology, 42, 1/2, pp. 39-62.

James, W. and Robinson, M. (1987), Hydrologic Modelling Of Continuous Urbanization And Consequent Effects Downstream," Proceedings, Eighth Canadian Hydrotechnical Conference, Canadian Society of Civil Engineering, Montreal, Quebec, pp. 523-531.

Kamedulski, G.E. and McCuen, R.H. (1979), "Evaluation Of Alternative Stormwater Dentention Policies," Journal Water Resources Planning and Management Division, ASCE, 105, WR2, pp. 171-186.

Karim, M.F. and Kennedy, J.F. (1982), "IALLUVIAL: A Computer-Based Flow- And Sediment- Routing Model For Alluvial Streams And Its Application To The Missouri River," Institute of Hydraulic Research, IIHR Report 250, Ia.

Katzer, T. and Bennett, J.P. (1983), "Sediment Transport Model For The East Fork Of The Carson River, Carson Valley, Nevada," Proceedings, 1983 International Symposium on Urban Hydrology, Hydraulics and Sediment Control, University of Kentucky, Lexington, pp. 421-436.

Keller, F.J. (1962), "Effect Of Urban Growth On Sediment Discharge, Northwest Branch Anacosta River Basin, Maryland," Professional Paper 450-C, U.S. Geological Survey, pp. C129-C131.

Kishi, T. and Ashida, K. (1974), "The Bed Configuration And Roughness Of Alluvial Streams," by Task Committee on the Bed Configuration and Hydraulic Resistance of Alluvial Streams, Committee on Hydraulics and Hydraulic Engineering, The Japan Society of Civil Engineering.

Knowles, A.J. (1971), "Channel Morphology And Flood Hydrology Of The River Greta, N. Riding Of Yorkshire," M.Sc. Thesis, University of Liverpool, Liverpool.

Koechlin, R. (1924), "Mecanisme de l'eau," Librairie Polytechnique, Béranger, Paris.

Krishnappan, B.G. (1981), "Users Manual: Unsteady, Nonuniform, Mobile Boundary Flow Model - MOBED," Hydraulics Division, National Water Research Institute, Environment Canada, Burlington, Ont.

Krishnappan, B.G. (1983), "MOBED - Users Mannual Update I," Hydraulics Division, National Water Research Institute, Burlington, Ont.

Krishnappan, B.G. (1985), "Comparison Of MOBED And HEC-6 River Flow Models," Canadian Journal of Civil Engineering, 12, pp. 464-471.

Lane, E.W. (1955), "Design Of Stable Channels," American Society of Civil Engineers, Transactions, 120, pp. 1234-1279.

Laursen, E.M. (1952), "Observations On The Nature Of Scour," Proceedings of Fifth Hydraulic Conference, Bulletin 34, University of Iowa, Iowa City, Iowa, June 9-11, pp. 179-197.

Lazar, T.R. (1978), "Urban Land Use And Its Impact On Streams: A Field Exercise," Science Education, 62, 2, pp. 165-171.

Lee, K. and Ham, P.J. (1988), "Effects Of Surrey's Storm Water Management Policy On Channel Erosion," Proceedings, International Symposium On Urban Hydrology and Municipal Engineering, Town Of Markham, Markham, Ontario.

Lee, K. (1990), Pers. Comm., Senior Water Resources Engineer, Gartner and Lee, Assoc. Ltd., Vancouver, British Columbia.

Lefebvre, G., Rohan, K. and Douville, S. (1985), "Erosivity Of Natural Intact Structured Clay: Evaluation," Canadian Geotechnical Journal, 22, pp. 508-517.

Lefebvre, G. (1986), "Slope Instability And Valley Formation In Canadian Soft Clay Deposits," Canadian Geotechnical Journal, 23, pp. 261-270.

Lefebvre G. and Rohan, K. (1986), "On The Principal Factors Controlling Erosivity Of Undistubed Clay," University of Sherbrooke, Sherbrooke, Quebec, pp. 170-195.

Leopold, L.B., Wolman, M.G. and Miller, J.P. (1964), "Fluvial Processes In Geomorphology," W.H. Freeman and Co., San Francisco, 522 pp.

Leopold, L.B (1968), "Hydrology For Urban Planning - A Guidebook On The Hydrologic Effects Of Urban Land Use," U.S. Geological Survey Circular 554, 18 pp.

Leopold, L.B. (1973), "River Channel Change Through Time: An Example," Bulletin 84, Geological Society of America, pp. 1845-60.

Leopold, L.B. (1982), "Water Surface Topography In River Channels And Implications For Meander Development, "In: Gravel Bed Rivers, R.D. Hey, J.C. Richards, and C.R. Thorne (ed.), John Wiley, New York, N.Y., pp. 359-388.

Lewin, J. (1978), "Floodplain Geomorphology," Progress in Physical Geography, 2, 3, pp. 408-437.

Liggett, J.A., Chiu, C.L. and Miao, L.S. (1965), "Secondary Currents In A Corner," Journal of the Hydraulics Division, ASCE, 91, HY6.

Lorant, F.I. (1983), "Erosion Control By Storm Water Management Is It Worth A Dam," Proceedings, Canadian Society of Civil Engineers, Annual Conference June 2-3, Ottawa, Ont., pp. 723-727.

Lorant, F.I. (1988), "Erosion Process In Urban Areas," Proceedings, International Symposium On Urban Hydrology and Municipal Engineering, Section C, Town Of Markham, Markham, Ontario.

Mansue, E.H. and Anderson, P.W. (1974), "Effects Of Land Use And Retention Practices On Sediment Yields In Stony Brook Basin, New Jersey," Water Supply Paper 1798-L, U.S. Geological Survey, 33 pp.

Mason, J.M. Jr., Rhomberg, E.J. and Gregory, G.G. Jr. (1982), "Effects Of Outlet Control Configuration On Detaining Stormwater," Proceedings, International Symposium On Urban Hydrology, Hydraulics and Sediment Control, University of Kentuky, Lexington, Kentucky, pp. 379-385.

Mather, C. (1990), Pers. Comm., Chief, Water Resource, Metropolitan Toronto and Region Conservation Authority.

McCuen, R.H. (1979), "Downstream Effects Of Storm Water Management Basins," Journal of the Hydraulics Division, ASCE, 1, 1, pp. 21-42.

McCuen, R.H. and Moglen, G.E. (1988), "Multicriterion Storm-water Management Methods," Journal of Water Resources Planning & Managment, ASCE, 114, 4, pp 414-431.

McGuire, J.G. (1987). "Determination Of Velocity Profiles And Shear Stress For The Rideau River Under Ice Cover," Water Quality Engineering Report, Civil 883, Queen's University, Kingston, Ont.

Mengis, R.C. (1981), "Modeling Of A Transient Streambed In The Rio Grande, Cochiti Dam To Near Albuquerque, New Mexico," U.S. Geological Survey, Open File Report, 82-106.

Middleton, G.V. (1976), "Hydraulic Interpretation Of Sand Size Distributions," Journal of Geology, 84, pp. 405-426.

Mirtskulava, T. E. (1966), "La stabilite a l'erosion des sols cohesifs," Journal de Recherches Hydrauliques, 4, 1, pp. 37-50.

MOE (1978), "Water Management - Goals, Policies, Objectives and Implementation Procedures of the Ministry of Environment, Ontario, November 1978," Ontario Ministry of Environment.

Morisawa, M.E. and LaFlure, E. (1979), "Hydraulic Geometry, Stream Equilibrium And Urbanization," In: Adjustments of the Fluvial System, D.D. Rhodes and G. Williams ed., Kendall Hunt Dubuque, Iowa, pp. 333-350.

Morse, B. and Townsend, R.D. (1988), "Considerations In The Numerical Modelling Of Alluvial Channel Transport Processes," Proceedings, VI International Water Resources Association World Congress On Water Resources, Ottawa.

National Research Council, Advisory Board On The Built Environment, (1983) "An Evaluation Of Flood-Level Prediction Using Alluvial-River Models," Technical Report, Committee on Hydrodynamic Computer Models for Flood Insurance Study, Washington, D.C.

Neff, E.L. (1967), "Discharge Frequency Compared To Long Term Sediment Yields," International Association for Scientific Hydrology, Berne Symposium, 75, pp. 236-242.

Ott, W.R. (1978), "Environmental Indices Theory And Practice," Ann Arbor Science, 371 pp.

Paaswell, R.E. (1973), "Causes And Mechanics Of Cohesive Soil Erosion: State Of The Art," Highway Research Board, Special Report 135, pp. 52-74.

Partheniades, E. and Paaswell, R.E. (1970), "Erodibility Of

Channels With Cohesive Boundary," Journal of the Hydraulics Division, ASCE, 96 (HY3), Proceedings Paper 7156, pp. 755-771.

Pitty, A. (1971), "Introduction To Geomorphology," Methuen, London, England.

Prasuhn, A.L. (1987), "Fundamentals Of Hydraulic Engineering," Holt, Rinehart and Winston, Toronto, 509 pp.

Preissmann, A. (1961), "Propogation des intumescences dans les cannaux et rivieres," 1re Congrs de l'association francaise de calcul, Grenoble.

PLUARG (1977), "Evaluation Of Remedial Measures To Control Non-Point Sources Of Water Pollution," Report from the Land Use Reference Group (PLUARG) to the International Joint Commission, IJC Report 77-014.

Richards, K.S. and Lorriman, N.R. (1987), "Basal Erosion And Mass Movement," In: Slope Stability, Geotechnical Engineering and Geomorphology, M.G. Anderson and K.S. Richards (ed.), John Wiley, Toronto, pp. 359-380.

Rohan, K, Lefebvre, G. and Douville, S. (1980), "Mecanismes d'erosion de l'airgle intacte/Erosion Mechanisms Of Intact Clay," Proceedings, Conference canadienne sur le littoral, Burlington, Ont., pp. 200-219.

Rossmiller, R.L. (1982), "Rational Formula Revisited," In: Stormwater Detention Facilities, W. DeGroot (ed.), ASCE, pp. 146-162.

Rowney, A.C., and MacRae, C.R. (1991(a)), "QUALHYMO User's Manual Version 2.1: A Language For Continuous Hydrologic Simulation," Dept. of Civil Eng., Royal Military College of Canada.

Rowney, A.C., and MacRae, C.R. (1991(b)), "QUALHYMO Technical Reference Manual Version 2.1: A Language For Continuous Hydrologic Simulation," Dept. of Civil Eng., Royal Military College of Canada.

Savini, J. and Krammerer, J.C. (1961), "Urban Growth And The Water Regime," Water Supply Paper 1591-A, U.S. Geological Survey, 42 pp., (Part 2).

Scheidegger, A.E. (1961), "Theoretical Geomorphology," Springer-Verlag, Berlin, 327 pp.

Schumm,S.A. and Lichty,R.W. (1963), "Channel Widening And Flood Plain Construction Along Cimarron River In South-western Kansas," Professional Paper 352-D, U.S. Geological Survey, pp. 71-88.

Scott, K.M. (1973), "Scour And Fill In Tujunga Wash - A Fanhead Valley In Urban Southern California - 1969," Professional Paper 732-B, U.S. Geological Survey, Washington, D.C.

Shen, H.W. and Komura, S. (1968), "Meandering Tendencies In Straight Alluvial Channels," Journal of the Hydraulics Division, ASCE, 94, HY4, pp. 997-1016.

Shen,W.W., ed. (1971), "Sedimentation," Water Resources Publications, Fort Collins, Colorado.

Simons, D.B., Li, R.M. and Brown, G.O. (1979), "Sedimentation Study Of The Yazoo River Basin-Users Manual For Program KUWASER, Report CER79-80DBS-R, Department of Civil Engineering, Colorado State University, Fort Collins, Colo.

Simons, D.B. and Li, R.M., (1982), "Engineering Analysis Of Fluvial Systems," Publ. by Simons, Li & Assoc. Ltd., Fort Collins, Colorado.

Smerdon, E.T. and Beasley, R.P. (1961), "Critical Tractive Forces In Cohesive Soils," Agricultural Engineering, 42, pp. 26-29.

Smith, H.T.U. (1940), "Notes On Historic Changes In Stream Courses Of Western Kansas, With A Plea For Additional Data," Transactions, Kansas Academy of Science, 43.

Soil Conservation Service (1972), "Hydrology National Engineering Handbook, Section 4," U.S. Department of Agriculture, 547 pp.

Stewart, J.H. and LaMarche, V.C. Jr. (1967), "Erosion And Deposition Produced By The Flood Of December 1964 On Coffee Creek, Trinity County, California," Professional Paper 422-K, U.S. Geological Survey, Washington, D.C.

Strahler, A.H. (1950), "Equilibrium Theory Of Erosional Slopes Approached From Frequency Distribution Analysis," American Journal of Science, 248, pp. 673-696, 800-814.

Tarapore, Z.S. (1956), "Scour Below A Submerged Sluice Gate,"M.Sc. Thesis, University of Minnesota, Minneapolis, Minn.

Thorne, C.R. (1978), "Processes Of Bank Erosion In River Channels, Ph.D. Thesis, University of East Anglia, Norwich.

Thorne, C.R. and Lewin, J. (1982), "Bank Processes, Bed

Material Movement, and Planform Development," In: Adjustments of the Fluvial System, D.D. Rhodes and G. Williams ed., Kendall Hunt Dubuque, Iowa, pp. 117-138.

Thorne, C.R. (1988), "River Bank Stability Analysis II: Applications," Journal of Hydraulic Engineering, ASCE, Vol. 114, No. 2. Feb., pp. 151-172.

Train, R.E. (1973), "Management Of The Future," presented at the National Conference on Managing the Environment, Washington, D.C.

Tsang, G. (1970), "Change Of Velocity Distribution In A Cross-Section Of A Freezing River And The Effects Of Frazil Ice Loading On Velocity Distribution," Proceedings, International Association on Hydraulics Research, Symposium on Ice and Its Action on Hydraulic Structures, pp. 7-10.

Twidale, C.R. (1964), "Erosion Of An Alluvial Bank At Birdwood, South Australia," Z. Geomorphol., 8, pp. 189-211.

U.S. Army Corps of Engineers (1956), "Snow Hydrology," Portland Oregon, North Pacific Division, Corps of Engineers, 437 pp.

UHREMAC (1987), "Fourth Annual Report Of The Upper Holmes Run Environmental Monitoring Advisory Committee (UHREMAC)," Fairfax County, Virginia.

Urbonas, B. (1980), "Drainageway Erosion In Semi-Arid Urbanizing Areas," Flood Hazard News, Urban Drainage And Flood Control, 10, 1.

Urbonas, B. (1988), Pers. comm., Chief, Master Planning and Maintenance Programs, Urban Drainage And Flood Control District - 69, Denver, Colorado.

Vanoni, V. A. (1975), "Sedimentation Engineering," American Society of Civil Engineers, 54, New York, New York.

Vetter, M. (1986), "Velocity Distribution And Von-Karmon Constant In Open Channel Flows With Sediment Transport," Proceedings, Third International Symposium On River Sedimentation, S.Y. Wang, H.W. Shen and L.Z. Ding eds., pp. 814-823.

Whipple, W. Jr., DiLouie, J.M. and Pytler, T. Jr. (1981), "Erosion Potential Of Streams In Urbanizing Areas," Water Resources Bulletin, AWRA, 17, 1, pp. 36-45.

White, C.M. (1940), "The Equilibrium Of Grains On The Bed Of A Stream" Proceedings, Royal Society of London, Series A, 958, 174, pp. 322-338.

Williams, G.P. (1978), "Bank-full Discharge Of Rivers," Water Resources Research, 14, 1141-1154.

Wisner, P.E. Cheung, P., P'ng, C., Kassem, A., Lam, A., Liang, W., and Fraser, H. (1983), "IMPSWM Methodology, 2nd. Ed.", University of Ottawa, Ottawa.

Wolman,M.G. and Eiler, J.P. (1958), "Reconnaissance Study Of Erosion And Deposition Produced By The Flood Of August 1955, In Connecticut," Transactions of the American Geophysical Union, 39, pp. 1-14.

Wolman, M.G. (1959), "Factors Influencing Erosion Of A Cohesive River Bank," American Journal of Science, 257, 3, pp 204-216.

Wolman, M.G. and Miller, J.P. (1960), "Magnitude And Frequency Of Forces In Geomorphic Processes," Journal of Geology, 68, pp. 54-74.

Wolman, M.G. (1967), "A Cycle Of Sedimentation And Erosion In Urban River Channels," Geogr. Ann., 49A, pp. 385-395.

Yu, B. and Wolman, M.G. (1986), "Bank Erosion And Related Washload Transport On The Lower Red River, Louisiana," Proceedings, Third International Symposium On River Sedimentation, The University Of Mississippi, pp. 1276-1285.